

An Innovative Seismic Risk Assessment Method and Implications of Strain-rate Dependency on Risk Estimates

Dissertation

submitted to, and approved by,

the Department of Architecture, Civil Engineering and Environmental Sciences
of the Technische Universität

Carolo-Wilhelmina
zu Braunschweig
and
the Faculty of Engineering
Department of Civil Engineering
of the University of Florence

in candidacy for the degree of a
Doktor-Ingenieur (Dr.-Ing.) /

Dottore di Ricerca in Risk Management on the Built Environment *)

by

Sadık Cem Topcuoğlu
from Antalya, Turkey

Submitted on 31 March 2006

Oral examination on 19 May 2006

Professorial advisor Prof. Udo Peil

Prof. Andrea Vignoli

Prof. Luca Facchini

2006

*) Either the German or the Italian form of the title may be used.

The dissertation is published in an electronic form by the Braunschweig university library at the address

<http://www.biblio.tu-bs.de/ediss/data/>

Contents

Abstract.....	4
Abbreviations and Symbols.....	5
1. Latin.....	5
2. Greek	8
Introduction	9
Chapter 1. Founding principles of risk management in built environment	10
1.1. Motive behind application of risk management in built environment.....	10
1.2. Risk management - definition	10
1.3. Risk management in built environment due to natural hazards - definition.....	11
1.4. Lack of a uniform framework.....	11
1.5. Principles of risk management in built environment due to natural hazards	13
Chapter 2. Innovative method for seismic risk assessment of a single facility	15
2.2. Phenomenological comprehension by means of a hazard tree.....	16
2.3. Risk measures decision.....	18
2.4. Detection of loss paths by loss trees.....	19
2.5. Assigning governing variables to events	24
2.6. Stating the mathematical model	26
2.7. Detection of potential hazard sources.....	28
2.8. Modeling hazard recurrence	30
2.9. Modeling intermediate events	34
2.9.1. Strong Motion Function	36
2.9.1.1. Source spectrum	37
2.9.1.2. Path model	39
2.9.1.3. Local soil and topographic effects model.....	41
2.9.1.4. Source duration model.....	43
2.9.1.5 Path delay model	43

2.9.1.6. Simulation.....	43
2.9.2. Strong motion - response intermediate function $f_{R S}(x)$	45
2.9.3. Response-damage intermediate function $f_{D R}(x)$	47
2.9.4. Damage-loss and response-collapse intermediate functions	52
2.9.4.1. Collapse probability model.....	52
2.9.4.2. Death and injury model	53
2.9.4.3. Restoration cost model	54
2.9.4.4. Serviceability interruption model	55
2.9.4.5. Monetary loss model -due to tangibles-	55
2.10. Solution and dealing with uncertainty	55
Chapter 3. Example application of the method	58
3.1. Problem statement	58
3.2. Construction of mathematical model.....	58
3.3. Hazard assessment.....	64
3.3.1. Investigation of seismological setting	64
3.3.4. Structural response analysis	71
3.3.5. Damageability and loss estimate	75
3.3.6. Presentation of results.....	77
Chapter 4. Investigations on sensitivity to strain-rate-dependency of seismic loss estimates in steel frame structures.....	87
4.1. On model sensitivity and motivation of the investigation.....	87
4.2. Rate dependency as a commonly neglected phenomenon in seismic response assessment	87
4.2.1. Rate dependency at material level	90
4.2.2. Local level (component and cross-section)	93
4.2.3. Global scale	94

4.3. Investigation on rate dependency sensitivity of seismic response of a steel frame under severe strong motion	95
4.3.1. Example structure	95
4.3.2. Finite element model	99
4.3.3. Material models and parameters.....	99
4.3.3. Modal analysis	100
4.3.4. Equivalent static analysis and code validation	100
4.3.4. Used time histories	104
4.3.5. Computational aspects of dynamic analyses	106
4.3.6. Data gathering and processing by Incremental Dynamic Analysis.....	106
4.4. Analysis of global results	111
4.4.1. Range of maximum strain rates	111
4.4.2. Variability of maximum strain rates among varying records	111
4.4.3. Variability of recorded velocity and connected maximum strain rate variability.....	115
4.4.4. Variability of global response parameters	122
Conclusions	131
ANNEX.I. MATLAB Script	132
ANNEX.II. ANSYS Script.....	142
Bibliography	183

Abstract

A probabilistic seismic risk assessment methodology for single facility is presented. It contains analyses of hazard, response, damage and loss. It is formed by synthesis of state-of-the-art approaches and own contributions. The consecutive steps of method are; (1) phenomenological comprehension, (2) source identification, (3) probabilistic hazard analysis, (4) stochastic strong motion simulation, (5) incremental dynamic time-history analysis, (5) probabilistic component-based damage and loss analysis. The method accounts for nonstructural and contents damage in addition to structural damage. The method is especially suitable for regions with poor instrumental seismic records, because of the use of stochastic strong motion simulation approach. The initial step of the method (phenomenological comprehension) can be implemented universally to other natural hazards' risks in built environment.

The method is applied on an example steel frame structure. The fictive structure is located in a certain near-field site in a highly seismic region in Turkey. Regional seismicity data is gathered. 7 discrete hazard intensity levels between moment magnitudes of 5.0 and 8.0 are considered. 10 strong motion displacement time histories are simulated for each discrete magnitude level. Dynamic structural time history analyses are carried out on a finite element model of the structure. Monte Carlo simulation is utilized to treat response and damage variability. Results show that loss is dominated by nonstructural components, followed by contents and structural components. It is expected that the developed method and the example serve both research and practical purposes in future.

In the second part, implications of strain-rate dependency on seismic response of steel frame structures are investigated. This question constitutes an example to model sensitivity. Model sensitivity is an important question in risk assessment. An example structure is excited with 12 near-field severe strong motion records. This is carried out at 8 amplification levels, making a total of 96 time history analyses. Three varying material models are utilized. Inter-event, intra-event and inter-model response variabilities are investigated. The strong motion time histories used are representative for near-field seismic hazard (12 among 22 available records fitting the initial assumptions are included, the assumptions being soil type C, and, $\text{PGA} > 0.6\text{g}$ or $\text{PGV} > 1\text{m/s}$). The results have shown that steel frames undergo strain rates up to 10^0 per second (on the brink of range for explosion and crash loading). The strain rates are shown to be depending on strong motion intensity and velocity characteristics. It is shown that global response is not affected by strain-rate-effects significantly (in the extreme cases in the order of 5%). This is shown by comparison of response data from time-independent and time-dependent multi-surface material models. So, modelling of time dependency is not significant for accurate risk estimates. This is not the case for modeling of progressive yielding. Multi-surface models deliver significantly different response results from that of the simpler multilinear model, especially at higher magnitude levels. This shows the considerable implications of material modeling on risk estimates.

Abbreviations and Symbols

1. Latin

a	regional constant for hazard recurrence equation
a_s	source acceleration spectrum
a_w	windowing function coefficient
A	fault rupture area
ASI	acceleration spectrum intensity
A_{v-30}	upper 30 m.-profile site amplification
b	slope of (the straight section of) hazard recurrence curve
b_w	windowing function coefficient
c	indicator variable of collapse
c_s	fault shape factor
c_w	windowing function coefficient
C	restoration cost of a component
C_L	mean loss ratio (loss / total facility value) in collapse state
C_{SI}	mean cost of unit time serviceability interruption cost
C_T	total facility value (structure,nonstructure and contents included)
	mean new construction cost of the whole facility
	(Note: the model assumes both equal)
CCPDF	cumulative complementary probability distribution function
d_s	depth of local soil considered in local effects
dam.	damaging
D	component damage random variable
DC	damageability curve
DS	damage state
el.	elastic
E	(event of) fault rupture at an effective distance
E_{diss}	dissipated energy
f	frequency
f_c	corner frequency
$f_{J K}(j,k)$	conditional probability distribution function of random variable J conditioned on random variable K
f_{max}	cutoff frequency
F	free surface effect
F_{base}	maximum base shear
$F_Y(y)$	cumulative probability distribution function of Y evaluated at y
FAS	fourier acceleration spectrum
FOSM	first order second moment method
g	gravity acceleration
$g(r)$	geometrical spreading function
G	(event of) site ground failure (fault crack, liquefaction, landslide)

$G_E(x)$	hazard recurrence function
$G_X(x)$	complementary cumulative probability distribution function of function X
HT	hazard tree
HV	hazard governing variable
HVAC	heating-ventilation-air condition systems
I	(random variable) number of earthquake induced injuries in one year
IDA	incremental dynamic analysis
interp.	interpolation
ISD_{max}	maximum peak interstorey drift ratio
L	(random variable) earthquake induced loss of use in one year
L_f	characteristic fault dimension
L_T	mean serviceability interruption time in collapse state
LT	loss tree
$L_a(d_s, f)$	local soil and topographic effects filter function
$L_a^s(d_s, f)$	wave impedance multiplier
$L_a^n(d_s, f)$	soil-nonlinearity multiplier
$L_a^d(d_s, f)$	site diminution multiplier
$L_a^b(d_s, f)$	sedimentary-basin related phenomena multiplier
$L_a^t(f)$	topographic multiplier
m	moment magnitude
m_{geo}	characteristic earthquake magnitude
m_{int}	intersection magnitude of characteristic frequency and b line
m_l	lower magnitude bound for risk assessment
m_{max}	maximum magnitude
m_{max}^{rec}	regional maximum recorded magnitude
m_{min}	lower cutoff magnitude
m_o	seismic moment
m_u	upper magnitude bound for risk assessment
mech.	mechanism
M	(random variable) number of earthquake induced deaths in one year
$\hat{M}_{R D}$	mean damageability vector of a component
$\hat{D}_{R D}$	standard deviation damageability vector of a component
MM1	material model 1; bilinear kinetic material model
MM2	material model 2; multilinear kinetic material model
MM3	material model 3; time independent two-surface material model
MM4	material model 4; time dependent two-surface material model
n	number of simulations at each magnitude level
n	number of component types in the facility
$n(m)$	number of earthquakes exceeding a magnitude level m
N	(random variable) earthquake induced restoration cost in one year
NAF	North Anatolian Fault (System)

NDA	nonlinear time-history dynamic analyses
NSA	nonlinear static analysis = pushover
$p_Y(y)$	probability (likelihood) of discrete random variable Y being equal to y
pl.	plastic
P	(random variable) earthquake induced monetary loss in one year
$P_a(r, f)$	path filter function
PFA_{\max}	maximum peak floor acceleration
PFV_{\max}	maximum peak floor velocity
PGA	peak ground acceleration
Q	mean number of occupants
$Q(f)$	attenuation operator
r	source-site distance
r_{\max}	maximum distance criteria for effective faults
rec.	record (time history record)
R	maximum structural response random variable
R_I	mean ratio of number of injured to number of occupants in collapse state
R_M	mean ratio of number of deaths to number of occupants in collapse state
R_R	ratio of loss (restoration cost) to value of a component
RMB	risk management in built environment due to natural hazards
RN	reverse-normal (fault)
RV	response governing variable
$R_{\Theta\Phi}$	radiation pattern
s	characteristic slip per earthquake
$s_{SM}(m)$	strong motion duration function
s_S	source duration (rupture duration)
s_p	path delay
s_L	local site delay
S	site strong motion random variable
S_a^{\max}	maximum pseudo-acceleration
$S(f)$	shape of source spectral
SS	strike-slip
ST	sensitivity type
S_v^{\max}	maximum pseudo-velocity
t	characteristic earthquake recurrence period
t_{act}	recency criterion for active faults
T	period
T_1	first natural period
T_c	characteristic recurrence period
T_D	maximum tip deflection
v	slip rate at the fault
v_s	shear-wave velocity at bedrock
v_s	shear wave velocity at source vicinity
\bar{v}_s	representative shear wave velocity of path

$\bar{v}_s(f)$	average shear wave velocity, from the surface down to a depth of $\frac{1}{4}$ wavelength
visc.	viscous
V	partition factor for shear waves and their energy in two components
VSI	velocity spectrum intensity
V_T	mean restoration cost in collapse state
w	fault width
$w(f)$	windowing function for simulation
X_d	(random variable) capacity of a component to resist the damage state d
Z_s	seismic impedance at bedrock
$\bar{Z}(f)$	time-weighted average of seismic impedance from the surface down to a depth of $\frac{1}{4}$ wavelength

2. Greek

Δm	spacing between discrete magnitude levels of strong motion simulation
Δt	time steps of earthquake records
$\Delta \sigma$	stress drop
ϵ	strain
ϵ	windowing function coefficient
$\dot{\epsilon}$	strain rate (time variation of strain, $d\epsilon / dt$)
$\dot{\epsilon}_{max}$	maximum strain rate
η	windowing function coefficient
μ	shear modulus of the crust at fault
μ	mean value
ρ	density at source vicinity
$\bar{\rho}(f)$	average density, from the surface down to a depth of $\frac{1}{4}$ wavelength
ρ_s	density at bedrock
σ	standard deviation
σ	stress
$\dot{\sigma}$	stress rate (time variation of stress, $d\sigma / dt$)
σ_{ave}	average hysteresis stress
$\bar{\sigma}_{pl}$	mean average yield stress
σ_u	tensile strength
σ_y	mean yield limit, initial yield strength
σ_y^{dyn}	mean yield limit under dynamic excitation
σ_y^{stat}	mean yield limit under quasi-static excitation

Introduction

This thesis has two objectives; (1) stating a consistent and innovative seismic risk assessment model, (2) investigating strain rate sensitivity of seismic loss estimates in steel frame structures.

Chapter 1 provides the fundamant for the succeeding chapters: It presents the essence of risk management in built environment due to natural hazards. It points out the origins of the subject in management science and its distinguishing characteristics from conventional civil engineering task (design for safety).

Chapter 2 presents a consistent and original framework for seismic risk assessment. It is based on synthesis of several state-of-the-art approaches. In several key points, it includes original solutions. Provided method is advanced but also practically applicable.

Chapter 3 is an example application of the subject method. It proves the applicability and practicality of the method.

Chapter 4 investigates a previously neglected phenomenon in earthquake engineering. It addresses sensitivity of response of steel moment resisting frames to strain-rate dependency. This phenomenon interacts with the particular velocity content phenomena in near field. The analysis provide detailed insight by analysis of global response data.

Chapter 1. Founding principles of risk management in built environment

1.1. Motive behind application of risk management in built environment

Users and owners demand lifetime-integrity of civil engineering facilities against potential perils. This should satisfy (1.) safety of life, (2.) security of inherent investment and (3.) continuity of activities. Providing these is the moral responsibility of the engineer. However, there are economical, temporal and epistemological limits to this effort. Therefore, the engineer has to optimize investment and time to satisfy his/her moral responsibility. Furthermore, he/she has to strive towards uniform safety levels due to equality principles. These explain the motive behind application of risk management methodology for civil engineering structures.

1.2. Risk management - definition

Risk management involves

- (1.) identification and assessment of potential future perils (risks),
- (2.) development and implementation of optimal strategies for risk prevention or mitigation.

It is a specific application of management science. Management science is a form of applied mathematics and refers to use of mathematical models, statistics and algorithms for decision-making in complex real-world systems to improve or optimize performance.

Risk management has a wide range of applications (for example in finance, business, industrial safety, environmental protection, public health, traffic, urban systems and civil engineering). Scale of applications range from single machinery, household, business or facility to whole countries, regions, sectors.

Typical risk management decisions can be listed as in the following:

- justification of investment for mitigation of a particular risk
- distribution of resources for management of an ensemble of risks,
- risk acceptability criteria.

1.3. Risk management in built environment due to natural hazards - definition

Built environment (the totality of civil engineering structures) is exposed to a series of natural hazards. They can be grouped according to their origins as in the following:

- geophysical (earthquake, landslide, volcanism),
- atmospheric (hurricane, tornado, extreme temperature, excessive precipitation),
- hydrological (flooding),
- combined (tsunami, avalanche).

These extreme events lead to varying degrees of partial damage or to collapse. The potential consequences are varying degrees of (1) life loss; (2) injury and health distraction; (3) wealth loss; (4) loss of social and business structures; (5) loss of historical or ecological heritage; and, (6) interruption of social and business activities.

In that context, risk management in built environment due to natural hazards (RMB) can be defined as follows:

“the task of scientific and proactive treatment of natural hazards’ consequences in planning and maintenance of civil engineering structures, carried out by optimizing investment, time and safety”.

The global humanitarian and economical significance of RMB is evident due to the (1) increasing disaster loss, (2) population and wealth concentration in hazardous areas.

It is worth to mention that RMB is not synonymous with and is distinct from (1) design for safety, (2) reliability engineering, (3) emergency management. (1) and (2) can occasionally serve RMB purposes. (3) is a reactive task which marks its difference from the essentially proactive RMB.

Some occasions for use of RMB decisions are safety-level decision in mitigation and design, insurance premium justification and remaining lifetime estimates.

1.4. Lack of a uniform framework

There is a lack of a uniform framework for RMB in related publications. Similar situation is reported for risk management in general in a comprehensive treatment of risk analysis (Aven, 2003).

In order to respond this, the five step process of management science as depicted in Fig.1.1 can be adapted to risk management as in Fig.1.2.

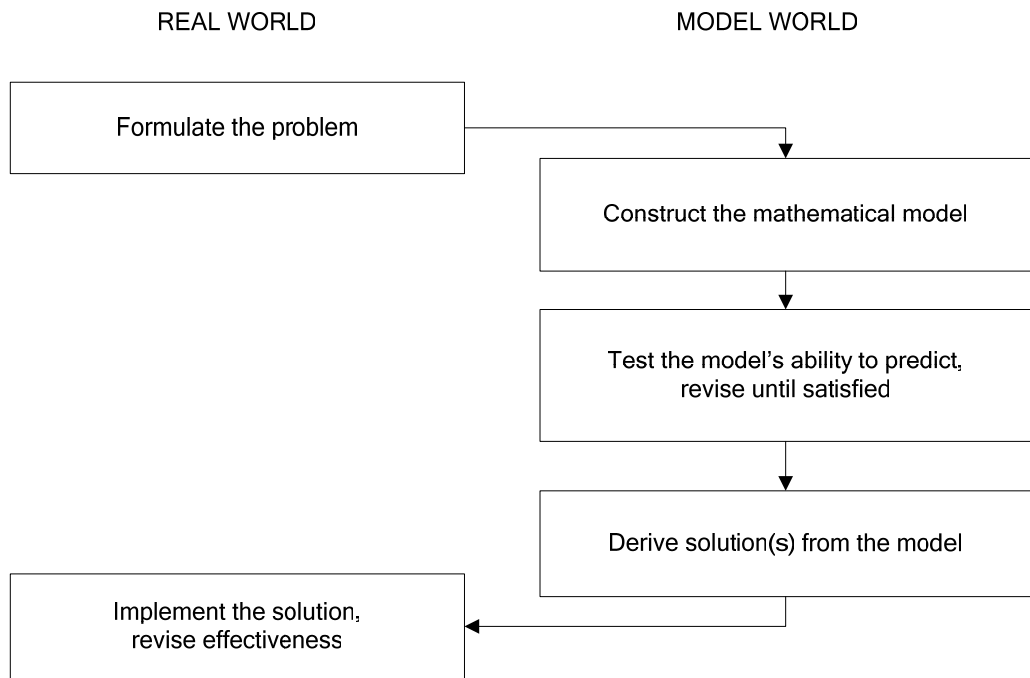


Fig.1.1: Five-step process of management science according to (Babcock, 1996)

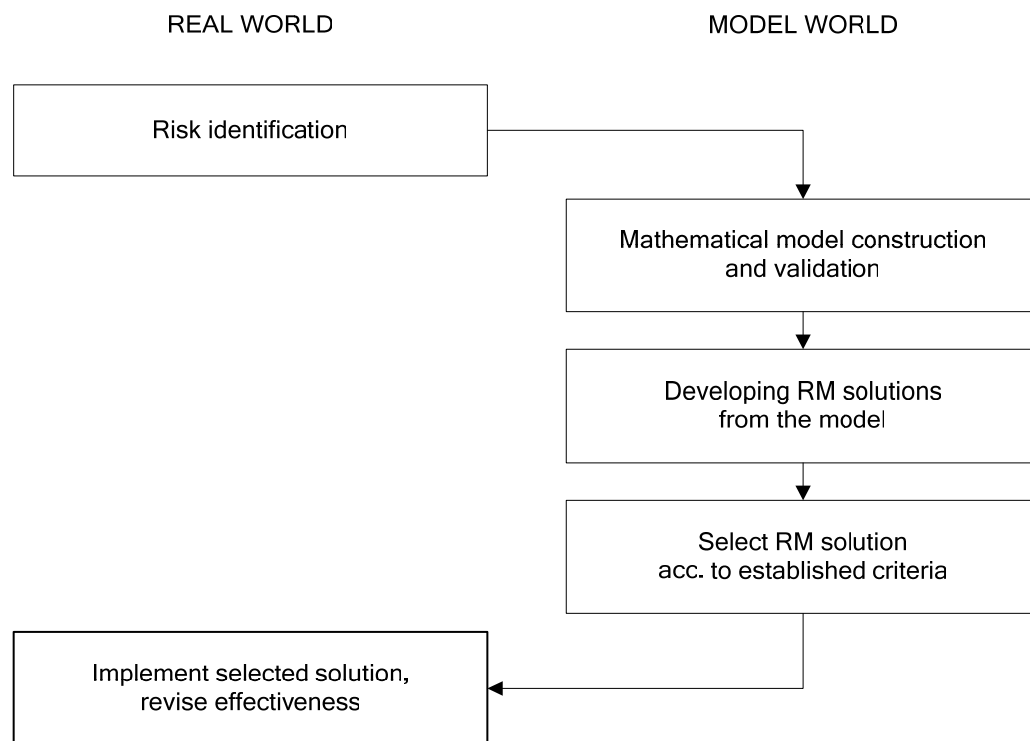


Fig.1.2: Framework for risk management in built environment against natural hazards, adapted from Fig.1.1

1.5. Principles of risk management in built environment due to natural hazards

As seen in Fig.1.2, risk management utilizes models in both risk assessment and solution development stages. Any model derives from synthesis of physical laws and empirical relations deriving from actuarial, experimental and simulation data. So, model uncertainty arises as an issue that should be treated by risk management alongside with the randomness of future phenomena.

From this point, following essential principles for a framework of risk management in built environment due to natural hazards could be drawn:

Principle I. Treatment of randomness and uncertainty

Since RM is based on model building, model uncertainty should be addressed alongside with randomness of hazard and consequences. The tool for these is probabilistic inference.

Principle II. Systems-view

RMB should adopt a systems-view of subject problem, (e.g. seismic risk management should consider source, path, site, structure, safety and economy). Segmented approaches can fail due to their inability to address (1) uncertainty propagation, (2) correlation between phenomena (e.g. relation between near-field fling pulse phenomena and rate dependency in seismic response of steel structures).

Principle III. Multi-disciplinary approach

As a consequence of Principle II, risk management operations should be multidisciplinary (e.g. seismic risk management in community level should involve at least seismology, geotechnical and structural engineering and public administration).

Principles II and III are in line with the distinguishing characteristics of management science as given by (Babcock, 1996). The latter author mentions additionally “emphasis on use of mathematical models, statistical and quantitative techniques” what we take for granted since Fig.1.1.

RMB can be carried out either for a single facility or for a group of facilities (defined geographically or over common characteristics like type, construction period, owner). This distinction can be referred by the terms micro-RMB and macro-RMB. This distinction is important for mathematical modeling, in terms of treatment of uncertainty (Bazurro and Luco, 2005) and risk acceptability criteria (Porter 2002).

A further distinction is between uni- and multi-hazard RMB. Multi-hazard RMB considers simultaneous or sequential occurrence of a group of natural hazards. Uni-hazard RMB considers only a single type of natural hazard.

RMB methodology can be applied to new projects (safety-investment optimization, site selection) or to existing facilities (decision among acceptance, mitigation, transfer, abandonment or relocation). This distinction may be addressed by the terms RMB in new project and RMB in existing facility.

This work focuses on seismic risk, one of the most significant natural hazards with record and increasing life and monetary losses.

Based on the principles drawn above, a generic procedure for seismic risk assessment in an existing facility is constructed and presented in the following.

Chapter 2. Innovative method for seismic risk assessment of a single facility

In this chapter, a framework method is presented for seismic risk assessment of an existing civil engineering facility. It is based on the principles stated in Chapter 1. It combines following approaches:

- (1) probabilistic seismic hazard analysis,
- (2) uniform hazard stochastic strong motion simulation,
- (3) incremental dynamic time-history analysis,
- (4) component based damage analysis.

The procedure answers the following questions for a single facility exposed to earthquake hazard:

- (1) what are the measures of risk?
- (2) how to proceed with risk assessment?
- (3) how to deal with randomness and model uncertainty?

The question of “how to decide among acceptance, mitigation, transfer, abandonment or relocation alternatives given a risk level?” is not investigated. This can be done with extending later with risk acceptability judgment and optimal strategy decision modules. Most of the introduced concepts in the method can be implemented in context of other natural hazards as well.

An example application of the method is given later in Chapter 3.

The method accounts only for facility-internal hazard consequences and neglects the exterior consequences. The exterior consequences can be of social, economic, ecologic, public-health nature. Those can be significant in several contexts like emergency-planning, city planning and subvention decisions. However, they are only weakly related to single facility risk assessment. Exceptions are (1) industrial and energy-production facilities (e.g. nuclear-, chemical plants, waste disposal facilities, dams, oil pipelines) with significant potential external effects to public-health and ecology, (2) historical / monumental structures with heritage value, (3) strategic public facilities.

Reminder: the subject is a single facility exposed to a earthquake hazard and the problem is “how to proceed with risk assessment?”.

2.2. Phenomenological comprehension by means of a hazard tree

The method starts with drawing an event tree as in Fig.2.3. This construction will be referred as hazard tree (HT) in this work. Hazard is given without specification of source, intensity or periodicity. HT simply answers the question “what are possible consequences of a seismic event of significant intensity and sufficient vicinity?”.

HT reflects the qualitative phenomenological knowledge on the problem in an extensive manner. So, it comprises also the events and paths which would be neglected in later stages of assessment (neglect can be due to low probability, low intensity, insignificance or non-conceivability). This approach helps to locate the assumptions taken later. HT does not contain probabilities, intensities or hazard sources, since gathering of such quantitative information is left to succeeding stages.

HT is an original proposal of this work and is based on conventional logical trees. For treatment of the latter, refer to (Faber, 2005).

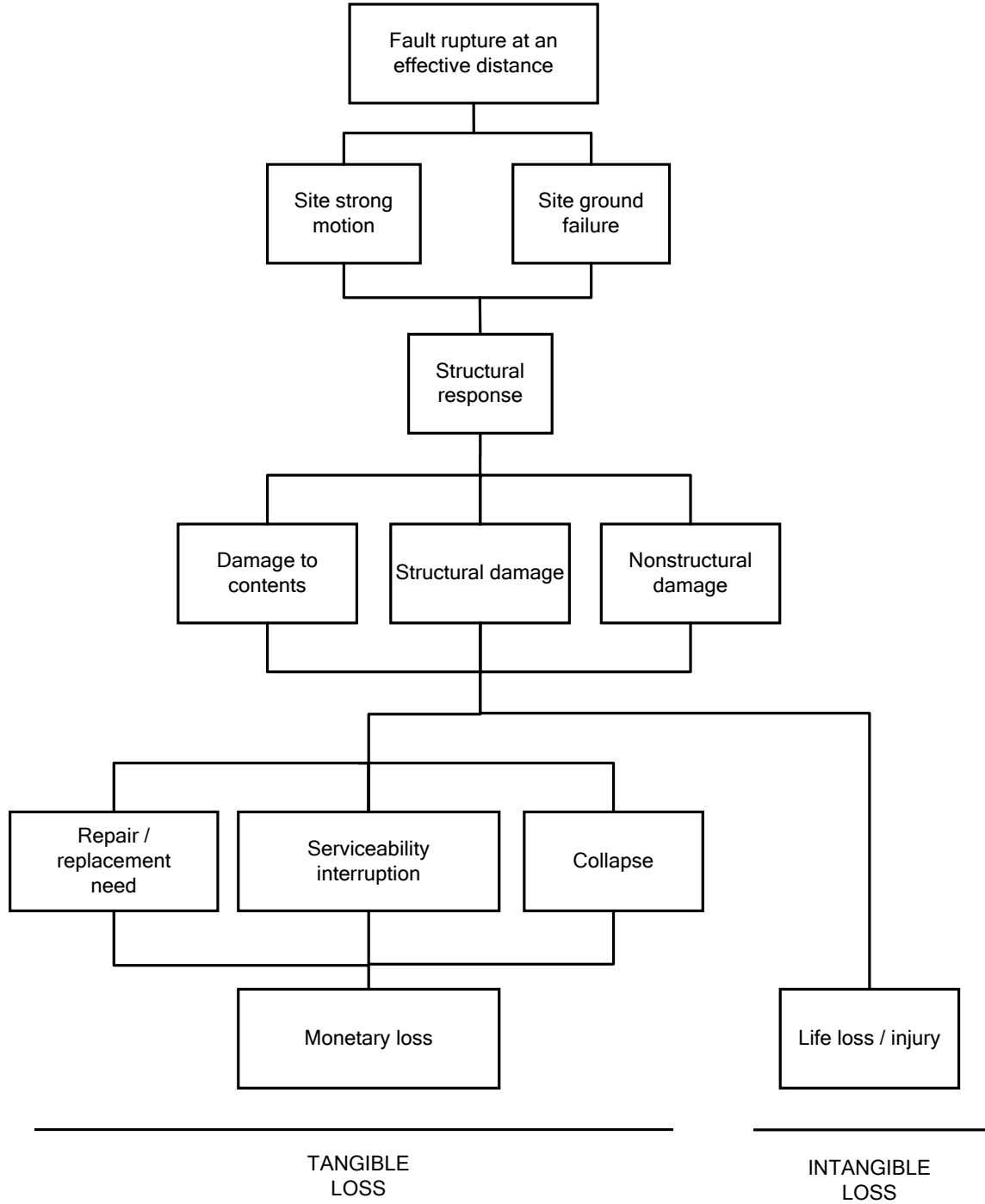


Fig.2.3: Hazard tree (HT) as tool for qualitative seismic risk identification. The initiator event is a generic one. Probabilities and intensities are not specified. HT provides preliminary inspection of cause-consequence relations.

2.3. Risk measures decision

Next step is the decision on (1) what constitutes the risk, and, (2) how to quantify it. The answers are respectively potential loss and loss estimates.

Potential loss comprises death, injury, monetary-loss and serviceability-interruption components. Using annual estimates in line with convention, random variables are defined as in following:

LOSS RANDOM VARIABLES	
M	number of earthquake induced deaths in one year
I	number of earthquake induced injuries in one year
N	earthquake induced restoration cost in one year
L	earthquake induced serviceability interruption in one year
P	earthquake induced monetary loss in one year

Table 2.1: Loss variables used in framework method

This reduces risk assessment problem to obtaining complementary cumulative probability distribution functions $G_M(m), G_I(i), G_N(n), G_L(l), G_p(p)$, namely the risk measures. Specifically, expected values (so, x for $G_X(x)=0.5$) are commonly taken as risk measure.

The term ‘restoration’ as used above covers both repair and replacement operations.

Selection of a time unit of one year as decisional basis is conventional, yet arbitrary. Its convenience stems from the typical projected life times of civil engineering facilities in the order of 10^1 years.

The above mentioned loss variables are used by default in most problems. However, some other loss variables can also be defined

- for limit state exceedance (e.g. collapse prevention, serviceability limit state, ultimate limit state, operability)
- occurrence of specified events (e.g. crack width > 5mm, breakdown of water supply).

For such cases, an indicator variable X with two possible values (1: occurrence, 0: non-occurrence) is defined and risk measure is then p_X ($x=1$) (annual probability of

exceedance or occurrence).

These risk measures can be utilized for compliance verification to standards or for comparison with other facilities. They can be associated with the facility as a whole, its structural/nonstructural components or contents. A commonly used one is exceedance of collapse prevention limit state, with $p_C(c=1)$ as risk measure where C = indicator variable of exceedance of collapse prevention limit state in one year.

Risk measures constitute criteria for risk acceptability and intervention decision.

It is worth to note that injury estimates could further be classified acc. to (1) degree of severity (e.g. minor, moderate, severe, critical, fatal), (2) treatment category (e.g. hospitalized, emergency dept. treat, self-treated), or (3) type (e.g. femur fracture). For further discussion on this point, refer to the work by (Porter et al., 2005) which demonstrates the vast numbers of injury cases even in moderate no-fatality events.

2.4. Detection of loss paths by loss trees

HT construction presented above facilitates qualitative comprehension by use of logical trees understandable by both experts and layman. But it does not provide a basis for risk measures quantification. For that end, another form of logical trees are necessary. Those are loss trees (LT) drawn separately for each risk measure.

A LT contains all scenarios leading to any change in the corresponding risk measure. It is drawn mainly with conventional fault tree notation, with the following distinctive features:

- (1) a LT provide an illustrative basis for mathematical modeling rather than a failure analysis,
- (2) intermediate events in a LT can be continuous nonlinear functions as well as discrete events.

Conventional fault trees are treated e.g. by (Faber, 2005).

Loss trees derived from HT in Fig.2.3 are given in Fig.s 2.4 to 2.9. The abbreviations and symbols used are explained in Table 2.2. There is no one-to-one correspondence between the given HT and LT's, due to these assumptions:

1. Contributions of nonstructural components' and contents' damage on death and injury risks are assumed negligible in line with statistics.

2. Collapse probability is related directly to structural response in line with state-of-the-art approach stated by (Krawinkler and Miranda, 2004).

The cause-consequence chain leading to loss is constructed as response→ damage→ loss. This is a useful construct for seismic risk assessment. Response refers to structure's mechanical behavior under excitation quantified by observable physical parameters (drift, strain, force, settlement etc.). Damage refers to permanent physical effects on structure, nonstructural components and contents. It is quantified by indicator variables of damage state exceedance (in other words, of damage state membership). Loss is the damage-associated monetary or social consequence, as formulated by (McGuire, 2004).

ABBREVIATIONS AND SYMBOLS IN LOSS TREES

E fault rupture at an effective distance

S site strong motion

G site ground failure (fault crack, liquefaction, landslide)

R structural response

SD structural damage

ND nonstructural damage

CD contents damage



OR gate



Excluding
OR gate

Table 2.2: Notation used for construction of loss trees

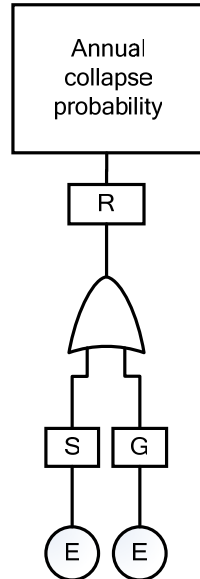


Fig.2.4: Collapse limit state tree

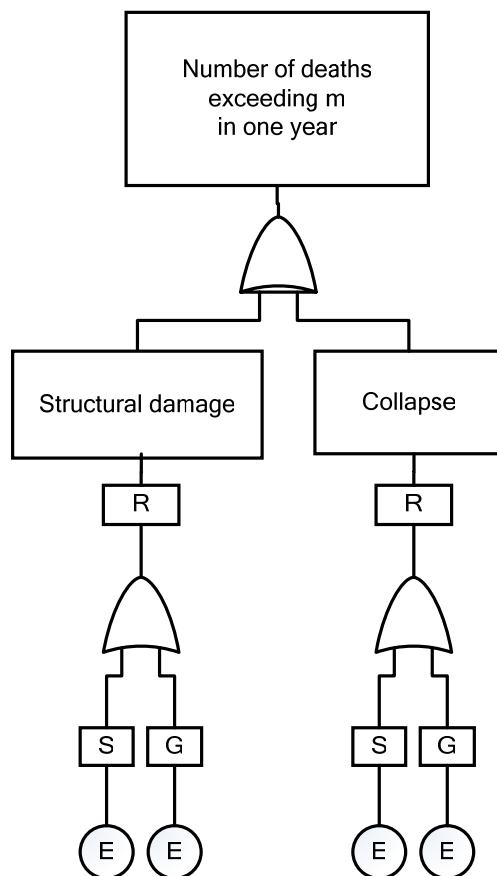


Fig.2.5: Death loss tree

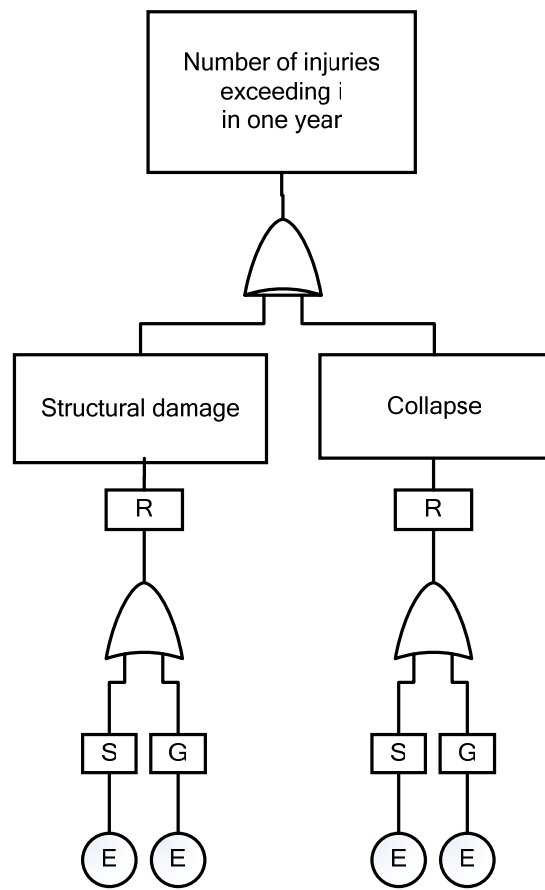


Fig.2.6. Injury loss tree

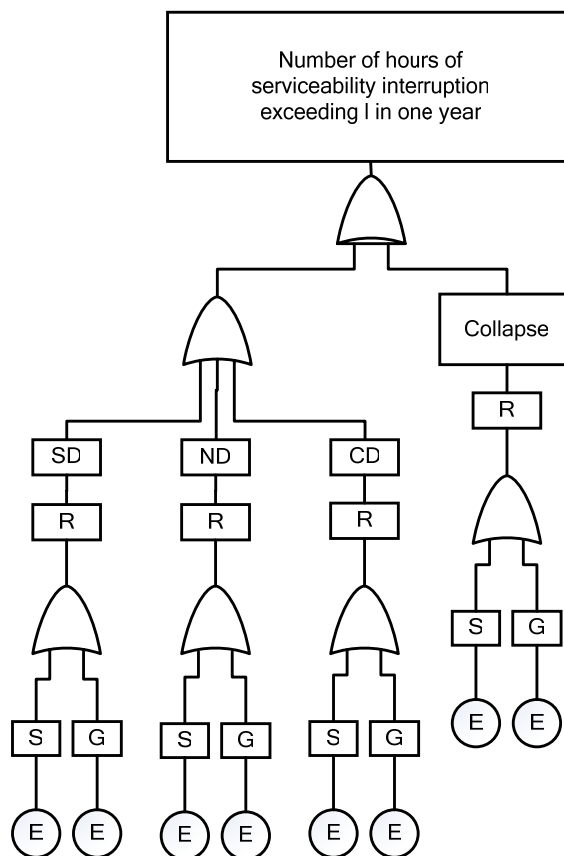


Fig.2.7. Serviceability interruption loss tree

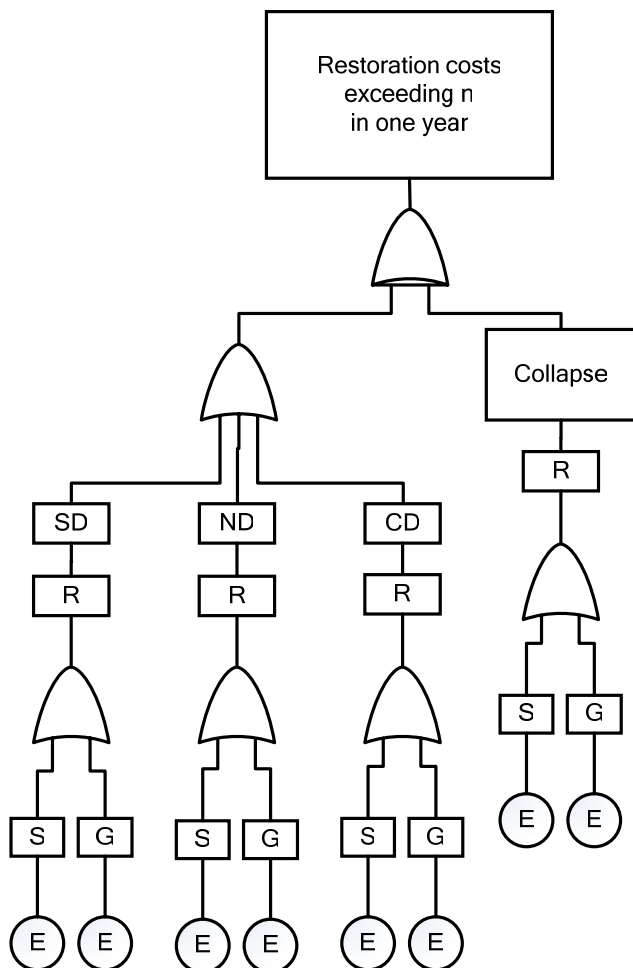


Fig.2.8. Restoration cost loss tree

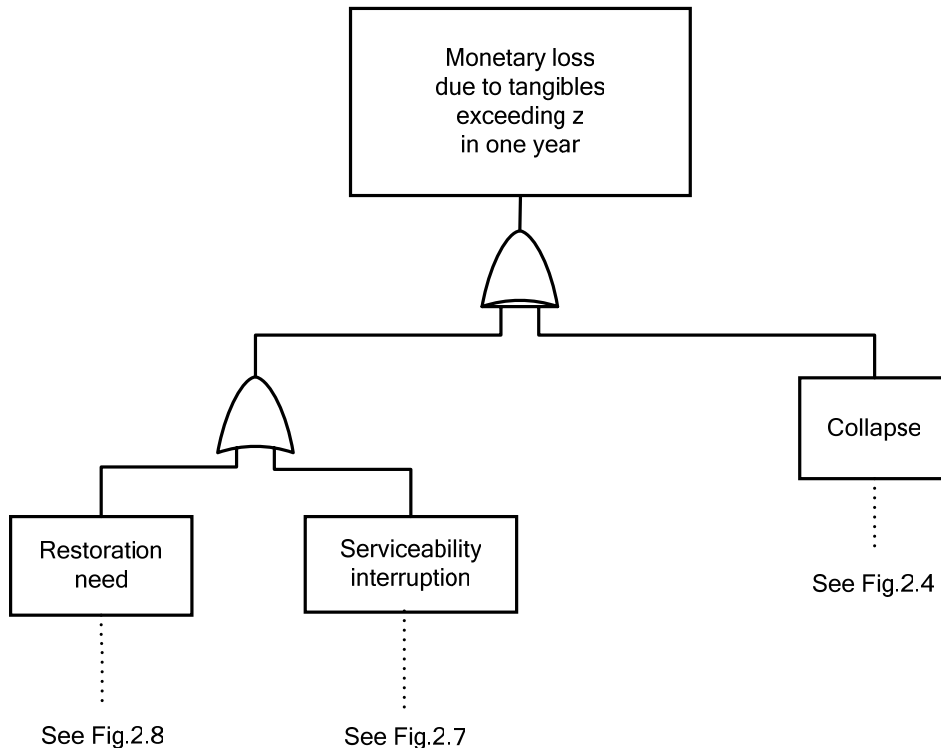


Fig.2.9: Monetary loss tree -due to tangibles-

2.5. Assigning governing variables to events

Most elements of loss trees are yet abstruse in mathematical sense. Since mathematical modeling requires quantification, random variables representative of each event should be assigned to those (e.g. flood height for flooding, peak ground acceleration for strong motion). These will be referred as governing variable of each phenomenological event.

If a scalar can not represent an event sufficiently, use of a $k \times 1$ governing variable vector or a $n \times m$ governing variable matrix is appropriate - at the expense of efficiency.

All above will be referred as governing variables in the remaining discussion.

Assigning a governing variable to an event is a challenging task, since a governing variable should fulfill several criteria: A governing variable should be

- (1) empirically observable,
- (2) good measure of event over varying intensities,
- (3) suitable as input in sequencing events.

(Vamsatsikos and Cornell, 2005) refer to these criteria as efficiency and sufficiency. In practical applications, reference to professional state of the art is advised. The decision on governing variables is a decisive step due to its effects on both model accuracy and model economy.

All governing variables should be defined as annual maxima. This is in line with time unit selection in Step2.

That implies that risk due to the annual maximum earthquake will be quantified (maximum in sense of consequences). So, the contribution of less severe events to annual loss is neglected. This neglect is discussed and validated by McGuire (2004). Furthermore, structural degradation due to repeated earthquakes in one year is not considered (as a reminder; (Wen and Loh, 2006) propose approaches to overcome this).

Table 2.3 gives the selected governing variables for the method. This is a state-of-the-art and consistent selection. Concerning response, common governing variables are maximum peak interstorey drift ratio (ISD_{max}), maximum peak floor velocity (PFV_{max}) and maximum peak floor acceleration (PFA_{max}) (so, $l=3$).

The decision for governing variable of max. strong motion at site (2. line in Table 2.3.) can be explained as follows: m= number of time steps of the longest simulated time history, n= number of simulated time histories. For simulations with less than m time steps, remaining elements are then zero. Then, S is composed of n vectors, each containing time series information of the corresponding simulated time history.

	EVENT (all in one year)	GOVERNING VARIABLE	ABB.
HAZARD	max. earthquake (separately for each seismogenic source)	moment magnitude	E
	max. strong motion at site	[nxm] suite of simulated displacement time histories	S
	max. ground failure at site	ground failure index	G
RESPONSE	max. structural response	[kxl], k:hazard levels, l: number of response governing variables	R
DAMAGE	max. component damage (defined separately for each component)	damage class	D
	max. death	number of deaths	M
	max. injuries	number of injured	I
	Collapse	indicator variable (1=occ., 0=non.)	C
LOSS	max. serviceability interruption	hours	L
	max. restoration cost (defined for all, a group or single element)	monetary unit	N
	max. monetary loss due to tangibles	monetary unit	P

Table 2.3: Governing variables for phenomenological loss tree events.

2.6. Stating the mathematical model

This step corresponds to translation of loss trees into mathematical form. This is done under consideration of governing variable selection.

Loss equations which form the risk assessment mathematical model are given in Table 2.4. They are derived from loss trees in Fig.2.4 to Fig.2.9 under consideration of governing variables of Table 2.3.

Consequences of earthquake-induced ground failure (denoted with G in loss trees) are not included in the model. This is done in order to maintain the limits of the discussion. Indeed, they have relatively small effect on earthquake loss in building structures¹.

Cornerstone of the model is the definitions of collapse prevention limit state and of partial damage range.

Partial damage range refers to the whole range between the original no-damage state and the collapse prevention limit state. In that range, loss is related to damage; damage to response; response to hazard.

Collapse prevention limit state capacity is defined probabilistically. On the consequences side, collapse loss is expressed deterministically. This can be justified with two arguments related to the nature of earthquake risk building structures:

- (1) Seismic collapse in building structures (especially high-rise) is a disastrous total breakdown case. The variation of loss at collapse can thus be neglected.
- (2) In case of modern structures, the probability of collapse is negligibly low. So, the neglect of variation of collapse loss has a negligible effect.

In Eq.s 4 and 5, first and second lines are respectively partial and collapse damage state contributions.

In stating the equations, several state-of-the-art approaches are consulted (e.g. PEER Performance Based Framework, assembly based vulnerability). Definition of collapse as the unique limit state is proposed by FEMA350 (2000).

¹ (*Bird and Bommer, 2004*) proves the relatively small and rare contribution of ground failure to earthquake loss in building structures by loss statistics from 50 globally-distributed severe earthquakes from 1989 to 2003 (this assertion is not valid for transportation and utility lifelines). For detailed treatment of earthquake loss due to ground failure, refer to the latter source.

MATHEMATICAL MODEL OF SEISMIC RISK ASSESSMENT

Collapse equation

$$p_C(c=1) = \int_r \int_s \int_x f_{C|R}(c=1, r) f_{R|S}(r, s) f_{S|E}(s, x) dG_E(x) \quad (1)$$

Loss Equation I. Deaths

$$G_M(m) = p_C(c=1) * Q * R_M \quad (2)$$

Loss Equation II. Injuries

$$G_I(i) = p_C(c=1) * Q * R_I \quad (3)$$

Loss Equation III. Serviceability interruption

$$G_L(l) = \sum_{a=1}^k \sum_{d=1}^n \int_r \int_s \int_x f_{L|D}^a(l, d) f_{D|R}^a(d, r) p_C(c=0 \mid R=r) f_{R|S}(r, s) f_{S|E}(s, x) dG_E(x) + p_C(C=1) * L_T \quad (4)$$

Loss Equation IV. Restoration cost

$$G_V(v) = \sum_{a=1}^k \sum_{d=1}^n \int_r \int_s \int_x f_{V|D}^a(v, d) f_{D|R}^a(d, r) p_C(C=0 \mid R=r) f_{R|S}(r, s) f_{S|E}(s, x) dG_E(x) + p_C(C=1) * V_T \quad (5)$$

Loss Equation V. Monetary loss -due to tangibles-

$$G_P(p) = G_P(V + (L * C_L)) \quad (6)$$

Abbreviations

a : component type

d: damage state

Q: number of occupants

R_M: mean death ratio given collapse state

R_I: mean injury ratio given collapse state

L_T: mean serviceability interruption in collapse state

V_T: mean restoration cost in collapse state

C_T: total facility value (str.+nonstructure+contents) = tangible loss in collapse state

C_L: mean loss ratio (loss / total facility value) in collapse limit state

For rest, see Table 2.1 to 2.3

Further explanations

p_C(c=1) : probability of exceedance of collapse prevention limit state

p_C(c=0 | R=r) : probability of non-exceedance of collapse prevention limit state

f_{R|S}(r,s) : response parameter R=r for a certain hazard intensity S=s

(other conditional functions similar like the latter)

Table 2.4

As the mathematical model is stated as above, the problem is reduced to obtaining the following:

- hazard recurrence function $G_E(x)$,
- remaining intermediate functions functions $f_{J|K}(j, k)$,
- deterministic facility-specific parameters ($Q, R_M, R_I, L_T, V_T, C_L$).

These will be obtained in next sections of the work.

There are two assumptions inherent in the model as stated in Table 2.4:

Causal Markovian dependence² is assumed for the event chain: hazard → response → damage → loss. This means that any $n+1^{\text{th}}$ element on the chain can be estimated solely from n^{th} element without considering preceding elements. So, for example, damage can be estimated from response without considering hazard. For most cases in civil engineering, Markov chain modeling of loss trees is suitable. The rare cases of limited applicability is due to strong interaction between loading and deformation (like vortex shedding in aerodynamics, frequency shift due to degradation in seismic response, soil-structure interaction). Such cases can be detected through correlation and sensitivity analysis, and then, models can be revised accordingly.

Damage functions ($f_{D|R}(d,r)$) of varying component types are assumed to be mutually independent between each other. Consequently, contributions from each component to each loss variable are also assumed to be independent.

2.7. Detection of potential hazard sources

Only active faults capable of producing significant magnitudes at a certain maximum distance can produce significant strong motion at the site. This step aims to find those faults to be considered for risk assessment at site. The output is termed as site-specific effective seismogenic sources.

Main sources are active fault maps, which are available for most seismic regions of the world. They are produced by synthesis of topographical, petrological (rock science) and instrumental data. They include exclusively faults which has undergone recent

² A Markov process is a continuous process of possibly dependent random variables (x_1, x_2, x_3, \dots) with the property that any prediction of the value of x_n , knowing $(x_1, x_2, x_3, \dots, x_{n-1})$ may be based on x_{n-1} alone. Refer to (Benjamin and Cornell, 1970) for detailed explanation.

significant seismic movement. The recency criterion (t_{act}) is defined in terms of geological time scale and is controversial among varying institutions; ranging from last $t_{act} = 10^4$ (Holocene) to $t_{act} = 0.5 \times 10^6$ years (Late Quaternary) (for details, refer to (Krinitzsky et al., 1993)).

Lower magnitude bound (m_l) refers to a magnitude level below which no damage and loss is expected. It is subjectively decided and typical values range from $m=6.0$ (Krinitzsky et al., 1993) to $m=4.0$ or $m=5.0$ (Kramer, 1996). (Stewart et al. 2002) mentions that smaller values are appropriate for brittle/stiff structures and soft soils.

Maximum distance criteria (r_{max}) is commonly taken as 100 km, but also may range from 20 to 400-500 km. In distance criteria decision, following criteria should be considered:

- fault size and potential
- seismological regime
- path and local soil characteristics
- facility vulnerability and criticality

Table 5.4 provides specific information for western United States. This can be taken as basis for regions with similar seismological characteristics.

MAXIMUM SOURCE-SITE DISTANCE r_{max} (in km) OF EFFECTIVE SEISMOGENIC SOURCES			
	VULNERABILITY TYPE		
Moment magnitude	Stable foundation	Liquefaction or permanent ground displacement exposure	Soft soil site amplification
5.3	-	1	-
6.0	20	10	-
7.0	32	50	230
8.0	50 (intraplate: 150)	150	400

Table 2.5: Distance criteria (maximum source-site distance for consideration in risk assessment) given engineered construction in western USA (Krinitzsky et al., 1993)

Fig.2.10. Identification of effective sources (criteria: r=100km, m=5.0)

2.8. Modeling hazard recurrence

Seismic risk assessment uses time-variant and time-invariant models respectively for short-term (instantaneous) and long-term prediction. The latter will be considered in this work.

Within this context, recurrence relation for each source will be obtained. This is denoted with $G_E(x)$, and is equivalent to the complementary cumulative probability distribution function, in other words, probability of exceedance of moment magnitude level x in 1 year.

There are two sources for relevant data: geology and seismicity.

Geological approach has two components: (1) estimation of characteristic earthquake recurrence period, (2) estimation characteristic earthquake size.

Characteristic earthquake recurrence period t is obtained according to the following equation after (Yeats and Gath, 2004)

$$t = s / v \quad (7)$$

where s is slip per earthquake and v is slip rate at the fault. Both are obtained through geological survey. The equation derives from elastic rebound theory.

s is estimated by measurement of surface ruptures or of offsets of features across a fault (e.g. streams, archeological ruins), due to recent and historical earthquakes. s is variable along the rupture, so an average value is used.

v is estimated from offset measurements on stratigraphic features, whose age are estimated using paleoseismic techniques like radiocarbon dating and stimulated

luminescence as mentioned by (Yeats and Gath, 2004).

Characteristic earthquake seismic moment and moment magnitude can be obtained by the following relations.

$$m_0 = \mu A s \quad (8)$$

$$m = \frac{2}{3} \log m_0 - 10.7 \quad (9)$$

Eq. 8 yields seismic moment and Eq. 9 moment magnitude. The latter one is used as magnitude measure³.

μ refer to shear modulus of the crust at fault ($\approx 3.0 - 3.5 \times 10^{11}$ dyn/cm² for crustal rocks acc. to latter source; typically $3.0 - 5.0 \times 10^{11}$ dyn/cm² for shallow earthquakes acc. to (Stein and Wysession, 2003)) (m_0 in dyn•cm).

A is fault rupture area and is estimated by aftershock area, analysis of surface waves and geodetic data from recent earthquakes at the particular fault (Scholz, 2002; Stein and Wysession, 2003, dePolo and Slemmons, 1990).

Geological data generally relieves characteristic earthquake, which a particular fault tend to produce repeatedly (but not necessarily periodically). This estimate is done within a certain magnitude range near maximum. (Kramer, 1996) gives this range as 0.5 magnitude unit.

On the other hand, seismicity data is commonly limited to lower magnitudes. It is gathered through regression on instrumental magnitude records (maximum 100 years span) and historical intensity records (maximum several 1000 years). This investigation is carried out for tectonic regions and not for single faults. Regional analysis is necessary due to scarcity of statistically significant data for single faults (particularly for intra-plate, developing or newly occupied regions). Basis of the method is Gutenberg-Richter Recurrence Law. This law relates number of earthquakes exceeding a magnitude level m ($n(m)$) to two regressive regional constants a and b :

$$n(m) = 10^a 10^{-bm} \quad (10)$$

³ Moment magnitude should be used in hazard analysis as magnitude measure, since it is (1) the unique non-saturating and non-filtering magnitude measure, (2) related to slip, rupture dimensions (Eq.s 2,3), energy and stress drop (for latter two, see (Scholz, 2002)).

where b is the slope of (the straight section of) the regional Gutenberg-Richter curve. This law was originally inferred from observations on Californian faults, but it applies globally (with $b \approx 1.0$) and on regional basis. It is an example to self-similarity (syn. scaling-invariance) in nature (Stein and Wyssession, 2003). For b regression algorithms, refer to (McGuire, 2004).

When a lower cutoff magnitude m_{\min} and a maximum magnitude m_{\max} (upper bound for the subject seismogenic zone) is incorporated into this law, CCPDF for earthquake magnitude can be written as in the following (after (McGuire, 2004)):

$$G_E(m) = \begin{cases} 1-k + k e^{-\beta(m-m_{\min})} & m_{\min} \leq m \leq m_{\max} \\ 0 & m > m_{\max} \end{cases} \quad (11)$$

where β is a regional constant related to b , and, k is given below and:

$$k = [1 - e^{-\beta(m_{\max} - m_{\min})}]^{-1} \quad (12)$$

The challenge is then to estimate β and m_{\max} , and, to choose m_{\min} .

β is simply given by

$$\beta = b \ln 10 \quad (13)$$

(b as explained previously).

m_{\min} is chosen subjectively and typical values in literature are 4.0 (Ordaz, 2004), 4.0 to 5.0 (Kramer, 1996). (Bayrak et. al, 2005) propose to define it as border between the straight and the convex parts of the regressed b-line (curvature is due to lack of small earthquake data). m_{\min} values used by the latter in a recent application for varying seismological regions of Turkey range from 3.2 to 4.5 depending on data availability. m_{\min} is not necessarily equal to m_l (which is explained previously).

m_{\max} will be referred as maximum extrapolated magnitude in the rest discussion. It is estimated by varying methods:

- (1) using geologic evidence (fault length),
- (2) geophysical data (crustal stress inference),
- (3) analogy to similar tectonic regimes or by judgment (e.g. increasing maximum historical earthquake by an amount) (1 to 3 after McGuire (2004)),

(4) by extrapolating from lower magnitudes (by e.g Gumbel III fit) (Bayrak et. al, 2005), or,

(5) by synthesis of methods.

(Krinitzsky et al. 1993) points out the subjective nature of this estimate. It is worth to remind that m_{\max} usually exceed maximum recorded magnitude (m_{\max}^{rec}) in subject region.

The synthesis of geological and seismicity data often lead to magnitude-recurrence relations similar to the one in Fig.2.11.

Typically, an inconsistency between geological and seismicity data is observed. This corresponds to the condition, when $f_c > G_E(m_{\text{geo}})$, where f_c is the characteristic frequency (equal to $1/T_c$, T_c is the characteristic recurrence period) and $G_E(m_{\text{geo}})$ is calculated according to Eq.5 by relaxing the range of definition. This inconsistency can be overcome by varying models discussed by e.g. (Ordaz, 2004), (McGuire, 2004), (Speidel and Mattson, 1997). The latter author mentions that model choice should depend on fault size, slip rate and length of historical seismicity observation.

An option is combining Eq.5 with uniform distribution for geologic-data-range, which can be demonstrated as in the following:

$$G_E(m) = \begin{cases} 1-k + k e^{-\beta(m-m_{\min})} & m_{\min} \leq m < m_{\text{int}} \\ f_{\text{geo}} & m_{\text{int}} \leq m < m_{\text{geo}} \\ 0 & m_{\text{geo}} \leq m \end{cases} \quad (14)$$

where, m_{geo} is the characteristic earthquake, m_{int} is the intersection magnitude of characteristic frequency and b line. m_{int} can be easily extracted by equating f_c to $G_E(m_{\text{int}})$. Upper limit can be augmented subjectively to $m_{\text{geo}} + 0.5$.

To remind, the output of this step is hazard function $G_E(x)$ for each source. The presented procedure is known as probabilistic seismic hazard analysis.

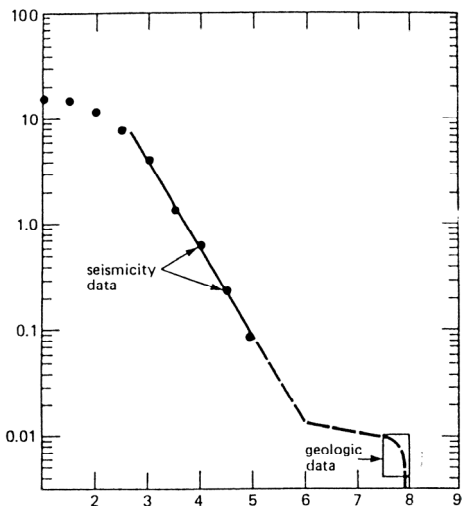


Fig.2.11: Magnitude vs. cumulative frequency of recurrence for a fault after (Schwartz and Coppersmith, 1984). The deviation from b-line is obvious for low magnitudes (due to undetected small earthquakes, insignificant for built environment) and for geologic data controlled high magnitudes (upper limit due to finite fault dimensions).

2.9. Modeling intermediate events

In the previous sections, hazard sources are detected and hazard recurrence functions are developed. In this section, intermediate functions will be developed from empirical data or physical relations. There are varying approaches to modeling. Model selection should consider analysis capacities, overall compatibility and consistency of model. For the variety of existing approaches in seismic risk assessment, refer to (McGuire, 2004) and (Meskouris et al. 1996). Only an advanced example depicted in Fig.2.12 will be treated in this work. Single steps are given in sections.

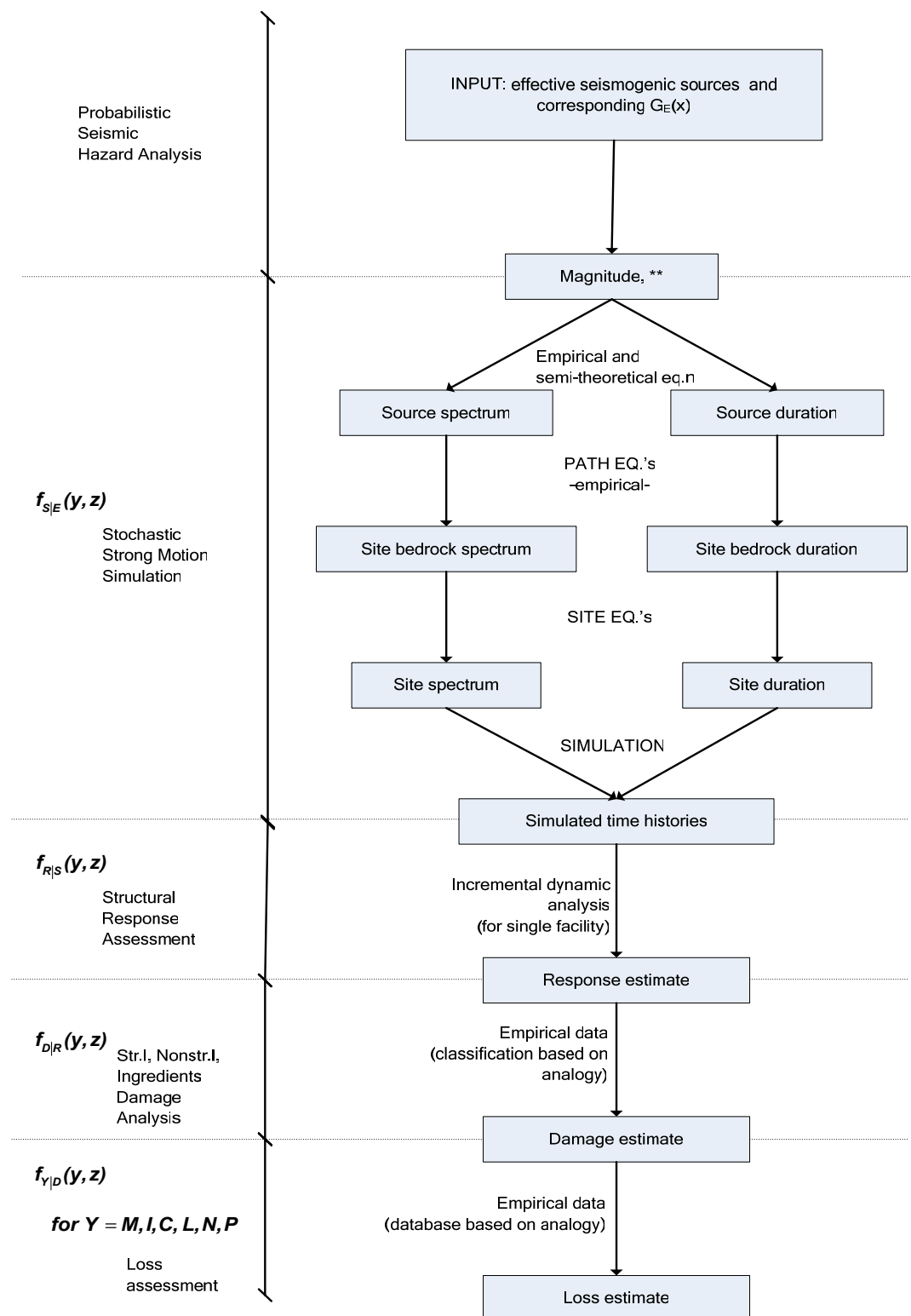


Fig.2.12: Risk assessment approach utilized in this work

2.9.1. Strong Motion Function

Aim in this section is to simulate a sufficient number of strong motion time histories to represent hazard at site.

The motive behind the simulation is the lack of sufficient strong motion records for most regions of the world. An example is Turkey as stated by (Akinci et al., 2001). Exceptions are few seismic regions in economically developed countries (like western North America, Japan and New Zealand). For alternative methods of utilizing processed instrumental records and deaggregation, see (Wen, 2004).

Previously, it was stated that the magnitudes produced by a fault vary between a lower and an upper value ($m_{\min} < m < m_{\max}$ or $m_{\min} < m < m_{\text{geo}}$). However, simulations will be carried out for the range of $m_l < m < m_u$, with m_l as described above and m_u referring to upper magnitude bound for risk assessment. m_u can be equal to or slightly smaller than m_{\max} . Accordingly, simulations will be carried out for discrete magnitude levels at this range. Decisions on the number of discrete levels and on the number of simulations for each level will be discussed later.

Let start with analysis of site strong ground motion.

Strong motion time series can be decomposed into two functions: acceleration spectrum and duration, each of which are dependent on characteristics of (1) source and rupture, (2) path, (3) local soil and topographic conditions⁴.

Acceleration spectrum of strong motion at an arbitrary site can be written as (modified from (Boore, 2003)):

$$a_{SM}(m, r, f) = a_s(m, f) P_a(r, f) L_a(d, f) \quad (15)$$

where m is magnitude level under consideration, r is the source-site distance, f is frequency, a_s is the source acceleration spectrum, P_a and L_a are respectively path and local filter functions, d is depth of local soil considered. Spectrum should be bounded for a frequency range significant for engineering purposes.

Strong motion duration function can be written as

$$S_{SM} = S_S + S_P + S_L \quad (16)$$

⁴ Strictly speaking, local site and topographic conditions are a part of path effects, but due to the high sensitivity of site strong motion on their variation, they are treated separately.

where s_s is the source duration function (syn. rupture duration), s_p and s_L are respectively path and local site delay functions. s_L can be neglected since $s_L \ll s_p$,

$$s_{SM} = s_s + s_p \quad (17)$$

The model deals only with absolute duration (not engineering duration) measures, so s_p is only source-site distance (r) dependent. Thus, problem reduces to obtaining $a_s(m, f)$, $P_a(r, f)$, $L_a(d, f)$, s_s , s_p and simulating sufficient number of time histories using these.

2.9.1.1. Source spectrum

Source spectrum can be expressed after (Boore, 2003) as following;

$$a_s(m, f) = C m S_s(m, f) \quad (18)$$

where C is a constant, m is magnitude level under consideration, $S_s(m, f)$ is displacement spectrum at source, named source spectral shape.

C is given by;

$$C = R_{\Theta\Phi} F V / (4\pi \rho v_s^3) \quad (19)$$

where $R_{\Theta\Phi}$ is the radiation pattern, F is the free surface effect, V is the partition factor of shear wave energy in two components, ρ and v_s are the density and shear wave velocity in the source vicinity (in SI units).

$R_{\Theta\Phi}$ is obtained by averaging over a range of azimuths and take-off angles (Boore, 2003), can be assumed approximately equal to 0.55 (Kramer 1996). F is usually assumed 2, which is actually exact only for SH waves (Boore, 2003). V is equal to $\sqrt{2}/2$.

Varying models differ in $S_s(m, f)$ expression, exhaustive list is given by Boore (2003).

A recent model by (Atkinson and Silva, 2000) follows:

$$S_s(m, f) = \frac{1-\varepsilon}{(1+(f/f_c)^2)} + \frac{\varepsilon}{(1+(f/f_{max})^2)^2} \quad (20)$$

Where f_c is corner frequency, f_{max} cutoff frequency and ε is a coefficient given by $\log \varepsilon = 0.605 - 0.255m$.

For southern Californian conditions, following values are given by (Atkinson and Silva,

2000): $\log f_c = 2.181 - 0.496m$ and $\log f_{max} = 2.41 - 0.408m$ (both in Hz)

f_{max} is otherwise obtained empirically for each geographical region (e.g. typically 15 and 40 Hz respectively for western and eastern North America (Kramer, 1996)).

f_c can be derived theoretically (Boore, 2003):

$$f_c = 4.9 \times 10^6 v_s \left(\frac{\Delta\sigma}{m_o} \right)^{1/3} \quad (21)$$

where v_s (km/sec) as described above, m_o (dyn·cm) as given in Eq.8, and $\Delta\sigma$ (bar) referring to stress drop. Eq.21 holds for all cases. $\Delta\sigma$ can be shown to be proportional to m_o and the characteristic fault dimension L_f (km) as in the following relation according to e.g. (Stein and Wyssession, 2003) and (Scholz, 2002):

$$\Delta\sigma = c_s m_o / L_f^3 \quad (22)$$

where c_s is fault shape factor. Eq.22 applied to strike-slip regime on a rectangular fault (which is the case for example in Chapter 3) yields

$$\Delta\sigma = \frac{2}{\pi} \frac{m_o}{w^2 L_f} \quad (23)$$

where w (km) is fault width. Simplifying Eq.11 by eliminating $\Delta\sigma$ and m_o , yields

$$f_c = 4.9 \times 10^6 v_s \left(\frac{2}{\pi w^2 L_f} \right)^{1/3} \quad (24)$$

Solutions for other shapes and regimes can be found in (Scholz, 2002).

Utilization of seismicity regression models (e.g. Eq.20) and f_{max} values developed for certain regions should be avoided in other seismologic settings.

The cornerstone of source spectrum models is the typical shape of ground motion spectrums marked with a corner frequency f_c on low side of the spectra, an intermediate plateau region and a cutoff frequency f_{max} on high side. This is seen in Fig.2.13. For theoretical support of the models, refer to (Stewart et al., 2002).

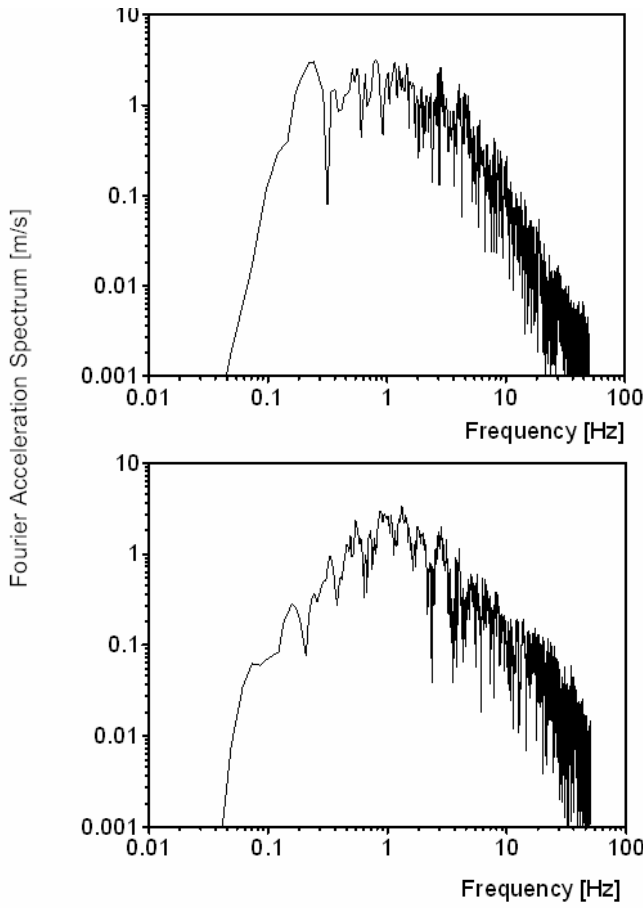


Fig. 2.13. Acceleration spectra from two instrumental records of a $m=7.1$ event (Düzce, Turkey, 11/12/1999) Source-instrument distances (closest to surface projection of rupture) are respectively 8.2 and 17.6 km. Similar corner and cutoff frequencies f_c and f_{max} at ca. 0.04 and 40 Hz are visible. This property constitutes cornerstone of stochastic source spectrum simulation method (source for records is (PEER, 2005), processed with software (SEISMOSIGNAL, 2005))

2.9.1.2. Path model

The aim of this step is modeling path effects on spectrum. Those effects depend on source-site distance and stratigraphy and rheology of the path.

Seismogenic sources (in other words active faults) are modeled as point, linear, areal or volumetric sources. The selection of model shape depend on two factors:

- (1) geometry of the source,
- (2) ratio of source-site distance to fault size (higher ratios justify simpler models).

Usual assumptions are:

- (1) all seismic energy is radiated from hypocenter,
- (2) hypocenters of potential earthquakes are uniformly distributed along the fault.

Assumption (2) does not necessarily imply a uniform distribution of source-site

distance. So, source-site distance can be modeled by probability density functions obtained through analytical or numerical methods, depending on the complexity of source. For an example, refer to (Kramer, 1996).

Given the spatial distribution of hypocenter along the fault, path effect on the source spectrum can be estimated by the following relation after (Boore, 2003) and (Kawase, 2003):

$$P_a(r, f) = g(r) \exp[-\pi f r / Q(f) \bar{v}_s] \quad (25)$$

where $g(r)$ and $Q(f)$ are described below and \bar{v}_s is the representative shear wave velocity of the whole path. Eq.25 is derived from theory of wave propagation.

$g(r)$, geometrical spreading function, is the measure of energy distribution according to (Lay and Wallace, 1995), and, is given by a piecewise continuous function after (Boore, 2003):

$$g(r) = \begin{cases} r_o / r & r < r_1 \\ Q r_1 (r_1 / r)^{p_1} & r_1 < r < r_2 \\ \vdots & \\ Q r_n (r_n / r)^{p_n} & r_n < r \end{cases} \quad (26)$$

r is usually taken as the closest distance to the rupture surface (D) (or as equal to $\sqrt{D^2 + h^2}$, where h is a period- and/or moment-dependent pseudo-depth). p_i and r_i for $1 < i < n$ are to be estimated empirically (h is more important for $< m=6.5$ and for near field, example values from an application by Atkinson and Boore (1995) for eastern North America: $n = 3$, $r_o = 1$, $r_1 = 70$, $r_2 = 130$, $p_1 = 0.0$, $p_2 = 0.5$).

$Q(f)$, attenuation operator, is the measure of energy loss. It can be idealized as a piecewise continuous exponential function after (Boore, 2003):

$$Q(f) = \begin{cases} a f^\alpha & f < f_{t1} \\ b f^\beta & f_{t1} < f < f_{t2} \\ c f^\varepsilon & f_{t2} < f \end{cases} \quad (27)$$

where a , b , c , α , β , ε , f_{t_1} , f_{t_2} are to be determined from regional analysis of weak-or strong-motion data as stated by (Boore 2003).

2.9.1.3. Local soil and topographic effects model

This step involves estimation of local effects filter function $L_a(d_s, f)$, d_s indicates the depth of soil profile considered and f frequency.

This function broadly includes;

- (i) amplification through local younger strata over bedrock (wave impedance)
- (ii) soil-nonlinearity induced de-amplification and predominant period prolongation
- (iii) site diminution
- (iv) sedimentary-basin related phenomena (basin-induced and -transduced surface waves, edge effect, focusing)
- (v) topographic amplification (ridge, hilltop) and deamplification (canyon, slope foot)

So, local effects on spectrum can be formulated as:

$$L_a(d_s, f) = L_a^s(d_s, f)L_a^n(d_s, f)L_a^d(d_s, f)L_a^b(d_s, f)L_a^t(f) \quad (28)$$

The study of these effects is commonly referred as geotechnical earthquake engineering⁵. Due to vastness of the whole subject, a model will be given only for (i), namely for $L_a^s(d_s, f)$ of Eq.28.

(Note: (ii) can be integrated by equivalent linear or nonlinear soil models after (Pecker, 2005). (iii) is discussed by (Boore, 2003) providing a filter function for it. (iv) requires 2D or 3D modeling as stated by (Kawase, 2003). Simple formula for (v) can be found in Kramer (1996) and EUROCODE 8, detailed discussion in (Faccioli and Vanini, 2003). (Kawase, 2003) mentions the difficulties in modeling (v) due to highly varying observations.)

According to (Pecker, 2005), (i) can be modeled in one-dimensional space with the following assumptions:

- (1) horizontally homogeneous and vertically varying medium (reasonable due to mechanics of deposition and weathering),
- (2) vertical wave propagation (justified by gradually upwards decreasing stiffness of

⁵ Its significance stems from the fact that site effects may cause amplifications in amplitudes up to two orders of magnitude, as stated by Kawase (2003).

strata over bedrock, which causes successive refraction)

In this context, exact theoretical amplification relation for a sinusoidal wave is given by e.g. Kawase (2003). (Boore, 2003) provides an approximate relation for this:

$$L_a^s(d_s, f) = \sqrt{Z_s / \bar{Z}(f)}$$

(29)

where Z_s is seismic impedance at bedrock given by

$$Z_s = \rho_s v_s \quad (30)$$

where ρ_s is density and v_s is shear-wave velocity at bedrock.

$\bar{Z}(f)$ is the time-weighted average of seismic impedance from the surface down to a depth of $\frac{1}{4}$ wavelength (this criteria determines sufficient d_s for $L_a^s(d_s, f)$ computation).

It is given by the following expression after (Boore, 2003):

$$\bar{Z}(f) = \bar{\rho}(f) \bar{v}_s(f) \quad (31)$$

where $\bar{\rho}(f)$ is the average density, $\bar{v}_s(f)$ is the average shear wave velocity, given by following expressions:

$$\bar{\rho}(f) = \frac{1}{z(f)} \int_0^{z(f)} \rho(z) dz \quad (32)$$

$$\bar{v}_s(f) = z(f) \left[\int_0^{z(f)} \frac{1}{v_s(z)} dz \right]^{-1} \quad (33)$$

where $z(f)$ is the depth of $\frac{1}{4}$ wavelength, $\rho(z)$ is the density at depth z , $v_s(z)$ is the shear wave velocity at depth z .

For the derivation of Eq.31 and following, refer to (Boore, 2003).

Implementation of the above formulae requires stratigraphic profile providing v_s (shear-wave velocity) and ρ_s (density) down to a depth of $\frac{1}{4}$ wavelength for the lowest frequency considered. This is commonly 1 Hz for engineering purposes after (Kramer and Stewart, 2004). This is usually an uneconomical task with existing borehole techniques. For that reason, common practice is using amplification factors derived from averaged v_s in upper 30 m. This empirically supported approach is referred as v_{s-30} scheme. In this scheme, variation of density (ρ_s) is not considered

due to the little variation at these depths. Selection of 30m as threshold is a convention without any scientific reason.

v_{s-30} scheme is the basis for amplification factors given by seismic design provisions. For detailed discussion, refer to (Kramer and Stewart, 2004).

2.9.1.4. Source duration model

Source duration is commonly modeled as inversely proportional to f_c (corner frequency):

$$s_s(m) = a \cdot f_c^{-1} \quad (34)$$

whereas the constant a range between 0.5 to 1.0 among varying models (Boore, 2003). An expression for f_c is given by Eq.11

In the example in Chapter 3, this model is used with $a=0.5$ in line with (Atkinson and Silva, 2000).

Logically, source duration should be proportional to source size (area or length) and rupture velocity. After (Kramer, 1996), s_s can be shown to be proportional to $\sqrt[3]{m_o}$.

Other theoretical and empirical approaches are not further discussed due to the limitations of this work. Note that, engineering duration measures (bracketed, significant etc.) are not of interest for the method.

2.9.1.5 Path delay model

According to Boore (2003), path delay can be related to source-site distance r with a piecewise function as in the following:

$$s_p(r) = \begin{cases} a r & r_1 > r \\ b / r & r_1 < r < r_2 \\ c r & r_2 < r \end{cases} \quad (35)$$

This relation is based on theoretical simulations and empirical data. However, observations relieve significant dispersion from formula according to (Boore, 2003).

2.9.1.6. Simulation

Initial decisions to take are

- (1) discrete magnitude levels for simulations,
- (2) number of simulations for each level.

Decision (1) - Magnitude levels for simulation:

For the magnitude range under consideration ($m_l < m < m_u$), a decision should be taken for the discrete magnitude levels at which simulation will be realized. A fair decision is simulating at uniform magnitude spacings of $\Delta m=0.5$ from m_l upwards. This is in line with state-of-the-art applications, e.g. (Wen, 2005) and (Vamsatsikos and Cornell, 2004).

Decision (2) – Number of simulations:

An inherent problem of simulation method is the misfit between spectra of single simulations and the original spectrum. The mean spectra of simulations, on the other hand, fit the original spectrum better with increasing numbers of simulations. So, the question is “how many simulations are sufficient to represent hazard sufficiently at a magnitude level?”. Let define the variable n as the number of simulations at each magnitude level under consideration.

In an application by (Boore, 2003), it was shown that mean acceleration spectrum of 640 simulations is almost coincident with the original spectrum. This is an infeasible number. Several seismic design codes give $n=3$ as a minimum. (Boore, 2003) and (Wen, 2005) mention $n=10$ as sufficient. This approach will be adapted for the method presented here.

A fair practice is visually checking each simulated spectra for significant misfit with originical spectrum - especially for frequencies near natural frequency of subject facility.

The above two decisions are subjective. There are no indications in literature for the sensitivity of estimates to these decisions. Alternatively, importance sampling methods for these decisions can be used.

Previously, site spectrum and duration are developed, magnitude levels for simulation and the number of simulations for each level are decided. Now, the method can proceed with time-domain simulation. This involves (1) white noise generation, (2) windowing, (3) transformation to frequency domain (obtaining fourier acceleration spectrum -FAS), (4) normalizing FAS with mean square amplitude spectrum, (5) multiplication of normalized FAS with site spectrum (filtering), (6) transformation back to the time domain, which relieves acceleration time history looked for. The procedure is explained in detail by (Boore, 2003). The order of windowing and filtering is important to avoid

distortion of low-frequency motion. A suitable windowing equation is given by Boore (2003):

$$w(t, \varepsilon, \eta, t_\eta) = a (t/t_\eta)^b \exp(-c(t/t_\eta)) \quad (36)$$

where a, b and c are determined so that $w(t)$ equals the maximum 1 when $t = \varepsilon t_\eta$ and $w(t) = \eta$ when $t = t_\eta$. a, b and c follow

$$b_w = -(\varepsilon \ln \eta) / (1 + \varepsilon(\ln \varepsilon - 1)) \quad (37)$$

$$c_w = b/\varepsilon \quad (38)$$

$$a_w = (e/\varepsilon)^{b_w} \quad (39)$$

The latter author propose $\varepsilon = 0.2$ and $\eta = 0.05$ for applications.

Several authors provide programs for time domain simulation. An example is the open-source Fortran program given and explained in (Boore, 2000). The reader is recommended to utilize this program, since its background is well documented in several publications like (Boore, 2003).

One must note that the variability in simulated time histories at a given magnitude level is not representative for actual variability of ground motion.

As reminder, the output from this stage is a suite of time histories for each hazard level (appr. 50 to 80 time histories) to represent site hazard.

2.9.2. Strong motion - response intermediate function $f_{R|S}(x)$

The aim in this step is obtaining response governing variables for the considered hazard range.

Initial decision is which response governing variables are sufficient and efficient indicators of damage and loss. (Vamsatsikos and Cornell, 2004) provide in this context the list in Table 2.6.

The approach presented there is in line with recent research: (Sarabandi et al., 2005) proves more than 80% correlation between percent loss and interstorey drift ratio among 24 steel structures effected by Northridge 1994 Earthquake. (Boatwright et al., 2001) shows similar high correlations between municipal safety tagging⁶ intensity and

⁶ Post-earthquake procedure of declaring buildings as uninhabitable by state officials.

interstorey drift ratio in a broad regional study after the same earthquake (both latter sources suggest also high correlations to effective peak velocity for this earthquake. However, since this observation lack evidence from other earthquakes, structural damage will be related here only to ISD).

RESPONSE GOVERNING VARIABLES

Damage type	Structural response governing v.
structural damage	max. peak interstorey drift ratio (ISD_{max})
contents' damage	max. peak floor acceleration (PFA_{max})
many types of nonstructural damage	
Several types of nonstructural damage	max. peak floor velocity (PFV_{max})

Table 2.6: Variables on the right hand side proved to be good indicators of damage types on the left hand side.

Following this, a structural analysis method is to be applied to relate response to the hazard. Since hazard is represented by a suite of time histories, the appropriate method is nonlinear time-history dynamic analyses (NDA)⁷.

Given the suite of time histories at varying hazard levels, classical NDA lets us to simulate structural response in time domain. Due to the focus on peak values of response, those correspond to discrete points in hazard-response curve. This is a limitation compared with NSA (nonlinear static analysis = pushover) which provides continuous response estimates up to collapse limit state.

Referred limitation can be overcome by

- (1) averaging the response at each hazard level under consideration, and then
- (2) linearly interpolating between the averages,

as proposed by (Wen, 2005) and (Vamsatsikos and Cornell, 2004).

⁷ Beyond NDA, there are other less sophisticated methods of seismic structural response analysis: nonlinear static (non-adaptive or -adaptive) (NSA), equivalent-linear dynamic, equivalent-linear static analyses (with or w/o modal combination). For details on NDA and these latter, refer to any structural dynamics textbook, e.g. (Chopra, 2005), (Filippou and Fenes, 2004).

2.9.3. Response-damage intermediate function $f_{D|R}(x)$

Current task is estimating damage from structural response governing variables. It is referred as damageability analysis⁸. A component-based approach will be adapted. This means that damage will be estimated separately for each component type.

The term “component” refers to all structural and nonstructural components and contents of the facility. Structural components are foundation components, columns, beams, girders, decks etc. Nonstructural components comprise architectural (claddings, ceilings, doors, windows, partitions etc.) and mechanical, electrical and plumbing components (elevators, lights, piping, ducts, heating-ventilation-air condition systems (HVAC), security systems, fire protection systems, communication systems etc.). Contents comprise equipment, furniture and stored goods.

Damageability data relates structural response to component damage and is obtained empirically (mainly experimentally) for each component type.

To enhance readability, the procedure is presented in steps:

Step I. Prepare a component inventory

Prepare an inventory of damageable component types making up the facility. A component type is group of components with same damageability property (e.g. solid brick wall of 3mx3m dimensions). If dimension is not relevant for damageability, a component type may comprise units with varying dimensions as well.

The inventory includes

- list of component types,
- component class of each type (structural, nonstructural or content),
- performance group of each type (drift-, acceleration- or velocity-sensitive), and,
- number of components of the particular type in varying floor levels.

Performance groups are given in Table.2.7. Distinguishing between floor levels in inventory enables to account for varying response at each floor level. The performance group classification is due to empirical evidence. An exhaustive list of component types can be found in (Taghavi and Miranda, 2003).

⁸ Used instead of “fragility” to avoid confusion, since latter is used interchangeably with vulnerability.

Damageability is not to more than two response governing variables here, for the sake of simplicity and in line with the state-of-the-art (Moehle et al. 2005, Porter et al. 2001).

PERFORMANCE GROUPS

Performance group	Comprises mainly	S_{RGV}	Examples
Drift sensitive	structural c.s	ISD _{max}	columns,beams,connections, walls,piping, glass,ornamentation
Acceleration sensitive	Content some nonstructural c.s	PFA _{max}	mechanical eq., electrical eq., suspended ceiling, elevators
Velocity sensitive	some nonstructural c.s	PFV _{max}	

Table 2.7: Performance group classification for building components. S_{REV} (structural response governing variable) selection is in line with evidence presented in section 2.9.2.2. after (Beck et al., 2002) (Moehle et al., 2005)

Step II. Define damage states

In this step, for each component type, a series of discrete damage states is defined. Those should be experimentally observable and meaningful for repair actions.

Accordingly, after any earthquake, any component would be in one of several damage states D=0,1,2,3,...n. D=0 denotes undamaged state.

(Porter et al. 2001) gives the assumptions in this approach as mutually-exclusiveness, collectively-exhaustiveness and progressiveness of damage states. Progressiveness means that the component under consideration should pass through damage state k to reach damage state k+1.

Step III. Extract damageability curve

A damageability curve (DC) exposes exceedance probability of each damage state in relation to a response governing variable. They are drawn separately for each component type with the appropriate response governing variable. So, taking $n = \text{number of component types in the facility}$, n damageability curves are needed. State-of-the-art for producing damageability curves is lognormal fit on experimental data.

The vastness of damageability information brings in a data management problem. To overcome this, the tabular presentation for each component type in Table 2.8 can be used. This table combines approaches by (Taghavi and Miranda, 2003), (Krawinkler and Miranda, 2004) and (Beck et al 2002).

Type no.	Component	Type	Dimensions	Class	Performance	Group	Damage State	Type of consequence	Information	Capacity						Duration hours/unit	
										μ	σ	μ	σ	μ	σ		
1	Solid brick wall	tvde	3m x 3m	Nonstructural	Acceleratiom-sensitive	0	0	Repair action	Minor repair of exterior finishes	-	-	-	-	-	-	0.40	
2	Solid brick wall	tvde	3m x 3m	Nonstructural	Acceleratiom-sensitive	1	1	Damage consequence	No	ISD	-	-	-	-	-	120	
3	Solid brick wall	tvde	3m x 3m	Nonstructural	Acceleratiom-sensitive	2	2	Building functionality	Fully functional	ISD	-	-	-	-	-	0.03	
								Life safety	None	ISD	-	-	-	-	-	0.0125	
								Component loss of function	None	Some parts may need demolition and reconstruction. Damaged area need repair exterior finish	0.10	0.01	0.10	0.20	0.20	0.40	
								Repair action	EMD on wall poss. stop function+ need repair	0.0045	0.0005	0.15	36	10	120	120	
								Damage consequence	Loss-of-use of adjacent rooms until end of repair	0.26	0.063	0.0039	0.10	0.10	0.03	0.03	
								Building functionality	Small	ISD	-	-	-	-	-	0.30	
								Life safety hazard	Moderate	Complete demolition of damaged area. Reconstruction.	0.09	0.09	0.09	0.09	0.09	0.09	0.09
								Component loss of function	EMS may break or not work	ISD	-	-	-	-	-	0.30	
								Repair action	Loss-of-use of adjacent rooms until end of reconstruction.	High	High	High	High	High	High	0.30	
								Damage consequence	High	High	High	High	High	High	High	0.30	
								Building functionality	High	High	High	High	High	High	High	0.30	
								Life safety	High	High	High	High	High	High	High	0.30	
								Component loss of function	High	High	High	High	High	High	High	0.30	

Table 2.8: Damageability and restoration cost data for a component. ** (column 11) restoration cost/component value

Step IV. Mathematical formulation of damageability

The aim in this section has been to model $f_{D|R}(d,r)$, conditional probability distribution function of membership to damage state d , conditioned on structural response. In the following, corresponding mathematical formulation will be presented. For a particular component and a damage state $d, d \in \{0, 1, 2, \dots, n\}$, one can write:

$$f_{D|R}(d,r) = p[D=d|R=r] \quad (40)$$

where D denotes damage state and R denotes structural response.

Let denote the capacity of the component to resist the damage state d by a random variable X_d . Then we can write;

$$p[D \geq d|R=r] = p[r > X_d] = F_{X_d}(r) \quad (41)$$

with $F_{X_d}(r)$ denoting the cumulative probability distribution function of X_d evaluated at r .

As stated earlier, lognormal probabilistic model is commonly used for $F_{X_d}(r)$, which can be given for any r by:

$$F_{X_d}(r) = \Phi\left(\frac{\ln(r/\mu_d)}{\sigma_d}\right) \quad (42)$$

where μ_d and σ_d is the mean and standard deviation of X_d and vary by component type and damage state (can be found in column 10 and 11 in Table 2.8). Since being in a damage state conditioned by response is lower-bounded by X_d and upper-bounded by X_{d+1} , we can write the following:

$$p[D=d|R=r] = p[r \geq X_d] - p[r \geq X_{d+1}] = F_{X_d}(r) - F_{X_{d+1}}(r) = \Phi\left(\frac{\ln(r/\mu_d)}{\sigma_d}\right) - \Phi\left(\frac{\ln(r/\mu_{d+1})}{\sigma_{d+1}}\right) \quad (43)$$

Where $\Phi(\)$ denotes the cumulative standard normal distribution evaluated at the term in parentheses. Equating Eq.40 and Eq.43 yields;

$$f_{D|R}(d,r) = \Phi\left(\frac{\ln(r/\mu_d)}{\sigma_d}\right) - \Phi\left(\frac{\ln(r/\mu_{d+1})}{\sigma_{d+1}}\right) \quad (44)$$

Using the fact that for $d = 0$; $\Phi\left(\frac{\ln(r/\mu_d)}{\sigma_d}\right) = 1$, and for $d = n$; $\Phi\left(\frac{\ln(r/\mu_{d+1})}{\sigma_{d+1}}\right) = 0$;

$$f_{D|R}(d, r) = \begin{cases} 1 - \Phi\left(\frac{\ln(r/\mu_1)}{\sigma_1}\right) & d = 0 \\ \Phi\left(\frac{\ln(r/\mu_d)}{\sigma_d}\right) - \Phi\left(\frac{\ln(r/\mu_{d+1})}{\sigma_{d+1}}\right) & 0 < d < n \\ \Phi\left(\frac{\ln(r/\mu_n)}{\sigma_n}\right) & d = n \end{cases} \quad (45)$$

To remind again, thus presented damageability function is to be evaluated separately for each component-type and floor level. The derivation above relied mainly on the work of (Porter et al., 2001, 2004).

The solution of Eq.45 can be carried out numerically, due to probabilistic nature of both of both response and damageability. An option is Monte Carlo Simulation, which will be utilized for the example in Chapter 3.

Damageability data (namely μ_i and σ_i for each damage state i) for a series of component types can be found e.g. in (Beck et al. 2002) and (Taghavi and Miranda, 2003). Damageability curves can also be partially or completely based on simulation results, expert opinion and from earthquake damage databases. For example, (Kao et al., 1999) provides nonstructural damage data with 3000 entries from 50 earthquakes from 1964 to 1999. Methods for processing such data to get damageability functions are discussed by (Porter et al. 2001).

As seen above, the presented approach provides seismic damage estimates for nonstructural components and contents in addition to structure. This is due to the dominating share of nonstructural components and contents in economic losses. This is stated by several authors, e.g. (Krawinkler and Miranda, 2004). (Bazurro, 2005-I) further mention the high sensitivity of seismic loss estimates to component damageability modeling. He mentions that replacement costs in average office buildings in USA is in average due to ca. 60% nonstructural, 20% contents and 20% structural damage. Similar figures for the same country are given by (Whittaker and Soong, 2005) for hospitals (45%, 45%, 10%), for hotels (70%, 15%, 15%) and for residential buildings (40%, 40%, 20%). For case stories proving the importance of nonstructural elements in seismic loss, refer to (Villaverde, 2004).

Above presented damageability approach differs in many ways from conventional fragility approaches, since it

- (1) accounts for nonstructural components and contents damage,
- (2) relates structural damage to response (instead of to hazard by means of conventional fragility curves⁹ or damage indices¹⁰),
- (3) utilizes probabilistic treatment of damage,
- (4) uses component-based damage states (instead of macroscopic – global performance levels).

2.9.4. Damage-loss and response-collapse intermediate functions

The task in this section is obtaining the remaining intermediate functions and facility-specific parameters.

2.9.4.1. Collapse probability model

Collapse probability is related to structural response as proposed by state-of-the-art.

The aim is to find collapse probability $f_{C|R}(c=1, r)$ in Eq.1, where c denotes the indicator variable of collapse ($c=1$ implying collapse, $c=0$ no collapse), and, r denotes the (uncertain) response.

Leaning on the discussion on damage states in section 2.9.2.3., one can write alternatively

$$f_{C|R}(C=1, r) = p[C=1|R=r] \quad (46)$$

Let treat the whole structure as a component in line with section 2.9.2.3.. Let denote the capacity to resist collapse with X_C . Research shows that lognormal distribution for the random variable X_C can be assumed. Probability of collapse can then be written as

$$p[C=1|R=r] = p[r \geq X_C] = F_{X_C}(r) \quad (47)$$

With $F_{X_C}(r)$ denoting the cumulative probability distribution function of X_C evaluated

⁹ For explanation of conventional fragility analysis, refer to (Shinozuka et al. 2000)

¹⁰ For treatment of conventional damage indices, refer to (Williams and Sexsmith, 1995).

at r . Since lognormal-modeled, $F_{X_c}(r)$ is given for any r by:

$$F_{X_c}(r) = \Phi\left(\frac{\ln(r/\mu_c)}{\sigma_c}\right) \quad (48)$$

So, using the latter three equation;

$$f_{C|R}(C=1, r) = \Phi\left(\frac{\ln(r/\mu_c)}{\sigma_c}\right) \quad (49)$$

where μ_c and σ_c (mean and standard deviation of collapse resisting capacity X_d) depend on structural characteristics.

Several state-of-the-art publications provide estimates in this format for a range of structural types. They use maximum peak interstorey drift as response governing variable for collapse probability. For example, (Yun et al. 2002) have found $\mu_c = 0.08$ and $\sigma_c = 0.30$ in analysis of post-Northridge steel moment frames. (FEMA, 2000) proposes twofold criteria for collapse:

- (1) 0.10 as a deterministic collapse prevention ISD limit or
- (2) local tangent reaching 20% of elastic slope on Incremental Dynamic Analysis curve.

2.9.4.2. Death and injury model

For the time being, death and injury modeling is practically impossible due to lack of data utilizable in a single facility loss model. The problem is presented recently in a prestigious earthquake engineering journal by (Porter et al. 2005):

"The authors are aware of no laboratory research in the United States to improve our understanding of and ability to model nonfatal earthquake injuries..., the same can be said of fatal injuries, beyond efforts to estimate collapse potential. Only a fraction of occupants in collapsed buildings are killed, and little is known about that process either."

The above statement for United States can be considered universal.

On the other hand, for risk assessment of a portfolio of structures, statistics can be used. Examples are given by Coburn and Spence (2002)¹¹.

¹¹ These authors provide 20th century statistics showing that 90% of earthquake related deaths are caused by collapse. However, these statistics are not suitable for utilization in our single facility model,

For the current model, a collapse dependent death and injury model is assumed, with 75% dead and 25% injured among occupants in collapse limit state and no injury or death due to any component or partial damage states.

Another component of this task is occupancy modeling. There are occupancy statistics in literature e.g. given by (Coburn and Spence, 2002). Adaptation of these for single facility case however can not be justified. So, considering lack of suitable information, approximate assumptions can be made. For example, 18 hour occupancy for residential use, 10 hour occupancy for other social use (public, business, recreational). The subject of occupancy models for single facility deserves extended research.

2.9.4.3. Restoration cost model

The aim of this step is to model restoration cost for each component. This is denoted by $f_{V|D}(v,d)$, referring to the probability distribution of normalized restoration cost conditioned on (uncertain) damage state. Normalized restoration cost means component restoration cost divided by mean new construction cost of the whole facility (C_T).

Similar to damage models, lognormal models are utilized. So, for each component type and each damage state, two parameters (mean and standard deviation) are needed for the model. In the previously given sample damageability table in Table 2.8, corresponding information is in Column 11.

Restoration cost data can be gathered from statistics and expert opinion. It is worth to note that, only the direct costs (costs of labor, material, equipment) due to construction and demolition are modeled in this task. For further discussion, refer to (Krawinkler and Miranda, 2004) and (Porter et al., 2001).

*since they are regressed from a population dispersed both in time and location. The authors moreover provide death data classified among reinforced concrete (RC) and masonry structures and among near-field/high-frequency and distant/low-frequency dominant ground motion. These statistics show that in RC structures, at average, 50 to 70% of occupants remain trapped after a collapse. Among the factors effecting the ratio is building height. Among the trapped, average survival rates range from 10 to 30%. For a rough approximation for our model –translating reinforced concrete data to all types of structures– using the worst case values of the above, we can assert; ratio of deaths in occupant population = 70%*90% = 63%~65%, injured among occupant population = 70%*10% = 7%~10% assuming that there are no injuries in case of no collapse. The assumptions are too tight and we use a regressive data from a very dispersed population both in time and location, which is rather suitable for using in macroseismic models.*

2.9.4.4. Serviceability interruption model

Related statistical data is scarce as stated by (Porter et al., 2001). The approach proposed here is to sum up all restoration durations for each single component. This is based on following assumptions:

- (1) Partial usability of the facility during restoration of a partial damage is neglected.
- (2) Possibility of simultaneous restoration for any two components is neglected.

Scarcity of related statistical data (stated e.g. by (Porter et al., 2001), (Coburn and Spence, 2002)) justifies the assumptions. Collapse state is excluded in the model.

Similar to the previous models, lognormal distribution is used. Necessary information is given in Column 12 of the proposed sample damageability table in Table 2.8.

2.9.4.5. Monetary loss model -due to tangibles-

There are three components of monetary loss due to tangibles:

- (1) restoration costs,
- (2) serviceability interruption costs,
- (3) loss due to collapse.

(1) and (2) are considered for partial damage range, (3) for collapse limit state. (1) and (2) are modeled probabilistically, whereas (3) is based on deterministic estimate. (3) contains by definition the serviceability interruption costs due to collapse

Two deterministic parameters should be estimated for this step:

C_{SI} : mean cost of unit time serviceability interruption cost

C_T : mean new construction cost of the whole facility (as referred in 2.9.4.3)

2.10. Solution and dealing with uncertainty

Each function contained in loss equations of Table 2.4 is explained above.

Solution of loss equations of Table 2.4 can not be carried out with analytical methods due to the probabilistic and nonlinear relations. Numerical iterative techniques (like Monte Carlo Simulation or First-Order Second Moment (FOSM)) should be utilized. In the example given in Chapter 3, Monte Carlo Simulation is used. For an alternative solution method (FOSM), refer to (Baker and Cornell, 2005).

The resulting risk estimates is called “risk profile”.

Accompanying the model solution, is the task of model validation. This is an important and complicated task. It can be explained as seeking evidence to support or reject the model.

This task include validation of following components of the model:

- (1) phenomenological understanding,
- (2) selection of governing variables,
- (3) hazard model,
- (4) probabilistic models and parameters of intermediate events.

Following strategies can be used for validation:

- (1) comparison with observed data,
- (2) comparison with other models,
- (3) expert-opinion and review.

Risk assessment model validation should be object-oriented. That means it should be validate that the model do not lead to wrong risk management decisions, rather than seeking precision.

The previously presented model is constructed on the basis of state-of-the-art publications. Due to this reason and due to the dimensions of this work, the task of model validation will be skipped.

An important validation issue is treatment of uncertainty in loss estimate models¹². A practical question for the presented model is if uncertainty treatment is integrated sufficiently.

The high uncertainty surrounding seismic loss estimate models is related to several factors. (Bazurro, 2005) mentions in this context high sensitivity of loss estimates to:

- (1) hazard analysis method,

¹² Motives for addressing uncertainty in earthquake engineering is discussed by several authors: (Wen, 2004) mentions the undefined collapse and damage reliability of conventional procedures. (Bazurro, 2005) compares analysis examples with and without uncertainty treatment and show fallacy of latter. Uncertainty treatment is introduced gradually into seismic design codes (e.g. FEMA 350). For detailed treatment, refer to (Wen, 2004) and (Coburn and Spence, 2002).

- (2) detailed soil description,
- (3) directivity effects (especially in case of flexible structures),
- (4) hazard description by a single ground motion parameter or a vector,
- (5) (for macro risk management) accounting or neglecting for ground motion correlation.

In the model presented, (1) and (4) are dealt with state-of-the-art methods; respectively, with probabilistic seismic hazard analysis and stochastic strong motion simulation. Concerning (2), only impedance effects are addressed. Factor (3) is not addressed in our model. The model can be extended for the lacking components with future work.

On the other hand, (Porter, 2002) lists the top three contributors to uncertainty in seismic loss estimates as:

- (1) component capacity,
- (2) shaking intensity, measured by damped elastic spectral acceleration,
- (3) details of the ground motion given elastic spectra.

(Porter, 2002) includes case studies proving this assertion.

In line with the discussion above, presented method addresses (2) and (3) by stochastic simulation of strong motion, and (1) by component-based approach.

(Wen, 2005) mention uncertainty in demand is much higher than that of capacity.

So, it can be asserted that the presented model treats major sources of uncertainty recognized by the state-of-the-art. Detailed soil description and directivity effects are lacking and can be integrated in the model by future work.

Chapter 3. Example application of the method

This chapter includes an example application of the risk assessment method discussed in Chapter 2. The method reflects state-of-the-art of earthquake engineering and seismic risk management. The method is actually applicable to more complex facilities with arbitrary number of components and contents.

3.1. Problem statement

An owner demands annual seismic loss estimates for a facility, in order to use them for risk management decisions. The facility is used for electrical supplies control and is classified as a critical facility with full-time occupancy and operation. Relevant facility data can be taken from Table 3.1, structural information from Fig.3.1 and Fig.s 5.5 and 5.6. Component inventory is depicted in Fig.s. 3.2 and 3.3. The task to be fulfilled is the calculation of appropriate loss estimates.

3.2. Construction of mathematical model

The solution follows the algorithm constructed in Chapter 2.

It starts with hazard tree construction in Fig.3.4. This figure demonstrates the client qualitatively the consequences of a potential earthquake on the facility.

Next step is risk measures decision. Appropriate risk measures are given in Table 3.2. This follows construction of loss trees (refer to previous Fig.s 2.4, 2.5, 2.6, 2.8, not repeated here). Next step is the decision on governing variables to represent each event in loss trees, summarized in Table 3.3. All these steps serve for construction of mathematical model presented in Table 3.4.

RELEVANT DATA FOR SEISMIC RISK ASSESSMENT	
Occupancy	3 persons full-time
Total structural reconstruction cost	300 000 euros
Cost of 1 hour loss of use	1000 euro
Geographical location	39.9160° N, 39.4064° E. In Province of Erzincan, Turkey.
Site soil conditions	average shear wave velocity at 30m profile, v_{s-30} 200 m/s susceptibility to topographic/basin amplification, ground failure (liquefaction, landslide, cracking) none according to expert opinion
Structural components inventory	column profile HEA200 3m (12), beam profile HEA 200 5m (6), beam profile HEA 140 3m (6), cross brace L70x70 4.3m (12) (see Fig. 3.1 and 4.2)
Nonstructural components inventory	reinforced concrete deck 5mx3m (3), brick wall 3mx3m (6), brick wall 5mx3m (6), window 1mx1m (3), door 1mx2m (1), spiral stair 0.8mx6m (1) (see Fig. 3.3)
Contents inventory	generator (1), PC (2), technical precision equipment (2), electrical wiring, furniture (see Fig. 3.3)

Table 3.1.

RISK MEASURES	
M	number of hazard induced deaths in one year
I	number of hazard induced injuries in one year
N	hazard induced restoration (repair and replacement) cost in one year
P	hazard induced monetary loss –due to tangibles- in one year

Table 3.2

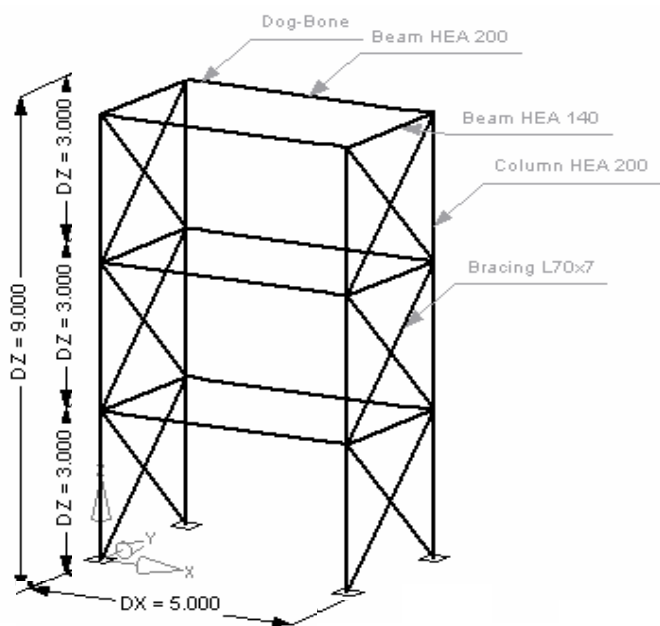


Fig. 3.1

STRUCTURAL COMPONENTS INVENTORY

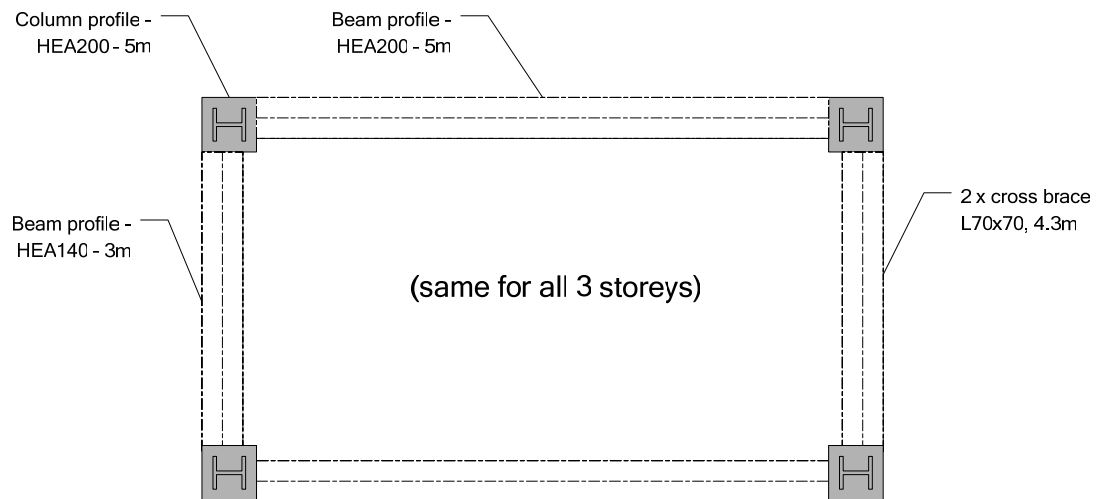


Fig. 3.2

NONSTRUCTURAL COMPONENTS AND CONTENTS INVENTORY

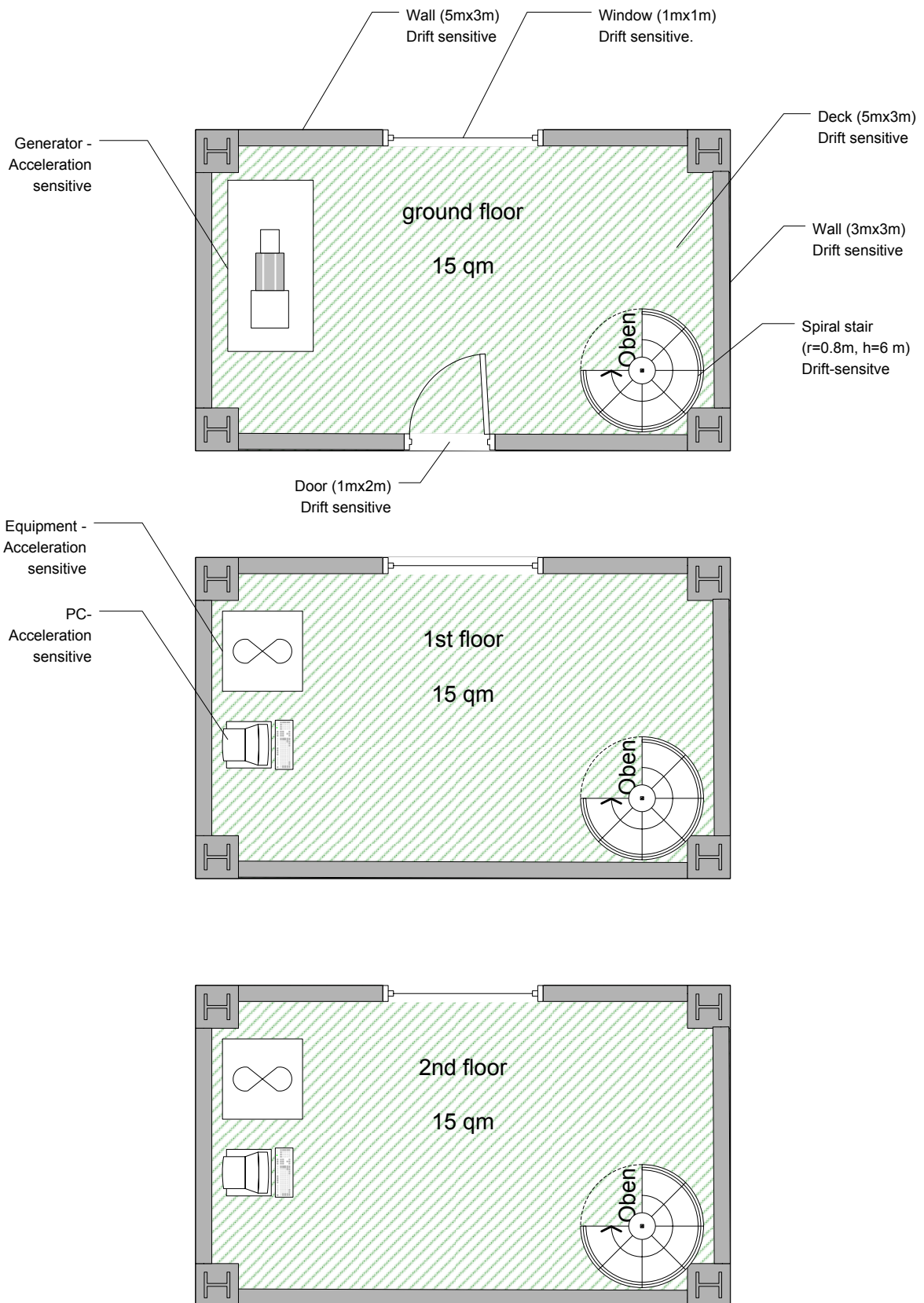


Fig. 3.3

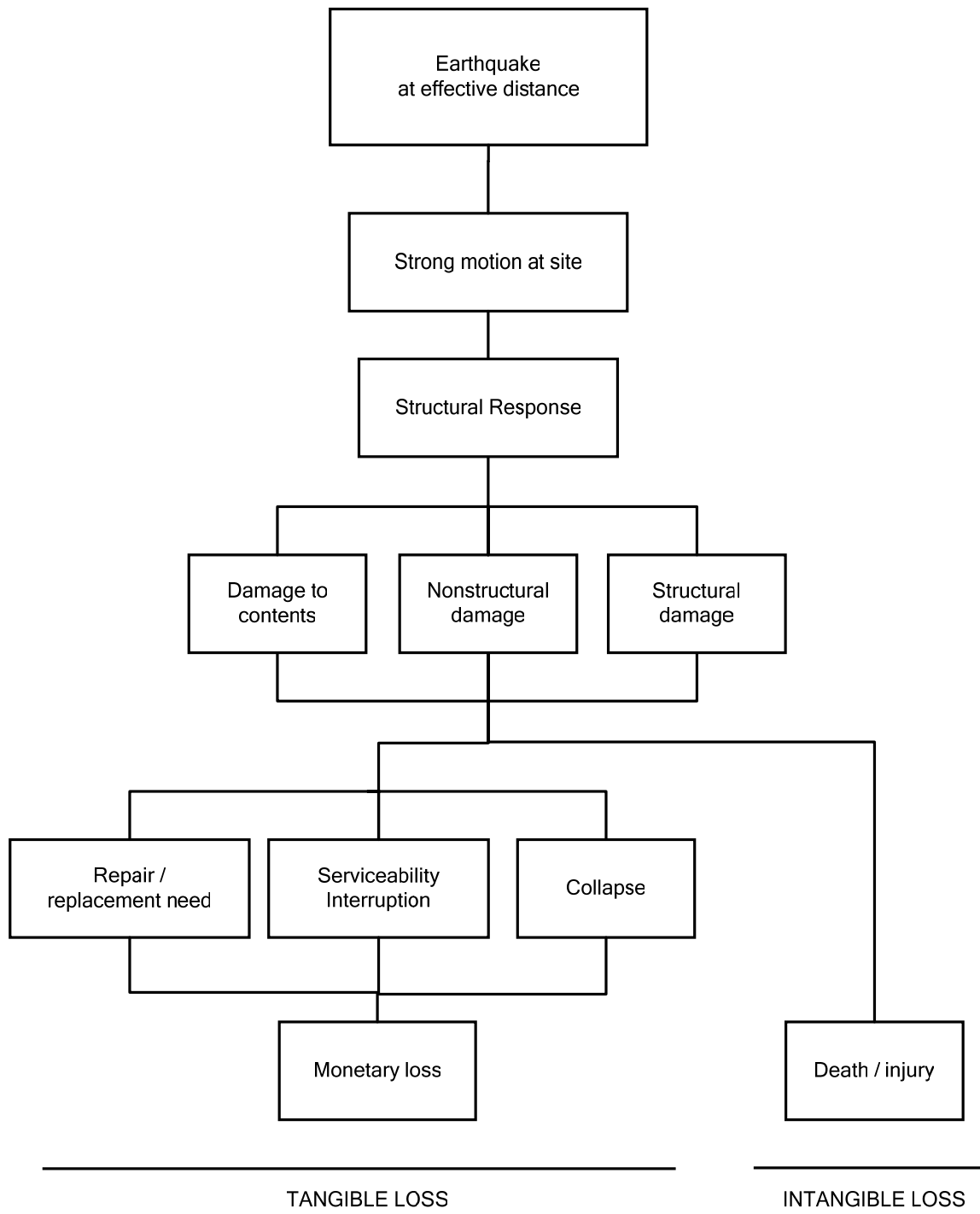


Fig. 3.4

GOVERNING VARIABLES DECISION			
	Event (annual maxima)	Governing variable	Abbr.
Hazard	earthquake (separately for each seismogenic source)	moment magnitude	E
	strong motion at site	suite of simulated displacement time histories	S
Response	structural response	ISD_{max} , PFA_{max} , PFV_{max}	R
Damage	component damage	damage class	D
Loss	death	number	M
	injuries	number	I
	collapse	indicator variable (1=occ., 0=non-occ.)	C
	restoration cost	monetary unit	N

Table 3.3

MATHEMATICAL MODEL OF SEISMIC RISK ASSESSMENT	
Collapse equation	
$p_C(C=1) = \int_r \int_s \int_x f_{C R}(C=1, r) f_{R S}(r, s) f_{S E}(s, x) dG_E(x)$	
Loss Equation I. Death	
$G_M(m) = p_C(C=1) * Q * R_M$	
Loss Equation II. Injury	
$G_I(i) = p_C(C=1) * Q * R_I$	
Loss Equation III. Restoration cost	
$G_V(v) = \sum_{a=1}^k \sum_{d=1}^n \int_r \int_s \int_x f_{V D}^a(v, d) f_{D R}^a(d, r) p_C(C=0 \mid R=r) f_{R S}(r, s) f_{S E}(s, x) dG_E(x)$ $+ p_C(C=1) * V_T$	
Loss Equation IV. Monetary loss -due to tangibles-	
$G_P(p) = G_P \langle V + (L * C_L) \rangle$	

Table 3.4

3. 3. Hazard assessment

3.3.1. Investigation of seismological setting

The site is located in the seismological region “Anatolian part of North Anatolian fault”, according to classification by (Bayrak et al. 2005). This classification is depicted in Fig. 3.5, with site coordinates drawn with red lines.

Maximum recorded magnitude in the region is $m_{\max}^{\text{rec}} = 7.9$. This is from 1939 Erzincan Earthquake with epicenter at 13 km from the site. This is actually the maximum instrumentally recorded magnitude in all Turkey.

(Bayrak et al. 2005) give maximum extrapolated magnitude as $m_{\max} = 8.1$.

In official seismic macrozonation map of Turkey, the site is in Zone I as seen in Fig. 3.6 with expected 475-year peak ground acceleration of at least 0.4g (ERD, 2006).

3.3.2. Effective sources identification and hazard recurrence modeling

Decisions on lower magnitude bound and maximum distance criteria are taken respectively as $m_l=5.0$ and $r_{\max}=50\text{km}$. These are taken from Table 3.5 given previously, considering the following conditions:

- (1) modern construction,
- (2) stable foundation,
- (3) absence of site amplification and ground failure susceptibility,
- (4) maximum regional magnitude approximately equal to 8.0.

As stated earlier, the referred Table 3.5. is developed originally for western USA. Its application for the current problem can be justified by:

- (1) similarity of San Andreas and North Anatolian Fault Systems discussed by various authors,
- (2) lack of relevant data for the region under consideration.

For location of site on active fault map of Turkey (ERD, 2006), see Fig.3.7, for focused view Fig.3.8. Fig.3.9 depicts 50 km vicinity of the site (r_{\max} criteria). The active fault within the circle is identified as site-specific effective seismogenic source.

As distance measure, closest distance to surface projection of the source will be used. Corresponding value obtained by measurement on the map is 10.60 km.

Necessary coefficients for hazard recurrence modeling are taken from the regional model by (Bayrak et al., 2005). These authors have analyzed data from over 20000 instrumental and historical events in Turkey, from which 707 occurred in the region under consideration. Accordingly; regional m_{\max} , m_{\min} and b are respectively 8.1, 4.5 and 0.9.

Those values are placed in Eq.s 13 and 14 and hazard recurrence curve in Fig. 3.10. is obtained. Discrete probability values from the curve are given in Table 3.5.

Characteristic earthquake is not considered due to lack of information. It is likely that such information is not available for the region considered.

Note that m_{\max} in model by (Bayrak et al., 2005) is 0.2 magnitude scale higher than m_{\max}^{rec} .

Risk assessment procedure will consider the range $m_l=5.0$ to $m_u =8.0$, due to following reasons:

- (1) for $m < 5.0$, no significant effects are expected,
- (2) for $8.0 < m < 8.1$, $p(m) \rightarrow 0$, namely the probabilities are very low.

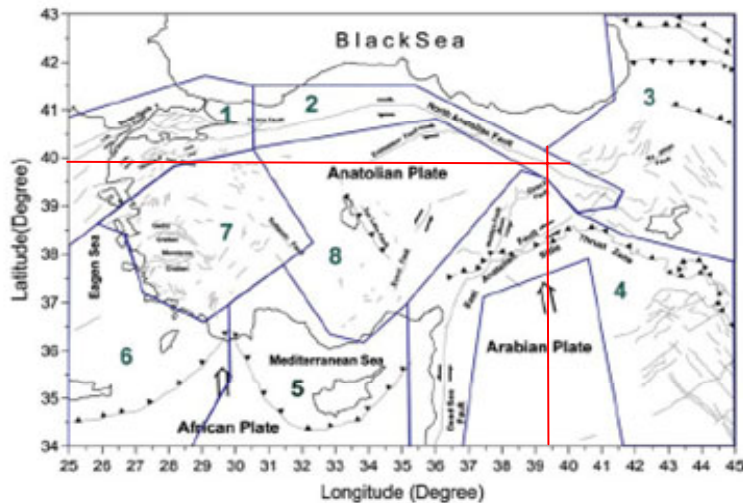
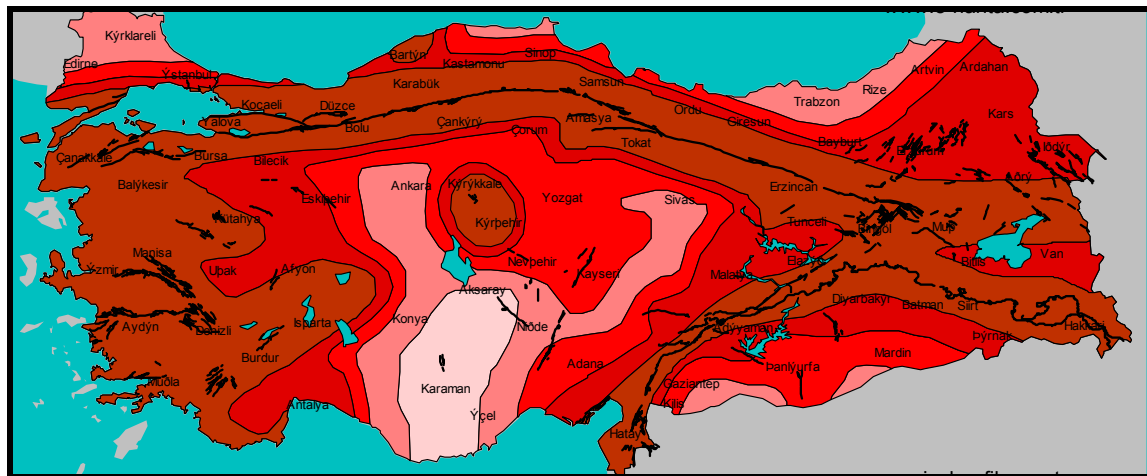


Fig. 3.5: Seismological regional classification of Turkey (Bayrak et al. 2004). Subject site marked with straight lines is in Region 2 (Anatolian Part of North Anatolian Fault).



*Fig. 3.6: Site location in seismic zonation map of Turkey after (DAD, 2005). Colors from dark to light denote respectively Zones I to V.
Subject site marked with a white star is in Zone I.*

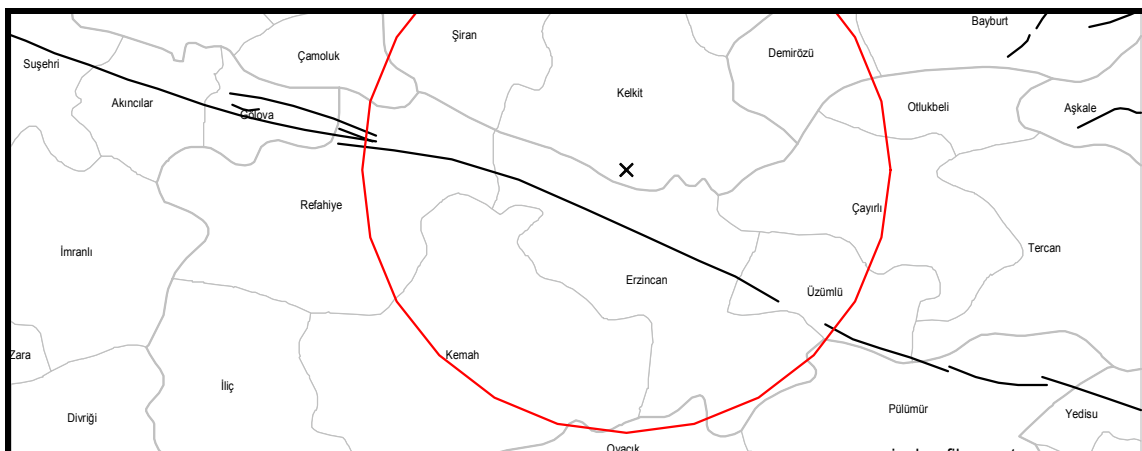
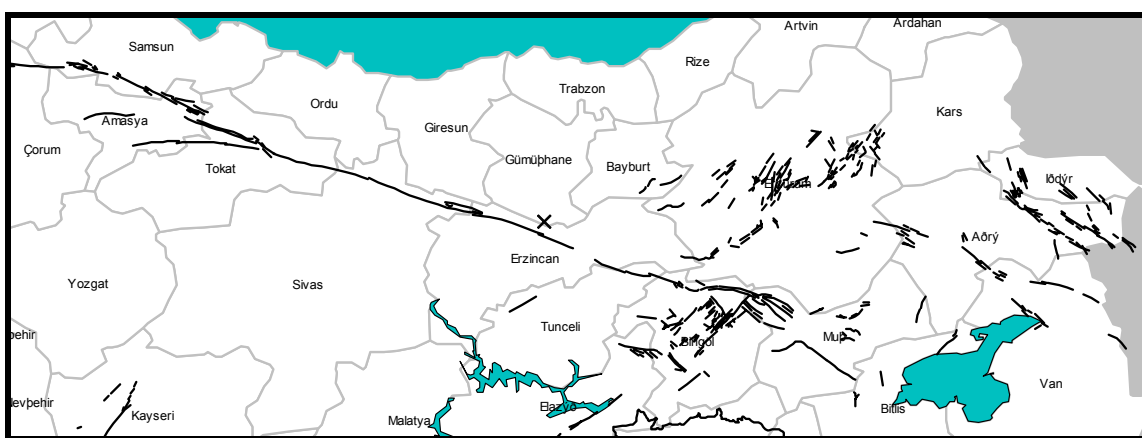


Fig.3.7,8,9

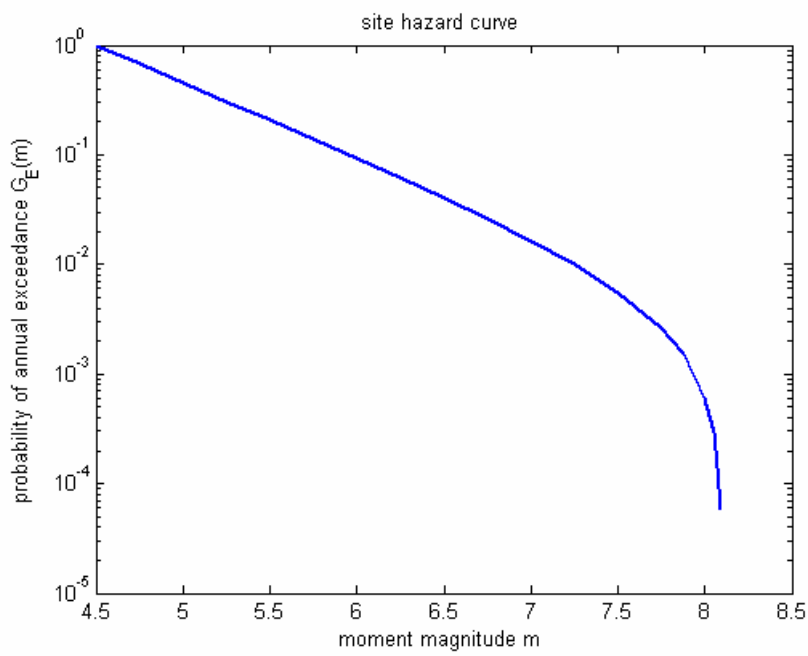


Fig. 3.10: Site hazard curve

	M	$G_E(m)$
m_{min}	4.5	1.0000
m_l	5.0	0.4551
	5.5	0.2061
	6.0	0.0923
	6.5	0.0402
	7.0	0.0164
	7.5	0.0056
m_u	8.0	0.0006
m_{max}	8.1	0.0001

Table 3.5: Moment magnitude vs. annual probability of exceedance for discrete points considered in risk assessment procedure ($m_l - m_u$) and two extremes m_{max} and m_{min} .

3.3.3. Stochastic strong motion simulation

In line with section 2.9.2.1., 10 simulations for each $\Delta m=0.5$ step between $m_l=5.0$ and $m_u=8.0$ are carried out. This makes a total of 70 simulations.

An open-source Fortran program given by (Boore, 2000) (refered in 2.9.1.6 as well) is used. The program uses time-domain stochastic strong motion simulation method after (Boore 2003).

Table 3.6 gives simulation parameters, most of which are taken from the work by (Akinci et al., 2001). These authors have determined source and attenuation characteristics through analysis of regional microseismicity. The region they considered was bounded by $39^{\circ}15'N-40^{\circ}00'N$ meridians and $39^{\circ}20'E-40^{\circ}15'$ parallels, so including the site considered in this problem.

For several other parameters, no regional data is available in literature. For those, state-of-the art publications on Californian / western North-American conditions are consulted. This approach can be justified by similarity of San Andreas and North Anatolian Fault Systems discussed by various authors.

Record duration vary with magnitude level ranging from 5 seconds for $m=5.0$ to 100 seconds for $m=8.0$, with equal time steps of 0.005 seconds.

Acceleration time history of a sample simulation is depicted in Fig.3.11 and compared to a real local record.

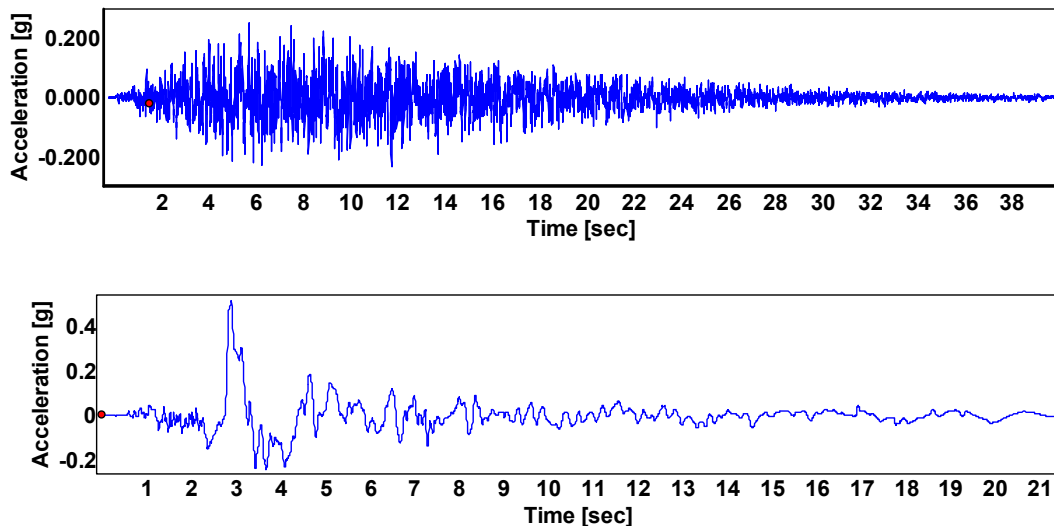


Fig. 3.11: Above is a simulated acceleration time history for a $m=7.0$ event at the site ($r=10.6$ km). Below is the only available real record from the region ($m=6.9$, source-site distance = 0.2 km, 13.03.1992). Simulated records have distinct time history patterns than real ones, especially in near field. However, they are useful considering scarcity of real records in vast seismic regions of the world.

STOCHASTIC STRONG MOTION SIMULATION PARAMETERS

Parameter	Abbr.	Value in this application	Source
Density	ρ	2.8 g / cm ³	
Shear wave velocity in source vicinity	v_s	3.5 km/sec	
Partition factor for shear waves	V	0.707	(Akinci et al., 2001)
Radiation pattern	$R_{\Theta\Phi}$	0.55	
Free surface effect	F	2	
Stress drop	$\Delta\sigma$	10 MPa	
Shape of source spectral	S(f)	Eq. 20	(Atkinson and Silva, 2000)
Reference distance		1km	Common in most applications
Geometrical spreading function	$g(r)$	$r^{-1.1} \quad r \leq 25\text{km}$ $r^{-0.5} \quad r \geq 25\text{km}$	(Akinci et al., 2001)
Attenuation operator	Q(f)	$40f^{0.45}$	
Source Duration	s_s	$\frac{1}{f_c}$	(Boore, 2000)
Path Duration	s_p	0.05r	
Site amplification -generic rock-		For parameters, see the source.	(Joyner 1997) , (Boore, 2000)
Site amplification -30 m profile-	A_{v-30}	1. 5	(EUROCODE 8)
Exponential window for simulation	w	Eq.s 36-39, $\epsilon = 0.2$, $\eta = 0.05$	(Boore 2003)

Table 3.6: Parameters used for stochastic strong motion simulation

3.3.4. Structural response analysis

A finite element model of the structure is constructed in ANSYS (a commercial software). Refer to Annex.II for ANSYS-script used and to section 4.3.2 for details of the model. Using this model, dynamic time history analyses are carried out for each of the 70 simulated displacement time histories (strong motion simulation was explained in section 3.3.3). Refer to section 4.3.5, for details of the time history computations. The statements given there are valid for this part of the work as well.

As given previously in Table 3.3, response governing variables are ISD_{max} , PFA_{max} and PFV_{max} . Corresponding data gathered from analyses is depicted in Fig.s 3.12 to 3.17. Normal or lognormal fits are used as seen there (commercial software MATLAB is used for this purpose). In succeeding steps, only lognormal model will be used, because maxima are defined in absolute values.

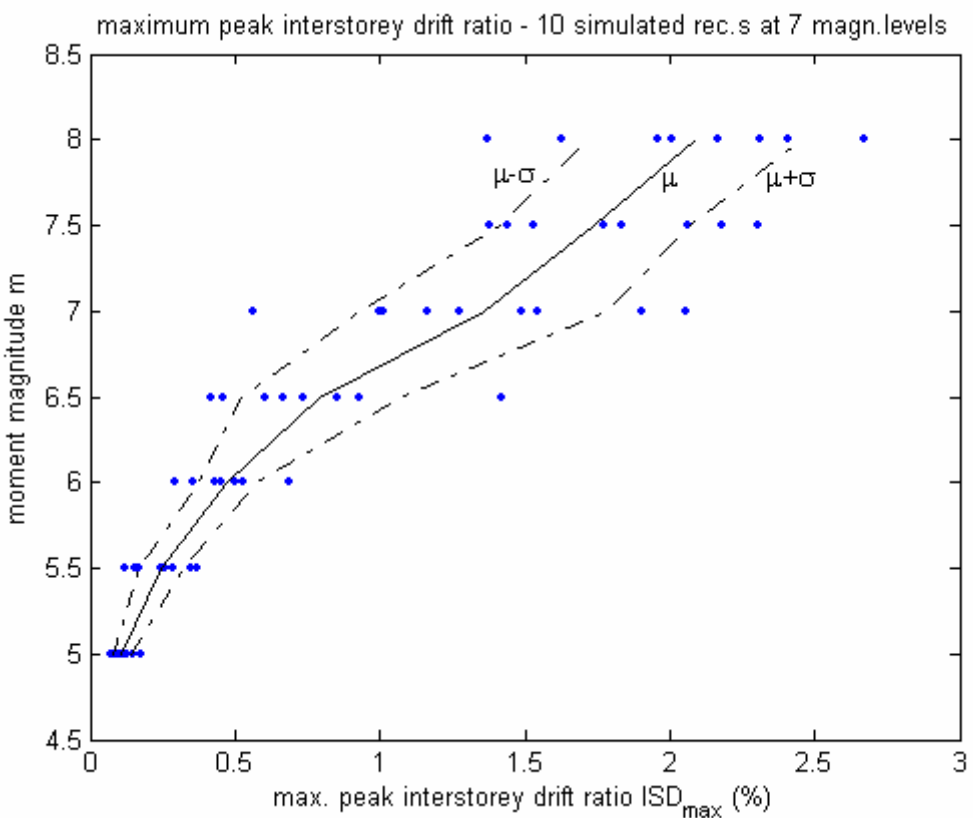


Fig.3.12: Normal fit to ISD data, piecewise linear interpolated over hazard levels

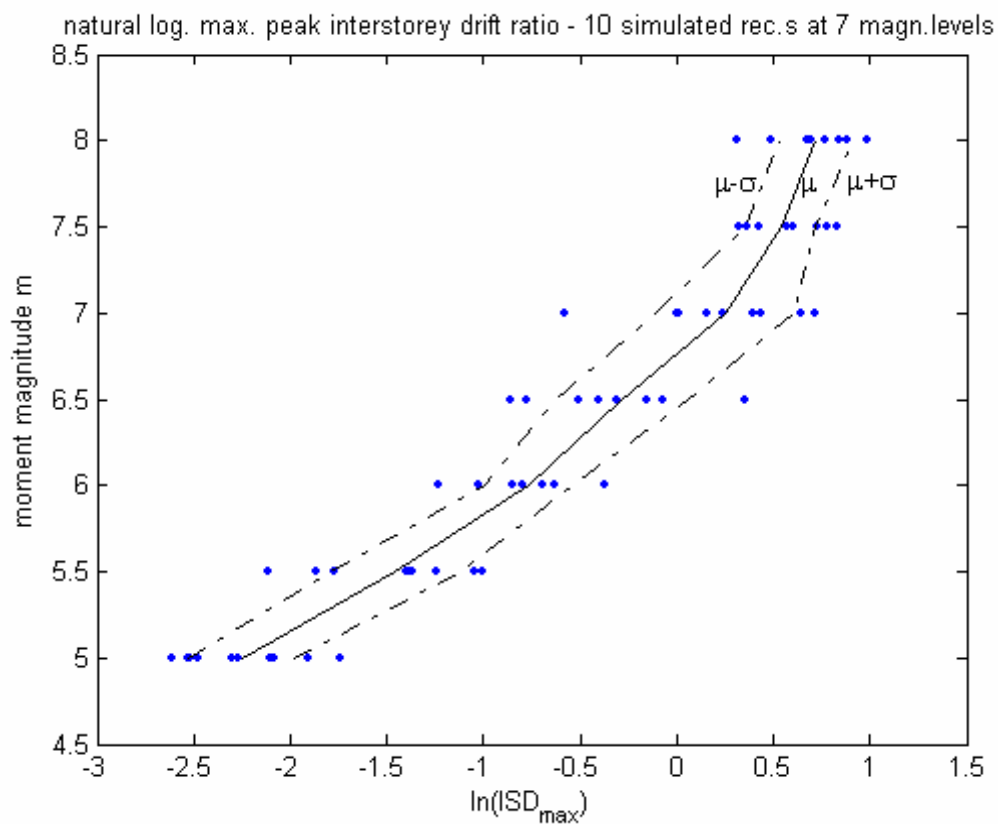


Fig.3.13: Lognormal fit to ISD data, piecewise linear interpolated over hazard levels

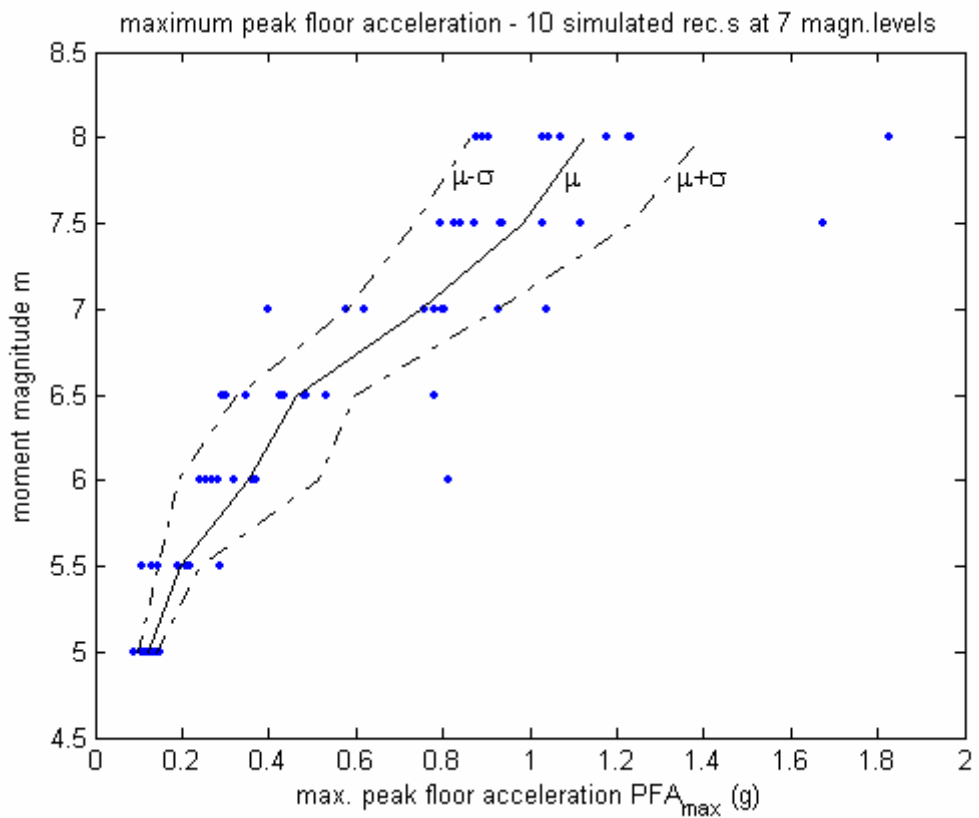


Fig.3.14: Normal fit to PFA data, piecewise linear interpolated over hazard levels

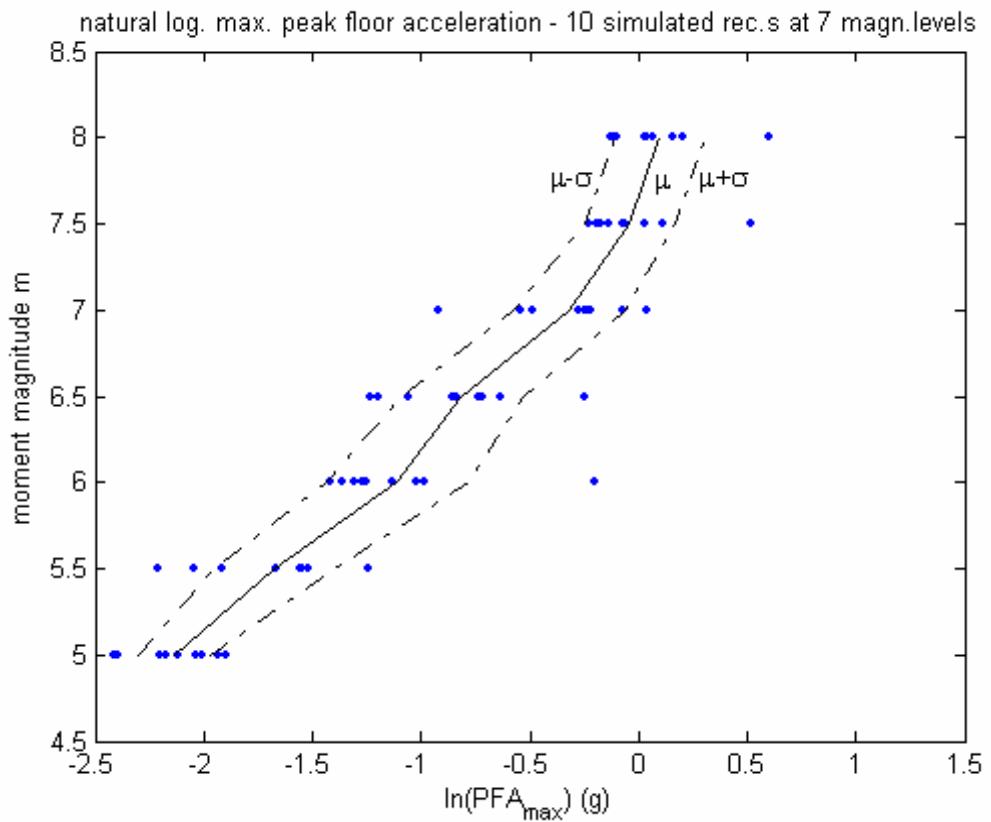


Fig.3.15: Lognormal to PFA data, piecewise linear interpolated over hazard levels

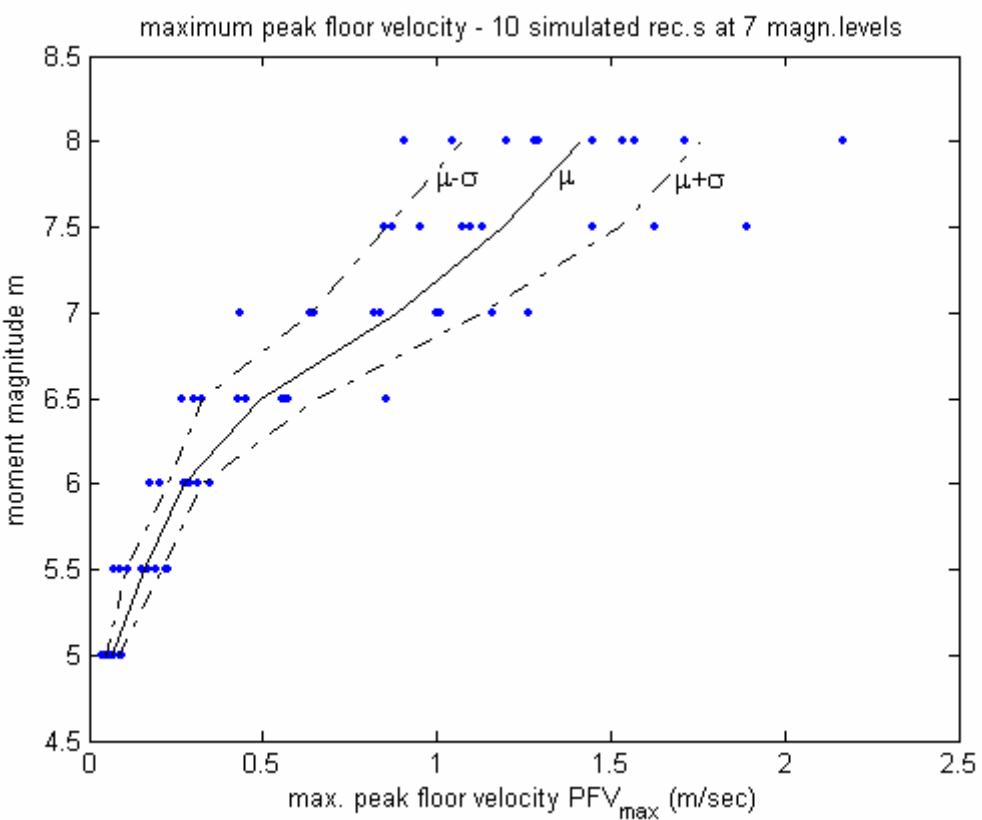


Fig.3.16: Normal fit to PFV data, piecewise linear interpolated over hazard levels

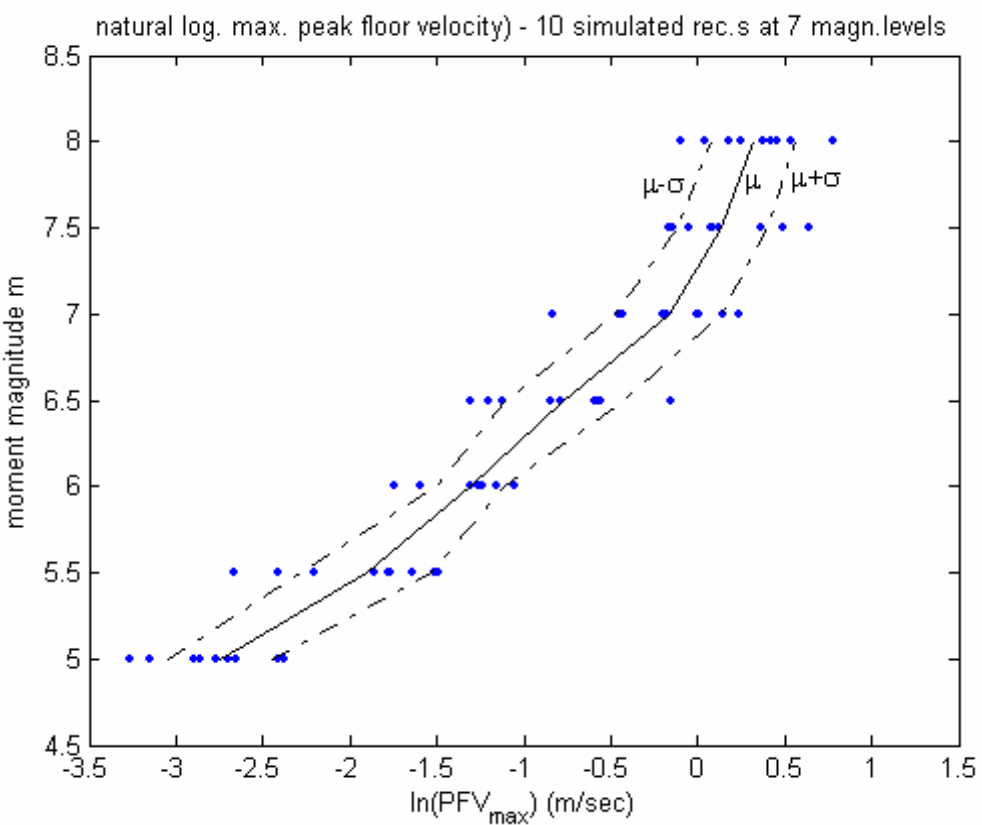


Fig.3.17: Lognormal fit to PFV data, piecewise linear interpolated over hazard levels

3.3.5. Damageability and loss estimate

Monte Carlo Simulation method is used for solution of loss equations given in Table 3.4. Input data is given in Tables 3.7 to 3.9. Cost breakdown information given there is fictive, however, in line with common trends given by (Bazurro and Luco, 2005).

The procedure for simulations follows:

- (1) Lognormal distribution is fit to response governing variable data at the 7 discrete hazard levels between $m=5.0$ and $m=8.0$ as seen in Fig.s. 3.13, 15 and 17. This reveals mean and standard deviation vectors for each response governing variable, namely for ISD, PFA and PFV. So, a total of 6 1×7 vectors in form of $\hat{M}_{R|S}$, $\hat{D}_{R|S}$ are obtained, whereas $R=ISD, PFA$ and PFV .
- (2) Overall structural and component damageability data is gathered. Refer to Tables 3.7 to 3.9 for this data. The sources for parameters are indicated there. Since a lognormal distribution is fit for damage state membership, the natural logarithm of the mean values are taken. So, for each component, two $n \times 1$ vectors are obtained: $\hat{M}_{R|D}$, $\hat{D}_{R|D}$. Those are, respectively, mean and standard deviation damageability vectors, with $R=ISD, PFA$ or PFV depending on performance group of component (refer to Table 2.7 for the concept).
- (3) Random vectors are generated from vectors $\hat{M}_{R|S}$ and $\hat{D}_{R|S}$. Then, for each element of generated vector, damage state membership probabilities are obtained in accordance with Eq.45. In this application, 10^6 simulations are used. The algorithm implemented in MATLAB is given in ANNEX.I.

Results are presented in following section 3.3.6.

STRUCTURAL SYSTEM DAMAGEABILITY							
C/ C _T	ST	DS	μ	σ	R _R		
Steel moment frame system	0.20	ISD	1	0.0288	0.64	0.3	Immediate occupancy
			2	0.0499	0.65	0.8	Life Safety
			3	0.08	0.30	1.3	Collapse Prevention
			4	0.10	0.001	1.5	Deterministic collapse

Table 3.7

NONSTRUCTURAL COMPONENTS' DAMAGEABILITY							
Comp. Type	C/C _T	ST	DS	μ	σ	R _R	
External Walls	0.10	ISD	1	0.0039	0.17	0.5	Patch need
			2	0.0085	0.23	1.2	Rplc. need
Windows	0.01	ISD	1	0.0230	0.28	1.8	Crack,rplc. need
Door	0.01	ISD	1	0.0350	0.25	1.1	Rplc. Need
Deck	0.10	Not considered due to low damageability					
Stair	0.01	Not considered due to low damageability					

Table 3.8: All data from (Beck et al., 2002).

CONTENTS' DAMAGEABILITY							
Content Type	C/ C _T	ST	DS	μ	σ	R _R	
Diesel generator *	0.30	PF A	1	0.87	0.51	0.10	Inoperative,service&reinstall
Motor control center *	0.15	PF A	1	0.79	0.52	0.10	Inoperative,service& reinstall
PC's **	0.05	PF A	1	3.5	0.25	0.10	Monitor falls from desk, rplc
			2	5.2	0.4	1.0	Monitor and unit fall, rplc
Automatic sprinklers**	0.05	PF A	1	4.2	0.87	1.56	Fractured pipe or head
Furniture	0.01	Not considered due to negligible value and low damageability					

(* (Swan and Kassawara, 1998), ** (Porter et al., 2001))

Table 3.9

Abbreviations: C / C_T : restoration cost of component to total facility value, ST : sensitivity type, DS : damage state, μ : mean damage state capacity, σ : standard deviation of damage state capacity, R_R : ratio of restoration cost to value of component (can be >1 due to additional demolition costs and post-earthquake demand surge)

3.3.6. Presentation of results

Significant results for risk management are listed in Table 3.10.

SIGNIFICANT RESULTS FOR RISK MANAGEMENT DECISIONMAKING	
Expected annual loss	0.83%
Expected annual loss due to structural components	0.03%
Expected annual loss due to nonstructural components	0.71%
Expected annual loss due to contents	0.09%
Annual structural collapse probability	0.384x10⁻⁶
Annual death expectancy for single occupant	0.288x10⁻⁶
Annual injury expectancy for single occupant	0.096x10⁻⁶

Table 3.10

The most significant result for risk management purposes is the expected annual loss, obtained as 0.83% of total value. This result can be used for risk management decisions Examples to such decisions are mitigation investment justification and insurance premium determination.

Collapse probability (annual probability of exceeding collapse limit state) is obtained as 0.384×10^{-6} per year. This value is in the same order of magnitude with target breakdown probability for civil engineering facilities, commonly taken as 10^{-6} as stated e.g. by (Porter, 2002).

Injury and death expectancy for a single occupant are obtained respectively as 0.096×10^{-6} and 0.288×10^{-6} per year. These values can be used for life safety verification decisions and for life safety insurance premium decisions.

Death expectancy figure is almost equal to target death expectancy 0.28×10^{-6} obtained by (Porter, 2002) for a fictive design after 1992 and 1994 NEHRP (National Earthquake Hazards Reduction Program, USA) Recommendations. The case studied by (Porter, 2002) was based on weekly 45 hours occupancy –office conditions- in highest seismicity region in USA.

As can be seen in Table 3.10, nonstructural components dominate expected loss, followed respectively by contents and structural loss. Table 3.11 provides a closer insight. It reveals that 86% of expected loss is due to walls, although value of walls is only 10% of facility value. On the other hand, although contents value is 50% of facility value, their share on loss is ca. 10% (the question of what constitutes the “value” of facility and components will not be discussed here).

BREAKUP OF LOSS DUE TO DAMAGE	
Component	% total annual loss expectancy due to damage
Structure	3.6
Walls	86.0
Windows	0.5
Door	0.0
Diesel generator	5.4
Motor control center	3.5
PC's	0.0
Automatic sprinkler system	1.0

Table 3.11

In the above, annual expected values are presented and analyzed. In the following, loss variability will be analyzed at varying hazard and probability levels. This provides also valuable insight to the problem.

According to Fig.3.18 expected loss ratios for respectively 50, 475 and 950 year events are 11%, 18% and 19%. For risk communication and risk acceptability decision purposes, these values can be used alongside with annual expectations.

Fig.3.19 demonstrates the breakup of loss among component types. As can be seen, the dominance of nonstructural loss spans over all hazard levels. $m=5.5$ and $m=6.0$ are respectively lower thresholds for contents' and structural losses. $m=6.0$ threshold for structural loss is typical for engineered modern buildings.

Fig.3.20 and Fig.3.21 provide insight into variation of nonstructural loss over hazard levels. Loss values larger than 100% of component value in Fig.3.21 are due to

additional demolition costs. Same relations for contents are given in Fig.s 3.22 and 3.23, and for structure in Fig.3.24.

Fig. 3.25 depicts variation of damage state probabilities over hazard levels. Considering damage state III, namely the collapse prevention damage state, an abnormality is obvious: Expected collapse probability for $m=7.0$ is exceeding that of $m=7.5$. This is despite monotonic increase of mean response parameters with increasing hazard intensity, depicted in Fig.s 3.12 to 3.17. This abnormality can be explained by the higher dispersion of response at $m=7.0$ level with respect to $m=7.5$ level, demonstrated in Fig.3.26 (see the twist at $m=7.0$). The higher dispersion $m=7.0$ is not coincidental and is related to material modeling: Multilinear material model used is based on a sudden and abrupt transition from elastic to inelastic regime. Where $m=7.5$ simulations lead probably to yielding for all cases, $m=7.0$ simulations may or may not lead to yielding, depending on pulse sequence or other arbitrary reasons. This leads to the increased dispersion of response at $m=7.0$. Detailed analysis of dispersion of response estimates is not the subject of this chapter, for further examples and explanation, refer to Chapter 4.

Fig.3.27 gives dispersion data for all response parameters at varying hazard levels. Similar weaving behavior is observable at lower hazard levels for PFA and PFV. This, on the other hand, can be either coincidental or related to hazard description (so, acceleration and velocity maxima of ground motion simulations). For precise risk assessment procedures, these phenomena should be investigated further. This is to some extent done in Chapter 4.

Finally, Fig.3.28 depicts a performance-acceptance-check according to (FEMA 350, 2000) criteria. This publication reflects the state-of-the-art of performance and reliability based provisions. Referred figure demonstrates the applicability of the presented method for performance acceptance decision.

The depicted linear target curve is bounded by

- (1) immediate occupancy drift criteria of 0.85% for 72 year event (50% in 50 years, annual probability of 0.01376), obtained for the recommended 50% confidence level for IO.
- (2) collapse prevention drift criteria of 4.54% for 2475 year event (50% in 50 years, annual probability of 0.01376), obtained for the recommended 90% confidence level for CP.

Procedure for developing the criteria can be found in (FEMA 350, 2000).

As seen in the referred figure, performance curve is partially in the unacceptable region. So, it can be stated that the overall performance is unacceptable according to (FEMA 350, 2000) criteria. Following statements explain the problem in detail with reference to Fig.3.28:

- (1) for hazard range $m=6.5-7.5$, it is likely -with 50% confidence- that the subject structure will not satisfy the FEMA-SAC performance criterion. That implies that excessive (more than acceptable) damage and loss can be expected. It can be stated with confidence that the problem is only related to material loss and not to life safety.
- (2) for the range of hazard levels significant for life safety, the structure satisfies the criterion with a significantly ample margin.

It is worth to note that the range over $m_u=8.0$ (1649-year event, annual probability of exceedance 0.6×10^{-3}) is not covered by hazard assessment. This can be noticed as a critical point to solution provided above. In applications, considering 2475 year event as m_u would be a good practice to conform to state-of-the-art conventions. However, in the investigated case, no significant implications to results should be expected, as explained in the following:

- (1) Since probabilities at $m_u = 8.0 - m_{max} = 8.1$ hazard range are very low; significant effects of neglect of hazard range $8.0 < m < 8.1$ to expected loss should not be expected.
- (2) There is an ample margin between performance curve and criteria around m_u . This can comfortably be extrapolated to m_{max} level. So, performance can be considered to be on the acceptable side at the considered range. As a result, life-safety considerations are not effected by neglect of hazard range $8.0 < m < 8.1$.

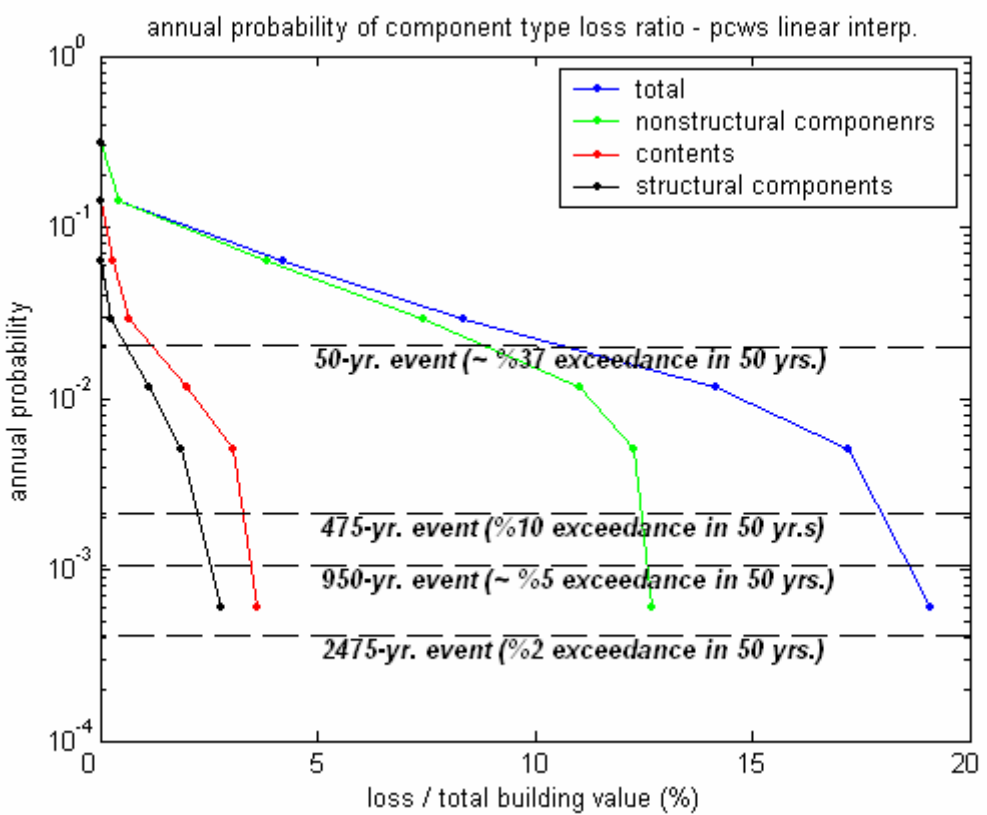


Fig.3.18

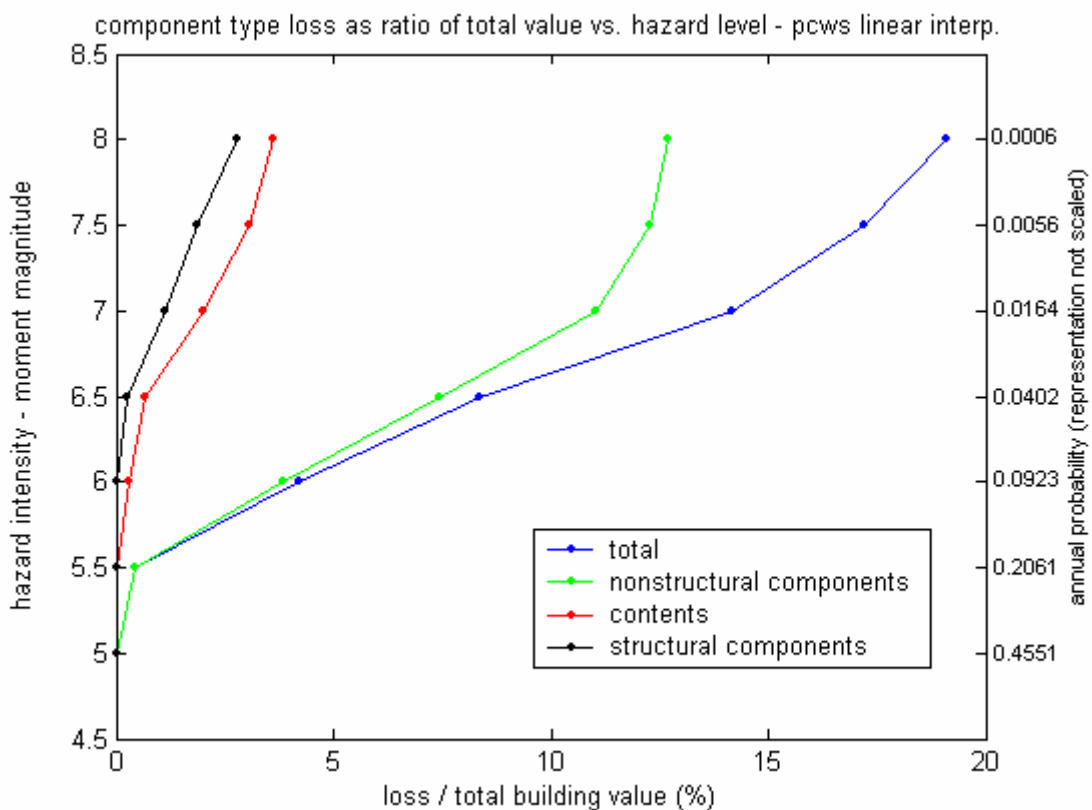


Fig.3.19

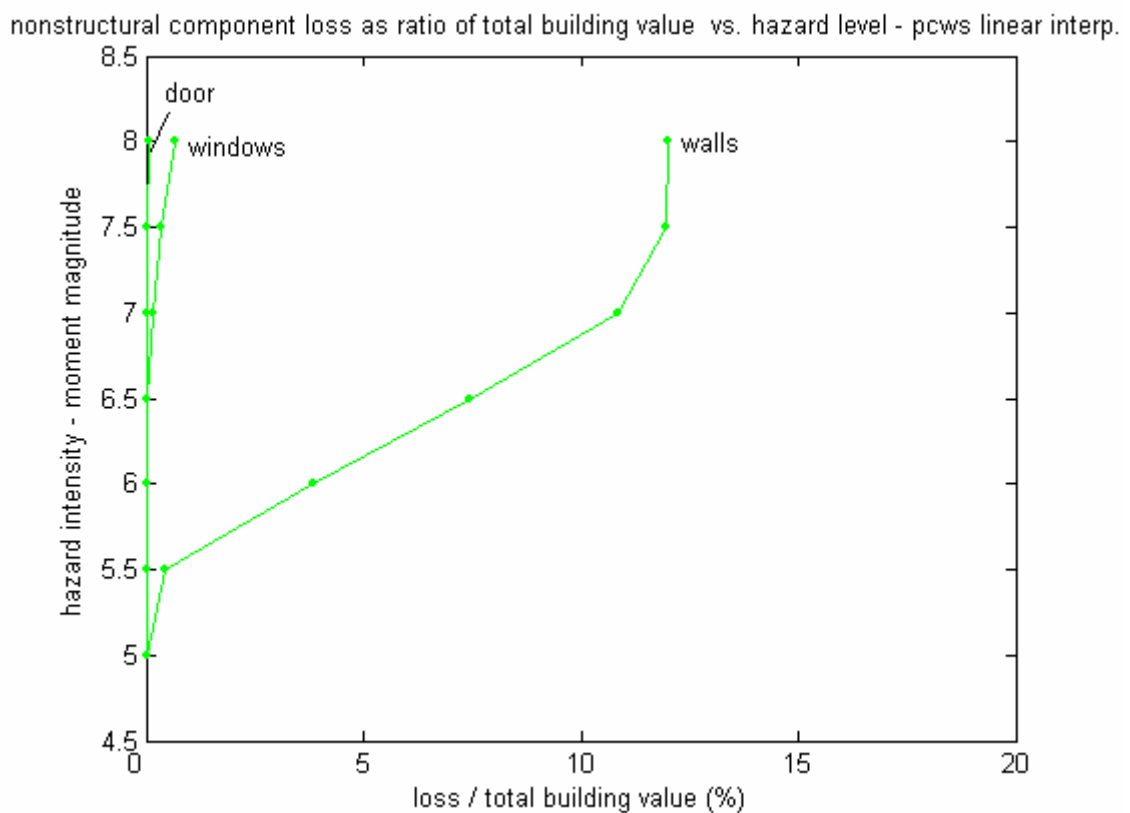


Fig.3.20

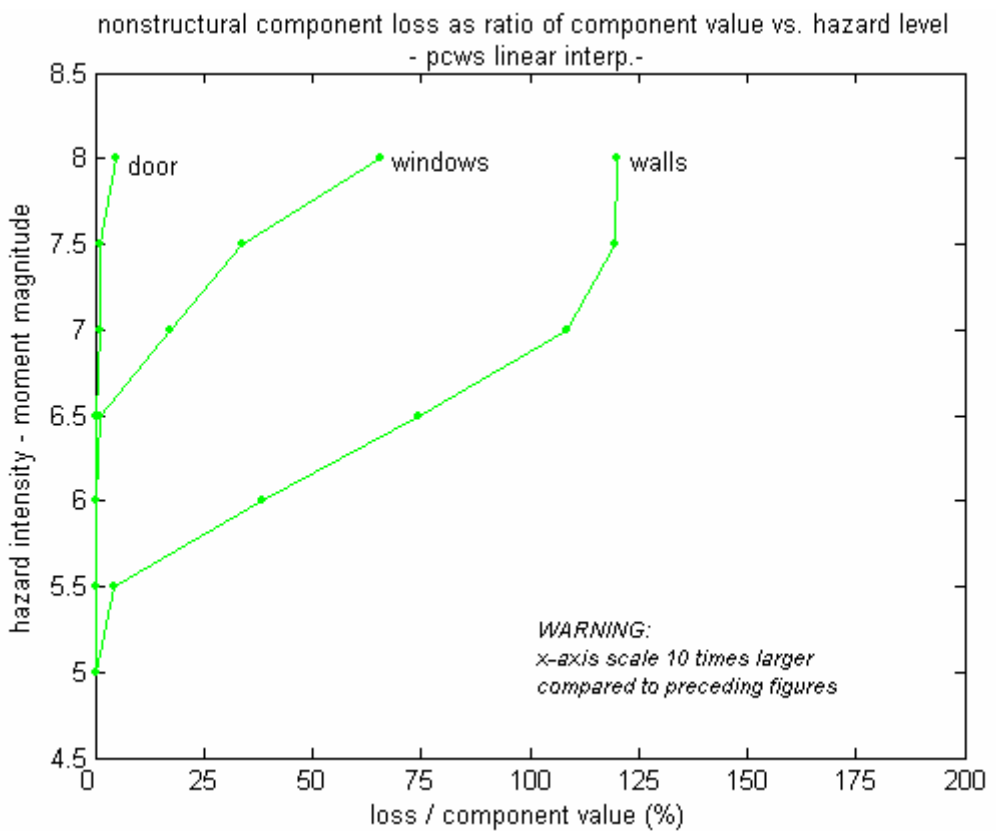


Fig.3.21

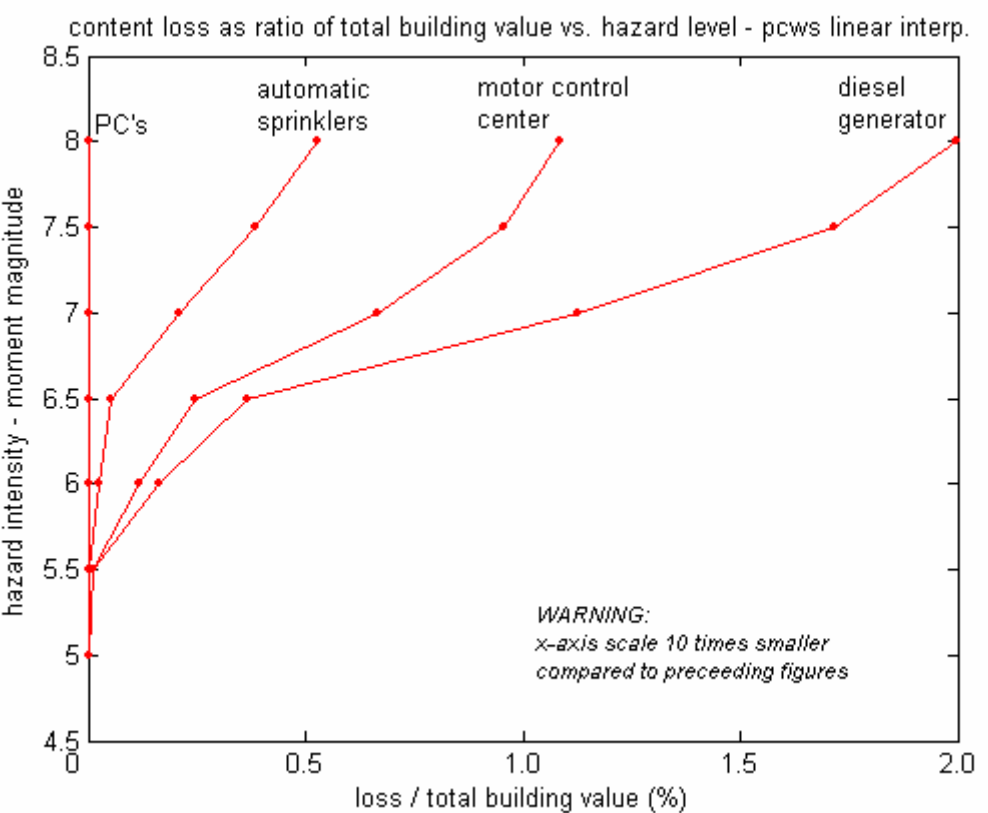


Fig.3.22

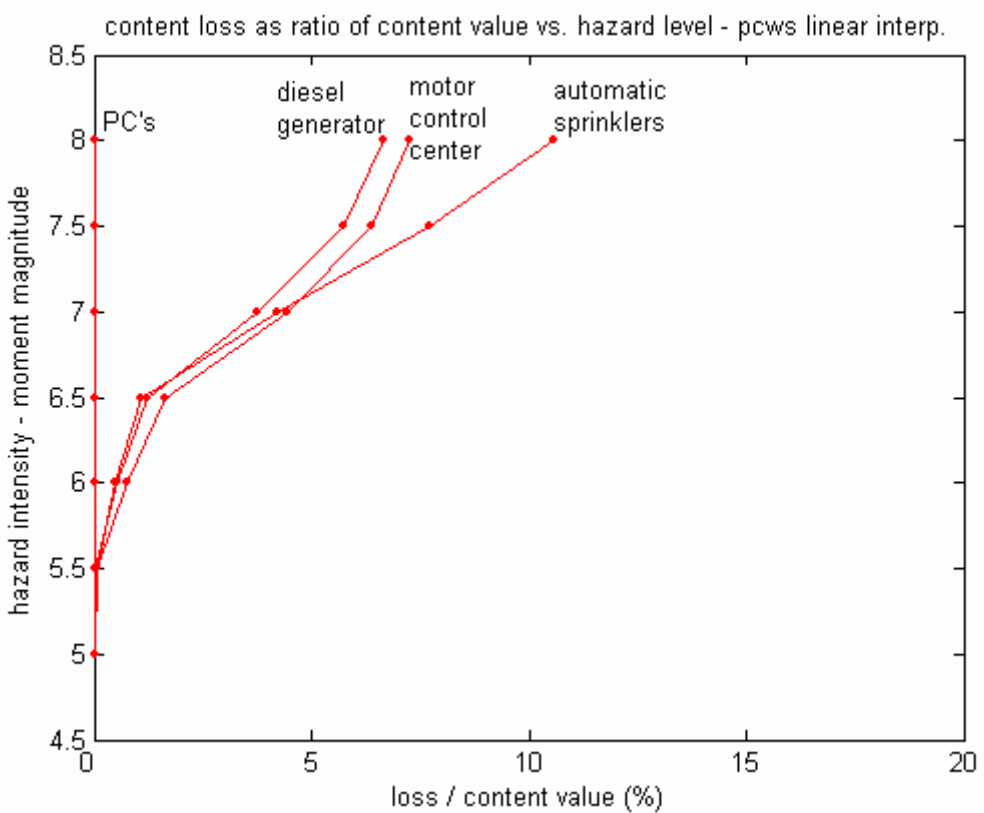


Fig.3.23

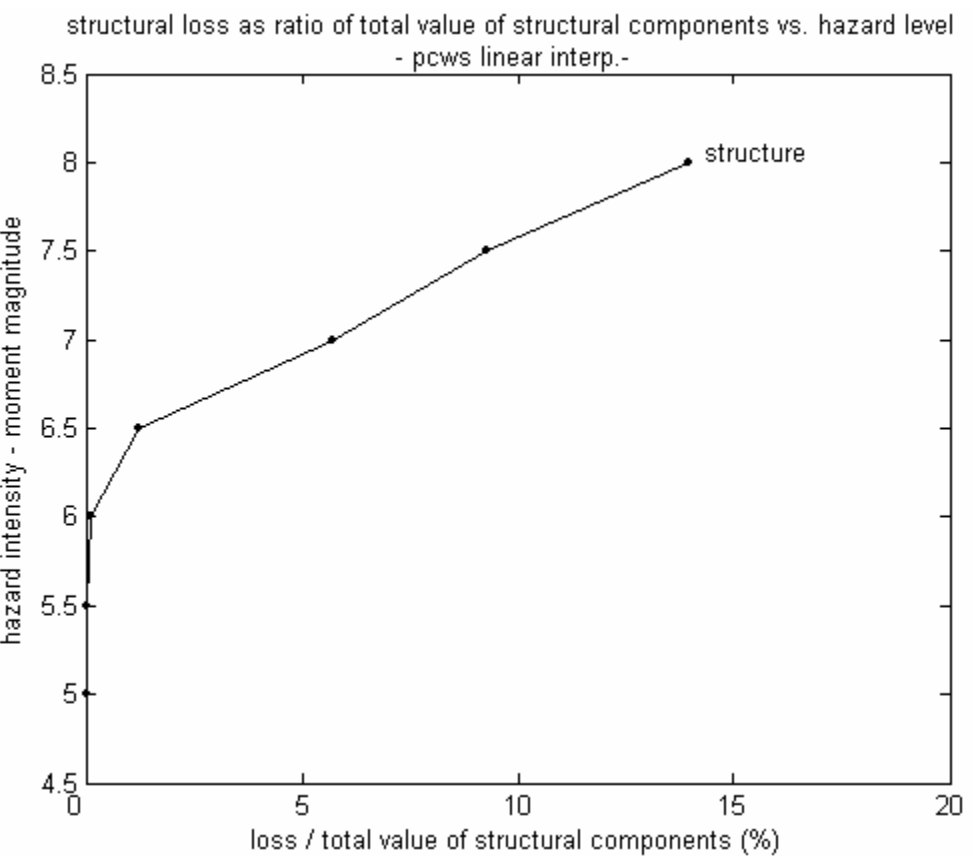


Fig.3.24

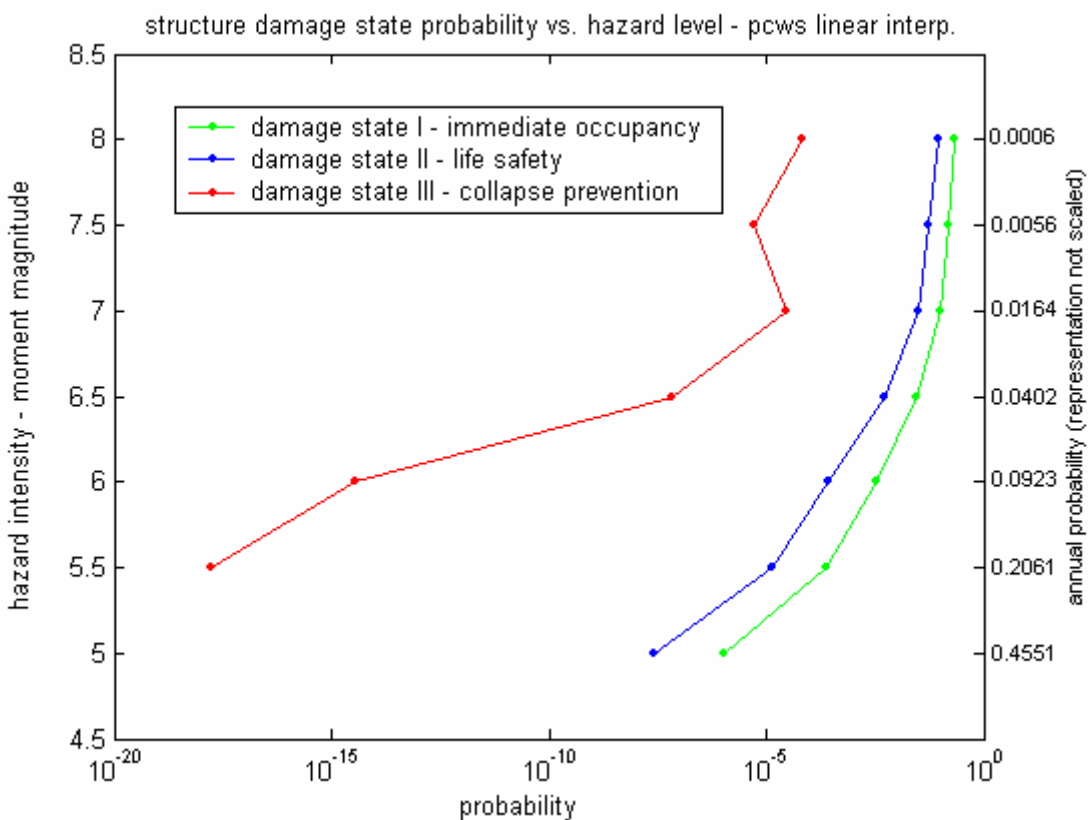


Fig.3.25

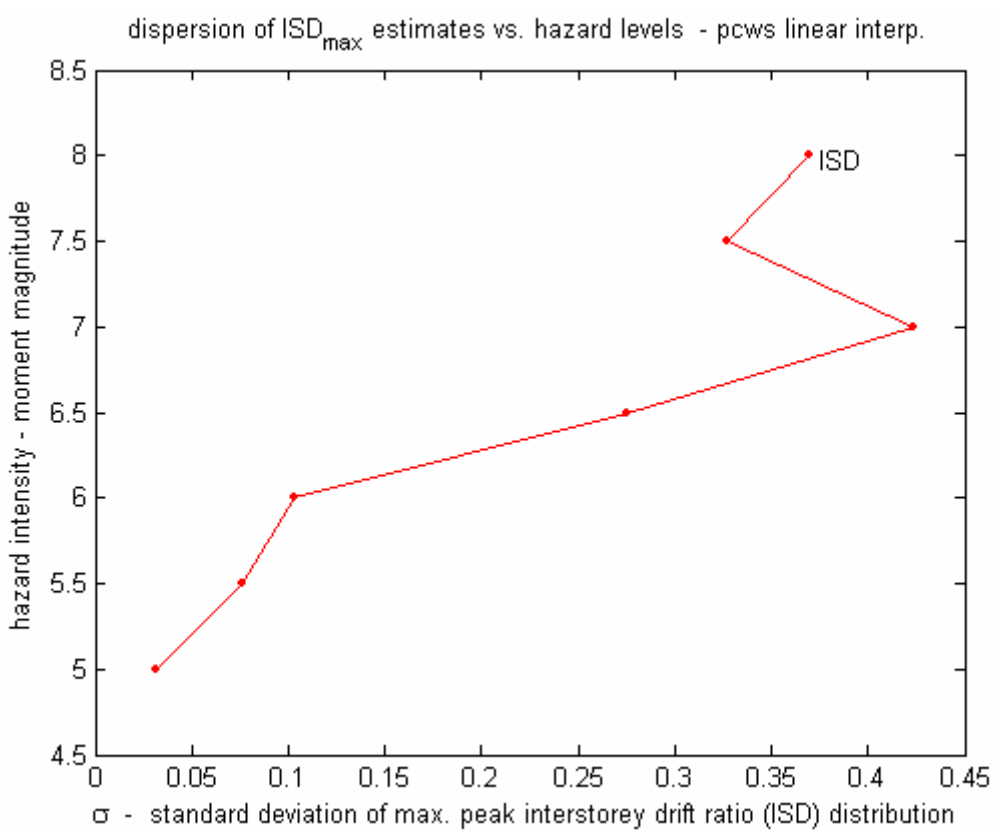


Fig.3.26

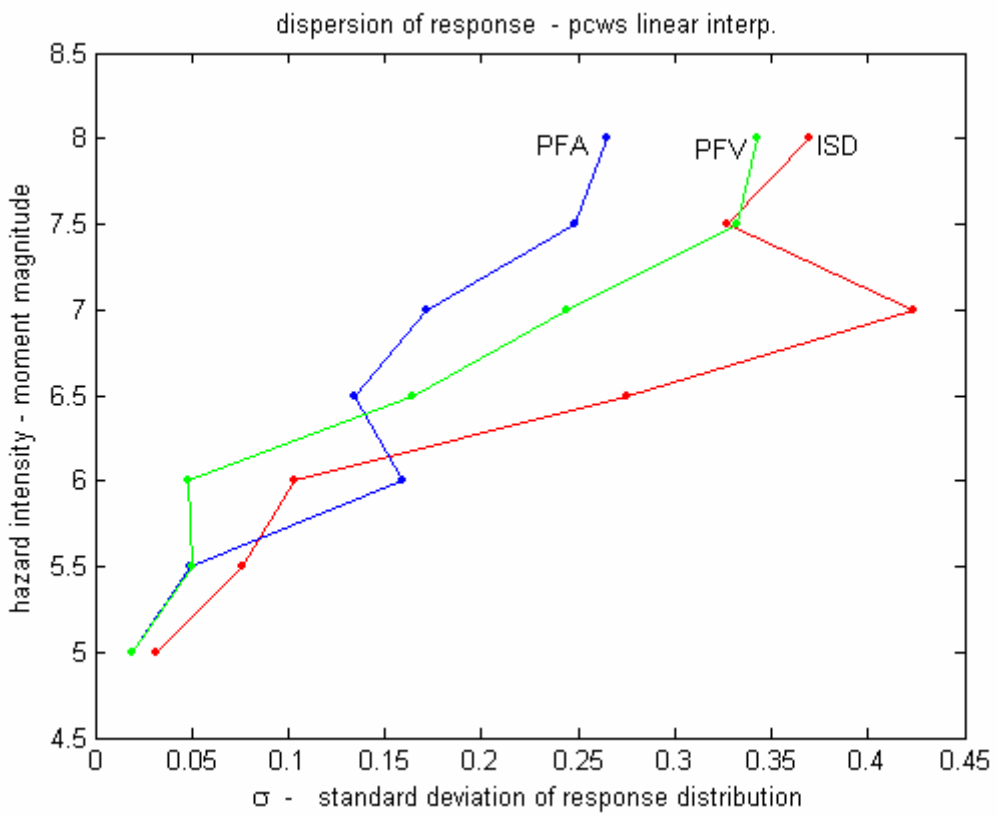


Fig.3.27

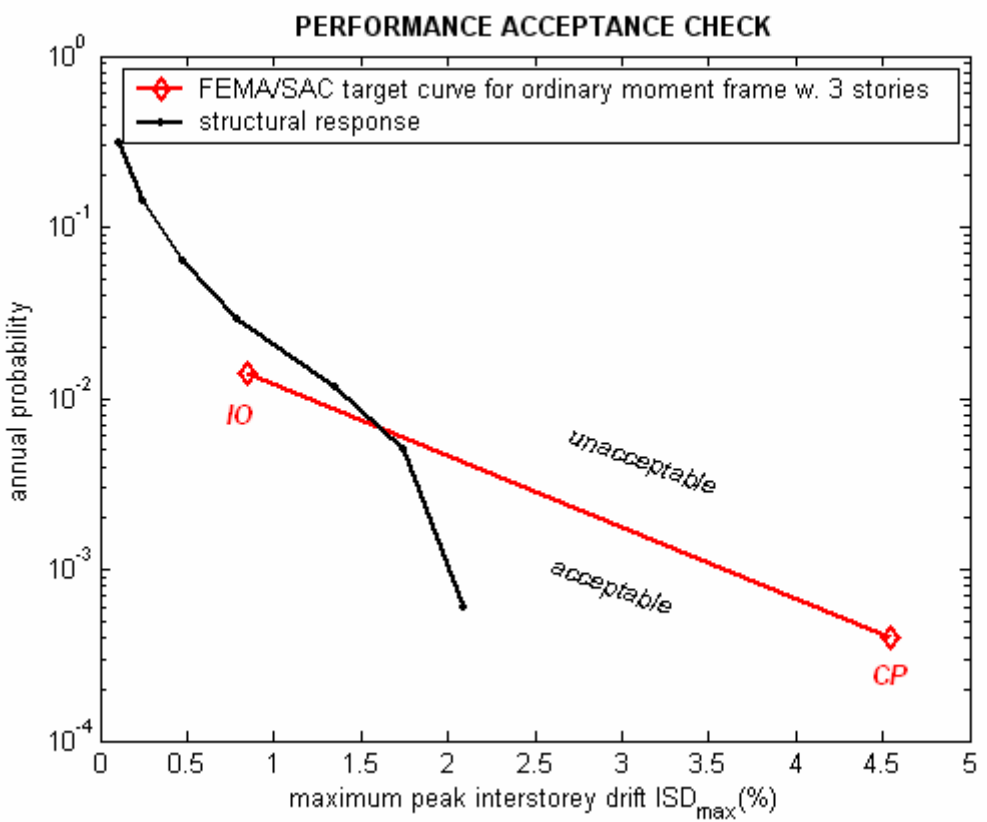


Fig.3.28

Chapter 4. Investigations on sensitivity to strain-rate-dependency of seismic loss estimates in steel frame structures

4.1. On model sensitivity and motivation of the investigation

As stated earlier, an important question of risk assessment schemes is that of model sensitivity. This is valid for natural hazards' risk assessment for civil engineering facilities as well. In this context, model sensitivity refers to sensitivity of loss estimates to mathematical modeling of physical phenomena.

Each model is a simplification of reality with assumptions, generalizations, inductive and deductive data. Each step of risk assessment task involves question of model selection. There are no upper bounds to better models, but to resources, capabilities and project time. So, one has to weigh between accuracy and economy of his/her model.

In this section, an example model selection problem is analyzed. The problem considered is related to seismic response assessment. More exactly, the sensitivity to strain rate-dependency modeling is analyzed. This is done for steel moment resisting frame structures, which is a common and efficient structural type for seismic regions.

It is well known that high strain rates alter yielding characteristics of steel. Analyses have shown that severe strong motion can lead to such rates as well. Despite an existing material model by (Böttcher, 2002) accounting for the phenomenon, there have been few investigations on implications of the phenomena on seismic response of steel frame structures.

The main question which will be investigated in this section is if it is worth modeling strain-rate-dependency for risk assessment of low-to-medium rise steel moment resisting frame structures in high seismicity regions.

4.2. Rate dependency as a commonly neglected phenomenon in seismic response assessment

Steel frame structures can undergo maximum strain rates ($\dot{\epsilon} = d\epsilon / dt$, time variation of strain) in the order of 10^{-1} sec⁻¹ during severe strong motion. An example is given in Fig.4.1. Under such high strain rates; structural steel demonstrate increased yield stresses relative to static loading (both in terms of mean yield limit σ_y and mean

average yield stress $\bar{\sigma}_{pl}$). This increase is due to change in microphysical processes which dominate plastic behavior.

Fig.4.1: Strain rate time history at a beam cross section of a 3-storey steel frame structure subjected to 12.11.1999 Düzce (Turkey) record (PGA=0.822g).

The dependence of plastic metal behavior on loading velocity is termed as rate-dependency. This term will be used in the following specifically for alteration of plastic parameters of structural steel under high strain rates during earthquake loading.

Strain rates at a given cross section of a frame structure are related to ground shaking velocity. Seismic loading is typically marked with sudden and rapidly changing velocities. This translates almost linearly to local strain rates in critical cross sections as shown in Fig.4.1. Moreover, strain rate show high variability along the height of the structure (among components and at cross section with relative location from center of inertia).

The practical problem related to rate dependency arises in two contexts:

- (1) conventional material models do not account for the phenomena,
- (2) material parameters utilized in structural design are gathered in static or quasi-static experiments with no consideration of rate-dependency effects, as stated by (Böttcher 2002).

Increased strength due to rate dependency effects can be comprehended as beneficiary. However, rate dependency has possible negative implications for global and local structural response as well. Examples are increased drift, increased ductility demand in connections due to beam overstrength and decreased connection ductility due to inelasticity concentrations.

The physical phenomenon rate-dependency in structural steel is known since more than one century according to (Böttcher 2002).

Microphysical explanation for the phenomenon is the gradual change of deformation patterns at molecular level depending on loading velocities. For detailed treatment, refer to (Böttcher 2002). The same author mentions that the effects are negligible at strain rates less than 10^{-4} . Accordingly, we can list the possible types of dynamic loads under which rate-dependency is of relevance to structural response as in Table 4.1 and Fig. 4.2.

Considering steel frame structures under seismic loading, implications of rate dependency on structural behavior can be analyzed at three levels:

- (1) material,
- (2) local,
- (3) global.

Material level refers to the governing stress-strain relation determined by microphysical processes (molecular, atomic) which will not be addressed in this work. Local level comprises both structural component behavior (columns, beams, connections, etc.) and the cross-sectional-behavior of given components. Global level refers to overall structural response formed by individual component action and interactions between them.

In the following, rate dependency effects to seismic response of steel moment resisting frame structures at these three scales are presented.

Parameter	Strain rates	Duration (μs)	Loading Velocity (m/s)	$\sigma_y^{\text{dyn}} / \sigma_y^{\text{stat}}$		Material behavior
	$\dot{\varepsilon}$ (1/s)			Comp.	Tens.	
Earthquake	10^{-3} - 10^0	10^7	-	1-1.3	1.8	Visc. el.-pl.
Ocean waves	10^{-3} - 10^{-1}	10^6	<5	1-1.3	1.7	Visc.-el.
Collapse loads	$<10^1$	10^6	<10	1-2.0	2.3	El.-pl.
Plane crash	10^{-2} - 10^2	10^5	<90	1-1.3	2.5	El.-pl.-dam.
Vehicle crash	10^{-2} - 10^2	10^4	<30	1-1.3	2.5	El.-pl.-dam.
Blast	10^1 - 10^3	10^3	<4000	1-2.0	5	El.-pl.-dam.
Conventional arms	10^2 - 10^3	-	-	1.5-2.0	-	Dam.
Contact explosion	$<10^8$	10^1	<9000	-	-	Hydro.-dam.
Comet impact	$<10^8$	10^1	>12000	-	-	Damped

Table 4.1: Engineering loading types with relevance to rate dependency. Given values are compiled by (Gebbeken and Ruppert, 1999) from various publications. Our dynamic time history analyses proved the strain rate range for earthquake loading.

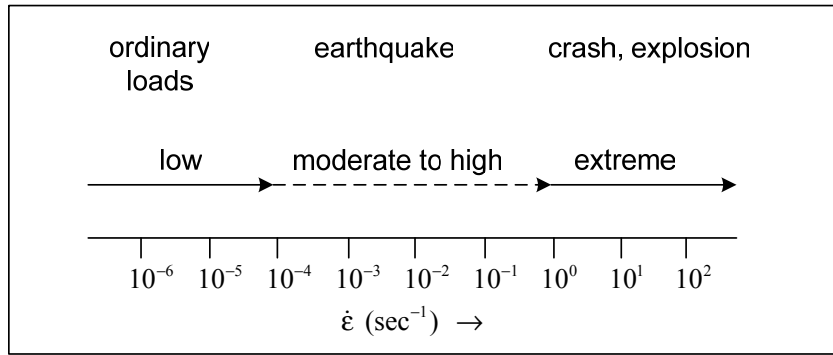


Fig. 4.2: Ranges of strain rates after (Böttcher et. al 2003)

4.2.1. Rate dependency at material level

Rate dependency phenomenon as described above is per definition related to deformation controlled experiments. In cyclic force-controlled experiments, a mirror image is observed: dependency of strain growth on stress rate $\dot{\sigma}$ (higher stress rates lead to less strain growth). This is termed as ratcheting phenomenon.

Both strain-rate-dependency and ratcheting are termed together as rate-dependency and have same microphysical causes. Moreover, it is shown that both are marked with identical qualitative patterns, as stated by (Böttcher, 2002). Since the focus of this work is on seismic loading, exclusively strain-rate-dependency will be discussed.

(Böttcher, 2002) demonstrated rate dependency phenomenon on steel type S355 with uniaxial quasi-static rod experiments. The experiment series included varying loading schemes (deformation-, strain- or force-controlled, monotonic or cyclic). Pronounced rate-dependent effects are verified independent of preloading level and loading type. The effects are observed increasingly from $\dot{\epsilon} = 10^{-4}$ to $\dot{\epsilon} = 10^{-2}$ ($\dot{\epsilon} = 10^{-2}$ was the maximum strain rate in referred experiments. It is also commonly accepted upper limit for isothermal assumption in steel).

It was shown that increased strain rates lead to increase in following parameters:

- (1) initial yield strength (σ_y),
- (2) average hysteresis stress (σ_{ave}),
- (3) length of yield plateau (as shown in Fig. 4.3).

For revision of dominant phenomena and relevant terms referred, see Fig. 4.4.

Beyond the changes in above stated parameters, the shape of stress-strain curves remained qualitatively stable with varying strain rates. No significant effects on initial elastic module and in linear-elastic range are observed. Strain-rate memory effect (memory of a previous strain-rate) is found to be negligible. Preloading mitigates rate-dependency but negligibly. Rate dependency effects are negligible in quasi-static strain-rate range; $\dot{\epsilon} < 10^{-4}$. It was also shown that multi-axial effects on rate dependency are negligible.

For details on rate-depending material testing, refer to (Bruhns and Fossa, 1996).

Despite the observed effects, rate-dependency remain a secondary factor in forming plastic behavior in comparison to the more dominant factors; loading intensity and sequence and number of load cycles.

(Böttcher, 2002) developed a time-dependent material model to account for the phenomena in finite element structural analyses. The model parameters were derived from the referred experimental results. This model will be named MM4 in the following.

MM4 combined two aspects:

- a time-dependent equilibrium definition,
- two-surface material model by (Scheibe, 1990) and (Reininghaus, 1994).

Scheibe-Reininghaus model will be named MM3 in the following. MM3 was based on a quadratic expression to define tangent modulus in hardening sector. It allowed exact computation of stress-strain curve of steel up to a strain level 8%.

For detailed treatment of Scheibe-Reininghaus model (MM3), refer to (Scheibe, 1990) and (Reininghaus, 1994), for the time dependent material model (MM4) to (Böttcher 2002), in summary by (Böttcher et al. 2003).

MM4 accounts for rate dependency effects up to strain rates of $\dot{\epsilon} = 10^{-2}$. It presents a unique opportunity to account for rate dependency effects in practical finite element dynamic analyses.

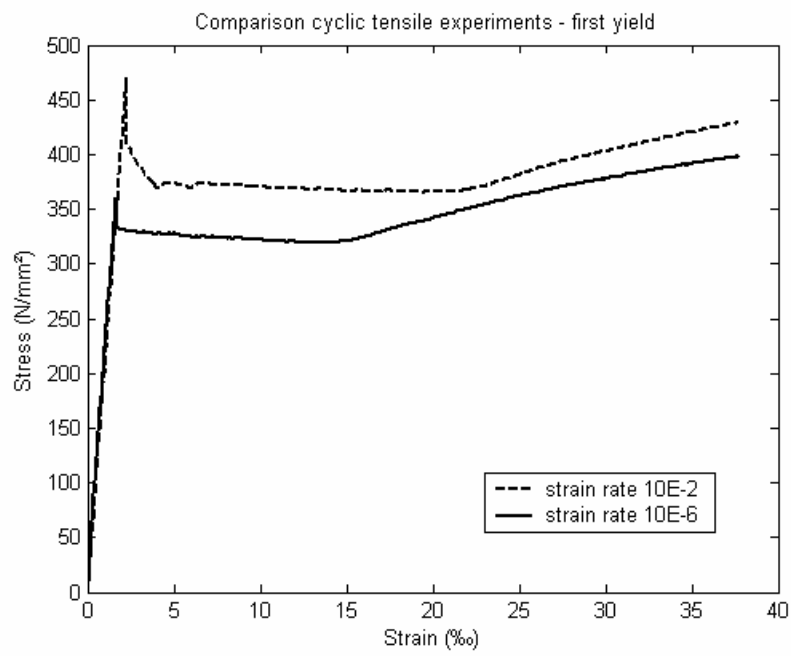


Fig. 4.3: Strain-rate dependency of initial yielding up to tensile strength observed in tensile experiments on rod specimens by (Böttcher, 2002).

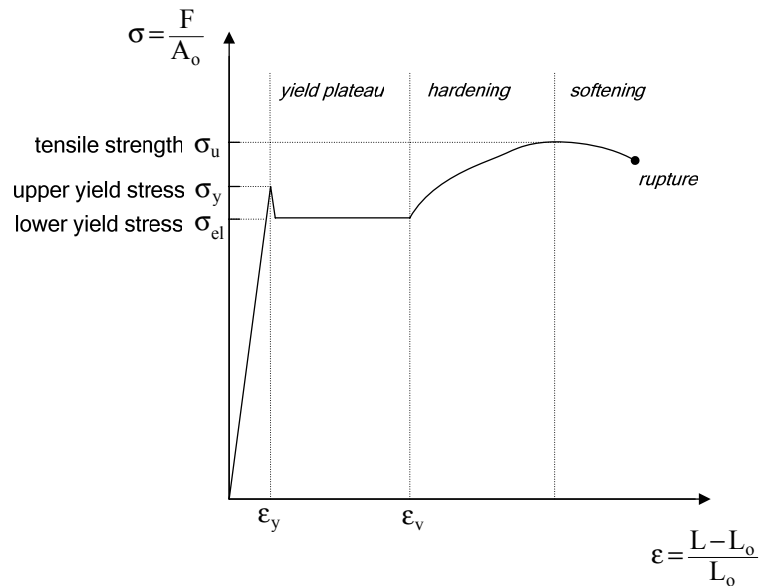


Fig. 4.4: Idealized stress-strain relationship of steel at initial loading (not scaled) (after Böttcher, 2002)

4.2.2. Local level (component and cross-section)

(Böttcher et al. 2003) mentions that the rate dependency effects were previously not considered in experimental fragility analysis in earthquake engineering.

In cyclic experiments, intensity and loading sequence are usually varied, but loading velocity and frequency was neglected. Recent examples are quasi-static tests by (Sugimoto et al., 2001) and (Jones et al., 2002).

(Note: cyclic experiments are used for investigation of e.g. moment-rotation behavior and rotation capacity of connections, low-cycle fatigue due to repeated plastic excursions).

Unexpected damage in steel frame connections in Northridge (USA, 1994) and Kobe (Japan, 1995) earthquakes gave impulse to consideration of rate dependency within experiments on structural components.

(Mazzolani, 2001) reports European experiments on frame structures. Those proved reduction of life-time due to rate-dependency effects in cyclic loaded moment resistant connections. The cause for this can be explained sequentially as in the following:

- (1) increased strain rates ($\dot{\epsilon}$) lead to increased σ_y/σ_u (yield limit to tensile strength ratio)
- (2) increased (σ_y/σ_u) lead to local concentration of inelastic deformations near connections
- (3) concentration results in higher local strains and strain rates at given global drift levels, which in turn leads to less ductile connection behavior.

(Böttcher, 2002) observed in a series of experiments on holed plate sections that rapidly changing loading velocities lead to sudden and significant changes in component behavior.

Experimental results after both (Mazzolani, 2001) and (Böttcher, 2002) verify that material-level rate dependency translates significantly to component behavior.

A previously not researched question is the implications on local sectional ductility at plastic hinges. Previous plastic hinge models assumed uniform yield limits all along the cross-section. This assumption can be questioned considering that flanges undergo larger strain rates than the central regions.

4.2.3. Global scale

The author of this work has found no publications dealing explicitly with rate dependency effects on seismic global behavior of steel frame structures. Exceptions are preliminary efforts in (Wichers, 2001) and (Böttcher, 2002).

Seismic response analysis reports and steel material models do not consider the phenomenon, e.g. (Fragiacomo et al. 2004), (Sivaselvan and Reinhorn, 2000). Seismic design codes do not refer to the phenomena and there are no indications that rate dependency is considered in their development. Several works dealing with explosion loads address the phenomena, e.g. (Gebbeken and Ruppert, 1999).

In the previous section, local effects of rate dependency was discussed. Deriving from these, one can suggest that rate dependency would lead in global scale to:

- (1) Increased deformations,
- (2) Decreased ductility.

In this work, only hypothesis (1) will be investigated by comparison of analyses results carried out with and without rate dependency consideration.

The criteria for hypothesis (1) is global deformations. This can be measured by maximum peak interstorey drift, peak floor acceleration and peak floor velocity. Those are also indicators for structural and nonstructural seismic damage and thus loss as stated previously. So, this enables to draw conclusions on implication of rate dependency on loss estimates, as well.

Considering the not investigated hypothesis (2), the mechanisms which lead to decreased ductility can be twofold;

- (i) Migration of plastic hinges from their ideal location (beam ends with a secure distance from connections) to relatively brittle connections due to beam overstrength caused by rate dependency, or,
- (ii) Decrease in individual component ductility (of connections, beams or columns).

4.3. Investigation on rate dependency sensitivity of seismic response of a steel frame under severe strong motion

To remind, subject matter is if rate-dependency effects deserve consideration in material models used in seismic response and loss analysis for steel structures. In other words, the aim is to verify or reject the common neglect of the phenomenon.

This question will be investigated by comparative analysis of simulated response of a 3-storey steel frame computed with varying material models under several severe strong motion records.

The results should be valid for similar structures (short storey steel moment resisting frames – up to ca. 5 storeys). Conclusions may not be valid for taller and more flexible structures. It is presumed that question of redundancy is irrelevant for rate-dependency, so the results apply to similar multi-bay structures.

4.3.1. Example structure

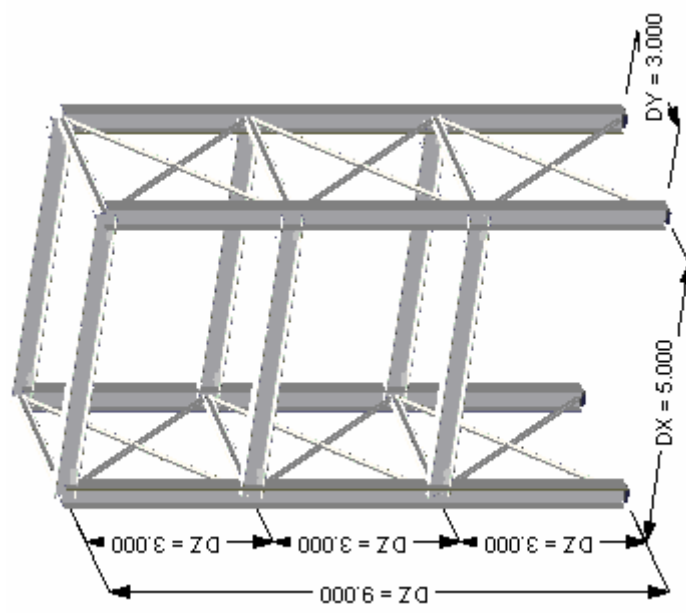
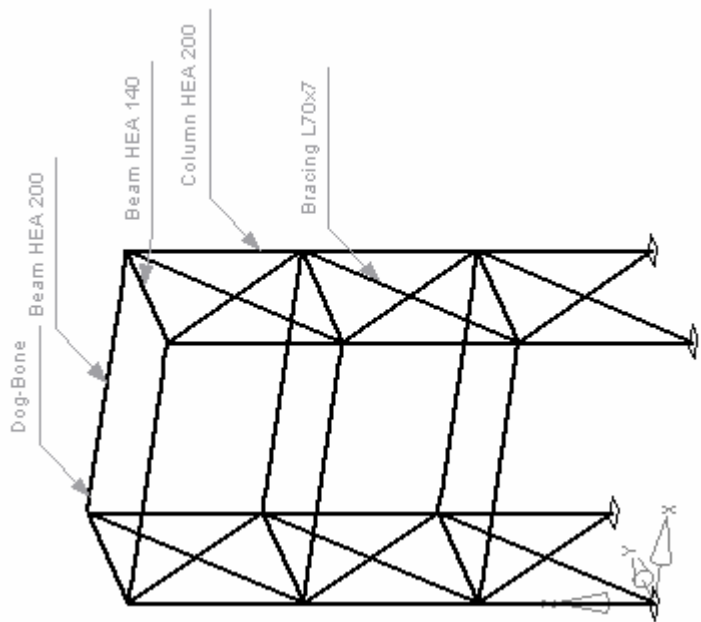
The structure under consideration is a 3-storey steel frame, with a storey height of 3m. The structure is depicted in Fig.s 4.5 to 4.9.

In X-axis, structural system consists of two one-bay moment resisting frames with haunched beam ends (dogbones). Baywidth is 5m. In Y-axis, there are two one-bay centrically cross-braced frames. Baywidth is 3m. Profiles are respectively HEA200 (columns), HEA 200 with 80% haunched ends (X-axis beams), HEA140 (Y-axis beams), L70x70 (Y-axis diagonal braces). Strong axis of columns is X axis. Beams are placed with their strong axes in Y axis.

As non-structural components, a reinforced concrete deck of 0.2m thickness and solid brick outer walls of 0.2m thickness are assumed.

Perfect rigidity of beam-column connections and column bases and ideally perfect decoupling of walls and decks from structural components are assumed.

Steel profiles are of type S355 according to EUROCODE 8 (previous notation: St52, modulus of elasticity=209000 N/mm², shear coefficient=0.3, density=7.85 t/m³). Density of deck concrete is 25 kN/m³. Density of solid bricks is 15 kN/m³. Live loads are 2 kN/m² (as given by EUROCODE 2 for office buildings).



Figs. 4.5, 4.6: 3D views of the structure

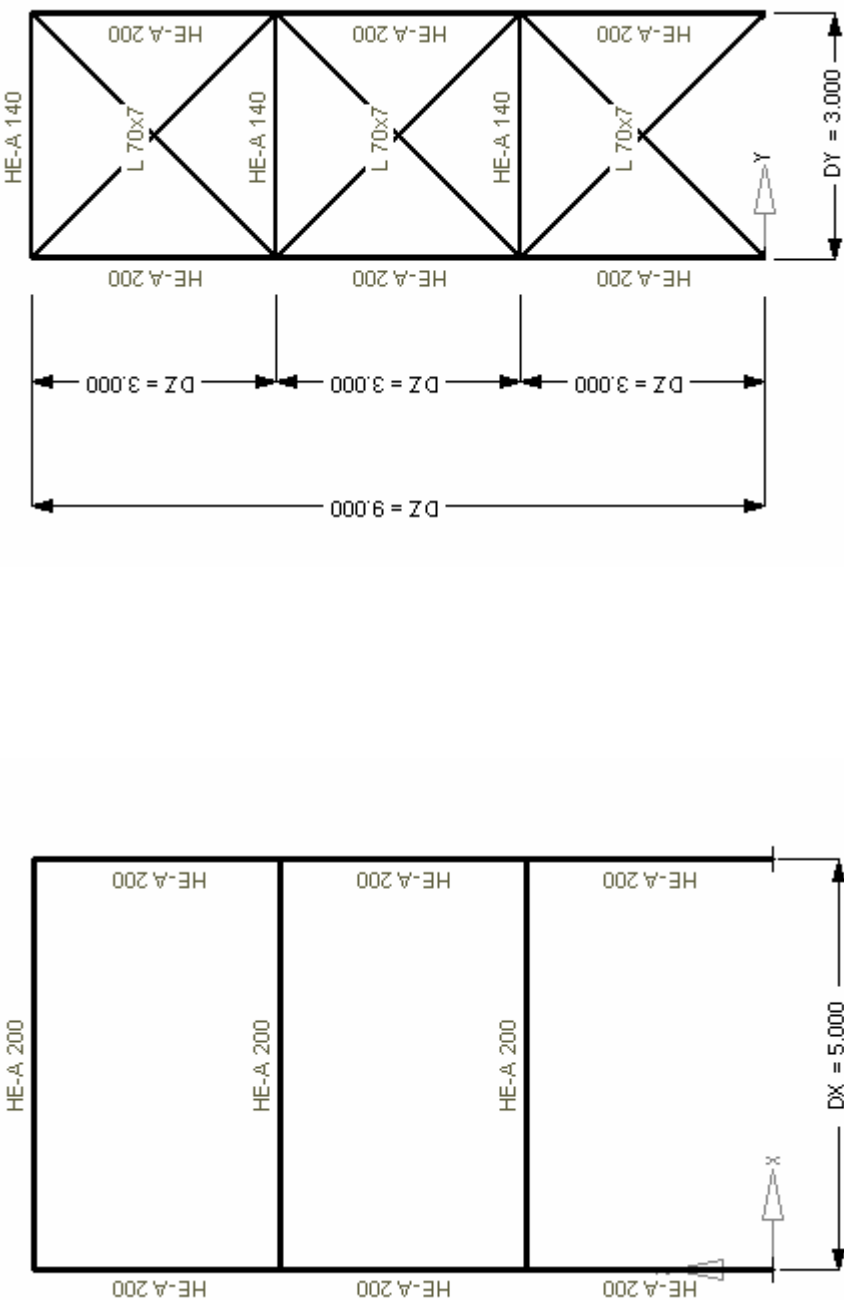


Fig.s. 4.7, 4.8: Sectional views of the structure

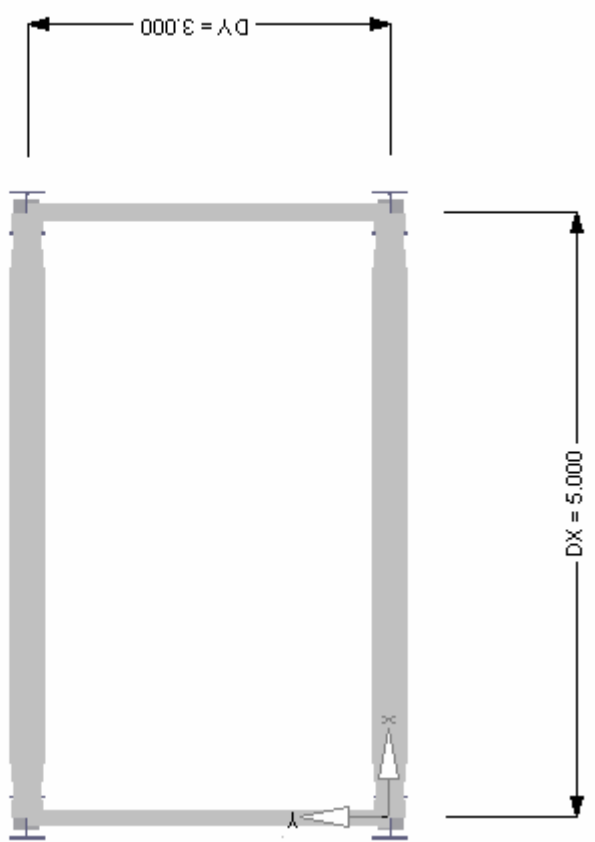


Fig. 4.9. Plan view of the structure with location of haunched beam ends depicted.

4.3.2. Finite element model

A 3-D finite element model of the structure is prepared with commercial finite element analysis program ANSYS. Corresponding ANSYS-script file is given in ANNEX.II.

The model consists of BEAM24 elements (simulating columns and beams) and MASS21 elements (simulating masses due to walls, decks and live loads).

BEAM24 is a layered uniaxial finite element. It has tension-compression, flexure, St.Venant torsion, shear deflection, plasticity, creep and swelling capabilities. It has 2 structural nodes with 3 deflectional and 3 rotational degree of freedoms for each. Definition of a third non-colinear node is necessary for definition of element axis system. Necessary profile data is extracted from a database provided by (Wichers, 2001). MASS21 is a point (one-node) element with 3 translational and 3 rotational degree of freedoms.

Rigid column bases and beam-column connections are simulated. In-plane stiffness of decks (diaphragm effect) and walls are neglected. These are in line with previous statements in section 4.3.1. Damping ratio of 5% is given in line with the common assumption for steel frame structures.

In the analyses, the structure will be excited simultaneously in two principal horizontal axes and the vertical axis to simulate 3D conditions. However, only the deformation results in the longer horizontal axis will be further analysed (namely for moment resisting frames).

4.3.3. Material models and parameters

Four material models are considered in computations:

- bilinear kinetic material model (MM1),
- multilinear kinetic material model (MM2),
- time-independent two-surface material model (MM3),
- time-dependent two-surface material model (MM4).

MM1 and MM2 are ANSYS standard material models. Necessary material properties input is provided in ANSYS-script file in ANNEX.II.

MM3 and MM4 work over an extensional Fortran interface by (Böttcher, 2002). Those readers who are interested to obtain the referred interface are recommended to contact

Institute of Steel Structures, TU Braunschweig.

For detailed explanation of all four models, refer to (Wichers, 2001).

The preliminary analyses with 5 time histories have shown that results from MM3 and MM4 show negligible variation in the order of 1-2% for global response parameters. The same is valid also for comparison of MM1 and MM2 results. Due to this negligible variation, the results are demonstrated only for MM2 and MM4 in the following.

4.3.3. Modal analysis

The first four natural periods are 0.77sec, 0.36sec., 0.30 sec., 0.23 sec. and 0.15 sec. according to the modal analysis of the finite element model. Modal shapes are depicted in Fig. 4.10.

For low-rise structures like the subject frame, it can be presumed that the behaviour is mainly dominated by the first eigenmode.

Note that, modal analysis model includes masses due to dead and live loads also, respectively with coefficients 1.0 and 0.3 (first natural period of the bare structure equals 0.27 sec which is unrealistic beyond construction phase).

Within the spectral regions concept¹³ depicted in 4.19, first natural period fits in the velocity-sensitive region. This region is typically from ca. 0.5 to 3.0-4.0 sec.s (depending on seismic regime). Response of structures with dominant modes in this region appears better related to ground velocity than any other parameter, as stated by (Chopra, 2004). Selection of a structure in this region is opportune for the purpose of this study, because rate-dependency effects should be expected to be relatively higher in this region due to the maximum pseudo-velocities

4.3.4. Equivalent static analysis and code validation

On a frame-stick model of the structure, lateral force method of analysis is carried out according to EUROCODE 8. For this purpose, commercial finite element programme RSTAB is used.

The site is assumed to be on type C ground and in seismic zone 4 acc. to EUROCODE 8 (maximum hazard zone). Earthquake loads are obtained based on EUROCODE 8 elastic

¹³ Spectral regions concept derives from the typical shapes of earthquake response spectra and is explained e.g. by (Chopra, 2004).

spectra. Accordingly, minimum design acceleration for 475 year earthquake is 0.4g modified with corresponding soil and behaviour factors. Load combinations are obtained accordingly.

Resulting tip deflection¹⁴ is 67% of code limit. This verifies conformity with EUROCODE 8 criterion of the structure under consideration. So, it is shown that the structure is a practical and realistic one. The details of the analysis are not given further.

¹⁴ *Tip deflection is the horizontal displacement of the highest floor level of the structure. It is an indicator of earthquake effects on structure like interstorey drift.*

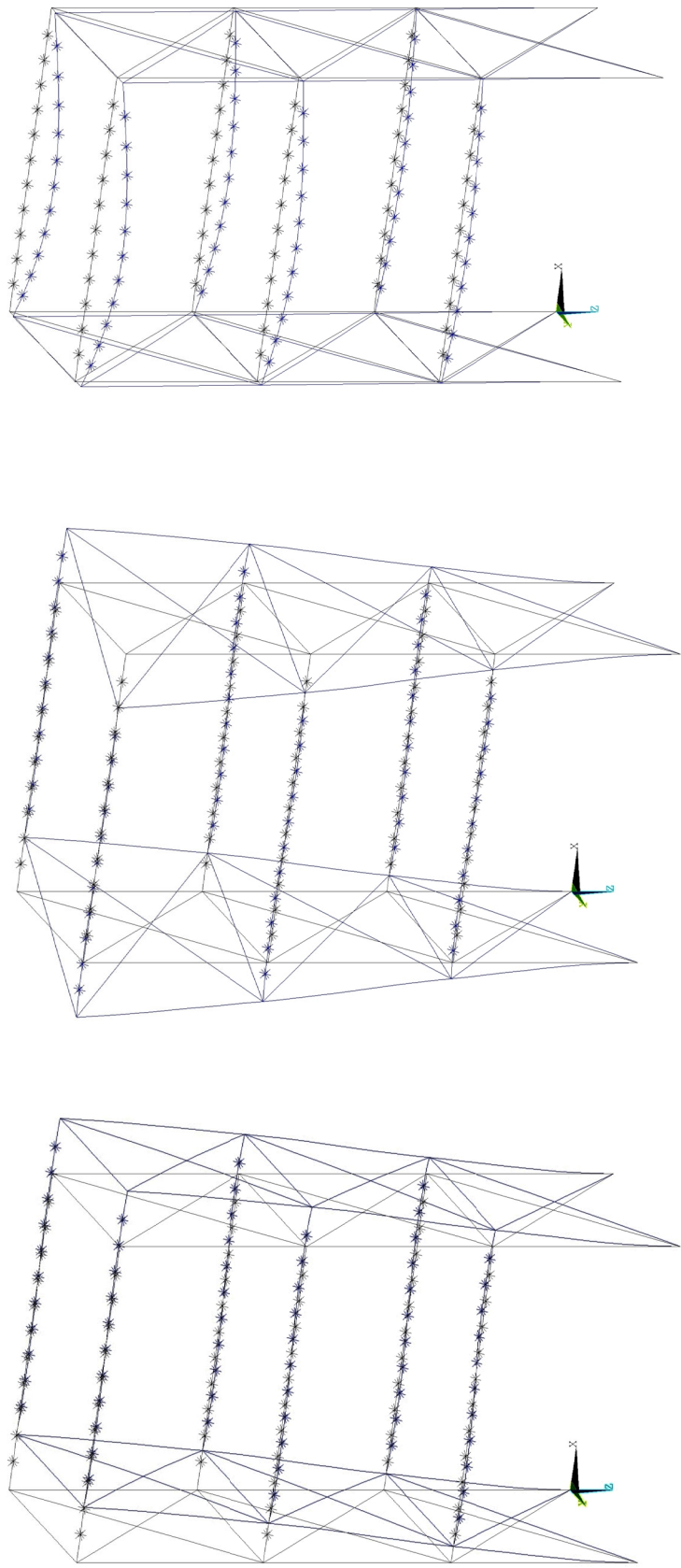
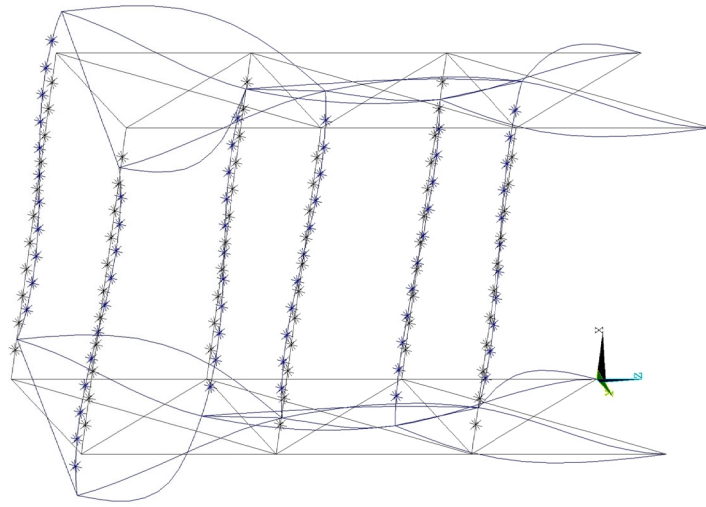
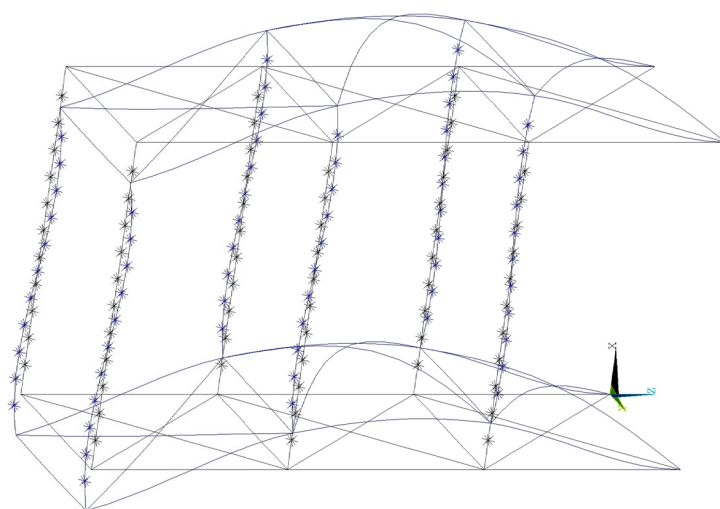


Fig. 4.10. 1st, 2nd, 3rd (above) 4th and 5th (next page) modal shapes



(cont. from previous page)



4.3.4. Used time histories

Strong motion records used in analyses are listed in Table 4.2. They are taken from the database (PEER, 2005). This open-source database is one of the most exhaustive and well prepared strong motion databases. It is especially suitable for structural engineering purposes.

Preliminary analyses have shown that the structure remains elastic when excited with records with peak ground accelerations (PGA) less than 0.6g. The subject demands, however, observation of inelastic behavior. So, the PGA=0.6g is selected as a lower threshold for selection of records.

Moreover, a decision had to be taken concerning the soil type of the hypothetical site. This is due to the significant variability of strong motion records among varying soil types. For that reason, the analyses will be carried assuming Soil Type C (according to both USGS (United States Geological Survey) and EUROCODE 8 classification). This is a commonly found soft soil type.

In PEER database, there are a total of 18 records from 5 earthquakes conforming the above conditions (PGA>0.6g, Soil Type C). Due to the time-intensive computations related to two-surface models, 10 records are selected for analyses. This is done by eliminating records with less peak ground velocities from the group. It can be stated that the resulting group is broadly representative of PGA>0.6 g records on Soil C, since it covers 10 of the 18 available records.

Moreover, further 5 records with peak ground velocities over 1 m/s are added to group. The peak ground accelerations of those latter are between 0.4g and 0.6g. This extension is done in order to include high velocity content records in analyses.

For each record, all 3 components (2 horizontal and 1 vertical) are acquired from the database. In the analyses, seismic loads are applied as 3-dimensional column base excitations. Loading at longer axis direction is always the horizontal component with higher peak acceleration.

Excitation on shorter axis and in vertical direction is done for simulating 3-dimensional loading conditions. Global deformation results will be gathered only at longer axis. Record parameters given in Fig.4.6 are those related with these components.

PEER Record no.	PEER record no.	Earthquake	Site- Source			PGV/ VSI		
			Mom.	Magn.	Distance (km)	Sa (T _i) (m/s) (g)	Sv (T _i) (m/s) (g)	PGV (m/s) PGA
1	P0809	Cape Mendocino, USA, 25.04.1992	RN	7.1	9.50	1.611	1.930	0.662
2	P1547	Düzce, Turkey, 12.11.1999	SS	7.1	17.60	1.324	1.592	0.822
3	P0161	Imperial Valley, USA, 15.10.1979	SS	6.5	2.50	0.899	1.080	0.775
4	P0180				3.80	0.500	0.607	0.602
5	P1441	Chi-Chi, Taiwan, 20.09.1999	RN	7.6	0.98	1.025	1.236	0.814
6	P0934				6.40	1.166	1.402	0.843
7	P1005				7.10	2.033	2.440	0.838
8	P0102	Northridge, USA, 17.01.1994	RN	6.7	0.40	1.429	1.718	0.939
9	P1021				14.60	1.159	1.395	0.877
10	P1023				0.20	1.620	1.946	0.897
11	P0178	Imperial Valley, USA, 15.10.1979	SS	6.5	1.30	0.590	0.710	0.439
12	P0963	Northridge, USA, 17.01.1994	RN	6.7	6.20	1.132	1.360	0.424
						1.060	2.497	0.291
							2.840	9.752

Table 4.2: Ensemble of strong motion records used in analyses, source: (PEER, 2005)
Mech.: mechanism, RN: reverse-normal, SS: strike-slip, ASI: acceleration spectrum intensity, VSI: velocity spectrum intensity

4.3.5. Computational aspects of dynamic analyses

Structural analyses are carried out with commercial finite element code ANSYS / Mechanical U Version 6.0. Corresponding ANSYS-script is given in ANNEX.II. For the computations with the two-surface material models (MM3 and MM4), an ANSYS-interface by (Böttcher, 2002) is additionally used.

Full-transient dynamic time-history analyses are carried out. Material damping is included. Newmark time integration method (with initial stiffness scheme without adaptive descent) and Newton-Raphson nonlinear procedure are used. The parameters used for Newmark method follow:

amplitude decay factor for 2nd order transient integration = 0.5,

oscillation limit criterion for automatic time stepping of 1st order transients = 50.

Time steps of earthquake records (Δt) are 0.005 sec. A criterion for checking resolution issue of time steps is: $20\Delta t <$ minimum significant period considered. This indicates that the analyses cover natural modes with $T > 0.1$ sec.s. Those are the first 5 natural modes of the structure. Knowing the dominancy of the first natural mode in low-rise frames, this is more than satisfactory.

In preliminary tries, there had been iteration problems and unexpected high responses at initial stages of records. This is found to be related to application of the dead loads and additional masses. The abnormality is overcome by inserting 30 initial load steps with only static loads. 15 of those are selected to be disproportionately long (10^5 times time-step of record) and remaining 15 normal (equal to time step of record). This “trick” of inserting a “relaxation period” between initial static gravity load application and start of dynamic excitation solved the problem of initial abnormal response.

4.3.6. Data gathering and processing by Incremental Dynamic Analysis

In the frame of this work, several hypotheses will be tested through time history analyses with 4 different material models and 12 strong motion records. Corresponding hazard governing variables for each of the records are given in Table 4.2.

An innovative method called Incremental Dynamic Analysis (IDA) is used. This method extends capacities of dynamic time-history analysis. It is developed at Stanford University e.g. by (Vamsatsikos and Cornell, 2002). It is based on carrying out dynamic analyses at varying amplification levels for a given record. For details of the method

refer to the latter source.

In the following, implementation of the method within this work is explained.

Let focus on a strong motion record (SM1) and a material model (MM4).

1. For the record under consideration, 5 hazard governing variables are obtained (HV) (see Table 4.2).
2. Record under consideration will be amplified / de-amplified with a series of factors (0.25, 0.5, 0.75, 1.0, 1.25, 1.5, 1.75, 2.0). Thus, one obtains a suite containing 8 time histories. Each record will be called an IDA record: for example “IDA 0.25 record of record 1” refer to record 1 deamplified with factor 0.25. Then “Record 1” itself corresponds to “IDA 1.00 record of record 1”. All the IDA records of record 1 will be referred as “IDA record set of record 1”. For each IDA record, HVs can be obtained by multiplication of HV of the original record with amplification factor.
3. Dynamic time history analyses are done separately for each IDA record in the set. So, 8 analyses are done for each record in Table 4.2. Each of these will be referred as IDA record analysis.

Global Analysis

4. Concerning global analysis, several maximum response governing variables (RV) are extracted from each IDA record analysis. RV's will assist in drawing conclusions on structural response. RV's are
 - ISD_{max} (maximum peak interstorey drift),
 - PFA_{max} (maximum peak floor acceleration),
 - PFV_{max} (maximum peak floor velocity),
 - T_D (maximum tip deflection),
 - F_{base} (maximum base shear),
 - E_{diss} (dissipated energy),
 - $\dot{\epsilon}_{max}$ (maximum strain rate).
5. The information obtained above enables to correlate response to hazard at varying amplification levels for a given record. For example, one can depict ISD_{max} vs. $S_a(T_1)$ as in Fig.4.11.

6. Interpolation curves are fit to the data as in Fig.4.12. Method of fit may depend on purpose of study. Within this section of this work, piecewise linear interpolation is sufficient. For risk computations, smooth splines are more suitable. Interpolation curves are termed as IDA curves. With these curves, the evolution of response at varying amplification levels can be easily traced. For example, in the case depicted in Fig.4.12, a severe hardening behaviour between IDA records 1.25 and 1.50 can be observed (IDA record 1.50 leads to smaller drift than IDA record 1.25). Such behaviour is caused by material nonlinearity. Examples are explained in detail by (Vamsatsikos and Cornell, 2005). By depicting 3D plots, one can obtain trends and relations to a third parameter as well, as done later in the work.
7. When the procedure is repeated for another material model, one can comparatively analyse the effects of material model selection at varying stages of hazard. An example is given in Fig. 4.13. As can be seen, two material models yield identical response in elastic range up to $S_a(T_1) \approx 0.75g$. Then, hardening can be observed in both results. Hardening is relatively retarded but more pronounced in time-dependent model.
8. When the procedure is repeated for other records, response variability at a hazard level can be traced.

Thus is explained how the results are obtained during the analyses which will be commented in following sections.

The procedure described above leans mainly on Incremental Dynamic Analysis (IDA) as stated previously. IDA is gaining increased acceptance due to its ability to trace structural behaviour at varying hazard levels as stated by (Wen, 2005).

Some capacities of IDA are the following:

- (1) Several phenomena (like hardening, softening, structural resurrection, collapse) can be traced in IDA-curves.
- (2) Limit states can be associated with hazard levels.
- (3) Variability of structural response under varying strong motion records of same intensity or as in our case sensitivity to material modelling at varying response and hazard ranges can be studied.

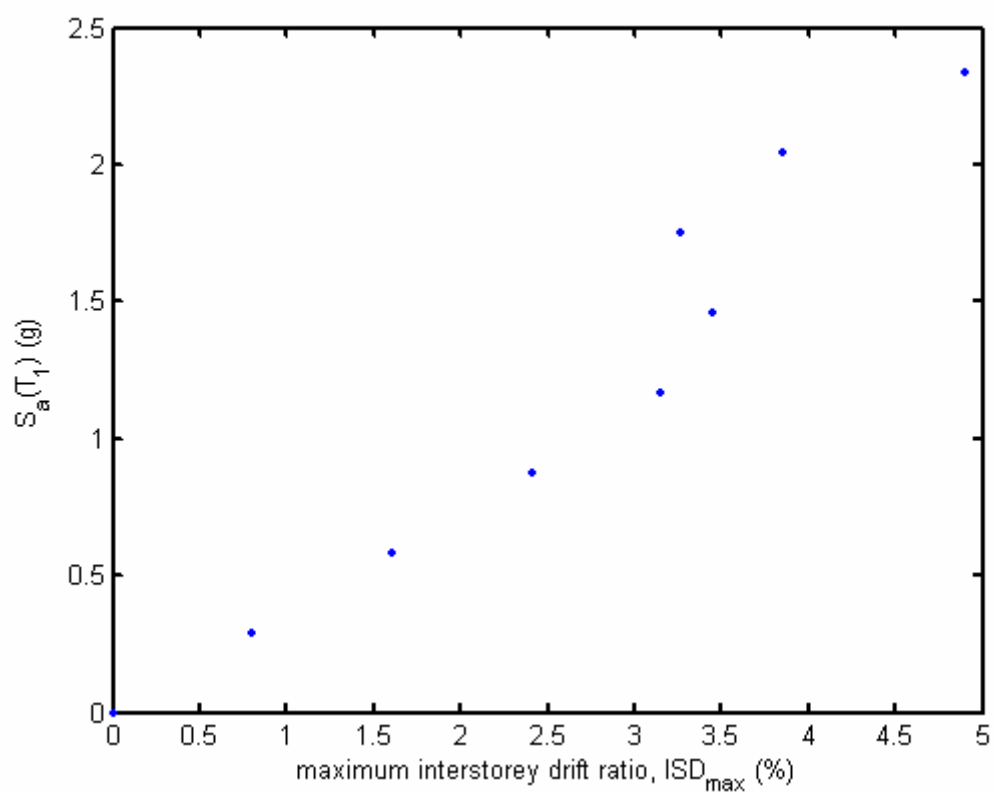


Fig.4.11

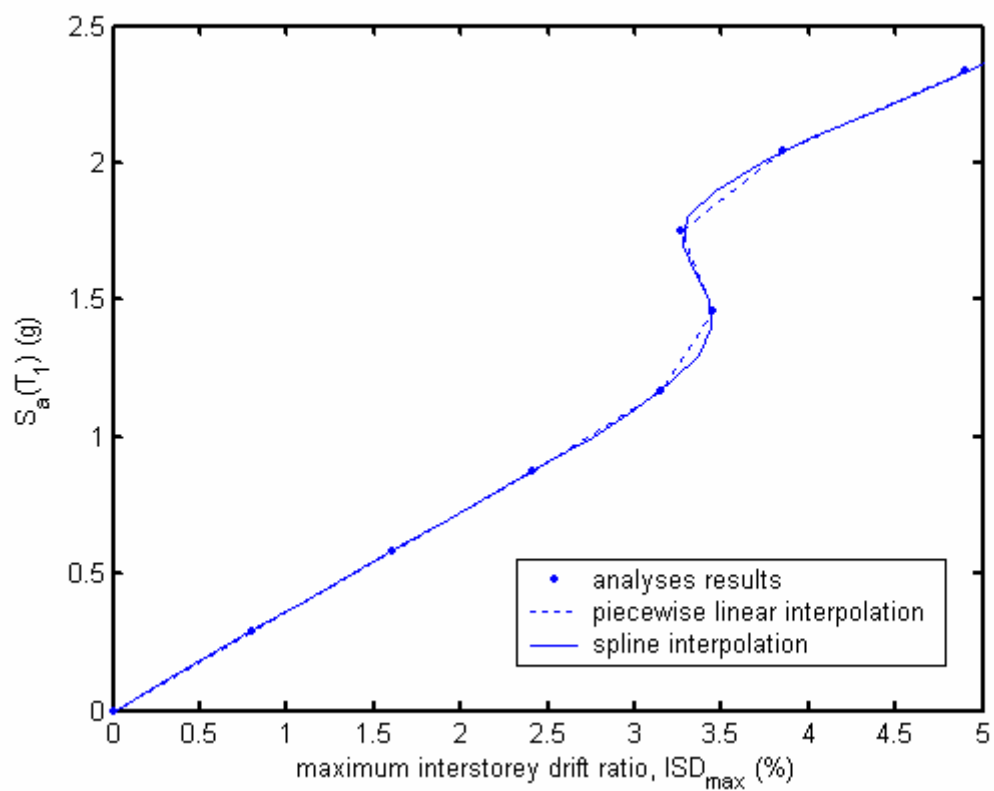


Fig.4.12

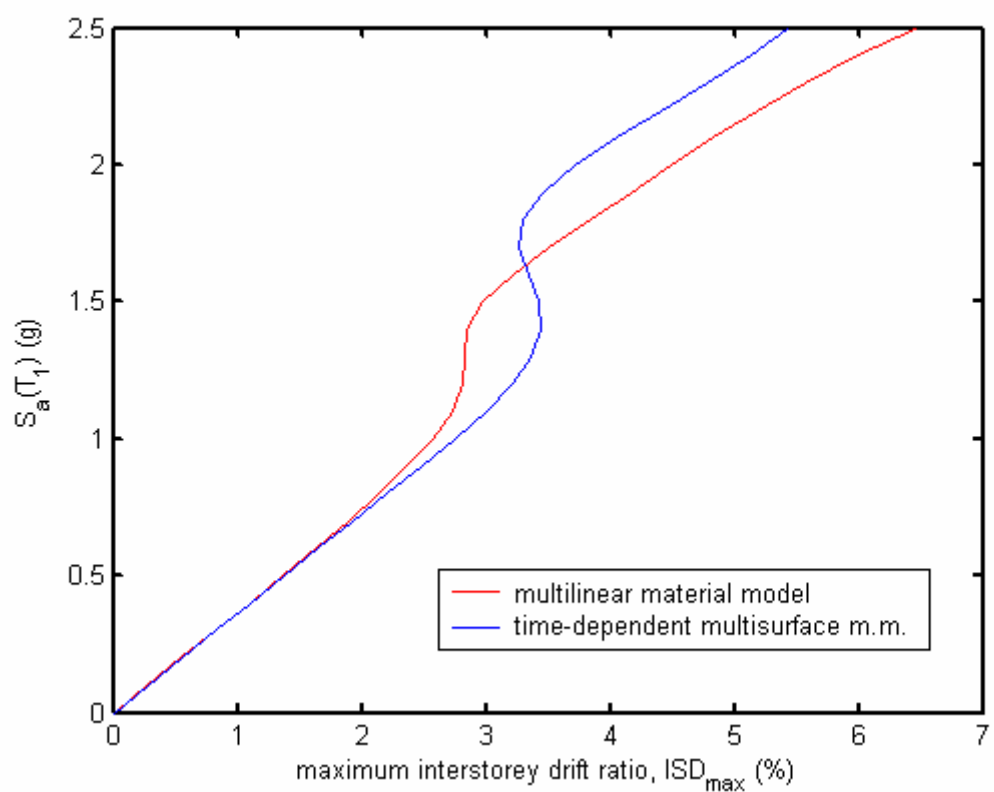


Fig.4.13

4.4. Analysis of global results

4.4.1. Range of maximum strain rates

In the beginning of the discussion, an approximate lower threshold of strain rate equal to 10^{-4} sec $^{-1}$ was set for significant rate dependency effects. This threshold is experimentally shown by (Böttcher et al. 2003)) and mentioned by (Gebbeken and Ruppert, 1999) as well.

(Gebbeken and Ruppert, 1999) suggest that earthquake loads lead to local strain rates up to 10^0 sec $^{-1}$. This latter hypothesis will be tested with the available results of this work: Fig.4.14 and Fig.4.15 give maximum strain rates recorded for IDA sets of 12 records (depicted vs. pseudo-acceleration at first natural period, respectively after time-dependent two-surface model - MM4 and multilinear kinetic model - MM2).

Depicted strain rates range between orders of magnitude of 10^{-2} and 10^0 sec $^{-1}$, justifying the hypothesis stated above. Moreover, they are in the rate-dependency sensitive range ($>10^{-4}$ sec $^{-1}$), even for the deamplified IDA records.

4.4.2. Variability of maximum strain rates among varying records

Several observations can be done concerning the subject:

OBSERVATION I.

Maximum strain rates show changing variability for different hazard levels and different material models, as seen in Fig.s 4.14 and 4.15. This is more obvious in Fig.s 4.16 and 4.17, where the data is linearly interpolated for each IDA set.

OBSERVATION II.

Records 10 and 11 show distinct patterns than others. The common characteristic of these records is their extremely short source-site distance (respectively 1.3 and 0.2 km). This alone, however, can not explain the deviation since the similar distances of records 5 and 8. It can be hypothetically stated that the deviations should be related to velocity content of subject records. This statement will be referred as HYPOTHESIS I and will be checked later.

OBSERVATION III.

Another point of remark is the deviation of record 2 from mainstream at higher hazard levels in MM4 results (Fig.4.16). This record distinguishes itself with the longest source-site distance of 17.6 km. This is beyond 15 km given commonly as threshold for near field effects. This may explain the deviation. In MM2 results, record 2 remains within mainstream.

OBSERVATION IV.

MM4 and MM2 data (respectively Fig.s 4.16 and 17) show relatively distinct variability patterns. Explanation can be the following hypotheses:

- (1). At lower hazard levels ($S_a(T_1) \sim <0.75$), the lower relative variability of MM4 data can be related to yield retardation due to rate dependency effects with respect to MM2 data (HYPOTHESIS II).
- (2). At medium levels ($0.75 < S_a(T_1) < 1.50$), inelasticity can be presumed to settle in both data (HYPOTHESIS III), leading to progressively increasing variability in MM4 data and vice versa in MM2 data. This is due to the two distinct inelasticity modelling; time-dependent two-surface model (MM4) is based on evolving yield criterion and patterns, and so, inelastic behaviour (in that case strain rates) is more and more marked by individual record characteristics with increasing hazard levels. On the other hand, multilinear kinetic model (MM2) data, following the abrupt yield onsets, stabilizes more and more with increasing hazard levels, and thus decreasing the dispersion within $0.75 < S_a(T_1) < 1.50$ range. This leads to the extreme hardening and weaving behaviour of the records to the right (weaving behaviour is defined by (Vamsatsikos and Cornell, 2005)).

OBSERVATION V.

Despite the inter-record variability at constant hazard level, the average ranges of both data remain stably comparable.

The hypotheses I,II and III, concerning observations II and IV will be checked in the following sections.

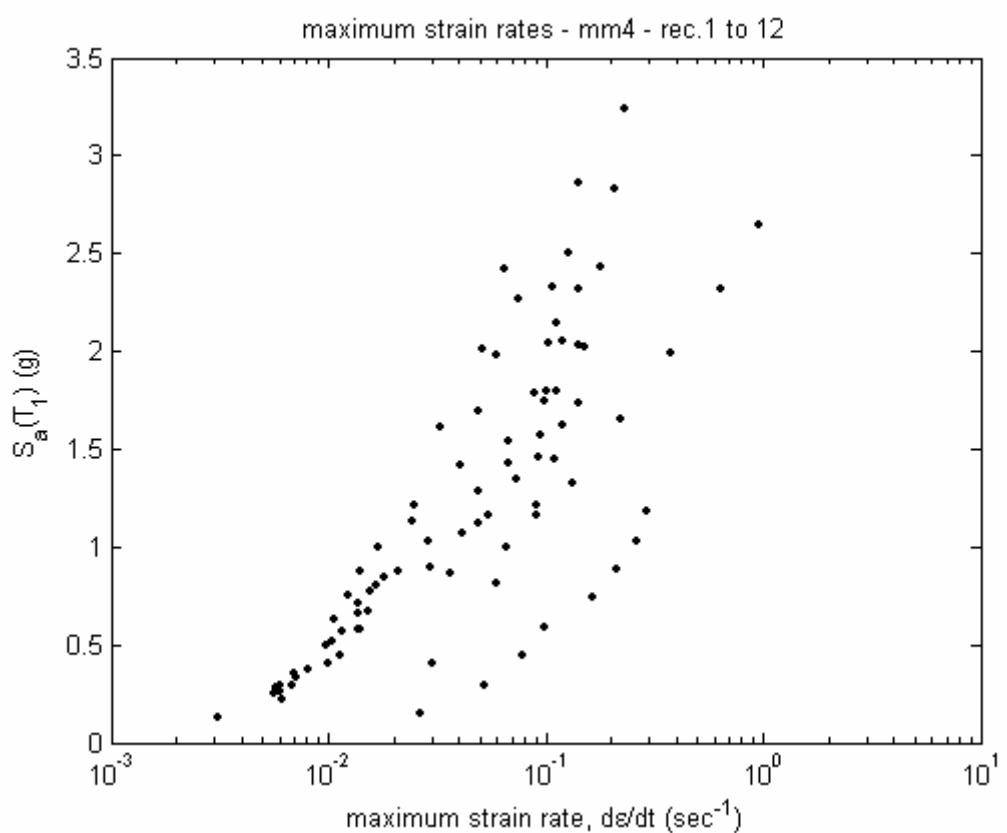


Fig.4.14

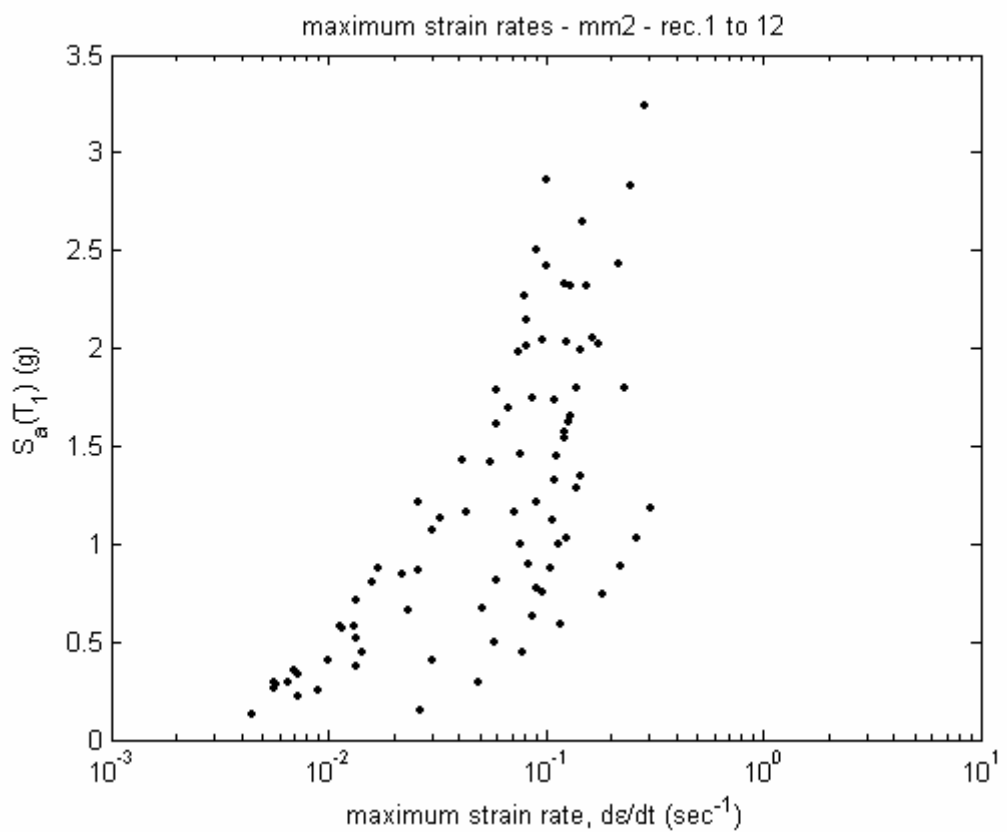


Fig. 4.15

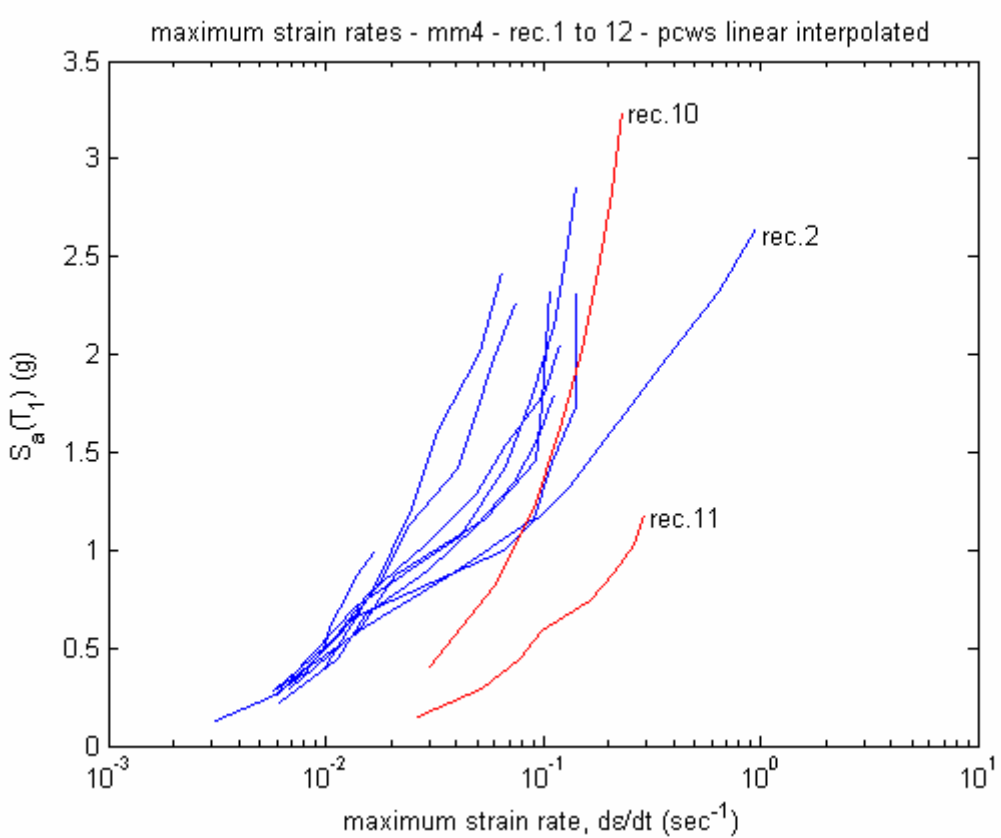


Fig.4.16

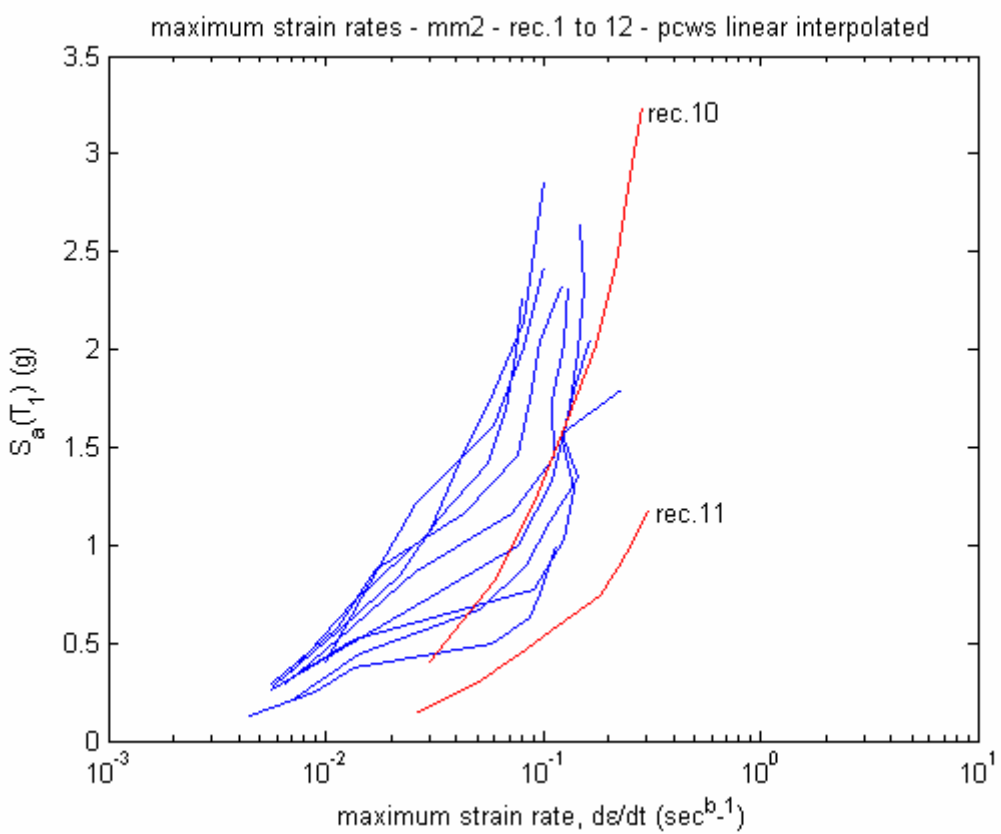


Fig.4.17

4.4.3. Variability of recorded velocity and connected maximum strain rate variability

The task of this section is to search for strong motion parameters related to variability of maximum strain rates at constant hazard levels. Within this task, particularly the reason behind high strain rates in rec.11 and less pronouncedly in rec.10 will be sought for. This problem is depicted in Fig.4.16 and 4.17. Preliminary hypothesis is that maximum strain rates can be estimated with analysis of velocity content of records, as stated in previous section.

Inspection of Table 4.2 and Table 4.3 reveals no significant correlation between the maximum strain rates observed and any hazard parameter given there. However, the common distinguishing property of rec.s 10 and 11 with less than 1.5 km source to site distance can be observed.

Fig.4.18 gives the dispersion of pseudo-velocity spectra of each record and the corresponding average. Despite the intra-record variability, average spectrum depicted with blue is rather smooth. Average spectrum is depicted as well in Fig.4.19. This figure contains the spectral regions concept. Accordingly, dispersion of spectral values in Fig. 4.18 is more dominant in displacement sensitive and to a lesser extent in velocity sensitive regions. This is in line with trends given in literature, e.g. by (Chopra, 2004).

Comparison of rec.10 and 11 with rest records reveal that these are marked with distinguishing characteristics of near field records¹⁵ -more pronouncedly for rec.11.-. This is expectable due to the low source-to-site distances of these records.

Such records have high maximum pseudo-velocity to maximum pseudo-acceleration ratios S_v^{\max} / S_a^{\max} . This parameter varies markedly among near field to far field. So, it could be an indicator for maximum strain rates at constant $S_a(T_1)$ levels. This hypothesis, however, is not verified by Fig.s. 4.20 and 4.21:

Regarding Fig.4.20, despite two local maxima due to rec.s 11 and 2 (at S_a ,levels ~ 1.25 and 2.75), contour curves are indifferent to S_v^{\max} / S_a^{\max} ratio.

Same is generally valid for Fig.4.21, as well, except a slight correlation trend at the

¹⁵ Distinguishing characteristics of mean near field spectra with respect to far field are: (1) slight shift in maximum pseudo-velocity region to higher periods, (2) sharper max. pseudo velocity peak related with higher pseudo velocities, rather than the typical plateau.

extreme S_a range 2.50 and 3.00.

One can try to refine the failed indicator by replacing the denominator by the structure-specific hazard parameter $S_a(T_1)$. $S_v^{\max} / S_a(T_1)$ related curves Fig. 4.22. and 4.23 show clearer trends:

Fig.4.22 indicate strong correlation of maximum strain rates to $S_v^{\max} / S_a(T_1)$ for MM4 beyond $S_v^{\max} / S_a(T_1)=2$. In the range $S_v^{\max} / S_a(T_1)<2$, the correlation is absent. This is partly due to interference by exceptional records 2 and 10 (at respectively $S_v^{\max} / S_a(T_1)=1.429$ and 1.908). This can be proven with the existence of the same trend in Fig.4.24, where dataset without records 2 and 10 is depicted.

MM2 data is depicted in Fig.4.23. There, the correlation beyond $S_v^{\max} / S_a(T_1)=2$ is slightly distorted in comparison to MM4 data in Fig.s 4.18 and 4.20. This is due to extreme hardening / weaving behaviour of rec.s 3, 4 and 5 observed previously in Fig.4.13 (these latter records are moderate $S_a(T_1)$ data with low site-source distances 1 to 4km, however this do not let us make a statement).

Since MM4 is a more realistic model than MM2, the conclusions will be drawn based on MM4 data:

ELASTIC REGIME (range of $S_a(T_1)<\sim 1.0g$ for our structure):

Mean maximum strain rates relate well to $S_a(T_1)$ - loglinearly and with low dispersion (Fig. 4.16). The deviations seen in Fig. 4.16 are due to near-fault records (rec.10 and 11) with $d<1.5\text{km}$. They presumably trigger yielding at lower $S_a(T_1)$ due to extreme directivity-related fling pulses. S_v measures are shown to be not governing. $S_d(T_1)$ measures are not checked.

INELASTIC REGIME (beyond $\sim 1.0g$ level for our structure)

Dispersion of maximum strain rates with respect to $S_a(T_1)$ is due to yield onset. It is well related to $S_v^{\max} / S_a(T_1)$, if $S_v^{\max} / S_a(T_1) > 2$ (high-velocity ground motion) (Fig.s. 4.22 and 4.24). For $S_v^{\max} / S_a(T_1) < 2$, $S_v^{\max} / S_a(T_1)$ and probably velocity content seem irrelevant to maximum strain rate (Fig.s. 4.22 and 4.24). At these conditions, maximum strain rate is probably related to acceleration content and to some other record-specific characteristic like shape.

Over all ranges, $S_v^{\max} / S_a(T_1)$ appears to be a better indicator for maximum strain rates than S_v^{\max} / S_a^{\max} .

The phenomena observed above in MM4 data is slightly dimmed and interfered in MM2 data at yield onset range due to MM2's less elaborate yield model.

Rec. no.	S_v^{\max} / S_a^{\max} (m/sec/g)	$S_v^{\max} / S_a(T_1)$ (m/sec/g)
1	4.258	1.245
2	5.228	1.429
3	2.897	2.007
4	3.986	2.448
5	7.720	2.969
6	2.928	1.749
7	5.664	1.411
8	2.654	1.297
9	3.158	1.403
10	7.393	1.908
11	9.314	4.261
12	8.478	2.113

Table 4.3. Tested velocity content indicators for maximum strain rates

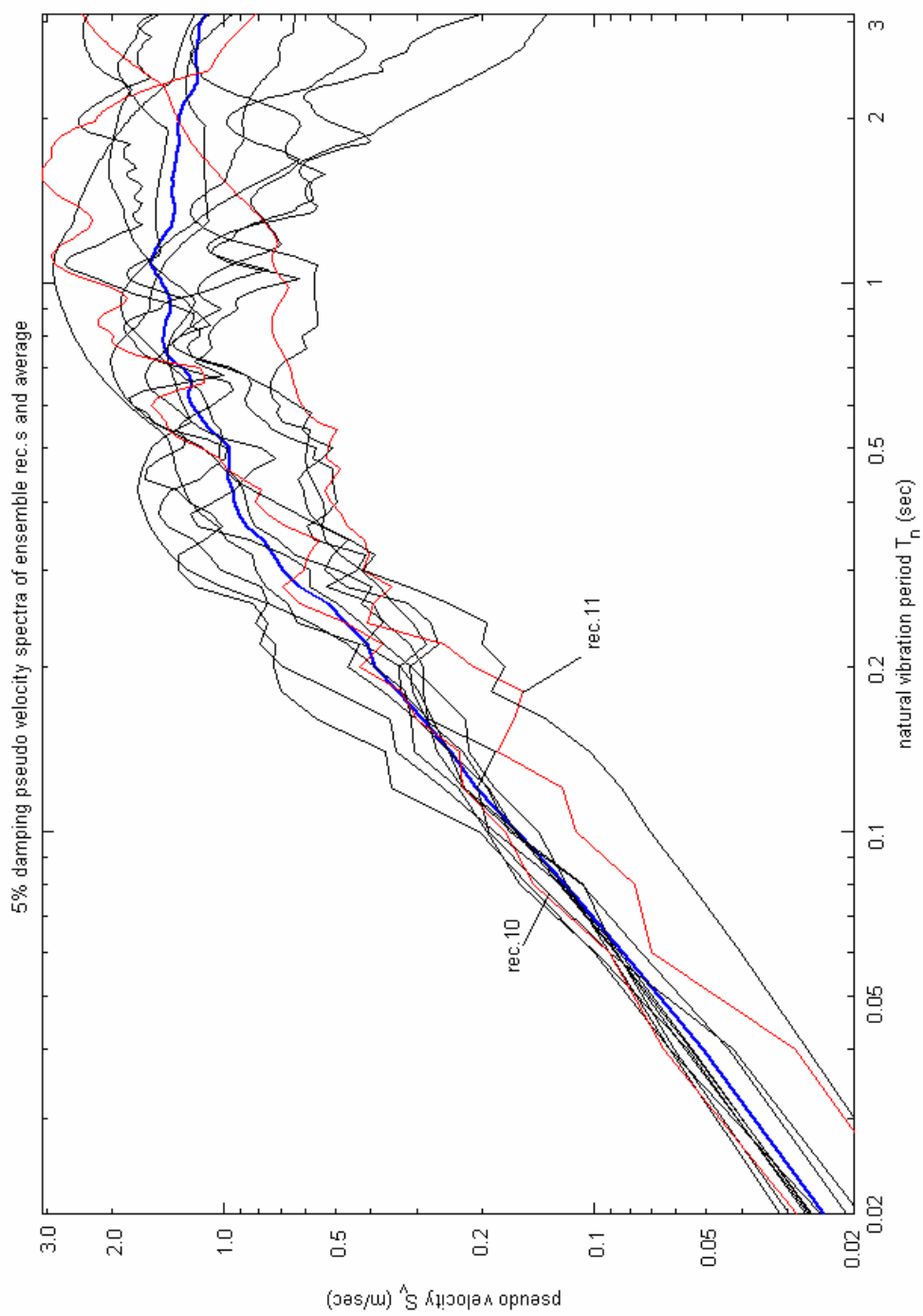


Fig. 4.18

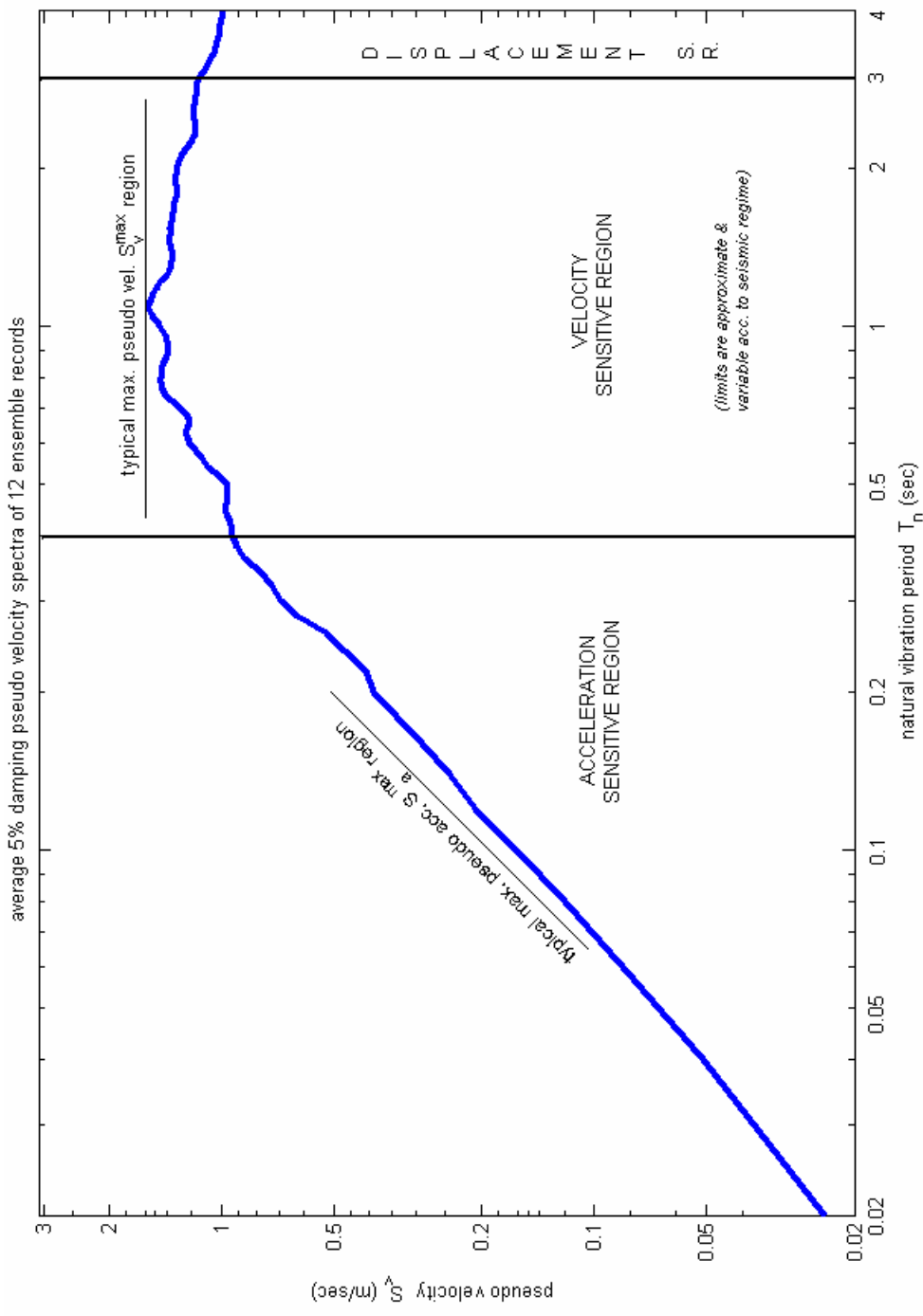


Fig. 4.19

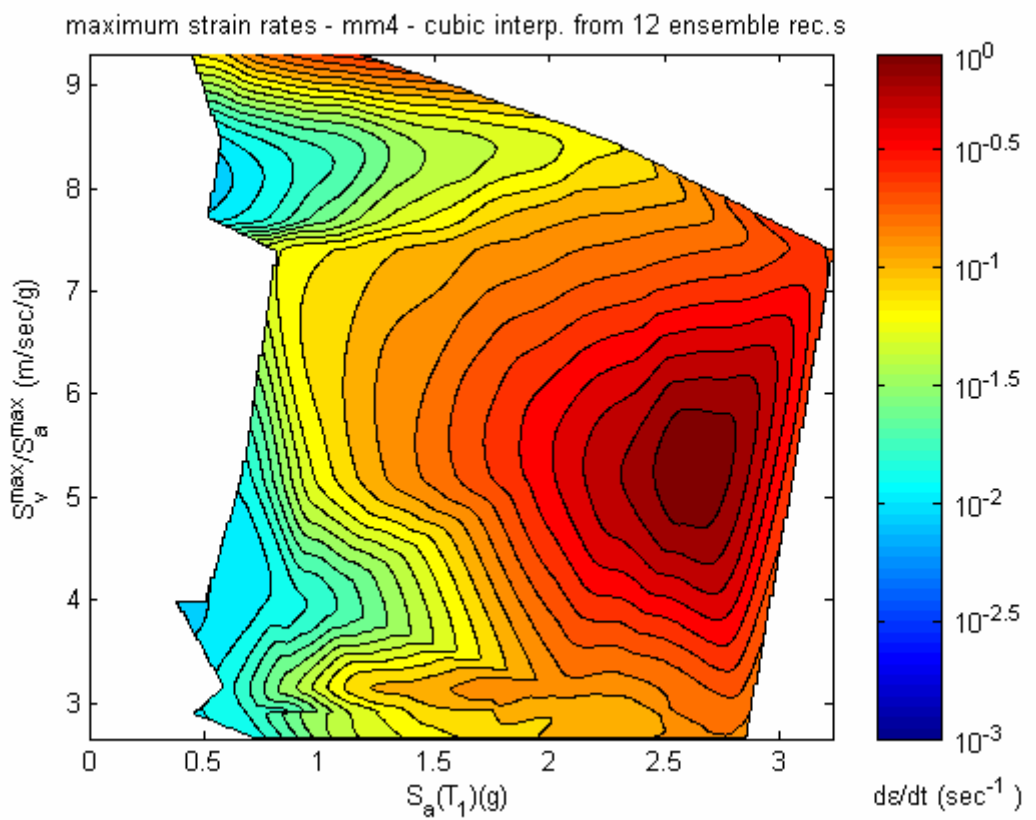


Fig. 4.20

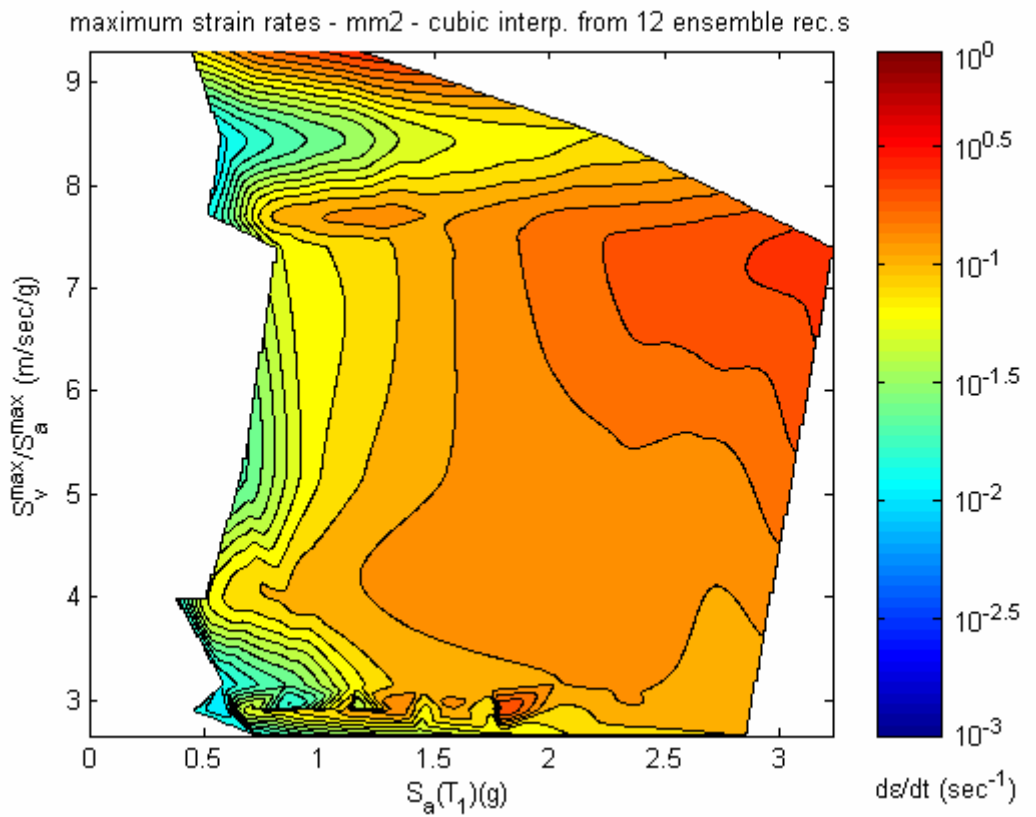


Fig. 4.21

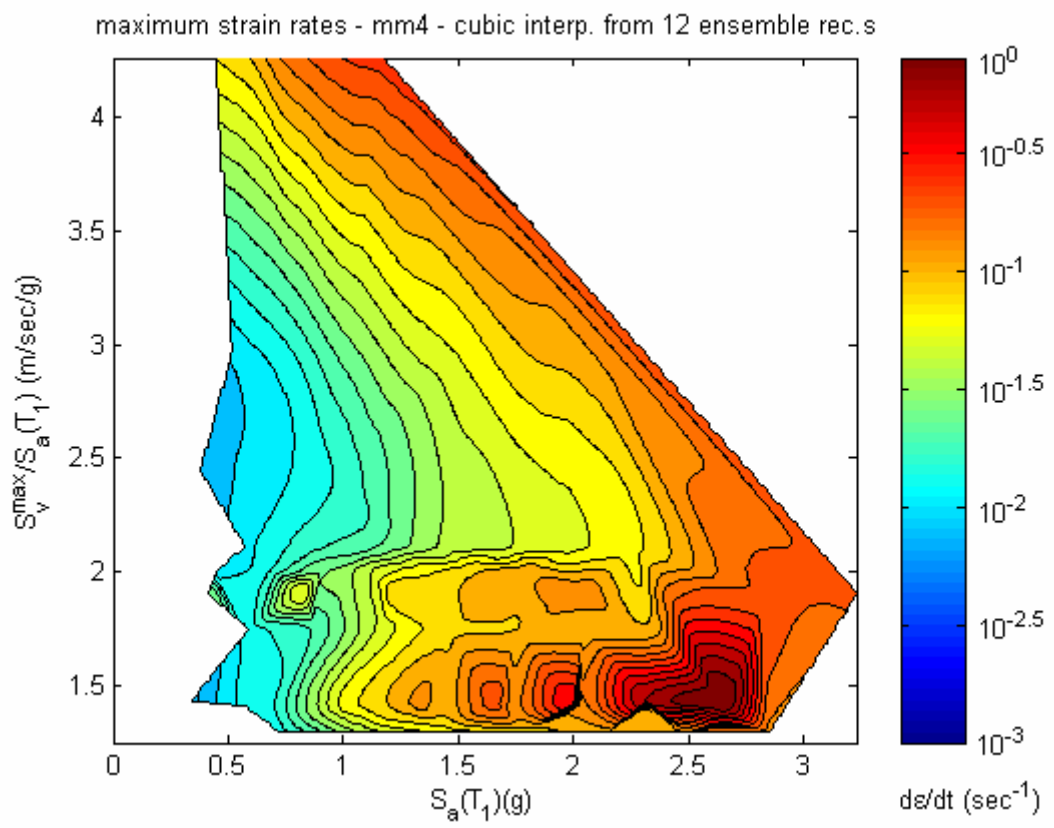


Fig. 4.22

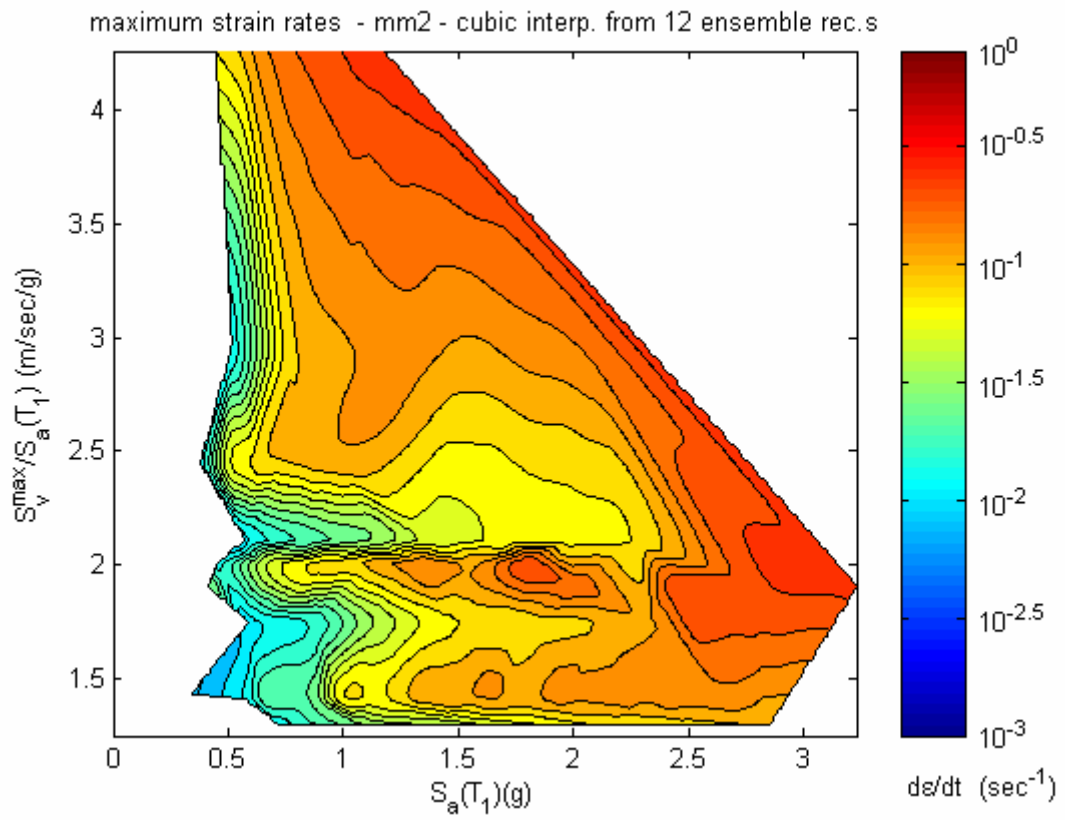


Fig. 4.23

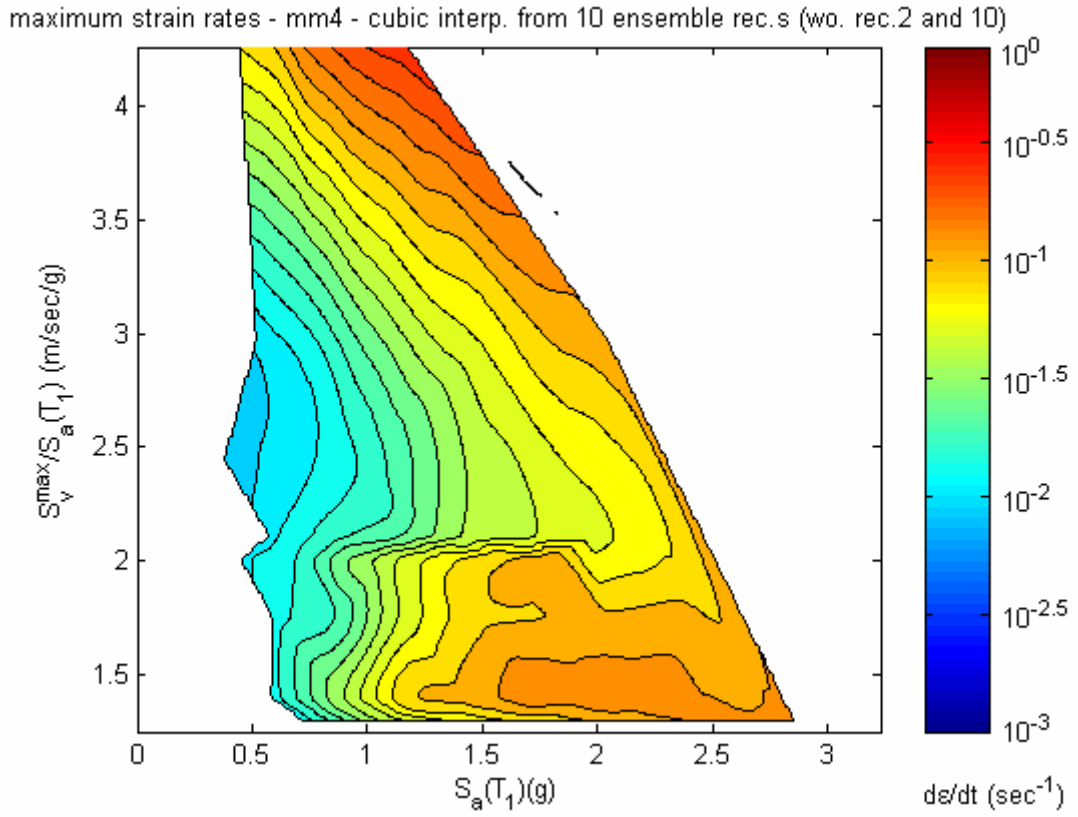


Fig. 4.24

4.4.4. Variability of global response parameters

In this section, the variability of global response parameters among varying records and the relation of this variability to maximum strain rates are investigated.

As stated earlier, the common global response parameters are the maximum interstorey drift ratio (for structural components), the maximum peak floor acceleration (for non-structural components and some contents) and the maximum peak floor velocity respectively (for remaining contents).

In Fig.s 25 and 26, ISD_{max} data from MM4 and MM2 computations are depicted. Previously deviating records in maximum strain rate figures (rec.s 10 and 11) are in both cases in line with mainstream.

Another observation is the deviation between MM2 and MM4 data for rec.2 at high hazard levels. Identical situation is observed in terms of maximum strain rates previously. To repeat, for the exceptional case of rec.2, different material models yield significantly varying results; at maximum hazard level respectively ISD_{max} = 9% and 7% and $\dot{\epsilon}_{\max} = 10^0$ and 10^{-1} . These can be due to an advancement of yield onset at higher hazard levels leading to increase in number of inelastic cycles. This may alter yield

sequence, which imprints MM4 data in contrast to MM2 data (since yield sequence is irrelevant for max MM2 data due to neglect of ratcheting and Bauschinger effects).

Another point of interest is the weaving forms observed especially in Fig.4.26, e.g. rec.5. The reason for this is the same as explained in section 4.4.2.

Fig.s 4.27 and 4.28 illustrate the attempts to explain ISD_{max} variability by a further parameter $S_v^{max} / S_a(T_1)$. Investigation of these figures reveal no correlation of ISD to $S_v^{max} / S_a(T_1)$. This means that ISD_{max} is indifferent to changes in $S_v^{max} / S_a(T_1)$ (valley at appr. $S_v^{max} / S_a(T_1)=1.8$ is due to lack of data from a record).

Hazard parameters incorporating spectral values at other periods like T_2 or $1.5T_1$ are not tested due to limitations of the work.

Let proceed further with response variability. Fig.s. 4.29 and 4.30 reveal increased variability of PFV_{max} values at higher hazard levels with respect to ISD_{max} . However, the variability over material models is much less. Fig.s 4.31 and 4.32 reveal strong correlation of PFV_{max} to $S_v^{max} / S_a(T_1)$ in a limited region, bounded by $S_a(T_1) > 1$ and $S_v^{max} / S_a(T_1) < 2$. This region corresponds to inelastic regime with low velocity strong motion. On the upper region bounded with $S_a(T_1) > 1$ and $S_v^{max} / S_a(T_1) > 2$, correlation is much less.

Fig.s 4.33 to 4.36 depict same relations for PFA measure. In Fig.s 4.33 and 4.34, yield onset at ca. $S_a(T_1) = 1g$ is more obvious than in ISD_{max} and PFV_{max} . General trend is saturation of PFA_{max} values after $S_a(T_1) = 1g$. This corresponds to moderate to significant yielding.

In all 3-D graphs, it is obvious that $S_a(T_1)$ strongly correlates to all response parameters at elastic range. In inelastic range, the correlation is partial.

Fig.s 4.37 and 4.38 depict maximum strain rate variability vs. PFV_{max} vs. $S_a(T_1)$. The first two parameters can be presumed intuitively to be correlated, since strain rates in general relate to excitation velocity. However, no such trends are recognizable in the referred figures.

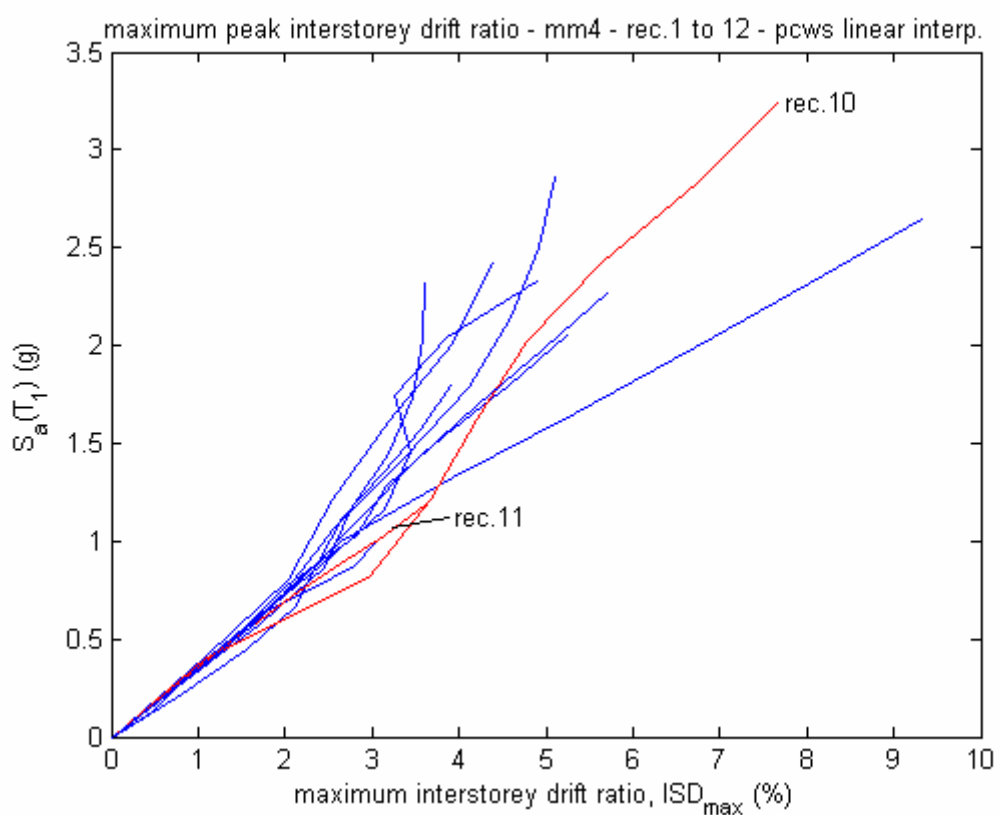


Fig. 4.25

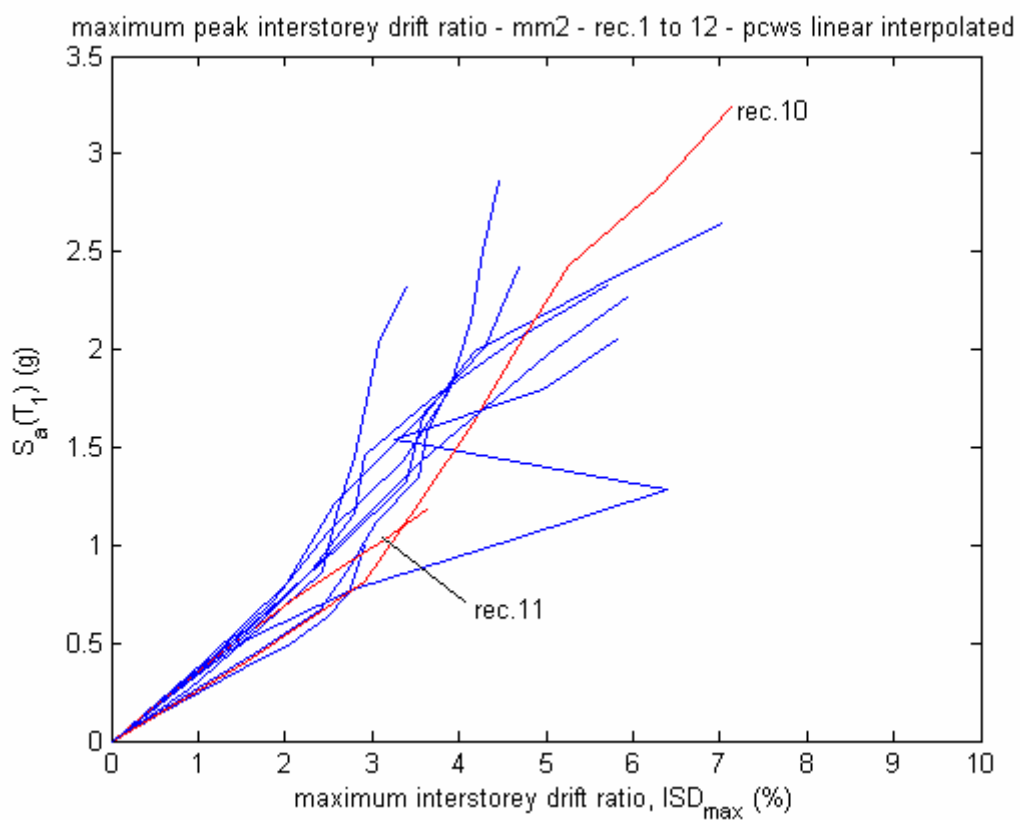


Fig.4.26

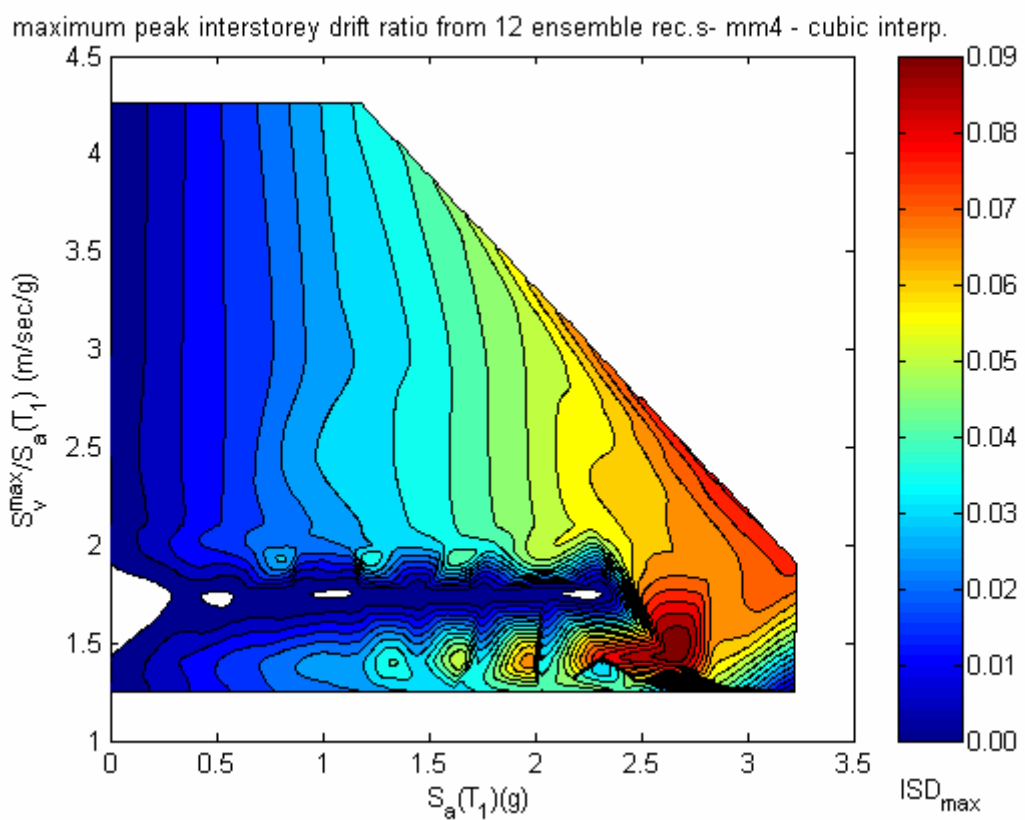


Fig. 4.27

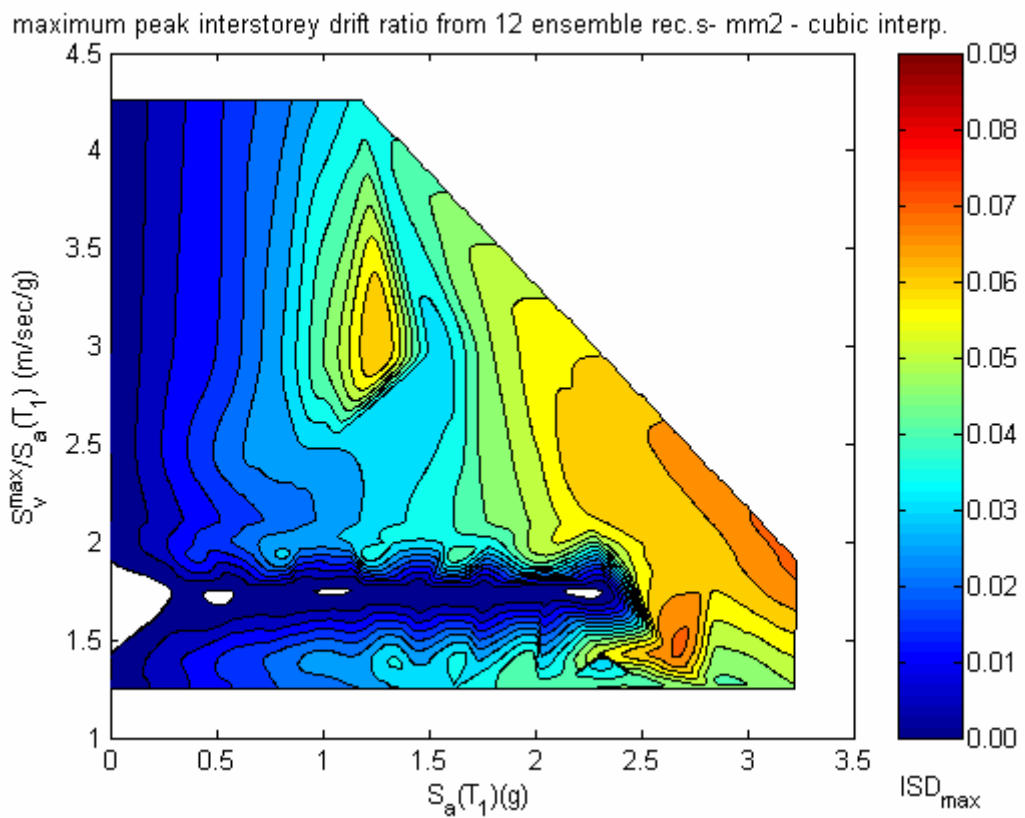


Fig. 4.28

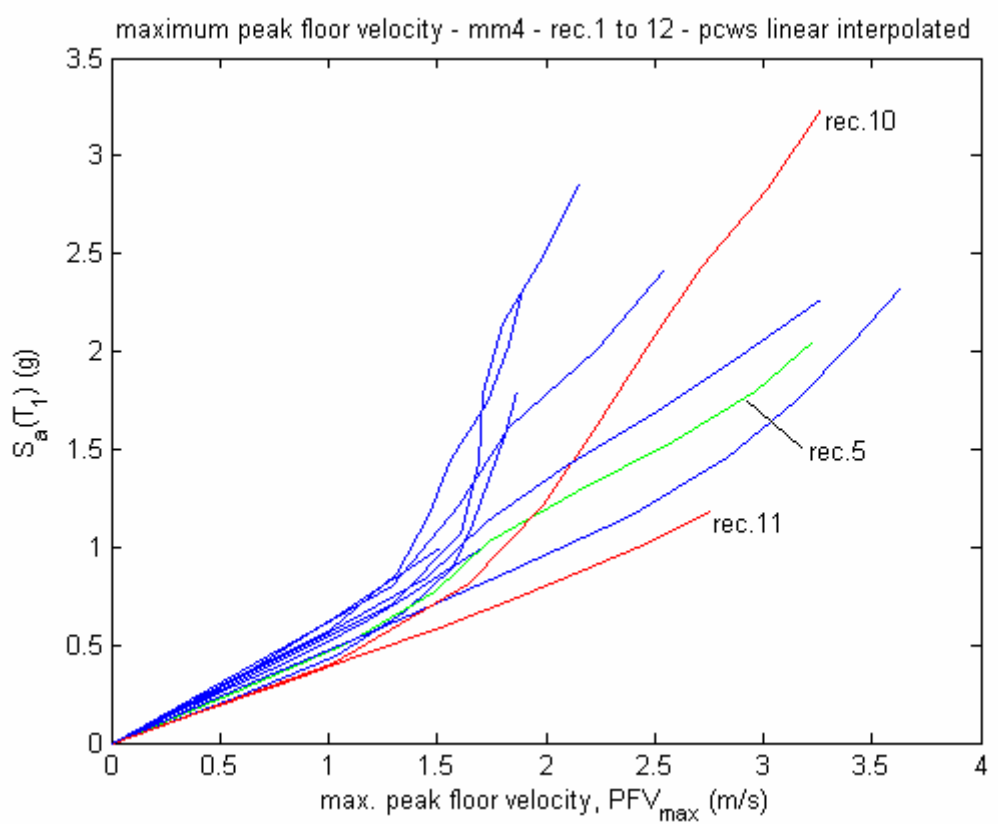


Fig. 4.29

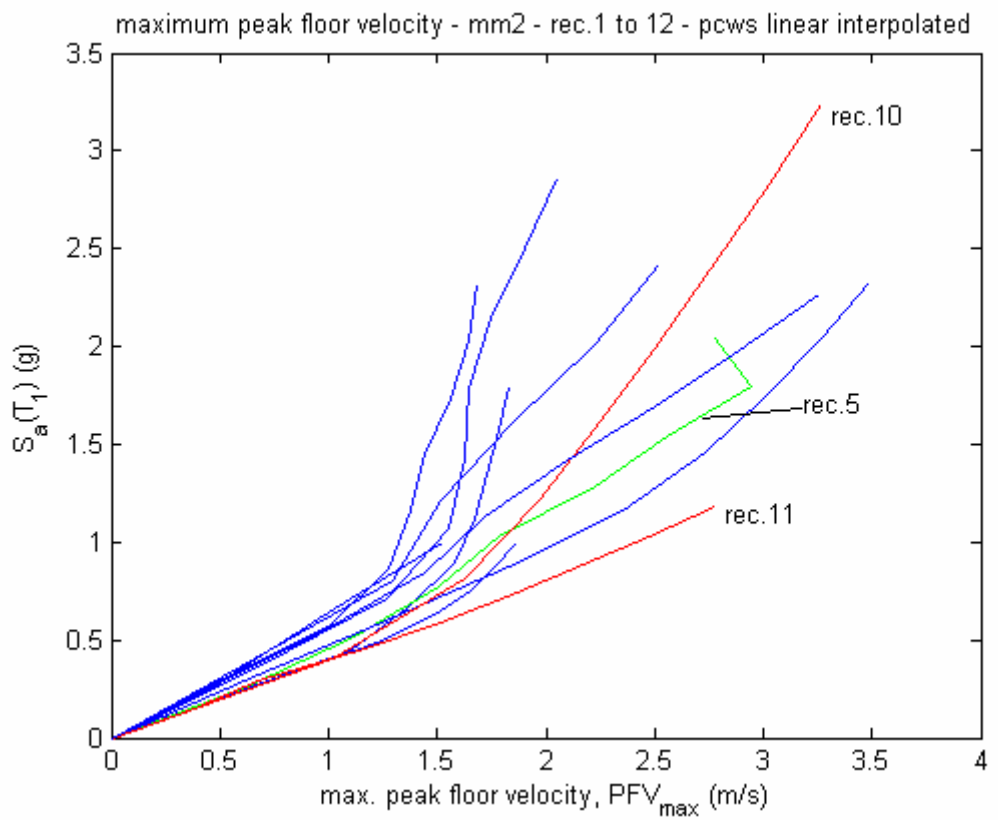


Fig. 4.30

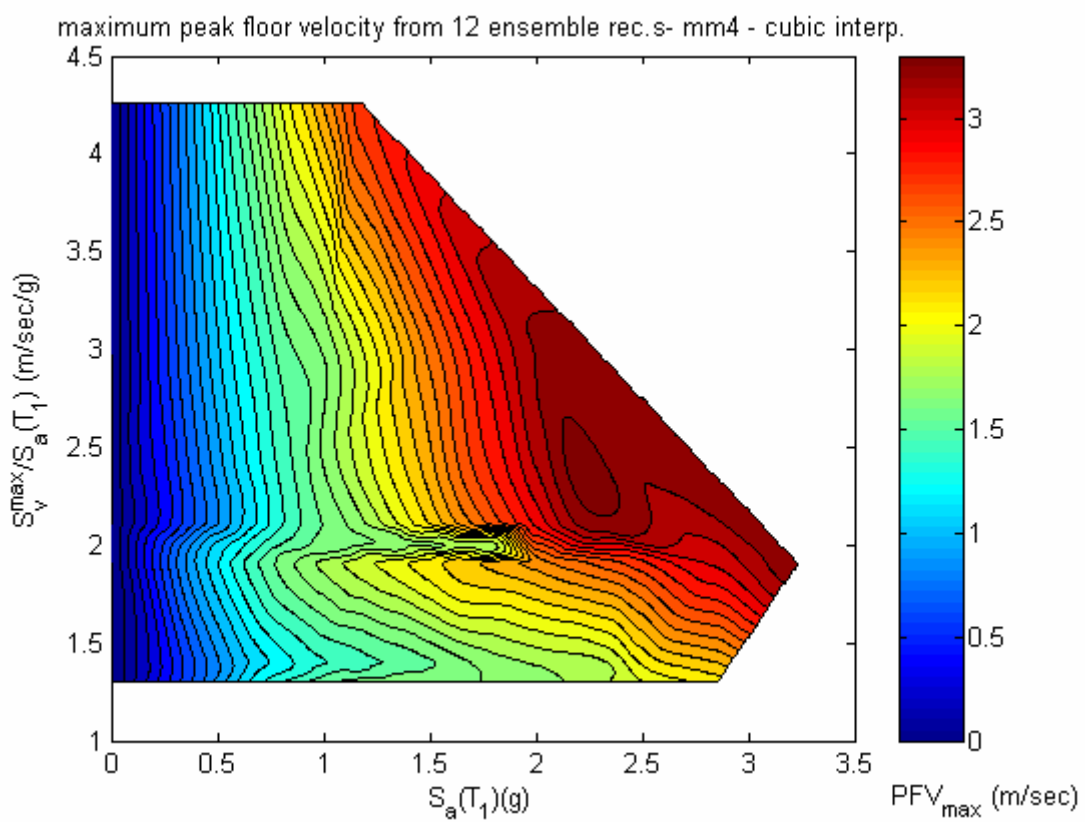


Fig. 4.31

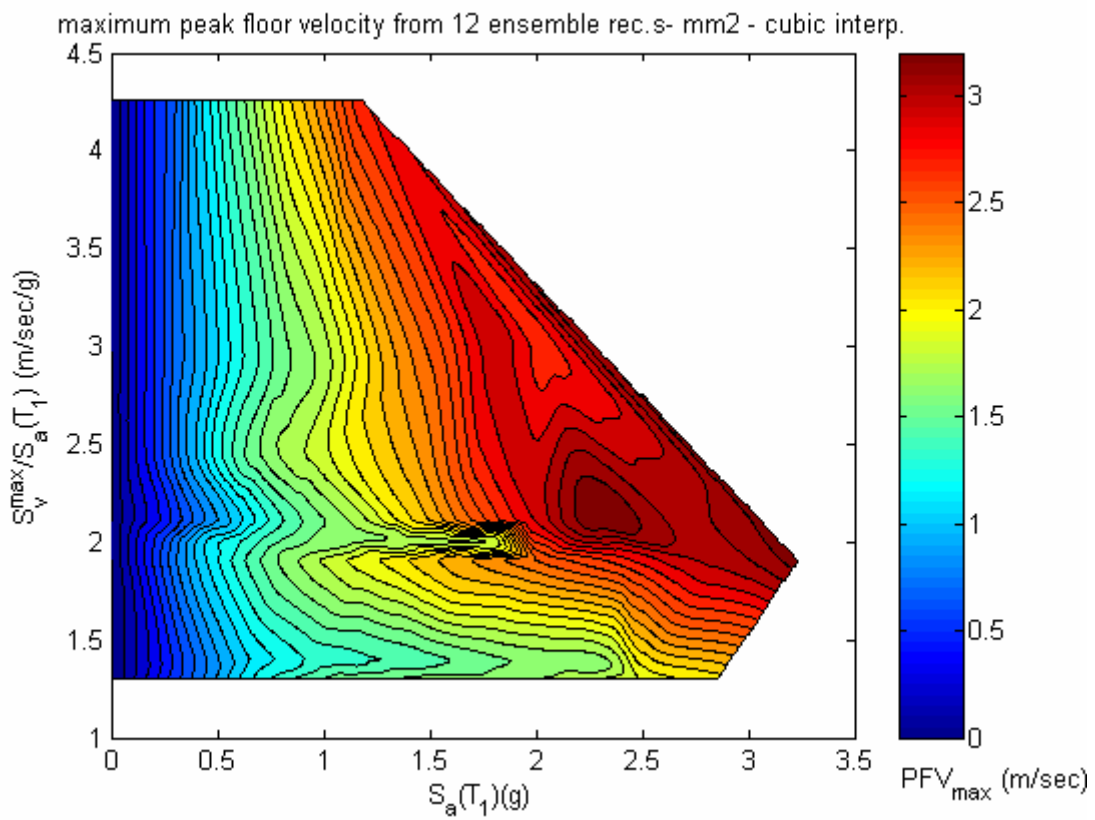


Fig. 4.32

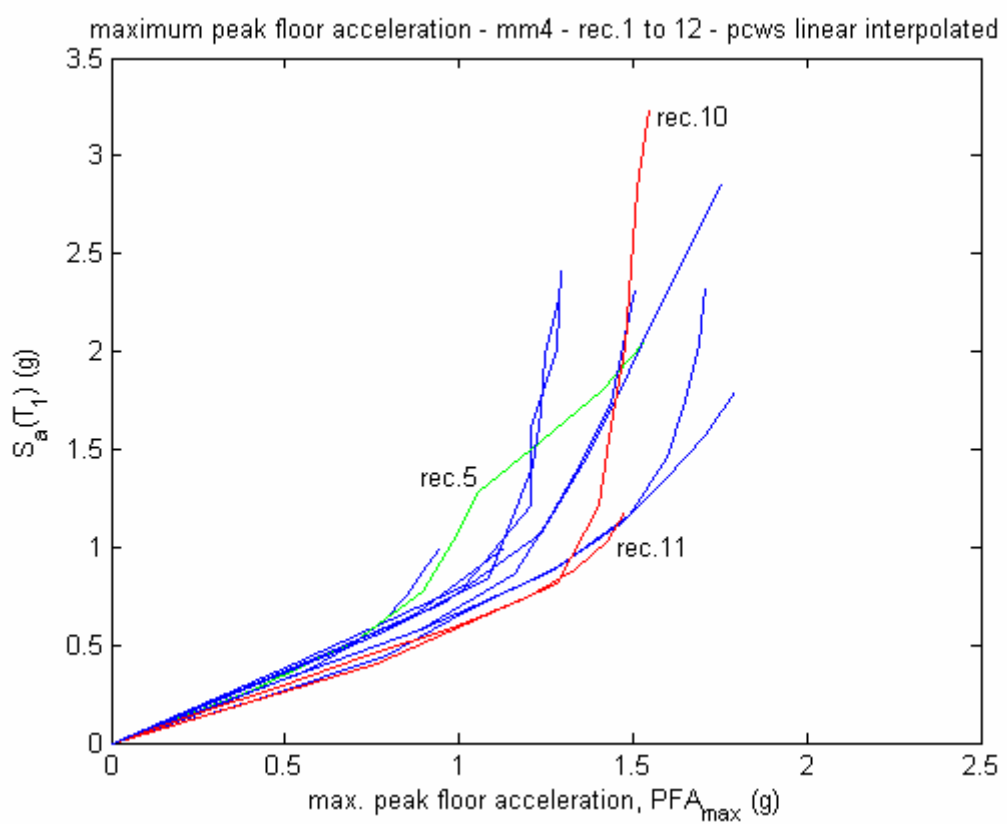


Fig. 4.33

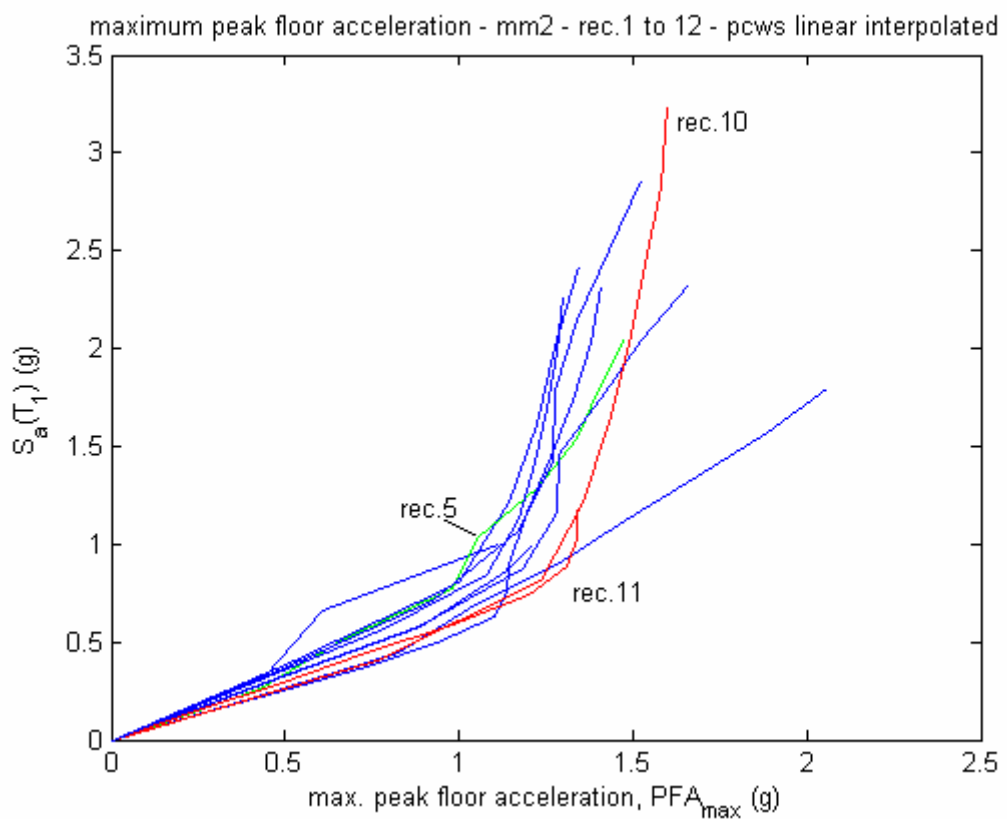


Fig. 4.34

maximum peak floor acceleration from 12 ensemble rec.s- mm4 - cubic interp.

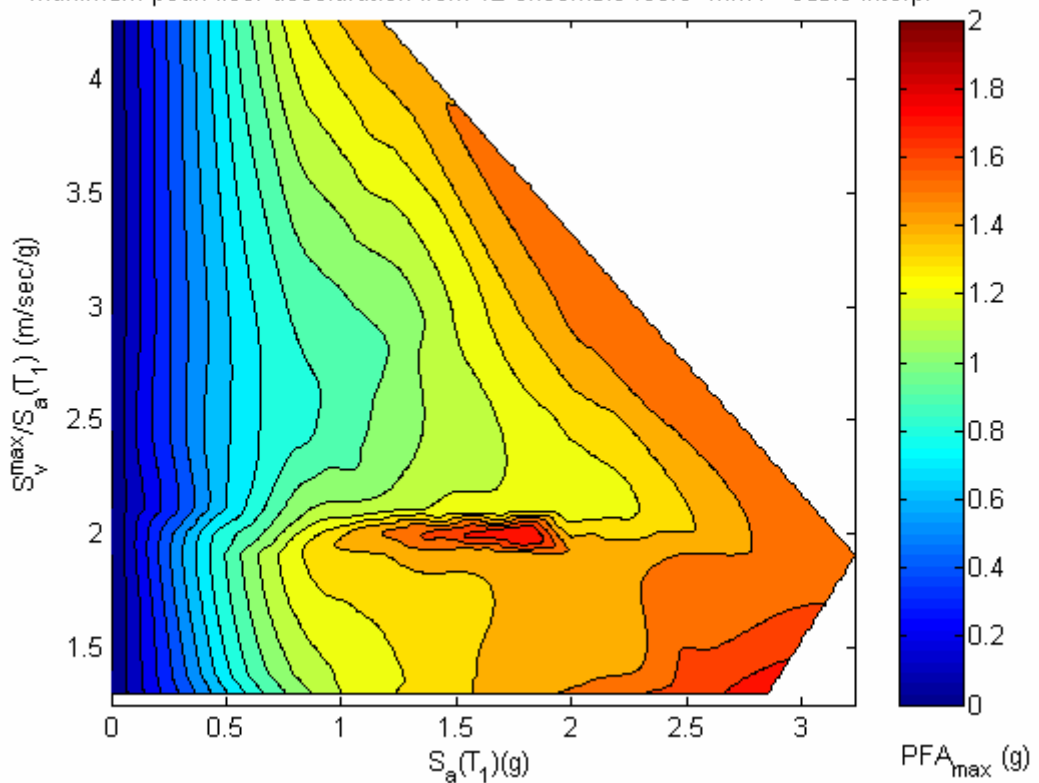


Fig. 4.35

maximum peak floor acceleration from 12 ensemble rec.s- mm2 - cubic interp.

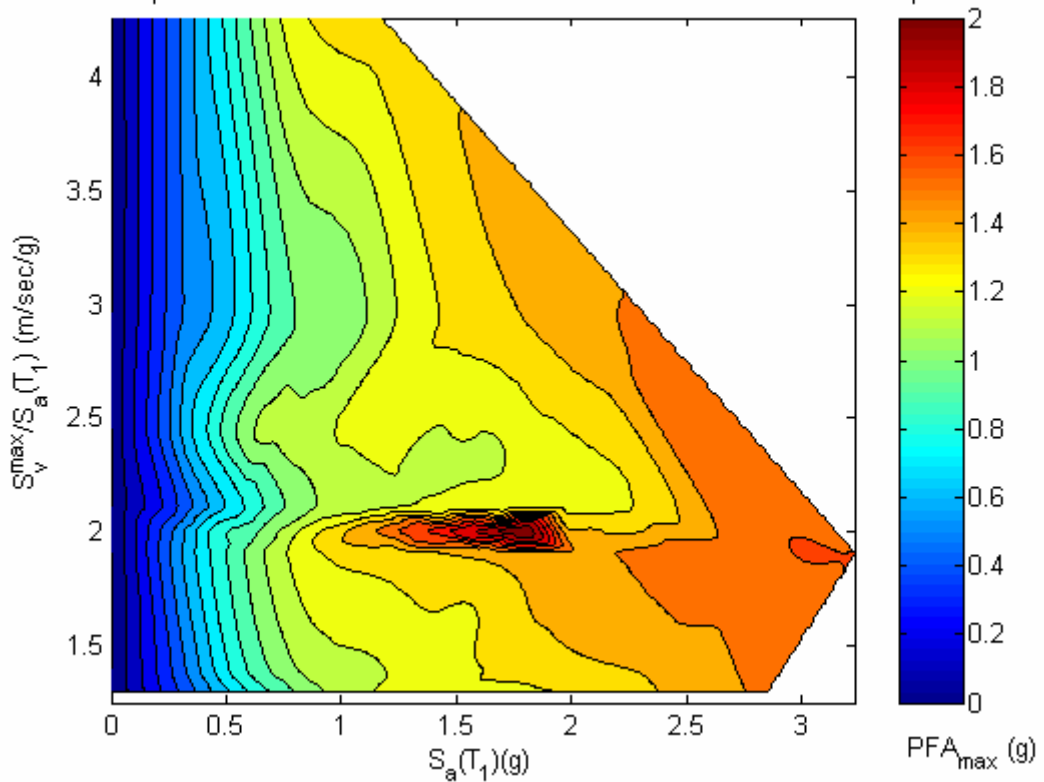


Fig. 4.36

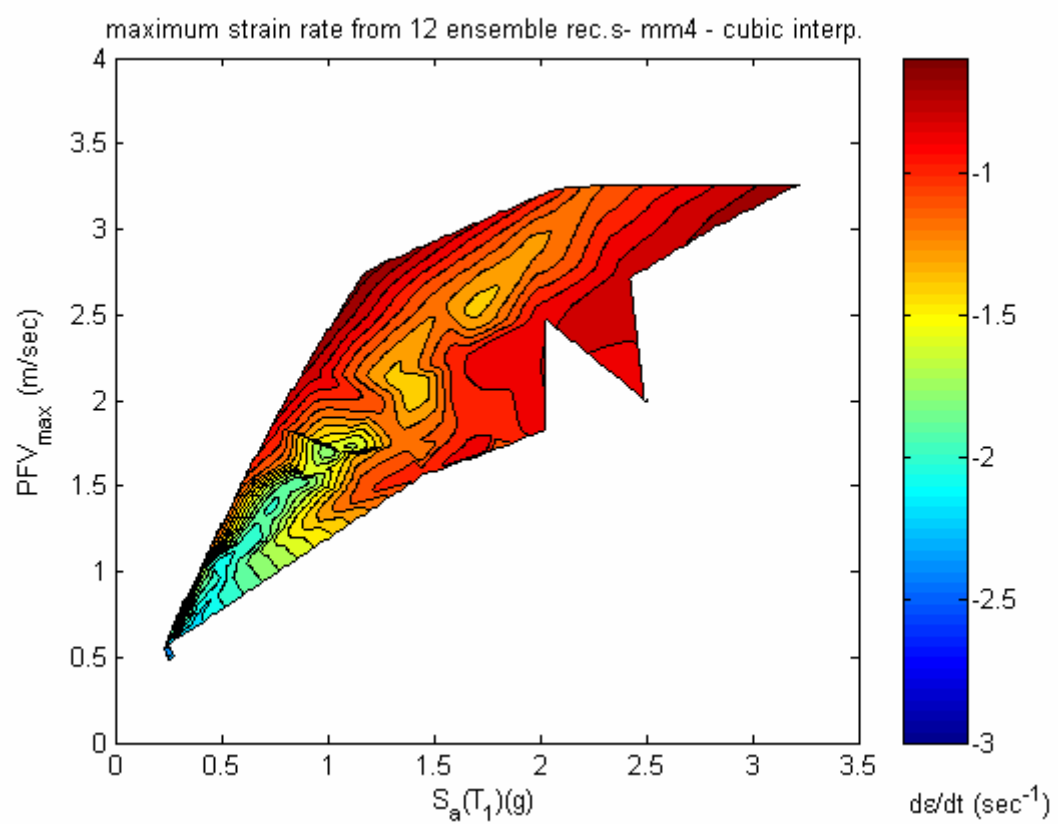


Fig. 4.37

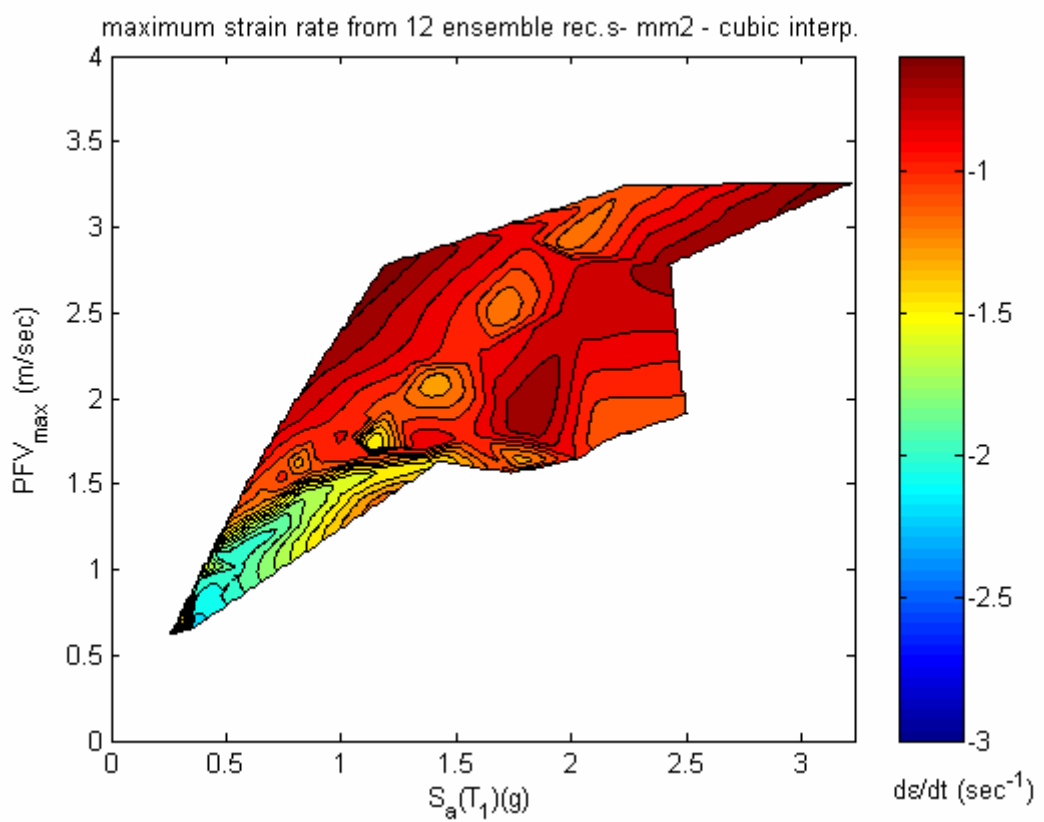


Fig. 4.38

Conclusions

In Chapter 2, an advanced state-of-the-art method is developed for seismic risk assessment. It is practically applicable as shown by the example in Chapter 3. The main problem of the method is the availability of both hazard and damageability data. This problem can be solved through more intensive efforts for creating open source databases. Among best practices in this context are websites of USGS (United States Geological Survey, USA) Hazard Program for hazard data and website of PEER (Pacific Earthquake Engineering Research Institute, USA) Framework for damageability data.

Continuing development of methods and tools in earthquake engineering leads to huge volumes of disorganized information which is not directly adaptable by risk assessment practice. An important contribution of this work has been to provide a complete method synthesizing state-of-the-art approaches and enriching them with original contributions.

Investigations on sensitivity to rate dependency have revealed that the phenomena is not significant for risk assessment purposes in terms of global response treatment. The question of local response sensitivity remains a further research need. This is particularly significant due to the very high strain rates on the brink of explosion load ranges proven by the simulations. On the other hand, response estimates are shown to be highly sensitive to progressive plasticity modeling demonstrated by comparison of multilinear and two-surface model data. Moreover, interaction of global response with near field seismological phenomena is observed. The outputs reveal that for better estimates of response and consequently of damage and risk, such interactions should be regarded.

As concluding remark, one can quote (Adams and Spence, 1999) “for all our present-day scientific and technical skill, the world’s earthquake problem is still a long way from being solved and so will require continuous attention” .

ANNEX.I. MATLAB Script

This annex is referred in section 3.3.5 of this work.

Following script is prepared as input for commercial software MATLAB. It is used for the application in Chapter 3. The method used therein is explained in Chapter 2.

```
disp('*****PROGRAM FOR SEISMIC RISK ASSESSMENT METHOD *****')
disp('*****prepared by: Sadik Cem Topcuoglu, 2006*****')

% PART I_HAZARD ASSESSMENT ****
% INPUT HAZARD PARAMETERS
% [this part assumes that the user has obtained the site hazard curve previously]

b=input('enter b coefficient for hazard curve (Gutenberg-Richter relation) \n')
% [b: slope of (the straight section of) the regional Gutenberg-Richter curve]
% [referred in eq. 10. obtained by regional seismicity analysis, see section 2.8. for details]

% [input all magnitudes in moment magnitude]

mmax=input('enter lower cutoff magnitude of hazard curve\n')
% [referred in eq.s 11 & 12. max. magnitude considered in hazard assessment, see section 2.8]

mmin=input('enter maximum magnitude of hazard curve\n')
% [referred in eq.s 11 & 12. min. magnitude considered in hazard assessment, see section 2.8]

ml=input('enter lower magnitude bound for risk assessment \n')
% [lower bound to be considered in risk assessment, see section 2.8]
% [varies between m=4-6]

mu=input('enter upper magnitude bound for risk assessment\n')
% [upper bound to be considered in hazard assessment, see section 2.9.1]
% [equal or slightly smaller than mmax]

nhl=input('enter number of considered hazard levels\n')
% [no. of hazard levels ml=<m=<mu, at which simulation will be carried out]
% [this is a subjective resolution decision, see section 2.9.1]
% [usual recommendation is 0.5 magnitude resolution, so nhl=(mu-ml)/0.5]
```

```
% [calculation of hazard parameters:]
```

```
dm=(mu-ml) / (nhl-1)
```

```
% [ $\Delta m$ , magnitude step between each hazard simulation level, see section 2.9.1.6]
```

```
bet=b*log(10)
```

```
% [ $\beta$ , eq.13, section 2.8]
```

```
k=1/(1-exp(-bet*(mmax-mmin)))
```

```
% [k, eq.12, section 2.8]
```

```
% [implementation of eq. 11, giving cumulative prob.s:]
```

```
m=ml
```

```
for h=1:nhl
```

```
% [cumulative prob.s of occurrence, eq.11:]
```

```
gem(hc)=k*(exp(-bet*(m-mmin)))-k+1
```

```
m=m+dm
```

```
end
```

```
% [computation for interval probabilities:]
```

```
hp(1,nhl)=gem(nhl)
```

```
for h=1:(nhl-1)
```

```
hp(1,nhl-h)=gem(nhl-h)-gem(1,nhl-h+1)
```

```
end
```

```
for h=1:nhl
```

```
HM(h)= ml-ms+(h*ms)
```

```
end
```

```
% [input number of simulations per hazard level:]
```

```
nth=input('enter number of simulated time histories per hazard level\n')
```

```
% [n, decision (2) in section 2.9.1.6]
```

```
% EXTERNAL WORK: Strong Motion Simulation
```

```
% [at this point, use an appropriate stochastic simulation program]
```

```
% to simulate nth time histories at each magnitude level ml, ml+dm, ml+2dm, ..., mu]
```

```
% [procedure and necessary tools are explained in section 2.9.1, especially in 2.9.1.6]
```

```
% EXTERNAL WORK: Structural Analysis (Response Assessment)
```

```
% [for each simulated time histories referred above,
```

```
% carry out structural analysis of the structure with appropriate methods and tools
```

```
% explained in section 2.9.2.]
```

```

% [from each analysis, extract necessary response governing variables]
% [which are ISDmax, PFAmax, PFVmax, refered in Table 2.6]

% PART II_RESPONSE INPUT ****
% [input of response governing variables to form necessary matrices for risk assessment,
% see section 2.9.2 for explanation]

% [response governing variables' matrices are initially set to zero to prepare for input]
isd=zeros(nth,nhl)
pfa=zeros(nth,nhl)
pfv=zeros(nth,nhl)

% [input results from structural analysis one by one at each hazard level:]
for hl=1:nhl
    disp('hazard level - magnitude')
    mh=ml-ms+(hl*ms)
    disp(mh)

% [input isd-max from structural analysis with each simulation at hazard level mh:]
isd(1:nth,hl)=input('enter isd-max from sim.s at the hazard level \n--bracketed & seperated with ;--\n')

% [input pfa-max from structural analysis with each simulation at hazard level mh:]
pfa(1:nth,hl)=input('enter pfa-max from sim.s at the hazard level \n--bracketed & seperated with ;--\n')

% [input pfv-max from structural analysis with each simulation at hazard level mh:]
pfv(1:nth,hl)=input('enter pfv-max from sim.s at the hazard level \n--bracketed & seperated with ;--\n')
end

% [natural logarithm of response governing variables,
% since lognormal distribution is assumed in line with literature:]
lisd=log(isd)
lpfa=log(pfa)
lpfv=log(pfv)

% [statistical inference of response governing variables at each hazard level:]
% [first three; mean values, rest; standard deviations]
lisdmu=mean(lisd)
lpfamu= mean(lpfa)
lpfvmu= mean(lpfv)
lisdsi=std(lisd)
lpfasi=std(lpfa)
lpfvsi=std(lpfv)

```

```

% PART III. DAMAGEABILITY INPUT*****
%
% [input of damageability parameters of each component,
% see section 2.9.3 for explanation]

%
% [whole structure is treated as one component. nonstr.l components and contents add one by one]
% [guiding list is in table 2.7 in section 2.9.3]
ndsc=input('enter number of drift sensitive components\n')
nasc=input('enter number of acceleration sensitive components\n')
nvsc=input('enter number of velocity sensitive components\n')

%
% [calculation, nc: total no. of components]
nc=ndsc+ nasc+nvsc

%
% [input, mcn: no of monte carlo simulations for each component]
% [input as 106 in application presented in chapter 3, explained in section 3.3.5]
mcn=input('enter number of simulations\n')

%
% [input, damage state capacity data,
% for an example: see Table 2.8,
% % concept is explained in section 2.9.3]

%
% [WARNING: enter damageability data first for drift-sensitive, then for acc.-sensitive,
% finally for vel.-sensitive components]

%
% PART IV. DAMAGE AND LOSS ASSESSMENT *****
%
% [loop for each component:]
for m=1:nc
    disp('COMPONENT no.:')
    disp(m)
    %
    % [input respectively mean capacity for 4 damage states for the component considered]
    % [if less than 4 ds's are defined for the component, give rest as very high numbers,
    % e.g. 10E8 times the last defined damage state capacity]

    dmu(1:4,m)=input('enter damage state mean capacities \n--bracketed & seperated with ;--\n')
    %
    % [example to mean capacity; Table 2.8., Column 10-left]

    dsi(1:4,m)=input('enter damage state capacity standard dev.s\n--bracketed &...
        seperated with ;--\n')
    %
    % [example to capacity standard dev.; Table 2.8., Column 10-right]

    plr(1:4,m)=input('enter ratio of_damage state loss_to_comp. restoration cost_\n--bracketed &...
        seperated with ;--\n')

```

```

% [example to mean capacity; Table 2.8., Column 11]

rct(1,m)=input('enter ratio of _component restoration cost_ to _bld. restoration...
...cost_\n--bracketed--\n')

end

%*****
% [damage state prob. matrices are initially set to zero to prepare for input:]

% [damage state 1 matrix, rows: magnitude levels, columns: components]
pd1=zeros(nhl,nc)

% [damage state 2 matrix, rows: magnitude levels, columns: components]
pd2=zeros(nhl,nc)

% [damage state 3 matrix, rows: magnitude levels, columns: components]
pd3=zeros(nhl,nc)

% [damage state 4 matrix, rows: magnitude levels, columns: components]
pd4=zeros(nhl,nc)

% *****

% [damage state membership and loss calculation for each component:]
for m=1:nc
    disp('calculation for component:')
    nc
    % [extraction of mean capacity vector for component considered:]
    dammu=log(dmu(:,m))
    % [extraction of capacity standard deviation vector for component considered:]
    damsi=dsi(:,m)
    % [extraction of appropriate response vector for the component:]
    if m<=ndsc
        respmu=lisdmu
        respsi=lisdssi
    elseif m<=(ndsc+nasc)
        respamu=lpfamu
        respsi=lpfasi
    else
        respamu=lpfamu
        respsi=lpfasi
    end

```

```

tp1=0
tp2=0
tp3=0
tp4=0

% [monte carlo simulation for the component considered,
% aim: obtain damage state membership conditional probabilities]
disp('simulation counter:')

for s=1:mcn
    s
    % [generate random vector from response distribution:]
    y=lognrnd(respmu,respsi)

    % [implementation of eq.s 41 & 42:] *****
    % [obtain probability of exceedance of damage state 1 capacity
    % ,for the generated number:]
    cp1=logncdf(y,dammu(1),damsi(1))

    % [same for damage state 2, 3 and 4 respectively:]
    cp2=logncdf(y,dammu(2),damsi(2))
    cp3=logncdf(y,dammu(3),damsi(3))
    cp4=logncdf(y,dammu(4),damsi(4))
    % *****
    % [implementation of eq.s 43 & 44:] *****
    % [obtain probability of damage state 1 membership for generated vector:]
    ap1=cp1-cp2
    % [same for damage state 2, 3 and 4]
    ap2=cp2-cp3
    ap3=cp3-cp4
    ap4=cp4
    % *****
    % [cumulate probabilities of damage state membership:]
    tp1=tp1+ap1
    tp2=tp2+ap2
    tp3=tp3+ap3
    tp4=tp4+ap4
end

```

```

% [extract probability of damage state 1 membership for component considered...
% by dividing cumulated probability vector to number of simulations:]
pd1(:,m)=tp1/mcn

% [same for damage states 2,3 and 4:]
pd2(:,m)=tp2/mcn
pd3(:,m)=tp3/mcn
pd4(:,m)=tp4/mcn

%[ loop for each magnitude level :] ****
for f=1:nhl
    % loss|hazard as ratio of comp value
    rplahl(f,m)=(pd1(f,m)*plr(1,m))+(pd2(f,m)*plr(2,m))+(pd3(f,m)*plr(3,m))+...
    (pd4(f,m)*plr(4,m))
    % loss|hazard as ratio of bld value
    aplahl(f,m)=rplahl(f,m)*rct(m)
end
% ****

% [compute absolute probs of damage state membership: ] ****
% [multiply hazard probability vector with damage state 1 membership vector:]
apd1(m)=(hp*pd1(:,m))
% [same for damage states 2,3 and 4:]
apd2(m)=(hp*pd2(:,m))
apd3(m)=(hp*pd3(:,m))
apd4(m)=(hp*pd4(:,m))
% ****

% [unite damage state vectors to form dam. state probability matrix for component considered:]
apd(:,m)=[apd1(m);apd2(m);apd3(m);apd4(m)]
% ****

% [rel. damage loss per component, percent of comp. value:]*****
rpl(m)=(plr(:,m))'*apd(:,m)
% *****

% [abs. damage loss vector per component - percent of total value:]*****
apl(m)=rpl(m)*rct(m)
% ****

```

```

% [total loss due to the component - percent of total value:]*****
apl(m)=sum(apl(m))

end

% [loop for each component ended]*****



% PART V. EXTRACTION OF RESULTS*****
% [total loss - percent of total value:]
EXPLOSS=sum(apl)
EXPLOSS2=sum(aplt)
% [check: exploss should be equal to exploss2.]


% [further necessary data for risk assessment purposes can also be extracted at that point]*****


% [extraction of graphs:]
% [in the following are example commands for extraction of graphs.
% see the titles for explanation. fig.s 3.18 to 3.28 are produced with these commands.]



figure(1)

lossvshaz=sum(aplahl,2)
plot(lossvshaz*100,HM,'b.-')
axis([0 20 4.5 8.5])
title('total percent loss estimate - pcws linear interp.'',...
xlabel('loss ratio (%)'),ylabel('moment magnitude')


figure(2)

lossstr=aplahl(:,1)
lossnstr=aplahl(:,2)+aplahl(:,3)+aplahl(:,4)
losscon=aplahl(:,5)+aplahl(:,6)+aplahl(:,7)+aplahl(:,8)
plot(lossvshaz,HM,'b.-',lossnstr,HM,'g.-',losscon,HM,'r.-',lossstr,HM,'k.-')
axis([0 0.20 4.5 8.5])
title('total loss ratio vs. hazard level - pcws linear interp.'',...
xlabel('loss / total building value (%)'),ylabel('hazard intensity - moment magnitude')


figure(3)

plot(lossvshaz,hp,'b.-',lossnstr,hp,'g.-',losscon,hp,'r.-',lossstr,hp,'k.-')
%axis([0 0.20 4.5 8.5])
title('total loss ratio vs. hazard level - pcws linear interp.'',...
xlabel('loss / total building value (%)'),ylabel('hazard intensity - moment magnitude')

```

```

figure(3)
set(gcf,'DefaultLineLineWidth',0.5)
plot(aplahl(:,2),HM','g.-',aplahl(:,3),HM','g.-',aplahl(:,4),HM','g.-',...
aplahl(:,5),HM','r.-',aplahl(:,6),HM','r.-',aplahl(:,7),HM','r.-',aplahl(:,8),HM','r.-')
axis([0 0.20 4.5 8.5])
title('component loss ratio vs. hazard level - pcws linear interp.'),...
xlabel('loss / total building value (%)'),ylabel('hazard intensity - moment magnitude')

```

```

figure(4)
set(gcf,'DefaultLineLineWidth',0.5)
plot(aplahl(:,2),HM','g.-',aplahl(:,3),HM','g.-',aplahl(:,4),HM','g.-')
axis([0 0.20 4.5 8.5])
title('nonstructural component loss ratio vs. hazard level - pcws linear interp.'),...
xlabel('loss / total building value (%)'),ylabel('hazard intensity - moment magnitude')

```

```

figure(5)
set(gcf,'DefaultLineLineWidth',0.5)
plot(aplahl(:,5),HM','r.-',aplahl(:,6),HM','r.-',aplahl(:,7),HM','r.-',aplahl(:,8),HM','r.-')
axis([0 0.20 4.5 8.5])
title('content loss ratio vs. hazard level - pcws linear interp.'),...
xlabel('loss / total building value (%)'),ylabel('hazard intensity - moment magnitude')

```

```

figure(7)
lossstr=rplahl(:,1)
lossnstr=rplahl(:,2)+rplahl(:,3)+rplahl(:,4)
losscon=rplahl(:,5)+rplahl(:,6)+rplahl(:,7)+rplahl(:,8)
plot(lossvshaz,HM','b.-',lossnstr,HM','g.-',...
losscon,HM','r.-',lossstr,HM','k.-')
axis([0 0.20 4.5 8.5])
title('component type loss ratio vs. hazard level - pcws linear interp.'),...
xlabel('loss / total value of component type value (%)'),ylabel('hazard intensity - moment magnitude')

```

```

figure(8)
set(gcf,'DefaultLineLineWidth',0.5)
plot(rplahl(:,1),HM','k.-')
axis([0 0.20 4.5 8.5])
title('structural loss ratio vs. hazard level - pcws linear interp.'),...
xlabel('loss / total value of structural components (%)'),ylabel('hazard intensity - moment magnitude')

```

```

figure(9)
set(gcf,'DefaultLineLineWidth',0.5)
plot(rplahl(:,2),HM,'g.-',rplahl(:,3),HM,'g.-',rplahl(:,4),HM,'g.-')
axis([0 2 4.5 8.5])
title('nonstructural component loss ratio vs. hazard level - pcws linear interp.'),...
xlabel('loss / component value (%)'),ylabel('hazard intensity - moment magnitude')

figure(10)
set(gcf,'DefaultLineLineWidth',0.5)
plot(rplahl(:,5),HM,'r.-',rplahl(:,6),HM,'r.-',rplahl(:,7),HM,'r.-',rplahl(:,8),HM,'r.-')
axis([0 1 4.5 8.5])
title('content loss ratio vs. hazard level - pcws linear interp.'),...
xlabel('loss / content value (%)'),ylabel('hazard intensity - moment magnitude')

figure(11)
set(gcf,'DefaultLineLineWidth',0.5)
plot(pd1(:,1),HM,'g.-',pd2(:,1),HM,'b.-',pd3(:,1),HM,'r.-')
%axis([0 1 4.5 8.5])
title('structure damage state probability vs. hazard level - pcws linear interp.'),...
xlabel('probability'),ylabel('hazard intensity - moment magnitude')

figure(11)
set(gcf,'DefaultLineLineWidth',0.5)
plot(pd1(:,1),hp,'g.-',pd2(:,1),hp,'b.-',pd3(:,1),hp,'r.-')
%axis([0 1 4.5 8.5])
title('structure damage state probability - pcws linear interp.'),...

figure(12)
set(gcf,'DefaultLineLineWidth',0.5)
plot(SDISD,HM,'r.-',SDPFA,HM,'b.-',SDPFV,HM,'g.-')
%axis([0 1 4.5 8.5])
title('dispersion of response - pcws linear interp.'),...
xlabel('/sigma standard deviation of response distribution'),ylabel('hazard intensity - moment magnitude')

% E N D ****

```

ANNEX.II. ANSYS Script

This annex is referred in sections 3.3.4, 4.3.2, 4.3.3 and 4.3.5 of this work.

Following script is prepared as input for commercial software MATLAB. It is used for the applications in Chapter 3 and Chapter 4. Due to the dimensions of this work, only one hazard amplification level for one time history and one material model is given as example (amplification level 0.125 for time history p0809 – p0809 being number of strong motion record in PEER Database (PEER, 2005)). Since it is necessary to clear database in ANSYS after each computation, all structural and material data should be input again after computation of each strong motion time-history.

The following script is based largely on a script in the work of (Wichers, 2001). Time history ensemble used here is a different one than that of Wichers'. Several further revisions are made in structural configuration and material properties. Profile database referred in the script is also provided in the work by (Wichers, 2001). Details on the script (e.g. generation of profiles, time history analysis aspects) are also given there. The referred author has given permission to use a modified version of his script within this work.

```
/BATCH
/CLEAR
/UNITS,SI
/CONFIG,NRES,2000

/CWD,d:\cem\p0809x0.125_m2
/FILNAME,p0809x0.125_m2,1
/CONFIG,NRES,500000
iwert=1814      !Anzahl der Werte, die aus der Erdbebendatei gelesen werden
ilang=1814      !Anzahl der Werte, die aus der Erdbebendatei gelesen werden
deltat=0.02

skalt1=0.125
Moanaly=0          ! 0:transient or static analysis  1:modal analysis
dynam=1            ! 0:static analysis(dl+ll)        1:transient analysis (dl+ll+eq)
mscal=0.7          ! Skalierung der Masse
weight=0.38692E+06 !weight of structure

! *** Werkstoffmodell *****
modell=2          ! 0: linear-elastische Rechnung
                  ! 1: bilineares Werkstoffmodell
                  ! 2: multilineares Werkstoffmodell
                  ! 3: TWO-Surface zeitunabhängig (Scheibe/Reinighaus)
                  ! 4: TWO-Surface Zeitabhängig (Scheibe/Reinighaus/Böttcher)

! *** Profile *****
profils='hea200'
profilr='hea200'
profilv='L70x7'
profilvr='hea140'           !Die Profil-Datenbank liegt in mm vor
profilba='d4hea200'
profilbb='d3hea200'
profilbc='d4hea200'
! *** Halterung Rahmeneckknoten in uy*****
decuy=0                !0:keine halterung, 1:halterung
```

```

!*** Lastparameter/Dynamik ***
masse=0.7
!Berücksichtigung der Massenträgheit 0: keine Berücksicht. 1: Berücksichtigung

massw=2.105*mscal
!Riegelmasse, corresponds to 21,05 kN/m when mscal=1 kg/m/1000

! *** Geometry ***
ibays=1      !0: 2D model, 1: rahmen in tiefe
istock=3     !Anzahl der Stockwerke des Rahmens,1,2,3      [Anzahl]      in Stück
breit=5000   !Rahmenbreite                                [Breite]      in mm
breitq=3000  !Abstand der Rahmen in der Tiefe          [Abstand]    in mm
hocbeg=3000  !Höhe Erdgeschoß                          [Höhe EG]    in mm
hochoga=3000 !Höhe 1.Obergeschoß                      [Höhe 1.OG]  in mm
hochogb=3000 !Höhe 2.Obergeschoß                      [Höhe 2.OG]  in mm
einsp=1      !Fußpunkt Stütze      0: gelenkiger Fußpunkt 1: eingespannter Fußpunkt
offset=0     !Abstand der Verbands-/Riegelknoten aus der Rahmenebene [Anzahl]      in mm
unts=10      !Anzahl der Elemente in der Stütze        [Anzahl]      in Stück
untr=10      !Anzahl der Elemente im Riegel           [Anzahl]      in Stück
untv=10      !Anzahl der Elemente im Verbandsstab       [Anzahl]      in Stück
bone=150     !Breite des 1/3-Bone-Elementes            [Breite]      in mm

! *** for calc of graphs
weightcoef=100/weight
hochcoef1=-100/hocbeg
hochcoef2=100/hochoga

! *** Sonstige Parameter ***
loese=1
langsa=40000  !Zeitliche Verzögerung der Lastdauer-genutzt für erste lastspiele
dskal=10*skalt1
askal=-9810   !Erdbeschleunigung                  [Beschleunigung] in mm/sec2

! *** Konvergenzkriterien ***
konv=0
konv2=0
cfak1=350
cfak2=0.05
iterat=1000

! *** Steuerungsvariablen für Erdbeben***
KBCWERT=1      !sprungartig
subzahl=1

! *** Schubverformung setzen, Kappa nach Ahrens/Duddek ***
DXI=0
DXJ=0
SHEARZ1=4.29   !      Stütze
SHEARY1=1.34   !      Stütze
SHEARZ2=4.29   !      Riegel
SHEARY2=1.36   !      Riegel
SHEARZ3=3.98   !      Dog-Bone innen
SHEARY3=1.40   !      Dog-Bone innen
SHEARZ4=3.66   !      Dog-Bone mitte
SHEARY4=1.45   !      Dog-Bone mitte
SHEARZ5=3.98   !      Dog-Bone außen
SHEARY5=1.40   !      Dog-Bone außen
SHEARZ6=4.58   !      Querriegel
SHEARY6=1.32   !      Querriegel
SHEARZ7=0      !      Verband
SHEARY7=0      !      Verband

! *** Parameter für Werkstoffmodelle ***
! *** Allg. Parameter Werkstoff ***
emod=209000   !E-Modul                         [E-Modul]      in N/mm2
den=7.85e-9   !Dichte                          [Dichte]      in
kg/mm3/1000 !                                         = g/mm3
nue=0.3       !Querdehnzahl                    [nue]         in ---

! *** Modellparameter Elast-Plast (BKIN) ***
*if,modell,eq,1,then
betas=360.0    !Streckgrenze                   [Spannung]    in N/mm2
emodv=0.01*emod !Steigung der Verfestigung   [Steigung]    in N/mm2
*endif

! *** Modellparameter MKIN ***
*if,modell,eq,2,then
epsy=360/emod !Dehnung der Streckgrenze   [Dehnung]    in %

```

```

epsy2=0.020          !Dehnung Punkt 2           [Dehnung]      in %
epsy3=0.040          !Dehnung Punkt 3           [Dehnung]      in %
epsy4=0.060          !Dehnung Punkt 4           [Dehnung]      in %
epsy5=0.100          !Dehnung Punkt 5           [Dehnung]      in %
betas=360            !Spannung im Punkt 1 (Streckgrenze) [Spannung]   in N/mm2
betas2=360           !Spannung im Punkt 2           [Spannung]   in N/mm2
betas3=430           !Spannung im Punkt 3           [Spannung]   in N/mm2
betas4=470           !Spannung im Punkt 4           [Spannung]   in N/mm2
betas5=520           !Spannung im Punkt 5           [Spannung]   in N/mm2
*endif

! *** Modellparameter TWO-SURFACE SCHEIBE/REININGHAUS ***
*if,modell,eq,3,then
!Einlesen Steuerwerte
/com

! *** Modellparameter TWO-SURFACE (Scheibe/Reininghaus/Böttcher) ***
c1=1                !!! NDIM             Dimension des Problems
c2=2                !!! KFLIB
c3=0                !!! KHARD/KBOUND/0:boundnurisotrop
c4=1                !!! KALFA/1:reinermroz
c5=1                !!! KBETA

/com                 !Einlesen der Sp.-Dehn.-diagramme
c6=36.0             !!! LOADING:k aktuell37.0        SEDKN(1,1)    Grundwert Fließplateau
c7=0.27             !!! LOADING:k monoton12.5       xmonfa y_1
c8=0.23             !!! LOADING:k saettigung10.0     xsaeaf y_3
/com
c9=36.0             !!! BOUNDING:k aktuell42.0        SEDKN(2,1)    Grundwert Fließplateau
/com
!sonstige Parameter Scheibe
c10=0.5             !!! CONMC1          c_a         Param. strain-memory
c11=0.5             !!! CONMC2          c_m         Param. strain-memory
c12=0.2             !!! CONMC3          c_s         Param. strain-memory
c13=5.0              !!! QSTERN
c14=2.0              !!! CONLA            b_1         Formparameter
c15=-4.0             !!! CONLB            b_2         Formparameter
c16=0.60             !!! CONGH
c17=3.0              !!! CONGC
c18=-10.0            !!! CONGD
c19=-1.8             !!! CONB             e_1         Formparameter bounding
c20=0.06             !!! DELBK            z_1         Größenparam. zykl. Verfest.

/com                 !Ergänzungen Reininghaus
c21=1               !!! IELP
c22=3.0              !!! h2                h_2         Formparam. kl. Dehn.-amplit.
c23=2.5              !!! h3                h_3         Formparam. kl. Dehn.-amplit.
c24=0.93             !!! a1=0.73286281      a_1         Größenparameter monot. Verfest.
c25=0.019            !!! a2=0.0162018       a_2         Größenparameter monot. Verfest.
c26=0                !!! IFT
c27=0                !!! IFZ
c28=10.5             !!! wzu
c29=0.5              !!! wgr
c30=0.35             !!! delfak0.35

/com                 !Steuerung WMTWOS
c31=0.1              !!! EPVMAX
c32=0.00001          !!! EPVMIN
c33=0.00010          !!! GRFLI
c34=0.00010          !!! grfile
c35=1.0              !!! f1
c36=1.0              !!! f2
c37=1.0              !!! f3

/com                 !Steuerung ANSYS-Ausgabe
!c38=10              !!! ausele
!c39=1              !!! ausgau
!c40=10              !!! plotele56
!c41=1              !!! plotgaul

/com                 !geändertes Qstern
c42=5.0              !!! qtmod6          q_4_*    %
c43=6.0              !!! qprop6          q_3_*    %
c44=6.8              !!! qbou1(Verfest.)9.5   q_1_* unterstr. %
c45=6.2              !!! qbou26          q_2_*    %
c46=5.0              !!! qquer6

/com                 !Ratcheting/ Mittelspannungsrelax.
c47=0                !!! KDEL
c48=2.4              !!! rexpo

```

```

c49=1.0      !!! rvorz
c50=0        !!! krat
c51=5        !!! wkinal=ddelta
c52=1000     !!! wkina210
c53=0.01     !!! CHAB11
c54=0.01     !!! CHAB12
c55=0.0005   !!! rata
c56=70       !!! forga
c57=40       !!! forgb
c58=3        !!! forgc
c59=0.0059   !!! chab21
c60=0.0041   !!! chab22
c61=0.0001   !!! chab23_3.1
c62=0.0      !!! fkinbo0=reinisotrop
c63=1.0      !!! xrat
c64=50       !!! yrat
c65=10       !!! betmax
c66=42       !!! offbetino %o
c67=1        !!! irel

/com          !Zeitabhängigkeit
c68=0        !!! izeit(0=rate-indep.)
c69=0.0      !!! ddelta/kN/cm2(ohnewurzel2/3) 0.5
c70=7.5      !!! skvmax0.4 dk_0_dach      kN/cm2 max Add. auf Grundwert
c71=0.8      !!! vmaxa      s_2
c72=0.2      !!! vmaxb      s_1
c73=0.001    !!! tmaxb      p_1
c74=4.0      !!! dqmax      dq_1_*      %o      max geschwind.-abhängig. Add. auf
Grundwert
c75=1        !!! imehr
c76=4.0      !!! rloafa      b_3      Formparameter
c77=1.0      !!! ymonfa      y_2      Faktor für ungesättigt
c78=1.0      !!! ysaefa      y_4      Faktor gesättigt
c79=0.0      !!! sosfak      u_1      Faktor für R_eH (FÜR OBERE STR.GR._Ausgeschaltet)
c80=4.0      !!! strfak      k_ostr_Dach kN/cm2
! Wert für R_eH (FÜR OBERE STR.GR._Ausgesch.)
*endif

! *** 1.5 Modellparameter TWO-SURFACE SCHEIBE/REINGHAUS/BÖTTCHER ***
*if,modell,eq,4,then
c1=1         !!! NDIM           Dimension des Problems
c2=2         !!! KFLIB
c3=0         !!! KHARD/KBOUND/0:boundnurisotrop
c4=1         !!! KALFA/1:reinerroz
c5=1         !!! KBETA

/com          !Einlesen der Sp.-Dehn.-diagramme
c6=32.0      !!! LOADING:k aktuell37.0      SEDKN(1,1) Grundwert Fließplateau
c7=0.27     !!! LOADING:k monoton12.5      xmonfa y_1
c8=0.23     !!! LOADING:k saettigung10.0  xsaeafa y_3
/com          !!! BOUNDING:k aktuell42.0      SEDKN(2,1) Grundwert Fließplateau
/com          !sonstige Parameter Scheibe
c10=0.5     !!! CONMC1      c_a      Param. strain-memory
c11=0.5     !!! CONMC2      c_m      Param. strain-memory
c12=0.2     !!! CONMC3      c_s      Param. strain-memory
c13=5.0      !!! QSTERN
c14=2.0      !!! CONLA       b_1      Formparameter
c15=-4.0    !!! CONLB       b_2      Formparameter
c16=0.60    !!! CONGH
c17=3.0      !!! CONGC
c18=-10.0   !!! CONGD
c19=-1.8    !!! CONB       e_1      Formparameter bounding
c20=0.06    !!! DELBK      z_1      Größenparam. zykl. Verfest.

/com          !Ergänzungen Reininghaus
c21=1        !!! IELP
c22=3.0      !!! h2          h_2      Formparam. kl. Dehn.-amplit.
c23=2.5      !!! h3          h_3      Formparam. kl. Dehn.-amplit.
c24=0.93    !!! a1=0.73286281   a_1      Größenparameter monet. Verfest.
c25=0.019   !!! a2=0.0162018   a_2      Größenparameter monet. Verfest.
c26=0        !!! IFT
c27=0        !!! IFZ
c28=10.5    !!! wzu
c29=0.5      !!! wgr
c30=0.35    !!! delfak0.35

/com          !Steuerung WMTWOS

```

```

c31=0.1      !!! EPVMAX
c32=0.00001  !!! EPVMIN
c33=0.00010  !!! GRFLI
c34=0.00010  !!! grfle
c35=1.0      !!! f1
c36=1.0      !!! f2
c37=1.0      !!! f3

/com          !Steuerung ANSYS-Ausgabe
!c38=10      !!! ausele
!c39=1       !!! ausgau
!c40=10      !!! plotele56
!c41=1       !!! plotgaul

/com          !geändertes Qstern
c42=5.0      !!! qtmod6      q_4_*   %o
c43=6.0      !!! qprop6      q_3_*   %o
c44=6.8      !!! qbou1(Verfest.)9.5 q_1_* unterstr.    %o
c45=6.2      !!! qbou26     q_2_*   %o
c46=5.0      !!! qquer6

/com          !Ratcheting/ Mittelspannungsrelax.
c47=0         !!! KDEL
c48=2.4      !!! rexo
c49=1.0      !!! rvorz
c50=0         !!! krat
c51=5         !!! wkinal=ddelta
c52=1000     !!! wkin210
c53=0.01     !!! CHAB11
c54=0.01     !!! CHAB12
c55=0.0005   !!! rata
c56=70        !!! forga
c57=40        !!! forgb
c58=3         !!! forgc
c59=0.0059   !!! chab21
c60=0.0041   !!! chab22
c61=0.0001   !!! chab23_3.1
c62=0.0      !!! fkinbo0=reinisotrop
c63=1.0      !!! xrat
c64=50        !!! yrat
c65=10        !!! betmax
c66=42        !!! offbetino %o
c67=1         !!! irel

/com          !Zeitabhängigkeit
c68=1         !!! izeit(0=rate-indep.)
c69=0.0      !!! ddelta/kN/cm2(ohnewurzel2/3)0.5
c70=7.5      !!! skvmax0.4 dk_0_dach      kN/cm2 max Add. auf Grundwert
c71=0.8      !!! vmaxa      s_2
c72=0.2      !!! vmaxb      s_1
c73=0.001   !!! tmaxb      p_1
c74=4.0      !!! dqmax      dq_1_*   %o      max geschwind.-abhängig. Add. auf Grundwert
c75=1         !!! imehr
c76=4.0      !!! rloafa     b_3      Formparameter
c77=1.0      !!! ymonfa     y_2      Faktor für ungesättigt
c78=1.0      !!! ysaefa     y_4      Faktor gesättigt
c79=0.0      !!! sosfak     u_1      Faktor für R_eH
!(FÜR OBERE STRECKGRENZE_Ausgeschaltet)
c80=4.0      !!! strfak     k_ostr_Dach  kN/cm2 Wert für R_eH
!(FÜR OBERE STRECKGRENZE_Ausgeschaltet, s. c79)
*endif

! STRUCTURAL SYSTEM

! *** Rahmen x/y/z-Ebene ***
! *** Lage der Keypoints für Erdgeschoß ***

x1=0
y1=0
z1=0

x2=0
y2=0
z2=-hocheg

x3=bone
y3=0
z3=-hocheg

```

```

x4=2*bone
y4=0
z4=-hocheg

x5=3*bone
y5=0
z5=-hocheg

x6=breit-3*bone
y6=0
z6=-hocheg

x7=breit-2*bone
y7=0
z7=-hocheg

x8=breit-bone
y8=0
z8=-hocheg

x9=breit
y9=0
z9=-hocheg

x10=breit
y10=0
z10=0

! *** Lage der Keypoints für 1. Obergeschoß ***

x11=0
y11=0
z11=z2-hochoga

x12=bone
y12=0
z12=z3-hochoga

x13=2*bone
y13=0
z13=z3-hochoga

x14=3*bone
y14=0
z14=z5-hochoga

x15=breit-3*bone
y15=0
z15=z6-hochoga

x16=breit-2*bone
y16=0
z16=z7-hochoga

x17=breit-bone
y17=0
z17=z8-hochoga

x18=breit
y18=0
z18=z9-hochoga

! *** Lage der Keypoints für 2. Obergeschoß ***

x19=0
y19=0
z19=z11-hochogb

x20=bone
y20=0
z20=z12-hochogb

x21=2*bone
y21=0
z21=z13-hochogb

x22=3*bone
y22=0

```

```

z22=z14-hochogb

x23=breit-3*bone
y23=0
z23=z15-hochogb

x24=breit-2*bone
y24=0
z24=z16-hochogb

x25=breit-bone
y25=0
z25=z17-hochogb

x26=breit
y26=0
z26=z18-hochogb

! *** Aussteifungsebenen ***

eben1=-2*offset
eben2=-offset
eben3=offset
eben4=breit-offset
eben5=breit+offset
eben6=breit+2*offset

! *** Referenzknoten K zur Definition der z-Achse am BEAM24-Element ***

! *** Referenz in Längsrichtung ***

xk1=breit/2

! *** Referenz in QUerrichtung ***

yk2=breitq/2

! *** PREPROCESSING ***

/PREP7          !Aufruf des Preprocessors

! *** Elementtyp ***

ET,1,BEAM24      !Element-Typennr. 1 * Balkenelement BEAM24 * Stützelementierung
ET,2,BEAM24      !Element-Typennr. 2 * Balkenelement BEAM24 * Riegellementierung
ET,3,BEAM24      !Element-Typennr. 3 * Balkenelement BEAM24
! * Dogbone-Elementierung innen
ET,4,BEAM24      !Element-Typennr. 4 * Balkenelement BEAM24
! * Dogbone-Elementierung mitte
ET,5,BEAM24      !Element-Typennr. 5 * Balkenelement BEAM24
! * Dogbone-Elementierung außen
ET,6,BEAM24      !Element-Typennr. 6 * Balkenelement BEAM24
! * Querriegellementierung
ET,7,BEAM24      !Element-Typennr. 7 * Balkenelement BEAM24 * Verbandselementierung

*if,masse,gt,0,then !Prüfung ob Massenträgheit berücksichtigt werden muß
ET,8,MASS21       !Element-Typennr. 8 * Massenelement MASS21
*endif

! *** Elementoptionen ***

KEYO,1,1,0        !!! Print additional cross-section check data !!!
KEYO,1,2,0        !!! Consistent mass matrix !!!
KEYO,1,3,1        !!! Centroid of Element at nodes !!!
KEYO,1,6,0        !!! Print member forces + moments !!!

KEYO,2,1,0        !!! Print additional cross-section check data !!!
KEYO,2,2,0        !!! Consistent mass matrix !!!
KEYO,2,3,1        !!! Centroid of Element at nodes !!!
KEYO,2,6,0        !!! Print member forces + moments !!!

KEYO,3,1,1        !!! Print additional cross-section check data !!!
KEYO,3,2,0        !!! Consistent mass matrix !!!
KEYO,3,3,1        !!! Centroid of Element at nodes !!!
KEYO,3,6,0        !!! Print member forces + moments !!!

KEYO,4,1,1        !!! Print additional cross-section check data !!!
KEYO,4,2,0        !!! Consistent mass matrix !!!

```

```

KEYO,4,3,1          !!! Centroid of Element at nodes !!!
KEYO,4,6,0          !!! Print member forces + moments !!!

KEYO,5,1,1          !!! Print additional cross-section check data !!!
KEYO,5,2,0          !!! Consistent mass matrix !!!
KEYO,5,3,1          !!! Centroid of Element at nodes !!!
KEYO,5,6,0          !!! Print member forces + moments !!!

KEYO,6,1,0          !!! Print additional cross-section check data !!!
KEYO,6,2,0          !!! Consistent mass matrix !!!
KEYO,6,3,1          !!! Centroid of Element at nodes !!!
KEYO,6,6,0          !!! Print member forces + moments !!!

KEYO,7,1,0          !!! Print additional cross-section check data !!!
KEYO,7,2,0          !!! Consistent mass matrix !!!
KEYO,7,3,1          !!! Centroid of Element at nodes !!!
KEYO,7,6,0          !!! Print member forces + moments !!!

*if,masse,gt,0,then !Elementoptionen nur bei Massenberücksichtigung
KEYO,8,3,2          !Keine Berücksichtigung der 3D-Massenträgheit infolge Rotation
*endif

! *** Werkstoffparameter setzen ***

!Festlegung der Werkstoffeigenschaften * Material-Nr.1 in Werkstofftabelle

MP,EX,1,emod        !Zuweisen des E-Moduls (Young's module)
MP,NUXY,1,nue        !Zuweisen der Querdehnzahl (Poisson's ratio, minor)
MP,DENS,1,den        !Zuweisen der Dichte

*if,modell,eq,1,then !Prüfung ob Werkstoffmodell 1 vorliegt
TB,BKIN,1,1          !Festlegung des bilinearen Werkstoffmodells
TBDATA,1,betas,emodv !Eintrag der Parameter
*endif

*if,modell,eq,2,then !Prüfung ob Werkstoffmodell 2 vorliegt
TB,MKIN,1,1          !Festlegung des multilineareren Werkstoffmodells
TBTEMP,,STRAIN        !Definiert die nachfolgenden Einträge als Dehnung
TBDATA,1,epsy,epsy2,epsy3,epsy4,epsy5 !Zuweisen der Dehnungen
TBTEMP,0.0            !Ausgangstemperatur zu Null Grad setzen
TBDATA,1,betas,betas2,betas3,betas4,betas5 !Eintrag der Spannungen zu Dehnungen
*endif

*if,modell,eq,3,then
TB,USER,1,,80
TBDATA,1,c1
TBDATA,2,c2
TBDATA,3,c3
TBDATA,4,c4
TBDATA,5,c5
TBDATA,6,c6
TBDATA,7,c7
TBDATA,8,c8
TBDATA,9,c9
TBDATA,10,c10
TBDATA,11,c11
TBDATA,12,c12
TBDATA,13,c13
TBDATA,14,c14
TBDATA,15,c15
TBDATA,16,c16
TBDATA,17,c17
TBDATA,18,c18
TBDATA,19,c19
TBDATA,20,c20
TBDATA,21,c21
TBDATA,22,c22
TBDATA,23,c23
TBDATA,24,c24
TBDATA,25,c25
TBDATA,26,c26
TBDATA,27,c27
TBDATA,28,c28
TBDATA,29,c29
TBDATA,30,c30
TBDATA,31,c31
TBDATA,32,c32
TBDATA,33,c33
TBDATA,34,c34

```

```

TBDATA, 35, c35
TBDATA, 36, c36
TBDATA, 37, c37
TBDATA, 38, c38
TBDATA, 39, c39
TBDATA, 40, c40
TBDATA, 41, c41
TBDATA, 42, c42
TBDATA, 43, c43
TBDATA, 44, c44
TBDATA, 45, c45
TBDATA, 46, c46
TBDATA, 47, c47
TBDATA, 48, c48
TBDATA, 49, c49
TBDATA, 50, c50
TBDATA, 51, c51
TBDATA, 52, c52
TBDATA, 53, c53
TBDATA, 54, c54
TBDATA, 55, c55
TBDATA, 56, c56
TBDATA, 57, c57
TBDATA, 58, c58
TBDATA, 59, c59
TBDATA, 60, c60
TBDATA, 61, c61
TBDATA, 62, c62
TBDATA, 63, c63
TBDATA, 64, c64
TBDATA, 65, c65
TBDATA, 66, c66
TBDATA, 67, c67
TBDATA, 68, c68
TBDATA, 69, c69
TBDATA, 70, c70
TBDATA, 71, c71
TBDATA, 72, c72
TBDATA, 73, c73
TBDATA, 74, c74
TBDATA, 75, c75
TBDATA, 76, c76
TBDATA, 77, c77
TBDATA, 78, c78
TBDATA, 79, c79
TBDATA, 80, c80
*endif

*if,modell,eq,4,then
TB,USER,1,,80
TBDATA,1,c1
TBDATA,2,c2
TBDATA,3,c3
TBDATA,4,c4
TBDATA,5,c5
TBDATA,6,c6
TBDATA,7,c7
TBDATA,8,c8
TBDATA,9,c9
TBDATA,10,c10
TBDATA,11,c11
TBDATA,12,c12
TBDATA,13,c13
TBDATA,14,c14
TBDATA,15,c15
TBDATA,16,c16
TBDATA,17,c17
TBDATA,18,c18
TBDATA,19,c19
TBDATA,20,c20
TBDATA,21,c21
TBDATA,22,c22
TBDATA,23,c23
TBDATA,24,c24
TBDATA,25,c25
TBDATA,26,c26
TBDATA,27,c27
TBDATA,28,c28
TBDATA,29,c29

```

```

TBDATA,30,c30
TBDATA,31,c31
TBDATA,32,c32
TBDATA,33,c33
TBDATA,34,c34
TBDATA,35,c35
TBDATA,36,c36
TBDATA,37,c37
TBDATA,38,c38
TBDATA,39,c39
TBDATA,40,c40
TBDATA,41,c41
TBDATA,42,c42
TBDATA,43,c43
TBDATA,44,c44
TBDATA,45,c45
TBDATA,46,c46
TBDATA,47,c47
TBDATA,48,c48
TBDATA,49,c49
TBDATA,50,c50
TBDATA,51,c51
TBDATA,52,c52
TBDATA,53,c53
TBDATA,54,c54
TBDATA,55,c55
TBDATA,56,c56
TBDATA,57,c57
TBDATA,58,c58
TBDATA,59,c59
TBDATA,60,c60
TBDATA,61,c61
TBDATA,62,c62
TBDATA,63,c63
TBDATA,64,c64
TBDATA,65,c65
TBDATA,66,c66
TBDATA,67,c67
TBDATA,68,c68
TBDATA,69,c69
TBDATA,70,c70
TBDATA,71,c71
TBDATA,72,c72
TBDATA,73,c73
TBDATA,74,c74
TBDATA,75,c75
TBDATA,76,c76
TBDATA,77,c77
TBDATA,78,c78
TBDATA,79,c79
TBDATA,80,c80
*endif

! *** Übertragung der Geometrieparameter auf die Elemente ***
! *** Stützen-Element BEAM24 * Element-Typennr. 1 ***
*DIM,ESTL,array,60,1
*VREAD,ESTL(1),profils,txt,d:\cem\profil\,,1
(1F9.2)
R,1,ESTL(1),ESTL(2),ESTL(3),ESTL(4),ESTL(5),ESTL(6)
RMORE,ESTL(7),ESTL(8),ESTL(9),ESTL(10),ESTL(11),ESTL(12)
RMORE,ESTL(13),ESTL(14),ESTL(15),ESTL(16),ESTL(17),ESTL(18)
RMORE,ESTL(19),ESTL(20),ESTL(21),ESTL(22),ESTL(23),ESTL(24)
RMORE,ESTL(25),ESTL(26),ESTL(27),ESTL(28),ESTL(29),ESTL(30)
RMORE,ESTL(31),ESTL(32),ESTL(33),ESTL(34),ESTL(35),ESTL(36)
RMORE,ESTL(37),ESTL(38),ESTL(39),ESTL(40),ESTL(41),ESTL(42)
RMORE,ESTL(43),ESTL(44),ESTL(45),ESTL(46),ESTL(47),ESTL(48)
RMORE,ESTL(49),ESTL(50),ESTL(51),ESTL(52),ESTL(53),ESTL(54)
RMORE,ESTL(55),ESTL(56),ESTL(57),ESTL(58),ESTL(59),ESTL(60)
RMORE,DXI,DXJ,SHEARZ1,SHEARY1

! *** Riegel-Element BEAM24 * Element-Typennr. 2 ***
*DIM,ERIL,array,60,1
*VREAD,ERIL(1),profilr,txt,d:\cem\profil\,,1
(1F9.2)
R,2,ERIL(1),ERIL(2),ERIL(3),ERIL(4),ERIL(5),ERIL(6)
RMORE,ERIL(7),ERIL(8),ERIL(9),ERIL(10),ERIL(11),ERIL(12)

```

```

RMORE,ERIL(13),ERIL(14),ERIL(15),ERIL(16),ERIL(17),ERIL(18)
RMORE,ERIL(19),ERIL(20),ERIL(21),ERIL(22),ERIL(23),ERIL(24)
RMORE,ERIL(25),ERIL(26),ERIL(27),ERIL(28),ERIL(29),ERIL(30)
RMORE,ERIL(31),ERIL(32),ERIL(33),ERIL(34),ERIL(35),ERIL(36)
RMORE,ERIL(37),ERIL(38),ERIL(39),ERIL(40),ERIL(41),ERIL(42)
RMORE,ERIL(43),ERIL(44),ERIL(45),ERIL(46),ERIL(47),ERIL(48)
RMORE,ERIL(49),ERIL(50),ERIL(51),ERIL(52),ERIL(53),ERIL(54)
RMORE,ERIL(55),ERIL(56),ERIL(57),ERIL(58),ERIL(59),ERIL(60)
RMORE,DXI,DXJ,SHEARZ2,SHEARY2

```

```
! *** Dogbone-Innen-Element BEAM24 * Element-Typennr. 3 ***
```

```

*DIM,EBAL,array,60,1
*VREAD,EBAL(1),profilba,txt,d:\cem\profil\,1
(1F9.2)
R,3,EBAL(1),EBAL(2),EBAL(3),EBAL(4),EBAL(5),EBAL(6)
RMORE,EBAL(7),EBAL(8),EBAL(9),EBAL(10),EBAL(11),EBAL(12)
RMORE,EBAL(13),EBAL(14),EBAL(15),EBAL(16),EBAL(17),EBAL(18)
RMORE,EBAL(19),EBAL(20),EBAL(21),EBAL(22),EBAL(23),EBAL(24)
RMORE,EBAL(25),EBAL(26),EBAL(27),EBAL(28),EBAL(29),EBAL(30)
RMORE,EBAL(31),EBAL(32),EBAL(33),EBAL(34),EBAL(35),EBAL(36)
RMORE,EBAL(37),EBAL(38),EBAL(39),EBAL(40),EBAL(41),EBAL(42)
RMORE,EBAL(43),EBAL(44),EBAL(45),EBAL(46),EBAL(47),EBAL(48)
RMORE,EBAL(49),EBAL(50),EBAL(51),EBAL(52),EBAL(53),EBAL(54)
RMORE,EBAL(55),EBAL(56),EBAL(57),EBAL(58),EBAL(59),EBAL(60)
RMORE,DXI,DXJ,SHEARZ3,SHEARY3

```

```
! *** Dogbone-Mitte-Element BEAM24 * Element-Typennr. 4 ***
```

```

*DIM,EBBL,array,60,1
*VREAD,EBBL(1),profilbb,txt,d:\cem\profil\,1
(1F9.2)
R,4,EBBL(1),EBBL(2),EBBL(3),EBBL(4),EBBL(5),EBBL(6)
RMORE,EBBL(7),EBBL(8),EBBL(9),EBBL(10),EBBL(11),EBBL(12)
RMORE,EBBL(13),EBBL(14),EBBL(15),EBBL(16),EBBL(17),EBBL(18)
RMORE,EBBL(19),EBBL(20),EBBL(21),EBBL(22),EBBL(23),EBBL(24)
RMORE,EBBL(25),EBBL(26),EBBL(27),EBBL(28),EBBL(29),EBBL(30)
RMORE,EBBL(31),EBBL(32),EBBL(33),EBBL(34),EBBL(35),EBBL(36)
RMORE,EBBL(37),EBBL(38),EBBL(39),EBBL(40),EBBL(41),EBBL(42)
RMORE,EBBL(43),EBBL(44),EBBL(45),EBBL(46),EBBL(47),EBBL(48)
RMORE,EBBL(49),EBBL(50),EBBL(51),EBBL(52),EBBL(53),EBBL(54)
RMORE,EBBL(55),EBBL(56),EBBL(57),EBBL(58),EBBL(59),EBBL(60)
RMORE,DXI,DXJ,SHEARZ4,SHEARY4

```

```
! *** Dogbone-Außens-Element BEAM24 * Element-Typennr. 5 ***
```

```

*DIM,EBCL,array,60,1
*VREAD,EBCL(1),profilbc,txt,d:\cem\profil\,1
(1F9.2)
R,5,EBCL(1),EBCL(2),EBCL(3),EBCL(4),EBCL(5),EBCL(6)
RMORE,EBCL(7),EBCL(8),EBCL(9),EBCL(10),EBCL(11),EBCL(12)
RMORE,EBCL(13),EBCL(14),EBCL(15),EBCL(16),EBCL(17),EBCL(18)
RMORE,EBCL(19),EBCL(20),EBCL(21),EBCL(22),EBCL(23),EBCL(24)
RMORE,EBCL(25),EBCL(26),EBCL(27),EBCL(28),EBCL(29),EBCL(30)
RMORE,EBCL(31),EBCL(32),EBCL(33),EBCL(34),EBCL(35),EBCL(36)
RMORE,EBCL(37),EBCL(38),EBCL(39),EBCL(40),EBCL(41),EBCL(42)
RMORE,EBCL(43),EBCL(44),EBCL(45),EBCL(46),EBCL(47),EBCL(48)
RMORE,EBCL(49),EBCL(50),EBCL(51),EBCL(52),EBCL(53),EBCL(54)
RMORE,EBCL(55),EBCL(56),EBCL(57),EBCL(58),EBCL(59),EBCL(60)
RMORE,DXI,DXJ,SHEARZ5,SHEARY5

```

```
! *** Querriegel-Element BEAM24 * Element-Typennr. 6 ***
```

```

*DIM,ERQL,array,60,1
*VREAD,ERQL(1),profilvr,txt,d:\cem\profil\,1
(1F9.2)
R,6,ERQL(1),ERQL(2),ERQL(3),ERQL(4),ERQL(5),ERQL(6)
RMORE,ERQL(7),ERQL(8),ERQL(9),ERQL(10),ERQL(11),ERQL(12)
RMORE,ERQL(13),ERQL(14),ERQL(15),ERQL(16),ERQL(17),ERQL(18)
RMORE,ERQL(19),ERQL(20),ERQL(21),ERQL(22),ERQL(23),ERQL(24)
RMORE,ERQL(25),ERQL(26),ERQL(27),ERQL(28),ERQL(29),ERQL(30)
RMORE,ERQL(31),ERQL(32),ERQL(33),ERQL(34),ERQL(35),ERQL(36)
RMORE,ERQL(37),ERQL(38),ERQL(39),ERQL(40),ERQL(41),ERQL(42)
RMORE,ERQL(43),ERQL(44),ERQL(45),ERQL(46),ERQL(47),ERQL(48)
RMORE,ERQL(49),ERQL(50),ERQL(51),ERQL(52),ERQL(53),ERQL(54)
RMORE,ERQL(55),ERQL(56),ERQL(57),ERQL(58),ERQL(59),ERQL(60)
RMORE,DXI,DXJ,SHEARZ6,SHEARY6

```

```
! *** Verbands-Element BEAM24 * Element-Typennr. 7 ***
```

```

*DIM, EVRL, array, 60, 1
*VREAD, EVRL(1), profilv, txt, d:\cem\profil\,1
(1F9.2)
R, 7, EVRL(1), EVRL(2), EVRL(3), EVRL(4), EVRL(5), EVRL(6)
RMORE, EVRL(7), EVRL(8), EVRL(9), EVRL(10), EVRL(11), EVRL(12)
RMORE, EVRL(13), EVRL(14), EVRL(15), EVRL(16), EVRL(17), EVRL(18)
RMORE, EVRL(19), EVRL(20), EVRL(21), EVRL(22), EVRL(23), EVRL(24)
RMORE, EVRL(25), EVRL(26), EVRL(27), EVRL(28), EVRL(29), EVRL(30)
RMORE, EVRL(31), EVRL(32), EVRL(33), EVRL(34), EVRL(35), EVRL(36)
RMORE, EVRL(37), EVRL(38), EVRL(39), EVRL(40), EVRL(41), EVRL(42)
RMORE, EVRL(43), EVRL(44), EVRL(45), EVRL(46), EVRL(47), EVRL(48)
RMORE, EVRL(49), EVRL(50), EVRL(51), EVRL(52), EVRL(53), EVRL(54)
RMORE, EVRL(55), EVRL(56), EVRL(57), EVRL(58), EVRL(59), EVRL(60)
RMORE, DXI, DXJ, SHEARZ7, SHEARY7

! *** Massen-Element MASS21 * Element-Typennr. 8 ***
*if,masse,gt,0,then                                !Prüfung ob Massenträgheit berücksichtigt
werden muß
massel=(massw*(breit-6*bone)/1000)/(untr+1)      !Masse am Knoten zwischen BEAM24-Elementen
R, 8, massel                                      !Element-Typennr. 8 Masse zuweisen
*endif

! *** 5.4 Solid Model ***

! *** Erzeugung der Keypoints für den Rahmen ***
! *** Keypoints EG, vorderer Rahmen ***
k,1,x1,y1,z1          !Verwendung der Geo.-Parameter zur Bildung von Keypoint-Nr. 1
k,2,x2,y2,z2          !Verwendung der Geo.-Parameter zur Bildung von Keypoint-Nr. 2
k,3,x3,y3,z3          !Verwendung der Geo.-Parameter zur Bildung von Keypoint-Nr. 3
k,4,x4,y4,z4          !Verwendung der Geo.-Parameter zur Bildung von Keypoint-Nr. 4
k,5,x5,y5,z5          !Verwendung der Geo.-Parameter zur Bildung von Keypoint-Nr. 5
k,6,x6,y6,z6          !Verwendung der Geo.-Parameter zur Bildung von Keypoint-Nr. 6
k,7,x7,y7,z7          !Verwendung der Geo.-Parameter zur Bildung von Keypoint-Nr. 7
k,8,x8,y8,z8          !Verwendung der Geo.-Parameter zur Bildung von Keypoint-Nr. 8
k,9,x9,y9,z9          !Verwendung der Geo.-Parameter zur Bildung von Keypoint-Nr. 9
k,10,x10,y10,z10     !Verwendung der Geo.-Parameter zur Bildung von Keypoint-Nr. 10
k,120,xk1,0,0          !Verwendung der Geo.-P. zur Bildung von Referenzpunkt-Nr. 120

*if,ibays,gt,0,then
! *** Keypoints EG, hinterer Rahmen ***
k,31,x1,breitq,z1    !Verwendung der Geo.-Parameter zur Bildung von Keypoint-Nr. 31
k,32,x2,breitq,z2    !Verwendung der Geo.-Parameter zur Bildung von Keypoint-Nr. 32
k,33,x3,breitq,z3    !Verwendung der Geo.-Parameter zur Bildung von Keypoint-Nr. 33
k,34,x4,breitq,z4    !Verwendung der Geo.-Parameter zur Bildung von Keypoint-Nr. 34
k,35,x5,breitq,z5    !Verwendung der Geo.-Parameter zur Bildung von Keypoint-Nr. 35
k,36,x6,breitq,z6    !Verwendung der Geo.-Parameter zur Bildung von Keypoint-Nr. 36
k,37,x7,breitq,z7    !Verwendung der Geo.-Parameter zur Bildung von Keypoint-Nr. 37
k,38,x8,breitq,z8    !Verwendung der Geo.-Parameter zur Bildung von Keypoint-Nr. 38
k,39,x9,breitq,z9    !Verwendung der Geo.-Parameter zur Bildung von Keypoint-Nr. 39
k,40,x10,breitq,z10   !Verwendung der Geo.-Parameter zur Bildung von Keypoint-Nr. 40
k,121,xk1,breitq,0    !Verwendung der Geo.-P. zur Bildung von Referenzpunkt-Nr. 121

! *** Keypoints EG, Querriegel ***
k,60,eben2,0,z2        !Verwendung der Geo.-Parameter zur Bildung von Keypoint-Nr. 60
k,61,eben2,breitq,z2   !Verwendung der Geo.-Parameter zur Bildung von Keypoint-Nr. 61
k,123,eben2,yk2,0       !Verwendung der Geo.-P. zur Bildung von Referenzpunkt-Nr. 123
k,62,eben5,0,z9        !Verwendung der Geo.-P. zur Bildung von Keypoint-Nr. 62
k,63,eben5,breitq,z9   !Verwendung der Geo.-Parameter zur Bildung von Keypoint-Nr. 63
k,126,eben5,yk2,0       !Verwendung der Geo.-P. zur Bildung von Referenzpunkt-Nr. 126

! *** Keypoints EG, Verband links ***
k,80,eben1,0,0          !Verwendung der Geo.-Parameter zur Bildung von Keypoint-Nr. 80
k,81,eben1,breitq,z2   !Verwendung der Geo.-Parameter zur Bildung von Keypoint-Nr. 81
k,122,eben1,yk2,0       !Verwendung der Geo.-P. zur Bildung von Referenzpunkt-Nr. 122
k,100,eben3,breitq,0    !Verwendung der Geo.-Parameter zur Bildung von Keypoint-Nr. 100
k,101,eben3,0,z2        !Verwendung der Geo.-Parameter zur Bildung von Keypoint-Nr. 101
k,124,eben3,yk2,0       !Verwendung der Geo.-P. zur Bildung von Referenzpunkt-Nr. 124

! *** Keypoints EG, Verband rechts ***
k,82,eben6,0,0          !Verwendung der Geo.-Parameter zur Bildung von Keypoint-Nr. 82

```

```

k,83,eben6,breitq,z9      !Verwendung der Geo.-Parameter zur Bildung von Keypoint-Nr. 83
k,127,eben6,yk2,0          !Verwendung der Geo.-P. zur Bildung von Referenzpunkt-Nr. 127
k,102,eben4,breitq,0        !Verwendung der Geo.-Parameter zur Bildung von Keypoint-Nr. 102
k,103,eben4,0,z9           !Verwendung der Geo.-Parameter zur Bildung von Keypoint-Nr. 103
k,125,eben4,yk2,0          !Verwendung der Geo.-P. zur Bildung von Referenzpunkt-Nr. 125

*endif

*if,istock,gt,1,then      !Prüfung ob mehr Stockwerke als EG vorhanden sind

! *** Keypoints 1.0G, vorderer Rahmen ***

k,11,x11,y11,z11          !Verwendung der Geo.-Parameter zur Bildung von Keypoint-Nr. 11
k,12,x12,y12,z12          !Verwendung der Geo.-Parameter zur Bildung von Keypoint-Nr. 12
k,13,x13,y13,z13          !Verwendung der Geo.-Parameter zur Bildung von Keypoint-Nr. 13
k,14,x14,y14,z14          !Verwendung der Geo.-Parameter zur Bildung von Keypoint-Nr. 14
k,15,x15,y15,z15          !Verwendung der Geo.-Parameter zur Bildung von Keypoint-Nr. 15
k,16,x16,y16,z16          !Verwendung der Geo.-Parameter zur Bildung von Keypoint-Nr. 16
k,17,x17,y17,z17          !Verwendung der Geo.-Parameter zur Bildung von Keypoint-Nr. 17
k,18,x18,y18,z18          !Verwendung der Geo.-Parameter zur Bildung von Keypoint-Nr. 18

! *** Keypoints 1.0G, hinterer Rahmen ***

k,41,x11,breitq,z11       !Verwendung der Geo.-Parameter zur Bildung von Keypoint-Nr. 41
k,42,x12,breitq,z12       !Verwendung der Geo.-Parameter zur Bildung von Keypoint-Nr. 42
k,43,x13,breitq,z13       !Verwendung der Geo.-Parameter zur Bildung von Keypoint-Nr. 43
k,44,x14,breitq,z14       !Verwendung der Geo.-Parameter zur Bildung von Keypoint-Nr. 44
k,45,x15,breitq,z15       !Verwendung der Geo.-Parameter zur Bildung von Keypoint-Nr. 45
k,46,x16,breitq,z16       !Verwendung der Geo.-Parameter zur Bildung von Keypoint-Nr. 46
k,47,x17,breitq,z17       !Verwendung der Geo.-Parameter zur Bildung von Keypoint-Nr. 47
k,48,x18,breitq,z18       !Verwendung der Geo.-Parameter zur Bildung von Keypoint-Nr. 48

! *** Keypoints 1.0G, Querriegel ***

k,64,eben2,0,z11           !Verwendung der Geo.-Parameter zur Bildung von Keypoint-Nr. 64
k,65,eben2,breitq,z11      !Verwendung der Geo.-Parameter zur Bildung von Keypoint-Nr. 65
k,66,eben5,0,z18           !Verwendung der Geo.-Parameter zur Bildung von Keypoint-Nr. 66
k,67,eben5,breitq,z18      !Verwendung der Geo.-Parameter zur Bildung von Keypoint-Nr. 67

! *** Keypoints 1.0G, Verband links ***

k,84,eben1,0,z2             !Verwendung der Geo.-Parameter zur Bildung von Keypoint-Nr. 84
k,85,eben1,breitq,z11      !Verwendung der Geo.-Parameter zur Bildung von Keypoint-Nr. 85
k,104,eben3,breitq,z2       !Verwendung der Geo.-Parameter zur Bildung von Keypoint-Nr. 104
k,105,eben3,0,z11           !Verwendung der Geo.-Parameter zur Bildung von Keypoint-Nr. 105

! *** Keypoints 1.0G, Verband rechts ***

k,86,eben6,0,z9             !Verwendung der Geo.-Parameter zur Bildung von Keypoint-Nr. 86
k,87,eben6,breitq,z18      !Verwendung der Geo.-Parameter zur Bildung von Keypoint-Nr. 87
k,106,eben4,breitq,z9       !Verwendung der Geo.-Parameter zur Bildung von Keypoint-Nr. 106
k,107,eben4,0,z18           !Verwendung der Geo.-Parameter zur Bildung von Keypoint-Nr. 107

*endif

*if,istock,gt,2,then      !Prüfung ob mehr Stockwerke als 1.0G vorhanden sind

! *** Keypoints 2.0G, vorderer Rahmen ***

k,19,x19,y19,z19           !Verwendung der Geo.-Parameter zur Bildung von Keypoint-Nr. 19
k,20,x20,y20,z20           !Verwendung der Geo.-Parameter zur Bildung von Keypoint-Nr. 20
k,21,x21,y21,z21           !Verwendung der Geo.-Parameter zur Bildung von Keypoint-Nr. 21
k,22,x22,y22,z22           !Verwendung der Geo.-Parameter zur Bildung von Keypoint-Nr. 22
k,23,x23,y23,z23           !Verwendung der Geo.-Parameter zur Bildung von Keypoint-Nr. 23
k,24,x24,y24,z24           !Verwendung der Geo.-Parameter zur Bildung von Keypoint-Nr. 24
k,25,x25,y25,z25           !Verwendung der Geo.-Parameter zur Bildung von Keypoint-Nr. 25
k,26,x26,y26,z26           !Verwendung der Geo.-Parameter zur Bildung von Keypoint-Nr. 26

! *** Keypoints 2.0G, hinterer Rahmen ***

k,49,x19,breitq,z19         !Verwendung der Geo.-Parameter zur Bildung von Keypoint-Nr. 49
k,50,x20,breitq,z20         !Verwendung der Geo.-Parameter zur Bildung von Keypoint-Nr. 50
k,51,x21,breitq,z21         !Verwendung der Geo.-Parameter zur Bildung von Keypoint-Nr. 51
k,52,x22,breitq,z22         !Verwendung der Geo.-Parameter zur Bildung von Keypoint-Nr. 52
k,53,x23,breitq,z23         !Verwendung der Geo.-Parameter zur Bildung von Keypoint-Nr. 53
k,54,x24,breitq,z24         !Verwendung der Geo.-Parameter zur Bildung von Keypoint-Nr. 54
k,55,x25,breitq,z25         !Verwendung der Geo.-Parameter zur Bildung von Keypoint-Nr. 55
k,56,x26,breitq,z26         !Verwendung der Geo.-Parameter zur Bildung von Keypoint-Nr. 56

```

```

! *** Keypoints          2.OG, Querriegel ***
k,68,eben2,0,z19      !Verwendung der Geo.-Parameter zur Bildung von Keypoint-Nr. 68
k,69,eben2,breitq,z19 !Verwendung der Geo.-Parameter zur Bildung von Keypoint-Nr. 69
k,70,eben5,0,z26      !Verwendung der Geo.-Parameter zur Bildung von Keypoint-Nr. 70
k,71,eben5,breitq,z26 !Verwendung der Geo.-Parameter zur Bildung von Keypoint-Nr. 71

! *** Keypoints 2.OG, Verband links ***
k,88,eben1,0,z11      !Verwendung der Geo.-Parameter zur Bildung von Keypoint-Nr. 88
k,89,eben1,breitq,z19 !Verwendung der Geo.-Parameter zur Bildung von Keypoint-Nr. 89
k,108,eben3,breitq,z11 !Verwendung der Geo.-Parameter zur Bildung von Keypoint-Nr. 108
k,109,eben3,0,z19      !Verwendung der Geo.-Parameter zur Bildung von Keypoint-Nr. 109

! *** Keypoints 2.OG, Verband rechts ***
k,90,eben6,0,z18      !Verwendung der Geo.-Parameter zur Bildung von Keypoint-Nr. 90
k,91,eben6,breitq,z26 !Verwendung der Geo.-Parameter zur Bildung von Keypoint-Nr. 91
k,110,eben4,breitq,z18 !Verwendung der Geo.-Parameter zur Bildung von Keypoint-Nr. 110
k,111,eben4,0,z26      !Verwendung der Geo.-Parameter zur Bildung von Keypoint-Nr. 111

*endif

! *** Erzeugung der Zwischen-Keypoints ***
nstut=unts-1    !Anzahl der Zwischen-Keypoints Stütze
nrieg=untr-1    !Anzahl der Zwischen-Keypoints Riegel
nverb=untv-1    !Anzahl der Zwischen-Keypoints Verband

! *** Erdgeschoß ***
! *** vorderer Rahmen ***
KFILL,1,2,nstut,500,1           !Einbau Zwischen-Keypoints Stütze links, ab Nr. 500
KFILL,5,6,nrieg,200,1           !Einbau Zwischen-Keypoints Riegel, ab Nr. 200
KFILL,10,9,nstut,600,1           !Einbau Zwischen-Keypoints Stütze rechts, ab Nr. 600

*if,ibays,gt,0,then
! *** hinterer Rahmen ***
KFILL,31,32,nstut,550,1           !Einbau Zwischen-Keypoints Stütze links, ab Nr. 550
KFILL,35,36,nrieg,250,1           !Einbau Zwischen-Keypoints Riegel, ab Nr. 250
KFILL,40,39,nstut,650,1           !Einbau Zwischen-Keypoints Stütze rechts, ab Nr. 650

! *** Querriegel ***
KFILL,60,61,nrieg,1100,1           !Einbau Zwischen-Keypoints Querriegel links, ab Nr. 1100
KFILL,62,63,nrieg,1150,1           !Einbau Zwischen-Keypoints Querriegel rechts, ab Nr. 1150

! *** Verbandsdiagonalen
KFILL,80,81,nverb,1400,1           !Einbau Zwischen-Keypoints Verband links, ab Nr. 1400
KFILL,82,83,nverb,1450,1           !Einbau Zwischen-Keypoints Verband rechts, ab Nr. 1450
KFILL,100,101,nverb,1700,1           !Einbau Zwischen-Keypoints Verband links, ab Nr. 1700
KFILL,102,103,nverb,1750,1           !Einbau Zwischen-Keypoints Verband rechts, ab Nr. 1750

*endif

! *** 1. Obergeschoß ***
*if,istock,gt,1,then  !Prüfung ob 1.Obergeschoß zu berücksichtigen ist

! *** vorderer Rahmen ***
KFILL,2,11,nstut,700,1           !Einbau Zwischen-Keypoints Stütze links, ab Nr. 700
KFILL,14,15,nrieg,300,1           !Einbau Zwischen-Keypoints Riegel, ab Nr. 300
KFILL,9,18,nstut,800,1           !Einbau Zwischen-Keypoints Stütze rechts, ab Nr. 800

! *** hinterer Rahmen ***
KFILL,32,41,nstut,750,1           !Einbau Zwischen-Keypoints Stütze links, ab Nr. 750
KFILL,44,45,nrieg,350,1           !Einbau Zwischen-Keypoints Riegel, ab Nr. 350
KFILL,39,48,nstut,850,1           !Einbau Zwischen-Keypoints Stütze rechts, ab Nr. 850

! *** Querriegel ***
KFILL,64,65,nrieg,1200,1           !Einbau Zwischen-Keypoints Querriegel links, ab Nr. 1200
KFILL,66,67,nrieg,1250,1           !Einbau Zwischen-Keypoints Querriegel rechts, ab Nr. 1250

! *** Verbandsdiagonalen
KFILL,84,85,nverb,1500,1           !Einbau Zwischen-Keypoints Verband links, ab Nr. 1500
KFILL,86,87,nverb,1550,1           !Einbau Zwischen-Keypoints Verband rechts, ab Nr. 1550
KFILL,104,105,nverb,1800,1           !Einbau Zwischen-Keypoints Verband links, ab Nr. 1800
KFILL,106,107,nverb,1850,1           !Einbau Zwischen-Keypoints Verband rechts, ab Nr. 1850

```

```

*endif

! *** 2. Obergeschoß ***
*if,istock,gt,2,then !Prüfung ob 2.Obergeschoß zu berücksichtigen ist

! *** vorderer Rahmen ***
KFILL,11,19,nstut,900,1      !Einbau Zwischen-Keypoints Stütze links, ab Nr. 900
KFILL,22,23,nrieg,400,1      !Einbau Zwischen-Keypoints Riegel,      ab Nr. 400
KFILL,18,26,nstut,1000,1      !Einbau Zwischen-Keypoints Stütze rechts, ab Nr. 1000

! *** hinterer Rahmen ***
KFILL,41,49,nstut,950,1      !Einbau Zwischen-Keypoints Stütze links, ab Nr. 950
KFILL,52,53,nrieg,450,1      !Einbau Zwischen-Keypoints Riegel,      ab Nr. 450
KFILL,48,56,nstut,1050,1      !Einbau Zwischen-Keypoints Stütze rechts, ab Nr. 1050

! *** Querriegel ***
KFILL,68,69,nrieg,1300,1      !Einbau Zwischen-Keypoints Querriegel links, ab Nr. 1300
KFILL,70,71,nrieg,1350,1      !Einbau Zwischen-Keypoints Querriegel rechts, ab Nr. 1350

! *** Verbandsdiagonalen
KFILL,88,89,nverb,1600,1      !Einbau Zwischen-Keypoints Verband links,    ab Nr. 1600
KFILL,90,91,nverb,1650,1      !Einbau Zwischen-Keypoints Verband rechts,   ab Nr. 1650
KFILL,108,109,nverb,1900,1      !Einbau Zwischen-Keypoints Verband links,    ab Nr. 1900
KFILL,110,111,nverb,1950,1      !Einbau Zwischen-Keypoints Verband rechts,   ab Nr. 1950

*endif

! *** Generierung der Knoten ***
istut=unts-2          !Laufvariable zur Schleifenbildung
irieg=untr-2          !Laufvariable zur Schleifenbildung
iverb=untv-2          !Laufvariable zur Schleifenbildung

! *** Erdgeschoß ***
! *** vorderer Rahmen ***
*DO,I,500,istut+500,1      !Schleife zur Knotenzuweisung, Stütze links
NKPT,I,I                !Knotenzuweisung ab Nr. 500
*ENDDO
*DO,I,200,irieg+200,1      !Schleife zur Knotenzuweisung, Riegel
NKPT,I,I                !Knotenzuweisung ab Nr. 200
*ENDDO
*DO,I,600,istut+600,1      !Schleife zur Knotenzuweisung, Stütze rechts
NKPT,I,I                !Knotenzuweisung ab Nr. 600
*ENDDO
NKPT,120,120              !Referenzknoten über Keypoint erzeugen

*if,ibays,gt,0,then
! *** hinterer Rahmen ***
*DO,I,550,istut+550,1      !Schleife zur Knotenzuweisung, Stütze links
NKPT,I,I                !Knotenzuweisung ab Nr. 550
*ENDDO
*DO,I,250,irieg+250,1      !Schleife zur Knotenzuweisung, Riegel
NKPT,I,I                !Knotenzuweisung ab Nr. 250
*ENDDO
*DO,I,650,istut+650,1      !Schleife zur Knotenzuweisung, Stütze rechts
NKPT,I,I                !Knotenzuweisung ab Nr. 650
*ENDDO
NKPT,121,121              !Referenzknoten über Keypoint erzeugen

! *** Querriegel ***
*DO,I,1100,irieg+1100,1      !Schleife zur Knotenzuweisung, Querriegel links
NKPT,I,I                !Knotenzuweisung ab Nr. 1100
*ENDDO
NKPT,123,123              !Referenzknoten über Keypoint erzeugen
*DO,I,1150,irieg+1150,1      !Schleife zur Knotenzuweisung, Querriegel rechts
NKPT,I,I                !Knotenzuweisung ab Nr. 1150
*ENDDO
NKPT,126,126              !Referenzknoten über Keypoint erzeugen

! *** Verband ***
*DO,I,1400,iverb+1400,1      !Schleife zur Knotenzuweisung, Verband links
NKPT,I,I                !Knotenzuweisung ab Nr. 1400

```

```

*ENDDO
NKPT,122,122
*DO,I,1450,iverb+1450,1
NKPT,I,I
*ENDDO
NKPT,127,127
*DO,I,1700,iverb+1700,1
NKPT,I,I
*ENDDO
NKPT,124,124
*DO,I,1750,iverb+1750,1
NKPT,I,I
*ENDDO
NKPT,125,125

*endif

! *** 1. Obergeschoß ***
*if,istock,gt,1,then !Prüfung ob 1.Obergeschoß zu berücksichtigen ist

! *** vorderer Rahmen ***
*DO,I,700,istut+700,1
NKPT,I,I
*ENDDO
*DO,I,300,irieg+300,1
NKPT,I,I
*ENDDO
*DO,I,800,istut+800,1
NKPT,I,I
*ENDDO

! *** hinterer Rahmen ***
*DO,I,750,istut+750,1
NKPT,I,I
*ENDDO
*DO,I,350,irieg+350,1
NKPT,I,I
*ENDDO
*DO,I,850,istut+850,1
NKPT,I,I
*ENDDO

! *** Querriegel ***
*DO,I,1200,irieg+1200,1
NKPT,I,I
*ENDDO
*DO,I,1250,irieg+1250,1
NKPT,I,I
*ENDDO

! *** Verband ***
*DO,I,1500,iverb+1500,1
NKPT,I,I
*ENDDO
*DO,I,1550,iverb+1550,1
NKPT,I,I
*ENDDO
*DO,I,1800,iverb+1800,1
NKPT,I,I
*ENDDO
*DO,I,1850,iverb+1850,1
NKPT,I,I
*ENDDO

*endif

! *** 2. Obergeschoß ***
*if,istock,gt,2,then !Prüfung ob 2.Obergeschoß zu berücksichtigen ist

! *** vorderer Rahmen ***
*DO,I,900,istut+900,1
NKPT,I,I

!Referenzknoten über Keypoint erzeugen
!Schleife zur Knotenzuweisung, Verband rechts
!Knotenzuweisung ab Nr. 1450

!Referenzknoten über Keypoint erzeugen
!Schleife zur Knotenzuweisung, Verband links
!Knotenzuweisung ab Nr. 1700

!Referenzknoten über Keypoint erzeugen
!Schleife zur Knotenzuweisung, Verband rechts
!Knotenzuweisung ab Nr. 1750

!Referenzknoten über Keypoint erzeugen

!Referenzknoten über Keypoint erzeugen
!Schleife zur Knotenzuweisung, Stütze links
!Knotenzuweisung ab Nr. 700

!Schleife zur Knotenzuweisung, Riegel
!Knotenzuweisung ab Nr. 300

!Schleife zur Knotenzuweisung, Stütze rechts
!Knotenzuweisung ab Nr. 800

!Schleife zur Knotenzuweisung, Stütze links
!Knotenzuweisung ab Nr. 750

!Schleife zur Knotenzuweisung, Riegel
!Knotenzuweisung ab Nr. 350

!Schleife zur Knotenzuweisung, Stütze rechts
!Knotenzuweisung ab Nr. 850

!Schleife zur Knotenzuweisung, Querriegel links
!Knotenzuweisung ab Nr. 1200

!Schleife zur Knotenzuweisung, Querriegel rechts
!Knotenzuweisung ab Nr. 1250

!Schleife zur Knotenzuweisung, Verband links
!Knotenzuweisung ab Nr. 1500

!Schleife zur Knotenzuweisung, Verband rechts
!Knotenzuweisung ab Nr. 1550

!Schleife zur Knotenzuweisung, Verband links
!Knotenzuweisung ab Nr. 1800

!Schleife zur Knotenzuweisung, Verband rechts
!Knotenzuweisung ab Nr. 1850

```

```

*ENDDO
*DO,I,400,irieg+400,1      !Schleife zur Knotenzuweisung, Riegel
NKPT,I,I                      !Knotenzuweisung ab Nr. 400
*ENDDO
*DO,I,1000,istut+1000,1      !Schleife zur Knotenzuweisung, Stütze rechts
NKPT,I,I                      !Knotenzuweisung ab Nr. 1000
*ENDDO

! *** hinterer Rahmen ***

*DO,I,950,istut+950,1      !Schleife zur Knotenzuweisung, Stütze links
NKPT,I,I                      !Knotenzuweisung ab Nr. 950
*ENDDO
*DO,I,450,irieg+450,1      !Schleife zur Knotenzuweisung, Riegel
NKPT,I,I                      !Knotenzuweisung ab Nr. 450
*ENDDO
*DO,I,1050,istut+1050,1      !Schleife zur Knotenzuweisung, Stütze rechts
NKPT,I,I                      !Knotenzuweisung ab Nr. 1050
*ENDDO

! *** Querriegel ***

*DO,I,1300,irieg+1300,1      !Schleife zur Knotenzuweisung, Querriegel links
NKPT,I,I                      !Knotenzuweisung ab Nr. 1300
*ENDDO
*DO,I,1350,irieg+1350,1      !Schleife zur Knotenzuweisung, Querriegel rechts
NKPT,I,I                      !Knotenzuweisung ab Nr. 1350
*ENDDO

! *** Verband ***

*DO,I,1600,iverb+1600,1      !Schleife zur Knotenzuweisung, Verband links
NKPT,I,I                      !Knotenzuweisung ab Nr. 1600
*ENDDO
*DO,I,1650,iverb+1650,1      !Schleife zur Knotenzuweisung, Verband rechts
NKPT,I,I                      !Knotenzuweisung ab Nr. 1650
*ENDDO
*DO,I,1900,iverb+1900,1      !Schleife zur Knotenzuweisung, Verband links
NKPT,I,I                      !Knotenzuweisung ab Nr. 1900
*ENDDO
*DO,I,1950,iverb+1950,1      !Schleife zur Knotenzuweisung, Verband rechts
NKPT,I,I                      !Knotenzuweisung ab Nr. 1950
*ENDDO

*endif

! *** Rahmeneckknoten ***

NKPT,1,1      !Keypoint-Nr. 1 wird Knoten-Nr. 1 zugewiesen, vorderer Rahmen
NKPT,2,2      !Keypoint-Nr. 2 wird Knoten-Nr. 2 zugewiesen, vorderer Rahmen
NKPT,3,3      !Keypoint-Nr. 3 wird Knoten-Nr. 3 zugewiesen, vorderer Rahmen
NKPT,4,4      !Keypoint-Nr. 4 wird Knoten-Nr. 4 zugewiesen, vorderer Rahmen
NKPT,5,5      !Keypoint-Nr. 5 wird Knoten-Nr. 5 zugewiesen, vorderer Rahmen
NKPT,6,6      !Keypoint-Nr. 6 wird Knoten-Nr. 6 zugewiesen, vorderer Rahmen
NKPT,7,7      !Keypoint-Nr. 7 wird Knoten-Nr. 7 zugewiesen, vorderer Rahmen
NKPT,8,8      !Keypoint-Nr. 8 wird Knoten-Nr. 8 zugewiesen, vorderer Rahmen
NKPT,9,9      !Keypoint-Nr. 9 wird Knoten-Nr. 9 zugewiesen, vorderer Rahmen
NKPT,10,10    !Keypoint-Nr. 10 wird Knoten-Nr. 10 zugewiesen, vorderer Rahmen

*if,ibays,gt,0,then
NKPT,31,31    !Keypoint-Nr. 31 wird Knoten-Nr. 31 zugewiesen, hinterer Rahmen
NKPT,32,32    !Keypoint-Nr. 32 wird Knoten-Nr. 32 zugewiesen, hinterer Rahmen
NKPT,33,33    !Keypoint-Nr. 33 wird Knoten-Nr. 33 zugewiesen, hinterer Rahmen
NKPT,34,34    !Keypoint-Nr. 34 wird Knoten-Nr. 34 zugewiesen, hinterer Rahmen
NKPT,35,35    !Keypoint-Nr. 35 wird Knoten-Nr. 35 zugewiesen, hinterer Rahmen
NKPT,36,36    !Keypoint-Nr. 36 wird Knoten-Nr. 36 zugewiesen, hinterer Rahmen
NKPT,37,37    !Keypoint-Nr. 37 wird Knoten-Nr. 37 zugewiesen, hinterer Rahmen
NKPT,38,38    !Keypoint-Nr. 38 wird Knoten-Nr. 38 zugewiesen, hinterer Rahmen
NKPT,39,39    !Keypoint-Nr. 39 wird Knoten-Nr. 39 zugewiesen, hinterer Rahmen
NKPT,40,40    !Keypoint-Nr. 40 wird Knoten-Nr. 40 zugewiesen, hinterer Rahmen

NKPT,60,60    !Keypoint-Nr. 60 wird Knoten-Nr. 60 zugewiesen, linker Querriegel
NKPT,61,61    !Keypoint-Nr. 61 wird Knoten-Nr. 61 zugewiesen, linker Querriegel
NKPT,62,62    !Keypoint-Nr. 62 wird Knoten-Nr. 62 zugewiesen, rechter Querriegel
NKPT,63,63    !Keypoint-Nr. 63 wird Knoten-Nr. 63 zugewiesen, rechter Querriegel

NKPT,80,80    !Keypoint-Nr. 80 wird Knoten-Nr. 80 zugewiesen, linker Verband
NKPT,81,81    !Keypoint-Nr. 81 wird Knoten-Nr. 81 zugewiesen, linker Verband
NKPT,82,82    !Keypoint-Nr. 82 wird Knoten-Nr. 82 zugewiesen, rechter Verband

```

```

NKPT,83,83          !Keypoint-Nr. 83 wird Knoten-Nr. 83 zugewiesen, rechter Verband
NKPT,100,100        !Keypoint-Nr. 100 wird Knoten-Nr. 100 zugewiesen, linker Verband
NKPT,101,101        !Keypoint-Nr. 101 wird Knoten-Nr. 101 zugewiesen, linker Verband
NKPT,102,102        !Keypoint-Nr. 102 wird Knoten-Nr. 102 zugewiesen, rechter Verband
NKPT,103,103        !Keypoint-Nr. 103 wird Knoten-Nr. 103 zugewiesen, rechter Verband

*endif

*if,istock,gt,1,then !Prüfung ob 1.Obergeschoß zu berücksichtigen ist

NKPT,11,11          !Keypoint-Nr. 11 wird Knoten-Nr. 11 zugewiesen, vorderer Rahmen
NKPT,12,12          !Keypoint-Nr. 12 wird Knoten-Nr. 12 zugewiesen, vorderer Rahmen
NKPT,13,13          !Keypoint-Nr. 13 wird Knoten-Nr. 13 zugewiesen, vorderer Rahmen
NKPT,14,14          !Keypoint-Nr. 14 wird Knoten-Nr. 14 zugewiesen, vorderer Rahmen
NKPT,15,15          !Keypoint-Nr. 15 wird Knoten-Nr. 15 zugewiesen, vorderer Rahmen
NKPT,16,16          !Keypoint-Nr. 16 wird Knoten-Nr. 16 zugewiesen, vorderer Rahmen
NKPT,17,17          !Keypoint-Nr. 17 wird Knoten-Nr. 17 zugewiesen, vorderer Rahmen
NKPT,18,18          !Keypoint-Nr. 18 wird Knoten-Nr. 18 zugewiesen, vorderer Rahmen

NKPT,41,41          !Keypoint-Nr. 41 wird Knoten-Nr. 41 zugewiesen, hinterer Rahmen
NKPT,42,42          !Keypoint-Nr. 42 wird Knoten-Nr. 42 zugewiesen, hinterer Rahmen
NKPT,43,43          !Keypoint-Nr. 43 wird Knoten-Nr. 43 zugewiesen, hinterer Rahmen
NKPT,44,44          !Keypoint-Nr. 44 wird Knoten-Nr. 44 zugewiesen, hinterer Rahmen
NKPT,45,45          !Keypoint-Nr. 45 wird Knoten-Nr. 45 zugewiesen, hinterer Rahmen
NKPT,46,46          !Keypoint-Nr. 46 wird Knoten-Nr. 46 zugewiesen, hinterer Rahmen
NKPT,47,47          !Keypoint-Nr. 47 wird Knoten-Nr. 47 zugewiesen, hinterer Rahmen
NKPT,48,48          !Keypoint-Nr. 48 wird Knoten-Nr. 48 zugewiesen, hinterer Rahmen

NKPT,64,64          !Keypoint-Nr. 64 wird Knoten-Nr. 64 zugewiesen, linker Querriegel
NKPT,65,65          !Keypoint-Nr. 65 wird Knoten-Nr. 65 zugewiesen, linker Querriegel
NKPT,66,66          !Keypoint-Nr. 66 wird Knoten-Nr. 66 zugewiesen, rechter Querriegel
NKPT,67,67          !Keypoint-Nr. 67 wird Knoten-Nr. 67 zugewiesen, rechter Querriegel

NKPT,84,84          !Keypoint-Nr. 84 wird Knoten-Nr. 84 zugewiesen, linker Verband
NKPT,85,85          !Keypoint-Nr. 85 wird Knoten-Nr. 85 zugewiesen, linker Verband
NKPT,86,86          !Keypoint-Nr. 86 wird Knoten-Nr. 86 zugewiesen, rechter Verband
NKPT,87,87          !Keypoint-Nr. 87 wird Knoten-Nr. 87 zugewiesen, rechter Verband
NKPT,104,104        !Keypoint-Nr. 104 wird Knoten-Nr. 104 zugewiesen, linker Verband
NKPT,105,105        !Keypoint-Nr. 105 wird Knoten-Nr. 105 zugewiesen, linker Verband
NKPT,106,106        !Keypoint-Nr. 106 wird Knoten-Nr. 106 zugewiesen, rechter Verband
NKPT,107,107        !Keypoint-Nr. 107 wird Knoten-Nr. 107 zugewiesen, rechter Verband

*endif

*if,istock,gt,2,then !Prüfung ob 2.Obergeschoß zu berücksichtigen ist

NKPT,19,19          !Keypoint-Nr. 19 wird Knoten-Nr. 19 zugewiesen, vorderer Rahmen
NKPT,20,20          !Keypoint-Nr. 20 wird Knoten-Nr. 20 zugewiesen, vorderer Rahmen
NKPT,21,21          !Keypoint-Nr. 21 wird Knoten-Nr. 21 zugewiesen, vorderer Rahmen
NKPT,22,22          !Keypoint-Nr. 22 wird Knoten-Nr. 22 zugewiesen, vorderer Rahmen
NKPT,23,23          !Keypoint-Nr. 23 wird Knoten-Nr. 23 zugewiesen, vorderer Rahmen
NKPT,24,24          !Keypoint-Nr. 24 wird Knoten-Nr. 24 zugewiesen, vorderer Rahmen
NKPT,25,25          !Keypoint-Nr. 25 wird Knoten-Nr. 25 zugewiesen, vorderer Rahmen
NKPT,26,26          !Keypoint-Nr. 26 wird Knoten-Nr. 26 zugewiesen, vorderer Rahmen

NKPT,49,49          !Keypoint-Nr. 49 wird Knoten-Nr. 49 zugewiesen, vorderer Rahmen
NKPT,50,50          !Keypoint-Nr. 50 wird Knoten-Nr. 50 zugewiesen, vorderer Rahmen
NKPT,51,51          !Keypoint-Nr. 51 wird Knoten-Nr. 51 zugewiesen, vorderer Rahmen
NKPT,52,52          !Keypoint-Nr. 52 wird Knoten-Nr. 52 zugewiesen, vorderer Rahmen
NKPT,53,53          !Keypoint-Nr. 53 wird Knoten-Nr. 53 zugewiesen, vorderer Rahmen
NKPT,54,54          !Keypoint-Nr. 54 wird Knoten-Nr. 54 zugewiesen, vorderer Rahmen
NKPT,55,55          !Keypoint-Nr. 55 wird Knoten-Nr. 55 zugewiesen, vorderer Rahmen
NKPT,56,56          !Keypoint-Nr. 56 wird Knoten-Nr. 56 zugewiesen, vorderer Rahmen

NKPT,68,68          !Keypoint-Nr. 68 wird Knoten-Nr. 68 zugewiesen, linker Querriegel
NKPT,69,69          !Keypoint-Nr. 69 wird Knoten-Nr. 69 zugewiesen, linker Querriegel
NKPT,70,70          !Keypoint-Nr. 70 wird Knoten-Nr. 70 zugewiesen, rechter Querriegel
NKPT,71,71          !Keypoint-Nr. 71 wird Knoten-Nr. 71 zugewiesen, rechter Querriegel

NKPT,88,88          !Keypoint-Nr. 88 wird Knoten-Nr. 88 zugewiesen, linker Verband
NKPT,89,89          !Keypoint-Nr. 89 wird Knoten-Nr. 89 zugewiesen, linker Verband
NKPT,90,90          !Keypoint-Nr. 90 wird Knoten-Nr. 90 zugewiesen, rechter Verband
NKPT,91,91          !Keypoint-Nr. 91 wird Knoten-Nr. 91 zugewiesen, rechter Verband
NKPT,108,108        !Keypoint-Nr. 108 wird Knoten-Nr. 108 zugewiesen, linker Verband
NKPT,109,109        !Keypoint-Nr. 109 wird Knoten-Nr. 109 zugewiesen, linker Verband
NKPT,110,110        !Keypoint-Nr. 110 wird Knoten-Nr. 110 zugewiesen, rechter Verband
NKPT,111,111        !Keypoint-Nr. 111 wird Knoten-Nr. 111 zugewiesen, rechter Verband

*endif

```

```

! *** Einbau der Stützen- und Riegelemente BEAM24 ***
! *** vorderer Erdgeschoß-Rahmen ***

TYPE,1                      !Anwendung des Stützenelementes
REAL,1
! *** Erdgeschoß Stütze links ***
E,1,500,120                  !Element Fußpunkt EG-Stütze links
*DO,I,500,500+istut-1        !Schleife zur Elementzuweisung
E,I,I+1,120                  !Elemente EG-Stütze links
*ENDDO
E,500+istut,2,120            !Element EG-Stütze oben links

! *** Dogbone links ***
TYPE,5                      !Anwendung des Element Dogbone außen
REAL,5
E,2,3,120

TYPE,4                      !Anwendung des Element Dogbone mitte
REAL,4
E,3,4,120

TYPE,3                      !Anwendung des Element Dogbone innen
REAL,3
E,4,5,120

TYPE,2                      !Anwendung des Riegelementes
REAL,2
! *** Erdgeschoß Riegel ***
E,5,200,120                  !Element Riegel EG links
*DO,I,200,200+irieg-1        !Schleife zur Elementzuweisung
E,I,I+1,120                  !Elemente Riegel EG
*ENDDO
E,200+irieg,6,120            !Element Riegel EG rechts

! *** Dogbone rechts ***
TYPE,3                      !Anwendung des Element Dogbone innen
REAL,3
E,6,7,120

TYPE,4                      !Anwendung des Element Dogbone mitte
REAL,4
E,7,8,120

TYPE,5                      !Anwendung des Element Dogbone außen
REAL,5
E,8,9,120

TYPE,1                      !Anwendung des Stützenelementes
REAL,1
! *** Erdgeschoß Stütze rechts ***
E,9,600+istut,120            !Element EG-Stütze oben rechts
*DO,I,600+istut,601,-1       !Schleife zur Elementzuweisung
E,I,I-1,120                  !Elemente Stütze rechts
*ENDDO
E,600,10,120                 !Element Fußpunkt EG-Stütze rechts

*if,ibays,gt,0,then
! *** hinterer Erdgeschoß-Rahmen ***

TYPE,1                      !Anwendung des Stützenelementes
REAL,1
! *** Erdgeschoß Stütze links ***
E,31,550,121                  !Element Fußpunkt EG-Stütze links
*DO,I,550,550+istut-1        !Schleife zur Elementzuweisung
E,I,I+1,121                  !Elemente EG-Stütze links
*ENDDO
E,550+istut,32,121            !Element EG-Stütze oben links

! *** Dogbone links ***
TYPE,5                      !Anwendung des Element Dogbone außen
REAL,5
E,32,33,121

TYPE,4                      !Anwendung des Element Dogbone mitte

```

```

REAL, 4
E, 33, 34, 121

TYPE, 3          !Anwendung des Element Dogbone innen
REAL, 3
E, 34, 35, 121

TYPE, 2          !Anwendung des Riegelementes
REAL, 2
! *** Erdgeschoß Riegel ***
E, 35, 250, 121
*DO, I, 250, 250+irieg-1
E, I, I+1, 121
*ENDDO
E, 250+irieg, 36, 121          !Element Riegel EG links
                                !Schleife zur Elementzuweisung
                                !Elemente Riegel EG
                                !Element Riegel EG rechts

! *** Dogbone rechts ***
TYPE, 3          !Anwendung des Element Dogbone innen
REAL, 3
E, 36, 37, 121

TYPE, 4          !Anwendung des Element Dogbone mitte
REAL, 4
E, 37, 38, 121

TYPE, 5          !Anwendung des Element Dogbone außen
REAL, 5
E, 38, 39, 121

TYPE, 1          !Anwendung des Stützenelementes
REAL, 1
! *** Erdgeschoß Stütze rechts ***
E, 39, 650+istut, 121          !Element EG-Stütze oben rechts
*DO, I, 650+istut, 651, -1      !Schleife zur Elementzuweisung
E, I, I-1, 121                  !Elemente Stütze rechts
*ENDDO
E, 650, 40, 121                !Element Fußpunkt EG-Stütze rechts

! *** EG Querriegel links ***
TYPE, 6          !Anwendung des Querriegellementes
REAL, 6
E, 60, 1100, 123
*DO, I, 1100, 1100+irieg-1
E, I, I+1, 123
*ENDDO
E, 1100+irieg, 61, 123          !Element Querriegel links
                                !Schleife zur Elementzuweisung
                                !Elemente Querriegel links
                                !Element Querriegel links

! *** EG Verband links ***
TYPE, 7          !Anwendung des Verbandselementes
REAL, 7
E, 80, 1400, 122
*DO, I, 1400, 1400+iverb-1
E, I, I+1, 122
*ENDDO
E, 1400+iverb, 81, 122          !Element Verband unten links
                                !Schleife zur Elementzuweisung
                                !Elemente Verband links
                                !Element Verband oben links

E, 100, 1700, 124
*DO, I, 1700, 1700+iverb-1
E, I, I+1, 124
*ENDDO
E, 1700+iverb, 101, 124          !Element Verband unten links
                                !Schleife zur Elementzuweisung
                                !Elemente Verband links
                                !Element Verband oben links

! *** EG Querriegel rechts ***
TYPE, 6          !Anwendung des Querriegellementes
REAL, 6
E, 62, 1150, 126
*DO, I, 1150, 1150+irieg-1
E, I, I+1, 126
*ENDDO
E, 1150+irieg, 63, 126          !Element Querriegel rechts
                                !Schleife zur Elementzuweisung
                                !Elemente Querriegel rechts
                                !Element Querriegel rechts

! *** EG Verband rechts ***
TYPE, 7          !Anwendung des Verbandselementes
REAL, 7

```

```

E,82,1450,127          !Element Verband unten rechts
*DO,I,1450,1450+iverb-1
E,I,I+1,127            !Schleife zur Elementzuweisung
*ENDDO
E,1450+iverb,83,127    !Elemente Verband rechts

E,102,1750,125          !Element Verband unten rechts
*DO,I,1750,1750+iverb-1
E,I,I+1,125            !Schleife zur Elementzuweisung
*ENDDO
E,1750+iverb,103,125    !Elemente Verband rechts

*endif

! *** 1.Obergeschoß ***
*if,istock,gt,1,then      !Prüfung ob 1.Obergeschoß zu berücksichtigen ist

! *** vorderer 1.OG-Rahmen ***
TYPE,1                  !Anwendung des Stützenelementes
REAL,1
! *** 1.OG Stütze links ***
E,2,700,120              !Element Fußpunkt 1.OG-Stütze links
*DO,I,700,700+istut-1
E,I,I+1,120            !Schleife zur Elementzuweisung
*ENDDO
E,700+istut,11,120      !Elemente 1.OG-Stütze links

! *** Dogbone links ***
TYPE,5                  !Anwendung des Element Dogbone außen
REAL,5
E,11,12,120

TYPE,4                  !Anwendung des Element Dogbone mitte
REAL,4
E,12,13,120

TYPE,3                  !Anwendung des Element Dogbone innen
REAL,3
E,13,14,120

TYPE,2                  !Anwendung des Riegelementes
REAL,2
! *** 1.OG Riegel ***
E,14,300,120              !Element Riegel 1.OG links
*DO,I,300,300+irieg-1
E,I,I+1,120            !Schleife zur Elementzuweisung
*ENDDO
E,300+irieg,15,120      !Elemente Riegel 1.OG

! *** Dogbone rechts ***
TYPE,3                  !Anwendung des Element Dogbone innen
REAL,3
E,15,16,120

TYPE,4                  !Anwendung des Element Dogbone mitte
REAL,4
E,16,17,120

TYPE,5                  !Anwendung des Element Dogbone außen
REAL,5
E,17,18,120

TYPE,1                  !Anwendung des Stützenelementes
REAL,1
! *** 1.OG Stütze rechts ***
E,18,800+istut,120      !Element 1.OG-Stütze oben rechts
*DO,I,800+istut,801,-1
E,I,I-1,120            !Schleife zur Elementzuweisung
*ENDDO
E,800,9,120             !Elemente Stütze rechts

! *** hinterer 1.OG-Rahmen ***
TYPE,1                  !Anwendung des Stützenelementes

```

```

REAL,1
! *** 1.OG Stütze links ***
E,32,750,121
*DO,I,750,750+istut-1
E,I,I+1,121
*ENDDO
E,750+istut,41,121
                                !Element Fußpunkt 1.OG-Stütze links
                                !Schleife zur Elementzuweisung
                                !Elemente 1.OG-Stütze links
                                !Element 1.OG-Stütze oben links

! *** Dogbone links **

TYPE,5
REAL,5
E,41,42,121
                                !Anwendung des Element Dogbone außen

TYPE,4
REAL,4
E,42,43,121
                                !Anwendung des Element Dogbone mitte

TYPE,3
REAL,3
E,43,44,121
                                !Anwendung des Element Dogbone innen

TYPE,2
REAL,2
! *** 1.OG Riegel ***
E,44,350,121
*DO,I,350,350+irieg-1
E,I,I+1,121
*ENDDO
E,350+irieg,45,121
                                !Anwendung des Riegellementes
                                !Element Riegel 1.OG links
                                !Schleife zur Elementzuweisung
                                !Elemente Riegel 1.OG
                                !Element Riegel 1.OG rechts

! *** Dogbone rechts **

TYPE,3
REAL,3
E,45,46,121
                                !Anwendung des Element Dogbone innen

TYPE,4
REAL,4
E,46,47,121
                                !Anwendung des Element Dogbone mitte

TYPE,5
REAL,5
E,47,48,121
                                !Anwendung des Element Dogbone außen

TYPE,1
REAL,1
! *** 1.OG Stütze rechts ***
E,48,850+istut,121
*DO,I,850+istut,851,-1
E,I,I-1,121
*ENDDO
E,850,39,121
                                !Anwendung des Stützenelementes
                                !Element 1.OG-Stütze oben rechts
                                !Schleife zur Elementzuweisung
                                !Elemente Stütze rechts
                                !Element Fußpunkt 1.OG-Stütze rechts

! *** 1.OG Querriegel links **

TYPE,6
REAL,6
E,64,1200,123
*DO,I,1200,1200+irieg-1
E,I,I+1,123
*ENDDO
E,1200+irieg,65,123
                                !Anwendung des Querriegellelementes
                                !Element Querriegel links
                                !Schleife zur Elementzuweisung
                                !Elemente Querriegel links
                                !Element Querriegel links

! *** 1.OG Verband links **

TYPE,7
REAL,7
E,84,1500,122
*DO,I,1500,1500+iverb-1
E,I,I+1,122
*ENDDO
E,1500+iverb,85,122
E,104,1800,124
*DO,I,1800,1800+iverb-1
E,I,I+1,124
*ENDDO
E,1800+iverb,105,124
                                !Anwendung des Verbandelementes
                                !Element Verband unten links
                                !Schleife zur Elementzuweisung
                                !Elemente Verband links
                                !Element Verband oben links
                                !Element Verband unten links
                                !Schleife zur Elementzuweisung
                                !Elemente Verband links
                                !Element Verband oben links

```

```

! *** 1.OG Querriegel rechts ***
TYPE,6
REAL,6
E,66,1250,126
*DO,I,1250,1250+irieg-1
E,I,I+1,126
*ENDDO
E,1250+irieg,67,126           !Anwendung des Querriegelelementes
                                !Element Querriegel rechts
                                !Schleife zur Elementzuweisung
                                !Elemente Querriegel rechts
                                !Element Querriegel rechts

! *** 1.OG Verband rechts ***
TYPE,7
REAL,7
E,86,1550,127
*DO,I,1550,1550+iverb-1
E,I,I+1,127
*ENDDO
E,1550+iverb,87,127          !Anwendung des Verbandselementes
                                !Element Verband unten rechts
                                !Schleife zur Elementzuweisung
                                !Elemente Verband rechts
                                !Element Verband oben rechts
E,106,1850,125
*DO,I,1850,1850+iverb-1
E,I,I+1,125
*ENDDO
E,1850+iverb,107,125         !Element Verband unten rechts
                                !Schleife zur Elementzuweisung
                                !Elemente Verband rechts
                                !Element Verband oben rechts
*endif

! *** 2.Obergeschoß ***
*if,istock,gt,2,then          !Prüfung ob 2.Obergeschoß zu berücksichtigen ist

! *** vorderer 2.OG-Rahmen ***
TYPE,1
REAL,1
! *** 2.OG Stütze links ***
E,11,900,120
*DO,I,900,900+istut-1
E,I,I+1,120
*ENDDO
E,900+istut,19,120          !Anwendung des Stützenelementes
                                !Element Fußpunkt 2.OG-Stütze links
                                !Schleife zur Elementzuweisung
                                !Elemente 2.OG-Stütze links
                                !Element 2.OG-Stütze oben links

! *** Dogbone links ***
TYPE,5
REAL,5
E,19,20,120                  !Anwendung des Element Dogbone außen

TYPE,4
REAL,4
E,20,21,120                  !Anwendung des Element Dogbone mitte

TYPE,3
REAL,3
E,21,22,120                  !Anwendung des Element Dogbone innen

TYPE,2
REAL,2
! *** 2.OG Riegel ***
E,22,400,120
*DO,I,400,400+irieg-1
E,I,I+1,120
*ENDDO
E,400+irieg,23,120          !Anwendung des Riegelementes
                                !Element Riegel 2.OG links
                                !Schleife zur Elementzuweisung
                                !Elemente Riegel 2.OG
                                !Element Riegel 2.OG rechts

! *** Dogbone rechts ***
TYPE,3
REAL,3
E,23,24,120                  !Anwendung des Element Dogbone innen

TYPE,4
REAL,4
E,24,25,120                  !Anwendung des Element Dogbone mitte

TYPE,5
REAL,5

```

E,25,26,120

```
TYPE,1           !Anwendung des Stützenelementes
REAL,1
! *** 2.OG Stütze rechts ***
E,26,1000+istut,120      !Element 2.OG-Stütze oben rechts
*DO,I,1000+istut,1001,-1  !Schleife zur Elementzuweisung
E,I,I-1,120            !Elemente Stütze rechts
*ENDDO
E,1000,18,120          !Element Fußpunkt 2.OG-Stütze rechts

! *** hinterer 2.OG-Rahmen ***
TYPE,1           !Anwendung des Stützenelementes
REAL,1
! *** 2.OG Stütze links ***
E,41,950,121      !Element Fußpunkt 2.OG-Stütze links
*DO,I,950,950+istut-1  !Schleife zur Elementzuweisung
E,I,I+1,121        !Elemente 2.OG-Stütze links
*ENDDO
E,950+istut,49,121  !Element 2.OG-Stütze oben links

! *** Dogbone links ***
TYPE,5           !Anwendung des Element Dogbone außen
REAL,5
E,49,50,121

TYPE,4           !Anwendung des Element Dogbone mitte
REAL,4
E,50,51,121

TYPE,3           !Anwendung des Element Dogbone innen
REAL,3
E,51,52,121

TYPE,2           !Anwendung des Riegelementes
REAL,2
! *** 2.OG Riegel ***
E,52,450,121      !Element Riegel 2.OG links
*DO,I,450,450+irieg-1  !Schleife zur Elementzuweisung
E,I,I+1,121        !Elemente Riegel 2.OG
*ENDDO
E,450+irieg,53,121  !Element Riegel 2.OG rechts

! *** Dogbone rechts ***
TYPE,3           !Anwendung des Element Dogbone innen
REAL,3
E,53,54,121

TYPE,4           !Anwendung des Element Dogbone mitte
REAL,4
E,54,55,121

TYPE,5           !Anwendung des Element Dogbone außen
REAL,5
E,55,56,121

TYPE,1           !Anwendung des Stützenelementes
REAL,1
! *** 2.OG Stütze rechts ***
E,56,1050+istut,121      !Element 2.OG-Stütze oben rechts
*DO,I,1050+istut,1051,-1  !Schleife zur Elementzuweisung
E,I,I-1,121            !Elemente Stütze rechts
*ENDDO
E,1050,48,121          !Element Fußpunkt 2.OG-Stütze rechts

! *** 2.OG Querriegel links ***
TYPE,6           !Anwendung des Querriegellelementes
REAL,6
E,68,1300,123      !Element Querriegel links
*DO,I,1300,1300+irieg-1  !Schleife zur Elementzuweisung
E,I,I+1,123          !Elemente Querriegel links
*ENDDO
E,1300+irieg,69,123  !Element Querriegel links
```

```

! *** 2.OG Verband links ***
TYPE,7
REAL,7
E,88,1600,122
*DO,I,1600,1600+iverb-1
E,I,I+1,122
*ENDDO
E,1600+iverb,89,122

E,108,1900,124
*DO,I,1900,1900+iverb-1
E,I,I+1,124
*ENDDO
E,1900+iverb,109,124

! *** 2.OG Querriegel rechts ***
TYPE,6
REAL,6
E,70,1350,126
*DO,I,1350,1350+irieg-1
E,I,I+1,126
*ENDDO
E,1350+irieg,71,126

! *** 2.OG Verband rechts ***
TYPE,7
REAL,7
E,90,1650,127
*DO,I,1650,1650+iverb-1
E,I,I+1,127
*ENDDO
E,1650+iverb,91,127

E,110,1950,125
*DO,I,1950,1950+iverb-1
E,I,I+1,125
*ENDDO
E,1950+iverb,111,125

*endif

! *** Koppelung der Knoten Rahmen/Verband ***
NSEL,ALL
NSEL,u,LOC,y,yk2
zseg=z2+hocheg/2
zsog1=z11+hochoga/2
zsog2=z19+hochgb/2
NSEL,u,LOC,z,zseg
NSEL,u,LOC,z,zsog1
1.0G
NSEL,u,LOC,z,zsog2
OG

CPINTF,UX,offset+15
CPINTF,UY,offset+15
CPINTF,UZ,offset+15
CPINTF,ROTY,offset+15

allsel

! *** Einbau der Knotenmassen MASS21 in Riegelebene ***
*if,masse,gt,0,then !Prüfung ob Massenträgheit berücksichtigt werden soll
type,8
REAL,8

! *** Erdgeschoß Riegel ***
! *** vorderer Rahmenriegel ***
E,5
*DO,I,200,200+irieg,1
E,I
*ENDDO

```

!Anwendung des Verbandselementes
!Element Verband unten links
!Schleife zur Elementzuweisung
!Elemente Verband links
!Element Verband oben links
!Element Verband unten links
!Schleife zur Elementzuweisung
!Elemente Verband links
!Element Verband oben links

!Anwendung des Querriegelelementes
!Element Querriegel rechts
!Schleife zur Elementzuweisung
!Elemente Querriegel rechts
!Element Querriegel rechts

!Anwendung des Verbandselementes
!Element Verband unten rechts
!Schleife zur Elementzuweisung
!Elemente Verband rechts
!Element Verband oben rechts
!Element Verband unten rechts
!Schleife zur Elementzuweisung
!Elemente Verband rechts
!Element Verband oben rechts

!Alle Knoten selektieren
!Deselektierung von allen Knoten im Bereich breitq/2
!Mittelebene im EG
!Mittelebene im 1.OG
!Mittelebene im 2.OG
!Deselektierung von allen Knoten im Bereich Mittelebene EG
!Deselektierung von allen Knoten im Bereich Mittelebene
!Deselektierung von allen Knoten im Bereich Mittelebene 2.
!Knoten sind im Toleranzbereich von 'offset' mit
!ihren Freiheitsgraden in der jeweiligen Richtung
!gekoppelt
!

```

E,6                               !Element Riegel EG rechts

*if,ibays,gt,0,then
! *** hinterer Rahmenriegel ***

E,35                               !Element Riegel EG links
*DO,I,250,250+irieg,1           !Schleife zur Elementzuweisung
E,I                                !Elemente Riegel EG
*ENDDO
E,36                               !Element Riegel EG rechts

*endif

*if,istock,gt,1,then      !Prüfung ob 1.Obergeschoß zu berücksichtigen ist
! *** 1.Obergeschoß Riegel ***

! *** vorderer Rahmenriegel ***

E,14                               !Element Riegel 1.OG links
*DO,I,300,300+irieg,1           !Schleife zur Elementzuweisung
E,I                                !Elemente Riegel 1.OG
*ENDDO
E,15                               !Element Riegel 1.OG rechts

! *** hinterer Rahmenriegel ***

E,44                               !Element Riegel 1.OG links
*DO,I,350,350+irieg,1           !Schleife zur Elementzuweisung
E,I                                !Elemente Riegel 1.OG
*ENDDO
E,45                               !Element Riegel 1.OG rechts

*endif

*if,istock,gt,2,then      !Prüfung ob 2.Obergeschoß zu berücksichtigen ist
! *** 2.Obergeschoß Riegel ***

! *** vorderer Rahmenriegel ***

E,22                               !Element Riegel 2.OG links
*DO,I,400,400+irieg,1           !Schleife zur Elementzuweisung
E,I                                !Elemente Riegel 2.OG
*ENDDO
E,23                               !Element Riegel 2.OG rechts

! *** hinterer Rahmenriegel ***

E,52                               !Element Riegel 2.OG links
*DO,I,450,450+irieg,1           !Schleife zur Elementzuweisung
E,I                                !Elemente Riegel 2.OG
*ENDDO
E,53                               !Element Riegel 2.OG rechts
*endif
*endif
FINI          !Beenden des Preprocessing-Moduls
SAVE          !Sichern der Daten

! *** AUFRUF DER SOLUTION ***
*if,moanaly,eq,1,then
*go,:Modalanal
*endif

/SOLU          !Aufruf des Lösungsprozessors
ANTYPE,trans,NEW        !Festlegen der Analyseart, transient=zeitabhängig
NLGEOM,OFF          !Große Verformungen werden nicht berücksichtigt
SSTIF,OFF           !Steifigkeitseffekte infolge Spannung werden nicht berücksichtigt
LUMPM,OFF           !Benutzung einer vom Element abhängig Massenmatrix
KBC,1                !Lastaufbringung stufenartig

TRNOPT,FULL,,,1       !Lösungsmethode ohne Ersatzsystem (Full Method)
TINTP,0.5,,,50,
SOLCONTROL,On

NROPT,init,,OFF
NEQIT,iterat          !Maximale Anzahl der Gleichgewichtsiterationen im Unterschritt
NCNV,2
ERESX,NO              !Keine Ableitung der Ergebnisse an den Iterationspunkten zu allen
Elementen
OUTPR,all,none         !Komplette Ausgabe der Ergebnisse - auch für die "Substeps"

```

```

OUTRES,all,all

cutcontrol,PLSLIMIT,0.01

parsav,all           !Sichern aller Parameter

rescontrol,define,none,none

autots,off          !Keine automatische Zeitschrittfolge

CNVTOL,U,,0.01*cfak2,konv2,1.0      !Festlegung der Konvergenzwerte für die
Verschiebungen

nSEL,s,node,,1      !Selektion des Knoten Nr. 1
d,all,ux,0          !Lagerbedingungen:   Halterung in x-Richtung
d,all,uy,0          !
d,all,uz,0          !
!d,all,rotz,0
*if,einsp,eq,1,then !Prüfung ob Stütze eingespannt ist
d,all,roty,0        !Halterung gegen Verdrehen um die y-Achse
d,all,rotx,0        !Halterung gegen Verdrehen um die x-Achse
*endif

allsel
nSEL,s,node,,10     !Selektion des Knoten Nr. 10
d,all,ux,0          !Lagerbedingungen:   Halterung in x-Richtung
d,all,uy,0          !
d,all,uz,0          !
!d,all,rotz,0
*if,einsp,eq,1,then !Prüfung ob Stütze eingespannt ist
d,all,roty,0        !Halterung gegen Verdrehen um die y-Achse
d,all,rotx,0        !Halterung gegen Verdrehen um die x-Achse
*endif

*if,ibays,gt,0,then
allsel
nSEL,s,node,,31     !Selektion des Knoten Nr. 31
d,all,ux,0          !Lagerbedingungen:   Halterung in x-Richtung
d,all,uy,0          !
d,all,uz,0          !
!d,all,rotz,0
*if,einsp,eq,1,then !Prüfung ob Stütze eingespannt ist
d,all,roty,0        !Halterung gegen Verdrehen um die y-Achse
d,all,rotx,0        !Halterung gegen Verdrehen um die x-Achse
*endif

allsel
nSEL,s,node,,40     !Selektion des Knoten Nr. 40
d,all,ux,0          !Lagerbedingungen:   Halterung in x-Richtung
d,all,uy,0          !
d,all,uz,0          !
!d,all,rotz,0
*if,einsp,eq,1,then !Prüfung ob Stütze eingespannt ist
d,all,roty,0        !Halterung gegen Verdrehen um die y-Achse
d,all,rotx,0        !Halterung gegen Verdrehen um die x-Achse
*endif
*endif

allsel           !Alles selektieren

*if,loese,eq,1,then !Wenn Parameter "loese" = 1, dann
*DIM,ZEIT,array,ilang+15,1
!Freihaltung von Speicher für Zeit, Felddaten, Werte bis ilang, eine Spalte
*DIM,SCHIEBX,array,ilang+15,1
!Freihaltung von Speicher für Schrieb, Felddaten, Werte bis ilang, eine Spalte
*DIM,SCHIEBY,array,ilang+15,1
!Freihaltung von Speicher für Schrieb, Felddaten, Werte bis ilang, eine Spalte
*DIM,SCHIEBZ,array,ilang+15,1
!Freihaltung von Speicher für Schrieb, Felddaten, Werte bis ilang, eine Spalte
*DIM,BESCHL,array,ilang+15,1
!Freihaltung von Speicher für Beschleunigung, Felddaten, Werte bis ilang, eine Spalte
*DIM,Ampli,array,ilang+15,1
!Freihaltung von Speicher für Amplitudenrechnung, Felddaten,
!Werte bis ilang, eine Spalte

! *** Einlesen der Bebendaten ***
*VREAD,ZEIT(1),timeg1090,inp,d:\cem\eqs\,1
!Einlesen der Zeitdaten in das dimensionierte Array, Datendatei: timekobe.inp
(1F14.5)

```

```

*VREAD,SCHIEBX(1),G01090_dth,inp,d:\cem\eqs\,1
!Einlesen der Schriebsdaten in das dimensionierte Array, Datendatei: akobe.inp
(5ES15.7E2)

nsubst,1           !Anzahl der "Substeps" die für den Lastschritt verwendet werden

! *** Berechnung des Lastfalles Eigengewicht ***
save

*if,erdbes,gt,0,then !Prüfung ob Eigengewicht berücksichtigt werden soll

! *** Einbau von Halterungen in y-Richtung für statische Analyse ***
D,2,uy,0
D,9,uy,0
*if,istock,gt,1,then !Prüfung ob 1.OG vorhanden
D,11,uy,0
D,18,uy,0
*endif
*if,istock,gt,2,then !Prüfung ob 2.OG vorhanden
D,19,uy,0
D,26,uy,0
*endif

allsel
xende=breit-offset-1
xanfang=offset+1
nsel,s,loc,x,xanfang,xende
d,all,rotx,0
allsel

ESEL,S,type,,7      !Selektion der Verbandselemente

EKILL,all          !Töten der Verbandselemente
allsel            !Alles selektieren

ACEL,0,0,-9810
!Beschreibung der linearen Beschleunigung der Struktur in z-Richtung
time,0.001*langsa
!Zeit am Ende der Lastaufbringung, keine Null, da sonst statische Analyse
timint,off,all
!Keine Berücksichtigung von Zeiteffekten, Anwendung auf alle geeigneten Einstellung
solve             !Starten der Lösungsberechnung
*endif

allsel

! *** Berechnung des Lastfalles Erdbeben ***
*if,dynam,gt,0,then !Prüfung ob Erdbeben berücksichtigt werden soll

! *** Aufhebung der Bindung der Rahmeneckknoten ***
*if,decuy,eq,0,then
DDELE,2,uy
DDELE,9,uy
*if,istock,gt,1,then !Prüfung ob 1.OG vorhanden
DDELE,11,uy
DDELE,18,uy
*endif
*if,istock,gt,2,then !Prüfung ob 2.OG vorhanden
DDELE,19,uy
DDELE,26,uy
*endif
*endif
! ***

ESEL,S,Type,,7      !Selektion der Verbandselemente
EALIVE,ALL          !Verbandselemente lebendig machen
allsel

TIMINT,ON,ALL
!Berücksichtung von Zeiteffekten, Anwendung auf alle geeigneten Einstellungen
KBC,KBCWERT
nsubst,subzahl       !Anzahl der "Substeps" die für den Lastschritt verwendet werden

! *** Aufbringung der Verschiebungen infolge Erdbeben bzw. zyklischer Last
*DO,i,1,iwert+15,1    !Einleitung der DO-Schleife
*if,i,gt,15,then
d,1,ux,dskal*SCHIEBX(i-15)   !Verschiebung der Auflagerknoten in x-Richtung
d,10,ux,dskal*SCHIEBX(i-15)  !Verschiebung der Auflagerknoten in x-Richtung

```

```

d,1,uy,dskal*SCHIEBY(i-15)           !Verschiebung der Auflagerknoten in y-Richtung
d,10,uy,dskal*SCHIEBY(i-15)
d,1,uy,dskal*SCHIEBZ(i-15)          !Verschiebung der Auflagerknoten in z-Richtung
d,10,uy,dskal*SCHIEBZ(i-15)
*if,ibays,gt,0,then                  !Verschiebung der Auflagerknoten in z-Richtung
d,31,ux,dskal*SCHIEBX(i-15)         !Verschiebung der Auflagerknoten in x-Richtung
d,40,ux,dskal*SCHIEBX(i-15)
d,31,uy,dskal*SCHIEBY(i-15)         !Verschiebung der Auflagerknoten in y-Richtung
d,40,uy,dskal*SCHIEBY(i-15)
d,31,uz,dskal*SCHIEBZ(i-15)        !Verschiebung der Auflagerknoten in z-Richtung
d,40,uz,dskal*SCHIEBZ(i-15)        !Verschiebung der Auflagerknoten in z-Richtung
*endif
*endif
save
*if,i,le,15,then
*if,i,lt,4,then
time,ZEIT(i)*langsa
*endif
*if,i,ge,4,then
time,(ZEIT(3)*langsa)+(ZEIT(i-3)*langsa/10000)
*endif
*endif
*if,i,gt,15,then
time,(ZEIT(3)*langsa)+(ZEIT(12)*langsa/10000)+ZEIT(i-15)
*endif
solve                                !Starten der Lösungsberechnung
*ENDDO                                !Sprung zum Schleifenanfang

*endif
*endif
save

FINI                                     !Ende der kompletten Daten-/Berechnungssequenz

*if,dynam,eq,0,then      !Prüfung ob Erdbeben berücksichtigt werden soll
*if,moanaly,eq,0,then   !Prüfung ob Erdbeben berücksichtigt werden soll
/POST1                                    !Aufruf der Ergebnisausgabe
NSEL,S,,,1,10,9
NSEL,A,,,31,40,9
/Output,_WEIGHT_TOTAL_,VER,
PRRSOL,FZ
/OUTPUT
allsel
FINI
*endif
*endif

*if,dynam,gt,0,then      !Prüfung ob Erdbeben berücksichtigt werden soll
/post26                                 !Aufruf des Postprocessors Time
Lines,5000                               !maximale Zeilenzahl pro Seite
NUMVAR,200                                !Maximale Anzahl der möglichen Variablen

! *** Definition von Variablen ***
TIMERANGE                                !Alle Variablen im durchlaufenden Zeitbereich definieren

*if,deltat,eq,0.02,then
pltime,2401.36,
*endif

*if,deltat,eq,0.01,then
pltime,1200.68,
*endif

*if,deltat,eq,0.005,then                 !Prüfung ob Beben 1090 berechnet werden soll
pltime,600.34,
*endif

STORE,NEW

! *** GLOBAL RESPONSE PARAMETERS ***
NSOL,2,1,U,X,UX_base                   !Ground Motion at base - ux - node1
NSOL,3,19,U,X,UX_tip                  !Tip deflection -absolute-ux- node19
ADD,4,2,3,,DRIFT_RATIO_X_percent_of_height,,,1/3*hochcoef1,1/3*hochcoef2
!story drift 1st stock-total drift for 1 storey bld

NSOL,48,2,U,X,UX_storey1              !Ground Motion at base - ux - node1
NSOL,49,11,U,X,UX_storey2             !Tip deflection -absolute-ux- node9

```

```

ADD,50,2,48,,STOREY1_ISD_X_percent_of_height,,,hochcoef1,hochcoef2
!story drift 1st stock-total drift for 1 storey bld
ADD,66,48,49,,STOREY2_ISD_X_percent_of_height,,,hochcoef1,hochcoef2
!story drift 1st stock-total drift for 1 storey bld
ADD,67,49,3,,STOREY3_ISD_X_percent_of_height,,,hochcoef1,hochcoef2
!story drift 1st stock-total drift for 1 storey bld

ESOL,5,1,1,F,X,FX_base_left      !Base shear_left_el1_n1
ESOL,6,36,10,F,X,FX_base_right   !Base shear_right_el36_n10
ADD,7,5,6,,BASE_SHEAR_Xdummy,,, save
ESOL,8,37,31,F,X,FX_base_left    !Base shear_left_el1_n1
ESOL,9,72,40,F,X,FX_base_right   !Base shear_right_el36_n10
ADD,10,7,8,9,BASE_SHEAR_X_percent_of_weight,,,weightcoef,weightcoef,weightcoef

ESOL,68,37,31,F,Z,FZ_base_col_comp  !Base shear_left_el1_n1
ESOL,69,72,40,F,Z,FZ_base_col_comp  !Base shear_right_el36_n10

DERIV,20,2,1,,_GROUND_VELOCITY_X,,,
DERIV,30,20,1,,_GROUND_ACCELERATION_X,,,
DERIV,46,3,1,,_TIP_VELOCITY_X,,,
DERIV,47,46,1,,_TIP_ACCELERATION_X,,,

DERIV,101,48,1,,_AFV_X_1,,,
DERIV,102,101,1,,_AFA_X_1,,,

DERIV,103,49,1,,_AFV_X_2,,,
DERIV,104,103,1,,_AFA_X_2,,,

DERIV,105,3,1,,_AFV_X_3,,,
DERIV,106,105,1,,_AFA_X_3,,,

/OUTPUT,PAFVX_PAFAX_max,VER,,
EXTREM,101,102
EXTREM,103,104
EXTREM,105,106
/output

/OUTPUT,PAFVX_PAFAX_th,VER,,
PRVAR,101,102
PRVAR,103,104
PRVAR,105,106
/output

/OUTPUT,GLOBAL_RESPONSE_X_th,VER,,      ! OUTPUT IN EL_TEST.VER
PRVAR,4,10          ! Table of drift & base shear
/output
/OUTPUT,GLOBAL_RESPONSE_X_max,VER,,     ! OUTPUT IN EL_TEST.VER
EXTREM,4,10,6
/output
/OUTPUT,ISD_X_th,VER,,
PRVAR,50,66,67
/output
/OUTPUT,ISD_X_max,VER,,
EXTREM,50
EXTREM,66,67
/output

! ***
NSOL,107,1,U,Y,UY_base      !Ground Motion at base - ux - node1
NSOL,108,19,U,Y,UY_tip      !Tip deflection -absolute-ux- node19
ADD,109,107,108,,DRIFT_RATIO_Y_percent_of_height,,,1/3*hochcoef1,1/3*hochcoef2
!story drift 1st stock-total drift for 1 storey bld

NSOL,110,2,U,Y,UY_storeyl   !Ground Motion at base - ux - node1
NSOL,111,11,U,Y,UY_storey2   !Tip deflection -absolute-ux- node9

ADD,112,107,110,,STOREY1_ISD_Y_percent_of_height,,,hochcoef1,hochcoef2
!story drift 1st stock-total drift for 1 storey bld
ADD,113,110,111,,STOREY2_ISD_Y_percent_of_height,,,hochcoef1,hochcoef2
!story drift 1st stock-total drift for 1 storey bld
ADD,114,111,108,,STOREY3_ISD_Y_percent_of_height,,,hochcoef1,hochcoef2
!story drift 1st stock-total drift for 1 storey bld

DERIV,115,107,1,,_GROUND_VELOCITY_Y,,,
DERIV,116,115,1,,_GROUND_ACCELERATION_Y,,,
DERIV,117,108,1,,_TIP_VELOCITY_Y,,,
DERIV,118,117,1,,_TIP_ACCELERATION_Y,,,

```

```

DERIV,119,110,1,,_AFV_Y_1,,
DERIV,120,119,1,,_AFA_Y_1,,

DERIV,121,111,1,,_AFV_Y_2,,
DERIV,122,121,1,,_AFA_Y_2,,

/OUTPUT,PAFV_PAFA_Y_max,VER,,
EXTREM,119,120
EXTREM,121,122
EXTREM,117,118
/output

/OUTPUT,PAFV_PAFA_Y_th,VER,,
EXTREM,119,120
EXTREM,121,122
EXTREM,117,118
/output

/OUTPUT,GLOBAL_RESPONSE_Y_th,VER,,      ! OUTPUT IN EL_TEST.VER
PRVAR,109                                ! Table of drift & base shear
/output
/OUTPUT,GLOBAL_RESPONSE_Y_max,VER,,      ! OUTPUT IN EL_TEST.VER
EXTREM,109
/output
/OUTPUT,ISD_Y_th,VER,,                   PRVAR,112,113,114
PRVAR,112,113,114
/output
/OUTPUT,ISD_Y_max,VER,,                  EXTREM,112
EXTREM,113,114
/output

! ***

/OUTPUT,COL_COMP_max,VER,,
EXTREM,68,69
/output

/SHOW,TIFF,,
/GFILE,2400
/GTHK,AXIS,3
/GTHK,GRID,0
/GTHK,CURVE,2
/GROPT,AXNM,front
/GROPT,CURL,1
/COLOR,AXES,BLAC
/COLOR,AXLAB,BLAC
/COLOR,CURVE,RED,1
/COLOR,GRID,LGRA
/COLOR,AXNUM,BLAC
/COLOR,WBAK,WHIT
XVAR,1
/AXLAB,X,_TIME_(sec)_
/AXLAB,Y,_GROUND_DISPLACEMENT_in_mm
PLVAR,2

XVAR,1
/AXLAB,X,_TIME_(sec)_
/AXLAB,Y,_GROUND_VELOCITY_in_mm/sec
PLVAR,20

XVAR,1
/AXLAB,X,_TIME_(sec)_
/AXLAB,Y,_GROUND_ACCELERATION_in_mm/sec^2
PLVAR,30

XVAR,1
/AXLAB,X,_TIME_(sec)_
/AXLAB,Y,_TIP_DEFLECTION_in_mm
PLVAR,3

XVAR,1
/AXLAB,X,_TIME_(sec)_
/AXLAB,Y,_TIP_VELOCITY_in_mm/sec
PLVAR,46

XVAR,1
/AXLAB,X,_TIME_(sec)_
/AXLAB,Y,_TIP_ACCELERATION_in_mm/sec^2

```

```

PLVAR, 47

/AXLAB,X,_TIME_(sec)
/AXLAB,Y,_DRIFT_RATIO_percent_of_height_
PLVAR, 4

/AXLAB,X,_TIME_(sec)
/AXLAB,Y,_BASE_SHEAR_percent_of_mass_
PLVAR, 10

/AXLAB,X,_TIME_(sec)
/AXLAB,Y,_COL_COMP_left
PLVAR, 68

/AXLAB,X,_TIME_(sec)
/AXLAB,Y,_COL_COMP_right
PLVAR, 69

XVAR, 2
/AXLAB,X,_GROUND_DISPLACEMENT_
/AXLAB,Y,_DRIFT_RATIO_percent_of_height_
PLVAR, 4

XVAR, 2
/AXLAB,X,_GROUND_DISPLACEMENT_
/AXLAB,Y,_BASE_SHEAR_percent_of_mass_
PLVAR, 10

XVAR, 4
/AXLAB,X,_DRIFT_RATIO_percent_of_height_
/AXLAB,Y,_BASE_SHEAR_percent_of_mass_
PLVAR, 10

! *****
! *** LOCAL RESPONSE PARAMETERS ***
! *** Beam ***
! *** Definition der Variablen für Rotation ***
Mitkno=untr/2           !Bestimmung der Riegelmittenknoten
EGRIEG=200+Mitkno
NSOL,11,EGRIEG,ROT,Y,RY_mid   !Variable Nr.11
NSOL,12,2,ROT,Y,RY_n2       !Variable Nr.12 für node2, Rotation um y-Achse
NSOL,13,3,ROT,Y,RY_n3       !Variable Nr.13 für node3, Rotation um y-Achse
NSOL,14,4,ROT,Y,RY_n4       !Variable Nr.14 für node4, Rotation um y-Achse
NSOL,15,5,ROT,Y,RY_n5       !Variable Nr.15 für node5, Rotation um y-Achse

NSOL,16,6,ROT,Y,RY_n6       !Variable Nr.16 für n6, Rotation um y-Achse
NSOL,17,7,ROT,Y,RY_n7       !Variable Nr.17 für n7, Rotation um y-Achse
NSOL,18,8,ROT,Y,RY_n8       !Variable Nr.18 für n8, Rotation um y-Achse
NSOL,19,9,ROT,Y,RY_n9       !Variable Nr.19 für n9, Rotation um y-Achse

! *** Definition der Variablen für Momente ***
allsel                  !Alles selektieren
NSEL,S,NODE,,EGRIEG
NSEL,A,NODE,,EGRIEG+1
NSEL,A,NODE,,120          !Selektion Referenzknoten
ESLN,S,1,ALL              !Element zwischen den Knoten selektieren
*GET,ELEMENT,ELEM,,NUM,MIN !Zuweisen der Elementnummer
ESOL,21,ELEMENT,EGRIEG,M,y,My_mid    !Variable für My am Knoten 2

allsel                  !Alles selektieren
NSEL,S,NODE,,2            !Selektion des Knoten Nr. 2
NSEL,A,NODE,,3            !Selektion des Knoten Nr. 3
NSEL,A,NODE,,120          !Selektion Referenzknoten
ESLN,S,1,ALL              !Element zwischen den Knoten selektieren
*GET,ELEMENT,ELEM,,NUM,MAX !Zuweisen der Elementnummer
ESOL,22,ELEMENT,2,M,y,My_n2    !Variable für My am Knoten 2

allsel                  !Alles selektieren
NSEL,S,NODE,,3            !Selektion des Knoten Nr. 3
NSEL,A,NODE,,4            !Selektion des Knoten Nr. 4
NSEL,A,NODE,,120          !Selektion Referenzknoten
ESLN,S,1,ALL              !Element zwischen den Knoten selektieren
*GET,ELEMENT,ELEM,,NUM,MAX !Zuweisen der Elementnummer
ESOL,23,ELEMENT,3,M,y,My_n3    !Variable für My am Knoten 3

allsel                  !Alles selektieren
NSEL,S,NODE,,4            !Selektion des Knoten Nr. 4
NSEL,A,NODE,,5            !Selektion des Knoten Nr. 5
NSEL,A,NODE,,120          !Selektion Referenzknoten

```

```

ESLN,S,1,ALL           !Element zwischen den Knoten selektieren
*GET,ELEMENT,ELEM,,NUM,min !Zuweisen der Elementnummer
ESOL,24,ELEMENT,4,M,y,My_n4 !Variable für My am Knoten 4
ESOL,25,ELEMENT,5,M,y,My_n5 !Variable für My am Knoten 4

allsel                  !Alles selektieren
NSEL,S,NODE,,6          !Selektion des Knoten Nr. 2
NSEL,A,NODE,,7          !Selektion des Knoten Nr. 3
NSEL,A,NODE,,120         !Selektion Referenzknoten
ESLN,S,1,ALL             !Element zwischen den Knoten selektieren
*GET,ELEMENT,ELEM,,NUM,min !Zuweisen der Elementnummer
ESOL,26,ELEMENT,6,M,y,My_n6 !Variable für My am Knoten 2

allsel                  !Alles selektieren
NSEL,S,NODE,,7          !Selektion des Knoten Nr. 3
NSEL,A,NODE,,8          !Selektion des Knoten Nr. 4
NSEL,A,NODE,,120         !Selektion Referenzknoten
ESLN,S,1,ALL             !Element zwischen den Knoten selektieren
*GET,ELEMENT,ELEM,,NUM,max !Zuweisen der Elementnummer
ESOL,27,ELEMENT,7,M,y,My_n7 !Variable für My am Knoten 3

allsel                  !Alles selektieren
NSEL,S,NODE,,8          !Selektion des Knoten Nr.
NSEL,A,NODE,,9          !Selektion des Knoten Nr.
NSEL,A,NODE,,120         !Selektion Referenzknoten
ESLN,S,1,ALL             !Element zwischen den Knoten selektieren
*GET,ELEMENT,ELEM,,NUM,max !Zuweisen der Elementnummer
ESOL,28,ELEMENT,8,M,y,My_n8 !Variable für My am Knoten 4
ESOL,29,ELEMENT,9,M,y,My_n9 !Variable für My am Knoten 4

INT1,146,10,4,,GLOBAL_diss_energy_intBASEshTIPdefl,,,1.0/weightcoef,3.0/hochcoef2,0.0
INT1,166,21,11,,Diss_Energy_mid_beam_intMOMdROT,,,1.0,1.0,0.0
INT1,167,22,12,,Diss_Energy_n2_beam_edge_intMOMdROT,,,1.0,1.0,0.0
INT1,168,23,13,,Diss_Energy_n3_beam_intMOMdROT,,,1.0,1.0,0.0
INT1,169,24,14,,Diss_Energy_n4_beam_intMOMdROT,,,1.0,1.0,0.0
INT1,170,25,15,,Diss_Energy_n5_beam_intMOMdROT,,,1.0,1.0,0.0

/OUTPUT,DISS_ENERGY_max_,VER,,
EXTREM,146
EXTREM,166,170,1
/output

XVAR,1
/AXLAB,X,_TIME_(sec)_
/AXLAB,Y,_GLOBAL_DISS_ENERGY
PLVAR,146

XVAR,1
/AXLAB,X,_TIME_(sec)_
/AXLAB,Y,_DISS_ENERGY_beam_mid_n2_3_4_5
PLVAR,166,167,168,169,170

/OUTPUT,BEAM_ROTY_th,VER,,
PRVAR,11,12,13,14,15,16,17,18,19
/output

/OUTPUT,BEAM_ROTY_max,VER,,
EXTREM,11,19,1
/output

/OUTPUT,BEAM_MOMY_th,VER,,
PRVAR,21,22,23,24,25,26,27,28,29
/output

/OUTPUT,BEAM_MOMY_max,VER,,
EXTREM,21,29,1
/output

! curves can be named**
XVAR,1
/AXLAB,X,_TIME_(sec)_
/AXLAB,Y,_BEAM_ROTY_th_
PLVAR,11,12,13,14,15
PLVAR,11,16,17,18,19
PLVAR,11,12,13,14,15,16,17,18,19

XVAR,1
/AXLAB,X,_TIME_(sec)_
/AXLAB,Y,_BEAM_MOMY_th_

```

```

PLVAR,21,22,23,24,25
PLVAR,21,26,27,28,29
PLVAR,21,22,23,24,25,26,27,28,29

XVAR,11
/AXLAB,X,_ROTY_mid_beam_
/AXLAB,Y,_MOMY_mid_beam_
PLVAR,21

XVAR,12
/AXLAB,X,_ROTY_n2_beam_edge_
/AXLAB,Y,_MOMY_n2_beam_edge_
PLVAR,22

XVAR,13
/AXLAB,X,_ROTY_n3_beam_
/AXLAB,Y,_MOMY_n3_beam_
PLVAR,23

XVAR,14
/AXLAB,X,_ROTY_n4_beam_
/AXLAB,Y,_MOMY_n4_beam_
PLVAR,24

XVAR,15
/AXLAB,X,_ROTY_n5_beam_
/AXLAB,Y,_MOMY_n5_beam_
PLVAR,25

XVAR,16
/AXLAB,X,_ROTY_n6_beam_
/AXLAB,Y,_MOMY_n6_beam_
PLVAR,26

XVAR,17
/AXLAB,X,_ROTY_n7_beam_
/AXLAB,Y,_MOMY_n7_beam_
PLVAR,27

XVAR,18
/AXLAB,X,_ROTY_n8_beam_
/AXLAB,Y,_MOMY_n8_beam_
PLVAR,28

XVAR,19
/AXLAB,X,_ROTY_n9_beam_
/AXLAB,Y,_MOMY_n9_beam_
PLVAR,29

allsel          !Alles selektieren

! ***NODE2***
NSEL,S,NODE,,2           !Selektion des Knoten Nr. 2
NSEL,A,NODE,,3           !Selektion des Knoten Nr. 3
NSEL,A,NODE,,120          !Selektion Referenzknoten
ESLN,S,1,ALL              !Element zwischen den Knoten selektieren
*GET,ELEMENT,ELEM,,NUM,MAX !Zuweisen der Elementnummer

ESOL,31,ELEMENT,2,LEPPL,1,PL_STRAIN_n2_s1_   !Variable für plastische Dehnung im Element
ESOL,32,ELEMENT,2,LEPEL,1,EL_STRAIN_n2_s1_   !Variable für elastische Dehnung im Element
ADD,33,31,32,,TOT_STRAIN_n2_s1_,,,          !Addition von plastischer und elastischer Dehnung im Bone 1
ESOL,34,ELEMENT,2,ls,1,AXL_STRESS_n2_s1_     !Längsspannung

DERIV,35,33,1,,_STRAIN_RATE_n2_s1_,,,,
XVAR,1
/AXLAB,X,_TIME_(sec)_      !Zeitangabe in Sekunden
/AXLAB,Y,_STRAIN_RATE_n2_s1_
PLVAR,35

XVAR,33
/AXLAB,X,_TOT_STRAIN_n2_s1_
/AXLAB,Y,_AXIAL_STRESS_n2_s1_
PLVAR,34

ESOL,36,ELEMENT,2,LEPPL,10,PL_STRAIN_n2_s10_ !Variable für plastische Dehnung im Element
ESOL,37,ELEMENT,2,LEPEL,10,EL_STRAIN_n2_s10_ !Variable für elastische Dehnung im Element
ADD,38,36,37,,TOT_STRAIN_n2_s10_,,,          !Addition von plastischer und elastischer Dehnung im Bone 1

```

```

ESOL,39,ELEMENT,2,ls,10,AXL_STRESS_n2_s10_ !Längsspannung

DERIV,40,38,1,,_STRAIN_RATE_n2_s10_...
XVAR,1
/AXLAB,X,_TIME_(sec)
/AXLAB,Y,_STRAIN_RATE_n2_s10_
PLVAR,40

XVAR,38
/AXLAB,X,_TOT_STRAIN_n2_s10_
/AXLAB,Y,_AXIAL_STRESS_n2_s10_
PLVAR,39

ESOL,41,ELEMENT,2,LEPPL,20,PL_STRAIN_n2_s20_ !Variable für plastische Dehnung im Element
ESOL,42,ELEMENT,2,LEPEL,20,EL_STRAIN_n2_s20_ !Variable für elastische Dehnung im Element
ADD,43,41,42,,TOT_STRAIN_n2_s20_...
!Addition von plastischer und elastischer Dehnung im Bone 1
ESOL,44,ELEMENT,2,ls,20,AXL_STRESS_n2_s20_ !Längsspannung

DERIV,45,43,1,,_STRAIN_RATE_n2_s20_...
XVAR,1
/AXLAB,X,_TIME_(sec)
/AXLAB,Y,_STRAIN_RATE_n2_s20_
PLVAR,45

XVAR,43
/AXLAB,X,_TOT_STRAIN_n2_s20_
/AXLAB,Y,_AXIAL_STRESS_n2_s20_
PLVAR,44

allsel
! *****
! ***NODE3***
NSEL,S,NODE,,3                      !Selektion des Knoten Nr. 3
NSEL,A,NODE,,4                      !Selektion des Knoten Nr. 3
NSEL,A,NODE,,120                     !Selektion Referenzknoten
ESLN,S,1,ALL                          !Element zwischen den Knoten selektieren
*GET,ELEMENT,ELEM,,NUM,MAX           !Zuweisen der Elementnummer

ESOL,51,ELEMENT,3,LEPPL,1,PL_STRAIN_n3_s1_ !Variable für plastische Dehnung im Element
ESOL,52,ELEMENT,3,LEPEL,1,EL_STRAIN_n3_s1_ !Variable für elastische Dehnung im Element
ADD,53,51,52,,TOT_STRAIN_n3_s1_...
!Addition von plastischer und elastischer Dehnung im Bone 1
ESOL,54,ELEMENT,3,ls,1,AXL_STRESS_n3_s1_ !Längsspannung

DERIV,55,53,1,,_STRAIN_RATE_n3_s1_...
XVAR,1
/AXLAB,X,_TIME_(sec)
/AXLAB,Y,_STRAIN_RATE_n3_s1_
PLVAR,55

XVAR,53
/AXLAB,X,_TOT_STRAIN_n3_s1_
/AXLAB,Y,_AXIAL_STRESS_n3_s1_
PLVAR,54

ESOL,56,ELEMENT,3,LEPPL,10,PL_STRAIN_n3_s10_ !Variable für plastische Dehnung im Element
ESOL,57,ELEMENT,3,LEPEL,10,EL_STRAIN_n3_s10_ !Variable für elastische Dehnung im Element
ADD,58,56,57,,TOT_STRAIN_n3_s10_...
!Addition von plastischer und elastischer Dehnung im Bone 1
ESOL,59,ELEMENT,3,ls,10,AXL_STRESS_n3_s10_ !Längsspannung

DERIV,60,58,1,,_STRAIN_RATE_n3_s10_...
XVAR,1
/AXLAB,X,_TIME_(sec)
/AXLAB,Y,_STRAIN_RATE_n3_s10_
PLVAR,60

XVAR,58
/AXLAB,X,_TOT_STRAIN_n3_s10_
/AXLAB,Y,_AXIAL_STRESS_n3_s10_
PLVAR,59

ESOL,61,ELEMENT,3,LEPPL,20,PL_STRAIN_n3_s20_ !Variable für plastische Dehnung im Element
ESOL,62,ELEMENT,3,LEPEL,20,EL_STRAIN_n3_s20_ !Variable für elastische Dehnung im Element
ADD,63,61,62,,TOT_STRAIN_n3_s20_...
!Addition von plastischer und elastischer Dehnung im Bone 1
ESOL,64,ELEMENT,3,ls,20,AXL_STRESS_n3_s20_ !Längsspannung

```

```

DERIV,65,63,1,,_STRAIN_RATE_n3_s20_...
XVAR,1
/AXLAB,X,_TIME_(sec)
/AXLAB,Y,_STRAIN_RATE_n3_s20_
PLVAR,65

XVAR,63
/AXLAB,X,_TOT_STRAIN_n3_s20_
/AXLAB,Y,_AXIAL_STRESS_n3_s20_
PLVAR,64

allsel
! *****

! ***NODE4***
NSEL,S,NODE,,4          !Selektion des Knoten Nr. 3
NSEL,A,NODE,,5          !Selektion des Knoten Nr. 3
NSEL,A,NODE,,120         !Selektion Referenzknoten
ESLN,S,1,ALL             !Element zwischen den Knoten selektieren
*GET,ELEMENT,ELEM,,NUM,Min !Zuweisen der Elementnummer

ESOL,71,ELEMENT,4,LEPPL,1,PL_STRAIN_n4_s1_   !Variable für plastische Dehnung im Element
ESOL,72,ELEMENT,4,LEPEL,1,EL_STRAIN_n4_s1_    !Variable für elastische Dehnung im Element
ADD,73,71,72,,TOT_STRAIN_n4_s1_...
!Addition von plastischer und elastischer Dehnung im Bone 1
ESOL,74,ELEMENT,4,ls,1,AXL_STRESS_n4_s1_     !Längsspannung

DERIV,75,73,1,,_STRAIN_RATE_n4_s1_...
XVAR,1
/AXLAB,X,_TIME_(sec)
/AXLAB,Y,_STRAIN_RATE_n4_s1_
PLVAR,75

XVAR,73
/AXLAB,X,_TOT_STRAIN_n4_s1_
/AXLAB,Y,_AXIAL_STRESS_n4_s1_
PLVAR,74

ESOL,76,ELEMENT,4,LEPPL,10,PL_STRAIN_n4_s10_ !Variable für plastische Dehnung im Element
ESOL,77,ELEMENT,4,LEPEL,10,EL_STRAIN_n4_s10_  !Variable für elastische Dehnung im Element
ADD,78,76,77,,TOT_STRAIN_n4_s10_...
!Addition von plastischer und elastischer Dehnung im Bone 1
ESOL,79,ELEMENT,4,ls,10,AXL_STRESS_n4_s10_   !Längsspannung

DERIV,80,78,1,,_STRAIN_RATE_n4_s10_...
XVAR,1
/AXLAB,X,_TIME_(sec)
/AXLAB,Y,_STRAIN_RATE_n4_s10_
PLVAR,80

XVAR,78
/AXLAB,X,_TOT_STRAIN_n4_s10_
/AXLAB,Y,_AXIAL_STRESS_n4_s10_
PLVAR,79

ESOL,81,ELEMENT,4,LEPPL,20,PL_STRAIN_n4_s20_ !Variable für plastische Dehnung im Element
ESOL,82,ELEMENT,4,LEPEL,20,EL_STRAIN_n4_s20_  !Variable für elastische Dehnung im Element
ADD,83,81,82,,TOT_STRAIN_n4_s20_...
!Addition von plastischer und elastischer Dehnung im Bone 1
ESOL,84,ELEMENT,4,ls,20,AXL_STRESS_n4_s20_   !Längsspannung

DERIV,85,83,1,,_STRAIN_RATE_n4_s20_...
XVAR,1
/AXLAB,X,_TIME_(sec)
/AXLAB,Y,_STRAIN_RATE_n4_s20_
PLVAR,85

XVAR,83
/AXLAB,X,_TOT_STRAIN_n4_s20_
/AXLAB,Y,_AXIAL_STRESS_n4_s20_
PLVAR,84

allsel

ESOL,86,ELEMENT,5,LEPPL,21,PL_STRAIN_n5_s21_ !Variable für plastische Dehnung im Element
ESOL,87,ELEMENT,5,LEPEL,21,EL_STRAIN_n5_s21_  !Variable für elastische Dehnung im Element
ADD,88,86,87,,TOT_STRAIN_n5_s21_...
!Addition von plastischer und elastischer Dehnung im Bone 1

```

```

ESOL,89,ELEMENT,5,ls,21,AXL_STRESS_n5_s21_      !Längsspannung

DERIV,90,88,1,,_STRAIN_RATE_n5_s21_...
XVAR,1
/AXLAB,X,_TIME_(sec)
/AXLAB,Y,_STRAIN_RATE_n5_s21_
PLVAR,90

XVAR,88
/AXLAB,X,_TOT_STRAIN_n5_s21_
/AXLAB,Y,_AXIAL_STRESS_n5_s21_
PLVAR,89

ESOL,91,ELEMENT,5,LEPPL,30,PL_STRAIN_n5_s30_ !Variable für plastische Dehnung im Element
ESOL,92,ELEMENT,5,LEPEL,30,EL_STRAIN_n5_s30_ !Variable für elastische Dehnung im Element
ADD,93,91,92,,TOT_STRAIN_n5_s30_...
!Addition von plastischer und elastischer Dehnung im Bone 1
ESOL,94,ELEMENT,5,ls,30,AXL_STRESS_n5_s30_      !Längsspannung

DERIV,95,93,1,,_STRAIN_RATE_n5_s30_...
XVAR,1
/AXLAB,X,_TIME_(sec)
/AXLAB,Y,_STRAIN_RATE_n5_s30_
PLVAR,95

XVAR,93
/AXLAB,X,_TOT_STRAIN_n5_s30_
/AXLAB,Y,_AXIAL_STRESS_n5_s30_
PLVAR,94

ESOL,96,ELEMENT,5,LEPPL,40,PL_STRAIN_n5_s40_ !Variable für plastische Dehnung im Element
ESOL,97,ELEMENT,5,LEPEL,40,EL_STRAIN_n5_s40_ !Variable für elastische Dehnung im Element
ADD,98,96,97,,TOT_STRAIN_n5_s40_...
!Addition von plastischer und elastischer Dehnung im Bone 1
ESOL,99,ELEMENT,5,ls,40,AXL_STRESS_n5_s40_      !Längsspannung

DERIV,100,98,1,,_STRAIN_RATE_n5_s40_...
XVAR,1
/AXLAB,X,_TIME_(sec)
/AXLAB,Y,_STRAIN_RATE_n5_s40_
PLVAR,100

XVAR,98
/AXLAB,X,_TOT_STRAIN_n5_s40_
/AXLAB,Y,_AXIAL_STRESS_n5_s40_
PLVAR,99

/OUTPUT,STRAIN_RATES_th,VER,,
PRVAR,35,40,45,55,60,65
PRVAR,75,80,85,90,95,100
/output

/OUTPUT,STRAIN_RATES_max,VER,,
EXTREM,35,100,5
/output

allsel
! ****
! ***NODE9***
NSEL,S,NODE,,9          !Selektion des Knoten Nr. 2
NSEL,A,NODE,,8          !Selektion des Knoten Nr. 3
NSEL,A,NODE,,120         !Selektion Referenzknoten
ESLN,S,1,ALL             !Element zwischen den Knoten selektieren
*GET,ELEMENT,ELEM,,NUM,MAX !Zuweisen der Elementnummer

ESOL,131,ELEMENT,9,LEPPL,21,PL_STRAIN_n9_s21_      !Variable für plastische Dehnung im Element
ESOL,132,ELEMENT,9,LEPEL,21,EL_STRAIN_n9_s21_      !Variable für elastische Dehnung im Element
ADD,133,131,132,,TOT_STRAIN_n2_s21_...
!Addition von plastischer und elastischer Dehnung im Bone 1
ESOL,134,ELEMENT,9,ls,21,AXL_STRESS_n2_s21_      !Längsspannung

DERIV,135,133,1,,_STRAIN_RATE_n9_s21_...
XVAR,1
/AXLAB,X,_TIME_(sec)
/AXLAB,Y,_STRAIN_RATE_n9_s21_
PLVAR,135

```

```

XVAR,133
/AXLAB,X,_TOT_STRAIN_n9_s21_
/AXLAB,Y,_AXIAL_STRESS_n9_s21_
PLVAR,134

ESOL,136,ELEMENT,9,LEPPL,30,PL_STRAIN_n9_s30_
!Variable für plastische Dehnung im Element
ESOL,137,ELEMENT,9,LEPEL,30,EL_STRAIN_n9_s30_
!Variable für elastische Dehnung im Element
ADD,138,136,137,,TOT_STRAIN_n9_s30_...
!Addition von plastischer und elastischer Dehnung im Bone 1
ESOL,139,ELEMENT,9,ls,30,AXL_STRESS_n9_s30_ !Längsspannung

DERIV,140,138,1,,_STRAIN_RATE_n9_s30_...
XVAR,1
/AXLAB,X,_TIME_(sec)
/AXLAB,Y,_STRAIN_RATE_n9_s30_
PLVAR,140

XVAR,138
/AXLAB,X,_TOT_STRAIN_n9_s30_
/AXLAB,Y,_AXIAL_STRESS_n9_s30_
PLVAR,139

ESOL,141,ELEMENT,9,LEPPL,40,PL_STRAIN_n9_s40_
!Variable für plastische Dehnung im Element
ESOL,142,ELEMENT,9,LEPEL,40,EL_STRAIN_n9_s40_
!Variable für elastische Dehnung im Element
ADD,143,141,142,,TOT_STRAIN_n9_s40_...
!Addition von plastischer und elastischer Dehnung im Bone 1
ESOL,144,ELEMENT,9,ls,40,AXL_STRESS_n9_s40_ !Längsspannung

DERIV,145,143,1,,_STRAIN_RATE_n9_s40_...
XVAR,1
/AXLAB,X,_TIME_(sec)
/AXLAB,Y,_STRAIN_RATE_n9_s40_
PLVAR,145

XVAR,143
/AXLAB,X,_TOT_STRAIN_n9_s40_
/AXLAB,Y,_AXIAL_STRESS_n9_s40_
PLVAR,144

allsel
! *****
! ***NODE8***
NSEL,S,NODE,,8                      !Selektion des Knoten Nr. 3
NSEL,A,NODE,,7                        !Selektion des Knoten Nr. 3
NSEL,A,NODE,,120                      !Selektion Referenzknoten
ESLN,S,1,ALL                           !Element zwischen den Knoten selektieren
*GET,ELEMENT,ELEM,,NUM,MAX            !Zuweisen der Elementnummer

ESOL,151,ELEMENT,8,LEPPL,21,PL_STRAIN_n8_s21_
!Variable für plastische Dehnung im Element
ESOL,152,ELEMENT,8,LEPEL,21,EL_STRAIN_n8_s21_
!Variable für elastische Dehnung im Element
ADD,153,151,152,,TOT_STRAIN_n8_s21_...
!Addition von plastischer und elastischer Dehnung im Bone 1
ESOL,154,ELEMENT,8,ls,21,AXL_STRESS_n8_s21_ !Längsspannung

DERIV,155,153,1,,_STRAIN_RATE_n8_s21_...
XVAR,1
/AXLAB,X,_TIME_(sec)
/AXLAB,Y,_STRAIN_RATE_n8_s21_
PLVAR,155

XVAR,153
/AXLAB,X,_TOT_STRAIN_n8_s21_
/AXLAB,Y,_AXIAL_STRESS_n8_s21_
PLVAR,154

ESOL,156,ELEMENT,8,LEPPL,30,PL_STRAIN_n8_s30_
!Variable für plastische Dehnung im Element
ESOL,157,ELEMENT,8,LEPEL,30,EL_STRAIN_n8_s30_
!Variable für elastische Dehnung im Element
ADD,158,156,157,,TOT_STRAIN_n8_s30_...
!Addition von plastischer und elastischer Dehnung im Bone 1

```

```

ESOL,159,ELEMENT,8,ls,30,AXL_STRESS_n8_s30_ !Längsspannung

DERIV,160,158,1,,_STRAIN_RATE_n8_s30_...
XVAR,1
/AXLAB,X,_TIME_(sec)
/AXLAB,Y,_STRAIN_RATE_n8_s30_
PLVAR,160

XVAR,158
/AXLAB,X,_TOT_STRAIN_n8_s30_
/AXLAB,Y,_AXIAL_STRESS_n8_s30_
PLVAR,159

ESOL,161,ELEMENT,8,LEPPL,40,PL_STRAIN_n8_s40_
!Variable für plastische Dehnung im Element
ESOL,162,ELEMENT,8,LEPEL,40,EL_STRAIN_n8_s40_
!Variable für elastische Dehnung im Element
ADD,163,161,162,,TOT_STRAIN_n8_s40_...
!Addition von plastischer und elastischer Dehnung im Bone 1
ESOL,164,ELEMENT,8,ls,40,AXL_STRESS_n8_s40_ !Längsspannung

DERIV,165,163,1,,_STRAIN_RATE_n8_s40_...
XVAR,1
/AXLAB,X,_TIME_(sec)
/AXLAB,Y,_STRAIN_RATE_n8_s40_
PLVAR,165

XVAR,163
/AXLAB,X,_TOT_STRAIN_n8_s40_
/AXLAB,Y,_AXIAL_STRESS_n8_s40_
PLVAR,164

allsel
! *****

! ***NODE7-6***
NSEL,S,NODE,,7           !Selektion des Knoten Nr. 3
NSEL,A,NODE,,6             !Selektion des Knoten Nr. 3
NSEL,A,NODE,,120           !Selektion Referenzknoten
ESLN,S,1,ALL               !Element zwischen den Knoten selektieren
*GET,ELEMENT,ELEM,,NUM,Min !Zuweisen der Elementnummer

ESOL,171,ELEMENT,7,LEPPL,21,PL_STRAIN_n7_s21_
!Variable für plastische Dehnung im Element
ESOL,172,ELEMENT,7,LEPEL,21,EL_STRAIN_n7_s21_
!Variable für elastische Dehnung im Element
ADD,173,171,172,,TOT_STRAIN_n7_s21_...
!Addition von plastischer und elastischer Dehnung im Bone 1
ESOL,174,ELEMENT,7,ls,21,AXL_STRESS_n7_s21_ !Längsspannung

DERIV,175,173,1,,_STRAIN_RATE_n7_s21_...
XVAR,1
/AXLAB,X,_TIME_(sec)
/AXLAB,Y,_STRAIN_RATE_n7_s21_
PLVAR,175

XVAR,173
/AXLAB,X,_TOT_STRAIN_n7_s21_
/AXLAB,Y,_AXIAL_STRESS_n7_s21_
PLVAR,174

ESOL,176,ELEMENT,7,LEPPL,30,PL_STRAIN_n7_s30_
!Variable für plastische Dehnung im Element
ESOL,177,ELEMENT,7,LEPEL,30,EL_STRAIN_n7_s30_
!Variable für elastische Dehnung im Element
ADD,178,176,177,,TOT_STRAIN_n7_s30_...
!Addition von plastischer und elastischer Dehnung im Bone 1
ESOL,179,ELEMENT,7,ls,30,AXL_STRESS_n7_s30_ !Längsspannung

DERIV,180,178,1,,_STRAIN_RATE_n7_s30_...
XVAR,1
/AXLAB,X,_TIME_(sec)
/AXLAB,Y,_STRAIN_RATE_n7_s30_
PLVAR,180

XVAR,178
/AXLAB,X,_TOT_STRAIN_n7_s30_
/AXLAB,Y,_AXIAL_STRESS_n7_s30_
PLVAR,179

```

```

ESOL,181,ELEMENT,7,LEPPL,40,PL_STRAIN_n7_s40_
!Variable für plastische Dehnung im Element
ESOL,182,ELEMENT,7,LEPEL,40,EL_STRAIN_n7_s40_
!Variable für elastische Dehnung im Element
ADD,183,181,182,,TOT_STRAIN_n7_s40_'''
!Addition von plastischer und elastischer Dehnung im Bone 1
ESOL,184,ELEMENT,7,ls,40,AXL_STRESS_n7_s40_ !Längsspannung

DERIV,185,183,1,,_STRAIN_RATE_n7_s40_...
XVAR,1
/AXLAB,X,_TIME_(sec)
/AXLAB,Y,_STRAIN_RATE_n7_s40_
PLVAR,185

XVAR,183
/AXLAB,X,_TOT_STRAIN_n7_s40_
/AXLAB,Y,_AXIAL_STRESS_n7_s40_
PLVAR,184

allsel

ESOL,186,ELEMENT,6,LEPPL,1,PL_STRAIN_n6_s1_ !Variable für plastische Dehnung im Element
ESOL,187,ELEMENT,6,LEPEL,1,EL_STRAIN_n6_s1_ !Variable für elastische Dehnung im Element
ADD,188,186,187,,TOT_STRAIN_n6_s1_...
!Addition von plastischer und elastischer Dehnung im Bone 1
ESOL,189,ELEMENT,6,ls,1,AXL_STRESS_n6_s1_ !Längsspannung

DERIV,190,188,1,,_STRAIN_RATE_n6_s1_...
XVAR,1
/AXLAB,X,_TIME_(sec)
/AXLAB,Y,_STRAIN_RATE_n6_s1_
PLVAR,190

XVAR,188
/AXLAB,X,_TOT_STRAIN_n6_s1_
/AXLAB,Y,_AXIAL_STRESS_n6_s1_
PLVAR,189

ESOL,191,ELEMENT,6,LEPPL,10,PL_STRAIN_n6_s10_
!Variable für plastische Dehnung im Element
ESOL,192,ELEMENT,6,LEPEL,10,EL_STRAIN_n6_s10_
!Variable für elastische Dehnung im Element
ADD,193,191,192,,TOT_STRAIN_n6_s10_'''
!Addition von plastischer und elastischer Dehnung im Bone 1
ESOL,194,ELEMENT,6,ls,10,AXL_STRESS_n6_s10_ !Längsspannung

DERIV,195,193,1,,_STRAIN_RATE_n6_s10_...
XVAR,1
/AXLAB,X,_TIME_(sec)
/AXLAB,Y,_STRAIN_RATE_n6_s10_
PLVAR,195

XVAR,193
/AXLAB,X,_TOT_STRAIN_n6_s10_
/AXLAB,Y,_AXIAL_STRESS_n6_s10_
PLVAR,194

ESOL,196,ELEMENT,6,LEPPL,20,PL_STRAIN_n6_s20_
!Variable für plastische Dehnung im Element
ESOL,197,ELEMENT,6,LEPEL,20,EL_STRAIN_n6_s20_
!Variable für elastische Dehnung im Element
ADD,198,196,197,,TOT_STRAIN_n6_s20_'''
!Addition von plastischer und elastischer Dehnung im Bone 1
ESOL,199,ELEMENT,6,ls,20,AXL_STRESS_n6_s20_ !Längsspannung

DERIV,200,198,1,,_STRAIN_RATE_n6_s20_...
XVAR,1
/AXLAB,X,_TIME_(sec)
/AXLAB,Y,_STRAIN_RATE_n6_s20_
PLVAR,198

XVAR,198
/AXLAB,X,_TOT_STRAIN_n6_s20_
/AXLAB,Y,_AXIAL_STRESS_n6_s20_
PLVAR,199

/OUTPUT,STRAIN_RATES_th,VER,,
PRVAR,135,140,145,155,160,165

```

```

PRVAR,175,180,185,190,195,200
/output

/OUTPUT,STRAIN_RATES_max,VER,,
EXTREM,135,200,5
/output

XVAR,1
/AXLAB,X,_TIME_(sec)
/AXLAB,Y,_STRAIN_RATES_s1
PLVAR,35,55,75,90,135,155,175,190
/AXLAB,Y,_STRAIN_RATES_s10
PLVAR,40,60,80,95,140,160,180,195
/AXLAB,Y,_STRAIN_RATES_s20
PLVAR,45,65,85,100,145,165,185,200

/AXLAB,X,_DUMMY
/AXLAB,Y,_DUMMY
PLVAR,197

allsel
fini
*endif
SAVE

/DELETE,d:\cem\p0809x0.25_m1\p0809x0.25_m1,rst,
/CLEAR

FINI
/EXIT,SOLU
FINI

! ****

```

Bibliography

- Adams R., Spence R., 1999. Earthquake. From: Natural Disaster Management- A presentation to commemorate IDNDR 1990-2000, Ed. J. Ingleton, Tudor Rose
- Akinci A., Malagnini L., Herrmann R.B., Pino N.A., Scognamiglio L., Eyidogan H., 2001. High-Frequency Ground Motion in the Erzincan Region, Turkey: Inferences from small earthquakes. Bulletin of the Seismological Society of America, 91, 6, pp. 1446-1455
- Aven T., 2003. Foundations of risk analysis: a knowledge and decision-oriented perspective. Wiley, Chichester
- Babcock D.L., 1996. Managing Engineering and Technology. 2nd Ed. Prentice Hall, New Jersey
- Baker J.W., Cornell C.A., 2005. Uncertainty Specification and Propagation for Loss Estimation using FOSM Methods. available in www
- Bayrak Y., Yilmaztürk A., Öztürk S., 2005. Relationships Between Fundamental Seismic Hazard Parameters for the Different Source Regions in Turkey. Natural Hazards, 36: 445-462
- Bazurro P., Luco N., 2005. Accounting for uncertainty and correlation in earthquake loss estimation. In: Proc. of IXth Int. Conf. on Structural Safety and Reliability, Ed.s Augusti G., Ciampoli M., Rome, Millpress, Rotterdam
- Beck J.L., Porter K.A., Shaikhutdinov R.V., Au S.K., Mizukoshi K., Miyamura M., Ishida H., Moroi T., Tsukada Y., Masuda M., 2002. Impact Of Seismic Risk On Lifetime Property Values. Report No. Eerl 2002-04, 2002, Pasadena
- Benjamin J.R., Cornell C.A., 1970. Probability, Statistics and Decision for Civil Engineers. McGraw-Hill, New York
- Bird J.F., Bommer J.J., 2004. Earthquake losses due to ground failure. Engineering Geology, 75, 147-179
- Boatwright J., Thywissen K., Seekins L.C., 2001. Correlation of Ground Motion and Intensity for the 17,January,1994 Northridge,California, Earthquake. Bulletin of the Seismological Society of America, 91, 4, pp.739-752
- Boore D.M., 2000. SMSIM – Fortran Programs for Simulating Ground Motions from Earthquakes: Version 2.0 – A Revision of OFR 96-80-A. USGS. available in www
- Boore D.M., 2003. Simulation of Ground Motion using the Stochastic Method. Pure appl. geophys., 160, 635-676, Birkhäuser Verlag, Basel
- Bozorgnia Y., Campbell K.W., 2004. Engineering Characterization of Ground Motion. From: Earthquake Engineering – From Engineering Seismology to Performance-Based Engineering, Ed.s Bozorgnia Y., Bertero V.V., CRC Press, Boca Raton
- Bozorgnia Y., Bertero V.V., 2003. Damage Spectra: Characteristics and Applications to Seismic Risk Reduction. Journal of Structural Engineering, Vol.129, No.10
- Böttcher C., 2002. Geschwindigkeitssensitivität des mechanischen Verhaltens unlegierter Baustähle bei wiederholter Beanspruchung bis in den inelastischen Bereich – experimentelle Untersuchung und Modellierung. Fortschritt-Berichte, Reihe 5, Grund- und Werkstoffe/Kunststoffe Nr.654, VDI Verlag, Düsseldorf
- Böttcher C., Reininghaus M., Peil U., 2003. Einfluß der Beanspruchungsgeschwindigkeit auf das mechanische Verhalten von unlegiertem Baustahl – Teil 1 u. 2. Stahlbau 72, Heft 11 u. 12

- Bruhns O.T., Fossa Bj., 1996. Rate-depending material testing. From: Dynamics of Civil Engineering Structures. Ed.s: Krätsig W.B., Niemann H.-J., Balkema, Rotterdam
- Chéry, J., 2001. A Physical Basis for Time Clustering of Large Earthquakes. In: Bulletin of the Seismological Society of America, Bd. 91, 6, p.1685-1693
- Chopra A. K., 2005. Earthquake dynamics of structures –a primer-. Earthquake Engineering Research Institute, 2nd Ed.
- Coburn A., Spence R., 2002. Earthquake Protection. 2nd Ed., John Wiley & Sons Ltd, Sussex, England
- ERD, 2006. Website of Earthquake Research Department, General Directorate of Disaster Affairs, Ankara, Turkey. www.deprem.gov.tr
- dePolo C., Slemmons D.B., 1990. Estimation of earthquake size for seismic hazards. In: Krinitzsky, E.L., Slemmons, D.B.. Neotectonics in earthquake evaluation. Boulder, Colorado, Geological Society of America Reviews in Engineering Geology, v.8.
- Faber M. H., 2005. Lecture Notes Risk and Safety in Civil Engineering. ETH Zurich, available in www
- FEMA, 1999. HAZUS – natural hazards loss estimation methodology software program, free distribution, info on <http://nibs.org/hazusweb>, Federal Emergency Management Agency, USA
- FEMA, 2000. Recommended Seismic Design Criteria for New Steel Moment-Frame Buildings, FEMA-350, Federal Agency for Emergency Management, USA
- Filippou F.C., Fenves G.L., 2004. Methods of Analysis for Earthquake Resistant Structures. From: Earthquake Engineering – From Engineering Seismology to Performance-Based Engineering, Ed.s. Bozorgnia Y., Bertero V.V., CRC Press, Boca Raton
- Fragiacomo M., Amadio C., Macorini L., 2004. Seismic response of steel frames under repeated earthquake ground motions. Engineering Structures 26, 2021-2035, available in www.sciencedirect.com
- Gebbeken N., Ruppert M., 1999. Ein Beitrag zur Simulation von Baustrukturen unter hochdynamischen Kurzzeitbeanspruchungen. Bauingenieur Bd. 74, Nr.11
- Jones S.L., Fry G.T., Engelhardt M.D., 2002. Experimental Evaluation of Cyclically Loaded Reduced Bea Section Moment Connections. Journal of Structural Engineering, Vol.128, No.4, 441-451
- Kao A., Soong T.T., Vender A., 1999. Nonstructural Damage Database. MCEER-99-0014, Microsoft Access Database, available in www
- Kawase H., 2003. Site Effects on Strong Ground Motions, from Int. Handbook of Earthquake and Engineering Seismology, Volume 81B, Int'l Assoc. Seismol. & Phys. Earth's Interior
- Kramer S.L., Stewart J.P., 2004. Geotechnical Aspects of Seismic Hazards. From: Earthquake Engineering – From Engineering Seismology to Performance-Based Engineering, Ed.s. Bozorgnia Y., Bertero V.V., CRC Press, Boca Raton
- Krawinkler H., Miranda E., 2004. Performance-Based Earthquake Engineering. From: Earthquake Engineering – From Engineering Seismology to Performance-Based Engineering, Ed.s. Bozorgnia Y., Bertero V.V., CRC Press, Boca Raton
- Krinitzsky E.L., 1993. Earthquake probability in engineering – Part 2: Earthquake recurrence and limitations of Gutenberg-Richter b-values for the engineering of critical structures – The Third Richard H. Jahns Distinguished Lecture in Engineering Geology. Engineering Geology, 36, 1-52, Elsevier

- Lay T., Wallace T.C., 1995. Modern Global Seismology. Academic Press Inc., London
- Luco N., Manuel L., Baldava S., Bazzurro P., 2005. Correlation of damage of steel moment-resisting frames to a vector valued set of ground motions. In: Proc. of IXth Int. Conf. on Structural Safety and Reliability, Ed.s Augusti G., Ciampoli M., Rome, Millpress, Rotterdam
- McGuire R.K., 2004. Seismic Hazard and Risk Analysis. Earthquake Engineering Research Institute, Monograph 10
- Meskouris K., Dorka U.E., Durán M., 1996. Structural response to earthquake loads. From: Dynamics of Civil Engineering Structures. Ed.s: Krätsig W.B., Niemann H.-J., Balkema, Rotterdam
- Moehle J., Stojadinovic B., Der Kiureghian A., Yang T.Y., 2005. An application of PEER Performance-Based Earthquake Engineering Methodology. PEER Research Digest No. 2005-1, available in www
- MTA. Active Fault Map of Turkey, 2005. Maden Tetkik Arama Enstitüsü - Institute of Mineral Research and Exploration. available at www.sayisalgrafik.com.tr/deprem
- Pecker A., 2005. Maximum Ground Surface Motion in Probabilistic Seismic Hazard Analysis. Journal of Earthquake Engineering, Vol.9, Imperial College Press
- PEER, 2005. Strong Motion Database, University of California, available in www
- Porter K., Kiremidjian A.S., LeGrue J.S., 2001. Component-Based Vulnerability of Buildings and Its Use in Performance Evaluation. Earthquake Spectra, 17 (2), p.291-312
- Porter K.. 2002. Life Safety Risk Criteria in Seismic Decisions. From: C.E. Taylor and E. VanMarcke, eds., Acceptable Risk Processes: Lifelines and Natural Hazards, Monograph No.21, ASCE
- Porter K., Shoaf K., Seligson H., 2005. Value of Injuries in the Northridge Earthquake - Technical Note. (accepted publication for Earthquake Spectra, 22 (2), May 2006). EERI, available in www
- Reininghaus M., 1994. Baustahl St 52 unter zweiachsiger plastischer Wechselbeanspruchung. Dissertation, TU Braunschweig
- Sarabandi P., Pachakis D., King S., Kiremidjian A., 2005. Development of Empirical Building Performance Functions Data from Past Earthquakes. Available in www. From John A. Blume Earthquake Engineering Center, Stanford
- Scheibe H.-J., 1990. Zum zyklischen Materialverhalten von Baustahl und dessen Berücksichtigung in Konstruktionsberechnungen. Dissertation, TU Braunschweig
- Schwartz D.P., 1984. Coppersmith K.J.. Fault behavior and characteristic earthquakes; Examples from Wasatch and San Andreas fault zones. Journal of Geophysical Research, v.89, p. 5681-5698
- Scholz C.H., 2002. Earthquakes and Faulting. Cambridge University Press, Cambridge, UK, 2nd Ed.
- SEISMOSIGNAL, 2005. open-source software for strong motion time series analysis
- Sivaselvan M.V., Reinhorn A.M., 2000. Hysteretic models for deteriorating inelastic structures. Journal of Engineering Mechanics, Vol.126, No.6
- Speidel, Mattson, 1997. Problems for Probabilistic Seismic Hazard Analysis. Natural Hazards 16: 165-179, Kluwer, Netherlands
- Stein S., Wyssession M., 2003. An Introduction to Seismology, Earthquakes and Earth Structure. Blackwell, Cornwall, UK

- Stewart J.P., Chiou S.-J., Bray J.-D., Graves R.W., Somerville P.G., Abrahamson N.A., 2002. Ground motion evaluation procedures for performance-based design. *Soil Dynamics and Earthquake Engineering* 22, 765-772
- Sugimoto H., Morita K., Takahashi Y., 2001. Prediction of Failure Mode of Haunched Beam to SHS Column Connections. *Steel Structures* 1, 185-199
- Swan S.W., Kassawara R., 1998. The Use of Earthquake Experience Data for Estimates of the Seismic Fragility of Standard Industrial Equipment. ATC-29-1. Proc. Seminar on Seismic Design and Performance of Nonstructural Components, Applied Technology Council
- Taghavi, S., Miranda E., 2003. Response Assessment of Nonstructural Building Elements. PEER Report 2003/05., University of California, Berkeley, open-source-report, available in www
- Vamsatsikos D., Cornell C.A., 2002. Incremental Dynamic Analysis. *Earthquake Engineering and Structural Dynamics*; 31: 491-514
- Vamsatsikos D., Cornell C.A., 2004. Applied Incremental Dynamic Analysis. *Earthquake Spectra*; Vol.20, p. 523-553
- Vamsatsikos D., Cornell C.A., 2005. Developing efficient scalar and vector intensity measures for IDA capacity estimation by incorporating elastic spectral shape information. *Earthquake Engineering and Structural Dynamics*; 34: 1573-1600
- Villaverde R., 2004. Seismic Analysis and Design of Nonstructural elements. From: *Engineering Seismology to Performance-Based Engineering*, Ed.s. Bozorgnia Y., Bertero V.V., CRC Press, Boca Raton
- Wen Y.K., 2004. Probabilistic Aspects of Earthquake Engineering. From: *From Engineering Seismology to Performance-Based Engineering*, Ed.s. Bozorgnia Y., Bertero V.V., CRC Press, Boca Raton
- Wen Y.K., 2005. Structural vulnerability and reliability-based design. In: Proc. of IXth Int. Conf. on Structural Safety and Reliability, Ed.s Augusti G., Ciampoli M., Rome, Millpress, Rotterdam
- Wen T.H., Loh C.H., 2006. Evaluation of the residual capacity of a structure in performance based seismic design (PBSD) through seismic hazard analysis. *Structure and Infrastructure Engineering*, Vol.2, No.1, p.1-11
- Whittaker A.S., Soong T.T., 2005. An overview of nonstructural components research at three US Earthquake Engineering Research Centers. From: Proc. of Seminar on Seismic Design, Performance, and Retrofit of Nonstructural Components in Critical facilities, ATC-29-2, Applied Technology Council, available in www
- Wichers M., 2001. Untersuchung des Einflusses des zeitabhängigen Materialverhaltens bei der Berechnung erdbebenbeanspruchter Stahlkonstruktionen. Diplomarbeit, TU Braunschweig
- Williams M.S., Sexsmith R.G., 1995. Seismic Damage Indices for Concrete Structures: A State-of-the-art Review. *Earthquake Spectra* Vol.11, No.2
- Yeats R.S., Gath E.M., 2004. The Role of Geology in Seismic Hazard Mitigation. From: *Engineering Seismology to Performance-Based Engineering*, Ed.s. Bozorgnia Y., Bertero V.V., CRC Press, Boca Raton